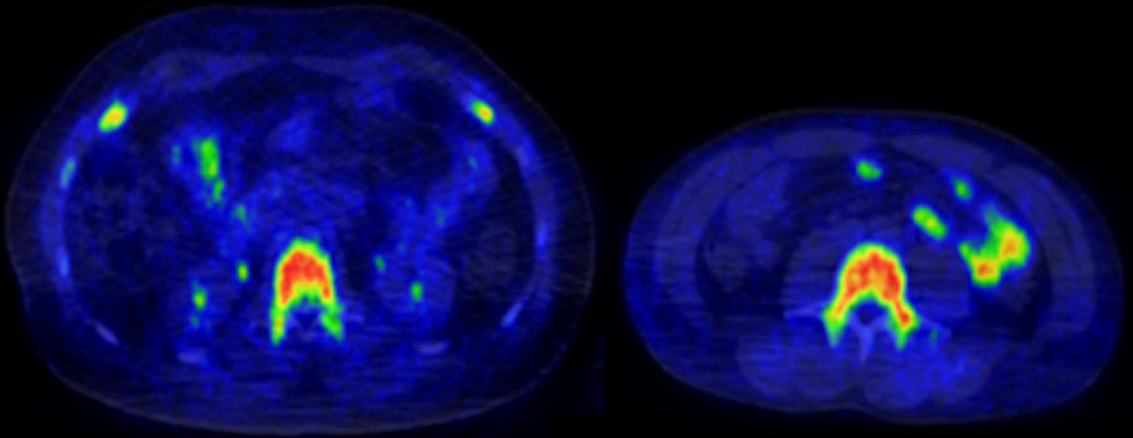




**TURUN
YLIOPISTO**
UNIVERSITY
OF TURKU



INSULIN SENSITIVITY AND ENDOCANNABINOID FUNCTION AS RISK FACTORS FOR OBESITY

Positron Emission Tomography Studies of
Insulin Sensitivity and CB1 Receptors

Laura Pekkarinen



**TURUN
YLIOPISTO**
UNIVERSITY
OF TURKU

INSULIN SENSITIVITY AND ENDOCANNABINOID FUNCTION AS RISK FACTORS FOR OBESITY

Positron emission tomography studies of insulin
sensitivity and CB1 receptors

Laura Pekkarinen

University of Turku

Faculty of Medicine
Department of Internal Medicine
Doctoral Programme in Clinical Research
Turku PET Centre
Turku, Finland

Supervised by

Professor Pirjo Nuutila, MD, PhD
Turku PET Centre
University of Turku and
Department of Endocrinology
Turku University Hospital
Turku, Finland

Professor Lauri Nummenmaa, PhD
Turku PET Centre
University of Turku
Turku, Finland

Reviewed by

Professor Hubert Preissl, Dr
Institute for Diabetes Research and
Metabolic Diseases of the
Helmholtz Center Munich
University of Tübingen
Tübingen, Germany

Docent Sanni Söderlund, MD, PhD
Endocrinology, Abdominal Center
Meilahti Hospital, Helsinki, Finland
Research Program for Clinical and
Molecular Metabolism
University of Helsinki
Helsinki, Finland

Opponent

Docent Kirsi Timonen, MD, PhD
Department of Clinical Physiology and
Nuclear Medicine at Hospital Nova
Wellbeing Services County of Central Finland
Jyväskylä, Finland

The originality of this publication has been checked in accordance with the University of Turku quality assurance system using the Turnitin OriginalityCheck service.

Cover image by Laura Pekkarinen. [^{18}F]FMPEP- d_2 PET image of one high and one low obesity risk subject.

ISBN 978-951-29-9574-5 (PRINT)
ISBN 978-951-29-9575-2 (PDF)
ISSN 0355-9483 (Print)
ISSN 2343-3213 (Online)
Painosalama, Turku, Finland 2023

To my family

UNIVERSITY OF TURKU

Faculty of Medicine

Internal Medicine

Turku PET Centre

LAURA PEKKARINEN: Insulin Sensitivity and Endocannabinoid Function as Risk Factors for Obesity. Positron Emission Tomography Studies of Insulin Sensitivity and CB1 Receptors.

Doctoral Dissertation, 155 pp.

Doctoral Programme in Clinical Research

December 2023

ABSTRACT

Obesity is a chronic disease with epidemic proportions, and it causes serious threats for human health and wellbeing. Obesity results from long-term positive energy balance, and is characterized by excessive fat accumulation. Insulin action in the brain regulates feeding behaviour and whole-body energy balance in interplay with peripheral metabolic organs. In addition, endocannabinoid system in brain and periphery modulates appetite and energy homeostasis.

Obesity is associated with increased brain insulin-stimulated glucose uptake (BGU), which in turn is linked with impaired insulin suppression of hepatic glucose production (EGP) and adipose tissue lipolysis. Subjects with obesity also exhibit lower endocannabinoid type 1 receptor (CB1R) availability in brain and abdominal adipose tissue. It remains unsolved, whether these alterations are present already before the development of obesity.

The aim of this thesis was to examine whether brain and peripheral tissue insulin sensitivity and CB1R availability are altered already in pre-obese state. We studied healthy non-obese young men with either high or low obesity risk using positron emission tomography. Tissue glucose uptake was quantified with a glucose analogue radiotracer [^{18}F]FDG during hyperinsulinemic-euglycemic clamp, and CB1R availability with CB1R inverse agonist radioligand [^{18}F]FMPEP- d_2 . Insulin-stimulated BGU was increased in high as compared to low obesity risk subjects, and it was associated with decreased whole-body glucose uptake and increased insulin-suppressed EGP and serum free fatty acid levels. Familial obesity risk was associated with increased BGU. Abdominal adipose tissue CB1R availability was lower in high than low obesity-risk subjects, and associated with enlarged mass and decreased insulin sensitivity of abdominal adipose tissue. Lower cerebral CB1R availability was associated with decreased whole-body insulin sensitivity, enlarged visceral adipose tissue mass and higher levels of circulating endocannabinoids.

Altogether, these results show that altered brain insulin action and crosstalk with periphery, as well as dysregulated endocannabinoid signalling may precede obesity.

KEYWORDS: Insulin sensitivity, glucose uptake, endogenous glucose production, cannabinoid type 1 receptor, obesity, brain, adipose tissue, positron emission tomography

TURUN YLIOPISTO

Lääketieteellinen tiedekunta

Sisätautioppi

Turun PET-keskus

LAURA PEKKARINEN: Insuliiniherkkyys ja endokannabinoidijärjestelmän toiminta lihavuuden riskitekijöinä. Positroniemissiotomografiatutkimuksia insuliiniherkyydestä ja CB1-reseptoreista.

Väitöskirja, 155 s.

Turun kliininen tohtoriohjelma

Joulukuu 2023

TIIVISTELMÄ

Lihavuus on pitkäaikainen sairaus, jonka esiintyvyys on saavuttanut epidemian mittasuhteet. Lihavuus aiheuttaa vakavan uhan terveydelle. Lihavuus on seurausta pitkäaikaisesta positiivisesta energiatasapainosta, ja sitä luonnehtii liiallinen kehon rasvamäärä. Aivojen insuliinisignalointi säätelee syömistä ja energiatasapainoa vuorovaikutuksessa ääreiskudosten kanssa. Myös aivojen ja ääreiskudosten endokannabinoidijärjestelmä vaikuttaa ruokahaluun ja energiatasapainoon.

Lihavuuteen liittyy kohonnut aivojen glukoosinotto insuliinialtistuksen aikana, mikä on yhteydessä heikentyneeseen glukoosin tuotannon ja rasvakudoksen rasvojen pilkkoutumisen estoon insuliinin vaikutuksesta. Lihavuuteen liittyy myös alentunut tyypin 1 endokannabinoidireseptorien (CB1R) saatavuus aivoissa ja vatsarasvassa. Ei kuitenkaan tiedetä, esiintyykö näitä muutoksia jo ennen lihavuuden kehittymistä.

Väitöskirjan tavoitteena oli selvittää, onko aivojen ja ääreiskudosten insuliiniherkyydessä ja CB1R-saatavuudessa muutoksia ennen lihavuuden kehittymistä. Tutkimme positroniemissiotomografian avulla terveitä, ei-lihavia ihmisiä, joilla lihomisriski on joko suuri tai pieni. Kudosten glukoosinotto määritettiin [¹⁸F]FDG-glukoosimerkkiaineen avulla hyperinsulineemisen-euglyseemisen clamp-tutkimuksen aikana, ja CB1R-saatavuus [¹⁸F]FMPEP-*d*₂-merkkiaineen avulla. Aivojen insuliinistimuloitu glukoosinotto oli suurempi suuren kuin pienen lihomisriskin henkilöillä, ja se oli yhteydessä pienentyneeseen kehon glukoosinottoon sekä suurentuneeseen glukoosin tuotantoon ja seerumin vapaiden rasvahappojen määrään. Perhetaustaan liittyvä lihomisriski oli yhteydessä aivojen suurentuneeseen glukoosinottoon. Vatsarasvan CB1R-saatavuus oli alhaisempi suuren kuin pienen lihomisriskin henkilöillä, ja liittyi vatsarasvan suurempaan määrään ja alentuneeseen insuliiniherkyyteen. Aivojen alhaisempi CB1R-saatavuus liittyi alentuneeseen kehon insuliiniherkyyteen sekä suurempaan sisäelinrasvan ja verenkierron endokannabinoidien määrään.

Tulokset osoittavat, että muutokset aivojen insuliinisignaloinnissa ja vuorovaikutuksessa ääreiskudosten kanssa sekä endokannabinoidijärjestelmän säätelyhäiriö voivat edeltää lihavuutta.

AVAINSANAT: Insuliiniherkkyys, glukoosin soluunotto, glukoosin tuotto, tyypin 1 kannabinoidireseptori, lihavuus, aivot, rasvakudos, positroniemissiotomografia

Table of Contents

Abbreviations	9
List of Original Publications	11
1 Introduction	12
2 Review of the Literature	14
2.1 Obesity – definition, prevalence and incidence	14
2.2 Central and peripheral regulation of energy homeostasis	15
2.3 The Pathogenesis of obesity	18
2.3.1 Impaired crosstalk between the brain and periphery ...	18
2.3.2 Environment and lifestyle	19
2.3.3 Genetic factors	20
2.4 Insulin action in energy and glucose metabolism	20
2.4.1 Insulin secretion and signalling	20
2.4.2 Insulin action on peripheral tissue metabolism in normal physiology	22
2.4.2.1 Skeletal muscle	22
2.4.2.2 White adipose tissue	23
2.4.2.3 Brown adipose tissue	23
2.4.2.4 Liver	24
2.4.3 Brain insulin signalling	25
2.4.3.1 Insulin transport and receptors	25
2.4.3.2 The hypothalamic and extrahypothalamic targets of insulin	25
2.4.3.3 Brain glucose metabolism and relation to insulin signalling	27
2.4.4 Physiological effects of brain insulin action	28
2.4.4.1 Regulation of feeding behaviour	28
2.4.4.2 Regulation of energy expenditure and thermogenesis	29
2.4.4.3 White adipose tissue lipolysis and lipogenesis	30
2.4.4.4 Regulation of hepatic glucose and lipid metabolism	31
2.4.4.5 Brain insulin action and peripheral insulin sensitivity	33
2.5 Obesity and insulin resistance	35
2.5.1 Mechanisms of obesity-induced insulin resistance	35
2.5.2 Tissue-specific changes in insulin resistance	36

2.5.3	Brain insulin resistance.....	37
2.5.4	Assessing brain changes associated with obesity with neuroimaging	39
2.5.4.1	Brain insulin resistance and dysregulation of peripheral tissues.....	40
2.6	Endocannabinoid system	42
2.6.1	Cannabinoid receptors and their ligands	42
2.6.2	Central endocannabinoid system and the regulation of energy balance.....	43
2.6.3	Peripheral endocannabinoid system and energy metabolism.....	44
2.6.4	Endocannabinoid system in obesity.....	45
2.6.5	Endocannabinoid system as a target to treat obesity... ..	46
3	Aims	48
4	Materials and Methods.....	49
4.1	Study subjects	49
4.2	PET studies.....	50
4.2.1	Principles of PET	50
4.2.2	Radiochemistry.....	51
4.2.3	PET image acquisition.....	53
4.2.3.1	[¹⁸ F]FDG PET scan with hyperinsulinemic– euglycemic clamp	53
4.2.3.2	[¹⁸ F]FMPEP- <i>d</i> ₂ scan.....	54
4.2.4	PET image analysis.....	55
4.2.4.1	Quantification of glucose uptake with [¹⁸ F]FDG	55
4.2.4.2	Quantification of peripheral tissue glucose uptake (II, III).....	58
4.2.4.3	Quantification of brain glucose uptake (I, II) ..	58
4.2.4.4	Measurement of endogenous glucose production (EGP) (II, III).....	59
4.2.4.5	Quantification of cannabinoid receptor availability in peripheral tissues (III)	60
4.2.4.6	Quantification of cannabinoid receptor availability in brain (I, III)	60
4.3	Anthropometric measurements.....	61
4.4	Biochemical analysis (I-III).....	61
4.5	Metabolic analysis (II, III)	62
4.6	Measurement of tissue masses (II, III).....	62
4.7	Statistical analysis	63
5	Results	64
5.1	Obesity risk associates with increased brain glucose uptake already in early adulthood.....	64
5.1.1	Study I-II: Increased brain glucose uptake in subjects with high versus low obesity risk.....	64
5.1.2	Study I: Familial obesity risk associates with increased brain glucose uptake	64

5.1.3	Study II: Whole-body insulin sensitivity associates negatively with brain glucose uptake	65
5.1.4	Study II: EGP associates positively with brain glucose uptake	69
5.2	Obesity risk associates with lower abdominal adipose tissue CB1 receptor availability	69
5.2.1	Study III: Lower abdominal adipose tissue CB1 receptor availability in subjects with high as compared to low obesity risk	69
5.2.2	Study III: Lower CB1 receptor availability is associated with decreased insulin sensitivity, higher body adiposity, unfavourable lipid profile and inflammatory markers.....	70
5.3	Obesity risk associates with central CB1 receptor availability	78
5.3.1	Study I: Familial obesity risk is associated with lower brain CB1 receptor availability.....	78
5.3.2	Study III: Lower whole-body insulin sensitivity, higher body adiposity and unfavourable lipid profile is associated with lower whole-brain CB1 receptor availability	79
6	Discussion.....	81
6.1	Impaired brain insulin sensitivity in the pre-obese state.....	81
6.2	Lower Abdominal adipose tissue CB1 receptor availability associates with metabolic dysregulation in the pre-obese state	82
6.3	Central CB1 receptor availability associates with metabolic dysregulation in the pre-obese state	85
6.4	Strengths and limitations.....	87
6.5	Clinical implications and future aspects.....	89
7	Conclusions	91
	Acknowledgements.....	93
	References	95
	Original Publications.....	117

Abbreviations

[¹⁸ F]FDG	[¹⁸ F]fluoro-D-glucose
[¹⁸ F]FMPEP- <i>d</i> ₂	(3R,5R)-5-(3-([¹⁸ F]fluoromethoxy-d ₂)phenyl)-3-((R)-1-phenylethylamino)-1-(4-(trifluoromethyl)phenyl)-pyrrolidin-2-one
1-AG	1-arachidonoylglycerol
2-AG	2-arachidonoylglycerol
AA	Arachidonic acid
AEA	Anandamide
AgRP	Agouti-related peptide
ApoA1	Apolipoprotein A1
ApoB	Apolipoprotein B
ARC	Arcuate nucleus
BAT	Brown adipose tissue
BBB	Blood-brain-barrier
BGU	Brain glucose uptake
CART	Cocaine- and amphetamine-regulated transcript
CB1R	Cannabinoid receptor type 1
CB2R	Cannabinoid receptor type 2
CNS	Central nervous system
CSF	Cerebrospinal fluid
CT	Computed tomography
DEA	Docosatetraenoyl ethanolamide
DIO	Diet-induced obese
DMH	Dorsomedial hypothalamic nucleus
DMN	Default-mode network
EGP	Endogenous glucose production
ECS	Endocannabinoid system
FFA	Free fatty acid
FDR	False discovery rate
FFM	Fat-free mass
fMRI	Functional magnetic resonance imaging

FUR	Fractional uptake rate
GIR	Glucose infusion rate
GlycA	Glycoprotein acetyls
GU	Glucose uptake
HFD	High-fat diet
HR	High-risk group
hs-CRP	High-sensitivity C-reactive protein
HU	Hounsfield unit
IR	Insulin receptor
K_i	Fractional uptake
LC	Lumped constant
α -LEA	α -linolenic acid
γ -LEA	γ -linolenic acid
LH	Lateral hypothalamic nucleus
LR	Low-risk group
Matsuda-ISI	Insulin sensitivity index by Matsuda
MRI	Magnetic resonance imaging
α -MSH	α -melanocyte-stimulating hormone
MUFA	Monounsaturated fatty acids
NALS	N-arachidonoyl-L-serine
NPY	Neuropeptide Y
OGTT	Oral glucose tolerance test
PET	Positron emission tomography
POMC	Pro-opiomelanocortin
PUFA	Polyunsaturated fatty acid
PVH	Paraventricular nucleus
Rd	Rate of glucose disappearance
ROI	Regions of interest
RWAT	Retroperitoneal adipose tissue
SAT	Subcutaneous adipose tissue
SPM	Statistical parametric mapping
TAC	Time-activity curve
T2D	Type 2 diabetes
VAT	Visceral adipose tissue
VOI	Volume of interest
VMH	Ventromedial hypothalamic nucleus
V_T	Volume distribution
WAT	White adipose tissue

List of Original Publications

This dissertation is based on the following original publications, which are referred to in the text by their Roman numerals:

- I Kantonen, T., Pekkarinen, L., Karjalainen, T., Bucci, M., Kalliokoski, K., Haaparanta-Solin, M., Aarnio, R., Dickens, A. M., von Eyken, A., Laitinen, K., Houttu, N., Kirjavainen, A. K., Helin, S., Hirvonen, J., Rönnemaa, T., Nuutila, P., & Nummenmaa, L. (2022). Obesity risk is associated with altered cerebral glucose metabolism and decreased μ -opioid and CB1 receptor availability. *International journal of obesity* (2005), 46(2), 400–407. <https://doi.org/10.1038/s41366-021-00996-y>.
- II Pekkarinen, L., Kantonen, T., Rebelos, E., Latva-Rasku, A., Dadson, P., Karjalainen, T., Bucci, M., Kalliokoski, K., Laitinen, K., Houttu, N., Kirjavainen, A. K., Rajander, J., Rönnemaa, T., Nummenmaa, L., & Nuutila, P. (2022). Obesity risk is associated with brain glucose uptake and insulin resistance. *European journal of endocrinology*, 187(6), 917–928. <https://doi.org/10.1530/EJE-22-0509>
- III Pekkarinen, L., Kantonen, T., Oikonen, V., Haaparanta-Solin, M., Aarnio, R., Dickens, A. M., von Eyken, A., Latva-Rasku, A., Dadson, P., Kirjavainen, A. K., Rajander, J., Kalliokoski, K., Rönnemaa, T., Nummenmaa, L., & Nuutila, P. (2023). Lower abdominal adipose tissue cannabinoid type 1 receptor availability in young men with overweight. *Obesity* (Silver Spring, Md.), 31(7), 1844–1858. <https://doi.org/10.1002/oby.23770>

The original publications have been reproduced with the permission of the copyright holders.

1 Introduction

Worldwide, obesity is recognized as a chronic disease that increases the risk for other non-communicable diseases, cancers and premature mortality [Bray et al., 2017; EASO, 2015; Jastreboff et al., 2019]. Obesity results from a long-term positive energy balance and is characterized by excess energy stored as fat in adipocytes enlarged in size and number, and as ectopic fat in other organs. The global obesity epidemic causes a serious burden to individuals and communities as worldwide over 650 billion adult have obesity [WHO, 2021]. Therefore, effective tools for preventing and treating obesity are needed, and to reach this, it is essential to understand the complex mechanisms in the pathogenesis of obesity.

Multiple neural and neuroendocrine circuits at central and peripheral levels coordinate appetite, food intake and energy expenditure in interplay with environment and genes [Wilson & Enriori, 2015]. Common obesity thus results from defective interaction between the brain and peripheral metabolic organs, and central resistance to nutritionally relevant signals arising from periphery. Disruption in the fine-tuned regulation of energy balance predisposes to excess eating and weight gain [Oussaada et al., 2019; Timper & Brüning, 2017; Wilson & Enriori, 2015].

Insulin in the brain acts as a satiety signal suppressing appetite particularly for palatable food [Kullmann, Kleinridders, et al., 2020]. In addition to regulation of eating behaviour, brain insulin action has several effects on whole-body metabolism. These include energy expenditure and thermogenesis [Sanchez-Alavez et al., 2010; Spiegelman & Flier, 2001], white adipose tissue and liver lipid metabolism [Scherer et al., 2021], control of blood glucose level by modulating hepatic endogenous glucose production (EGP) [Lewis et al., 2021] and potentially peripheral tissue glucose uptake [Heni et al., 2017], and cognitive performance [Dutta et al., 2022]. Impaired insulin action in the brain, “brain insulin resistance”, in turn is linked with disturbances in central and peripheral metabolism, and has been recognized as central characteristic of obesity [Kullmann, Kleinridders, et al., 2020].

Positron emission tomography (PET) with a labelled glucose analogue radiotracer 2- deoxy-2- ^{18}F fluoro-D-glucose (^{18}F FDG) allows detecting brain insulin sensitivity *in vivo*. Previous studies have demonstrated increased insulin-stimulated brain glucose uptake (BGU) in subjects with obesity [Rebelos et al., 2021;

Tuulari et al., 2013] and impaired glucose tolerance [J. W. Eriksson et al., 2021; Hirvonen et al., 2011; Latva-Rasku et al., 2018] as compared to lean and insulin sensitive subjects. However, it is not known whether altered brain insulin signalling is present already in subjects with overweight and risk factors for developing obesity.

Endocannabinoid system (ECS), consisting of two G-protein-coupled receptors, cannabinoid type 1 and type 2 (CB1R and CB2R, respectively), their endogenous ligands and ligand-metabolizing enzymes, has a central role in the control of energy homeostasis [Silvestri & Di Marzo, 2013]. CB1Rs are widely expressed in brain regions controlling feeding behaviour and energy balance [Di Marzo et al., 2009] and in peripheral tissues, including white and brown adipose tissue, skeletal muscle, endocrine pancreas and gastrointestinal tract [Matias, Petrosino, et al., 2008]. In the brain, activation of CB1Rs stimulate appetite and food intake in interaction with dopaminergic and opioidergic signalling pathways [Silvestri & Di Marzo, 2013]. In addition, the central ECS modulates peripheral metabolism including thermogenesis [Cota et al., 2003] hepatic EGP and white adipose tissue lipid metabolism [O'Hare et al., 2011]. Peripheral ECS modulates metabolic functions locally, and has central role especially in white adipose tissue and liver metabolism [Silvestri & Di Marzo, 2013]. Obesity and associated metabolic disorders are characterized by ECS dysregulation with altered CB1R availability and endocannabinoid levels in tissues and in circulation. CB1R antagonism in turn reduces food intake, body weight and improve the signs of metabolic disorders [Quarta et al., 2011; Silvestri & Di Marzo, 2013]. Withdrawal of the first CB1R inverse agonist Rimonabant (SR141716) from market due to neuropsychiatric side effects, has led to investigate new therapeutic approaches in order to control the overactive ECS in obesity [Simon & Cota, 2017].

ECS function can be studied *in vivo* by quantifying tissue CB1R availability with PET and an CB1R inverse agonist radioligand [3R,5R]-5-[3-methoxy-phenyl]-3-[(R)-1-phenyl-ethylamino]-1-[4-trifluoro-methyl-phenyl]-pyrrolidin-2-one ($[^{18}\text{F}]$ FMPEP- d_2). The radioligand binds to CB1Rs that are not occupied with their natural ligands. A previous study from our centre showed lower CB1R availability in the brain and abdominal adipose tissue depots of healthy males with obesity as compared to lean males [Lahesmaa et al., 2018].

The aim of the present thesis is to investigate brain and peripheral tissue insulin sensitivity and endocannabinoid receptors, and their associations with the risk of developing obesity using PET imaging.

2 Review of the Literature

2.1 Obesity – definition, prevalence and incidence

Obesity is a chronic disease defined as excessive fat accumulation in adipose tissue due to energy imbalance, presenting a significant risk for health [Bray et al., 2017]. Obesity can be classified using body mass index (BMI) - body weight in kilograms divided by the square of height in meters (kg/m^2) – as $\text{BMI} \geq 30 \text{ kg/m}^2$ defined as obesity [WHO, 2021]. While BMI does not take into account body composition, waist circumference is an additional measurement of abdominal obesity. Waist circumference $\geq 88 \text{ cm}$ for women and $\geq 102 \text{ cm}$ for men is considered to associate with significant health consequences [Jensen et al., 2014].

The prevalence of obesity has increased worldwide, and today, there are more people living with obesity than with underweight in all areas except Sub-Saharan Africa and South Asia [World Obesity, 2023]. In 2016, 13% of adults aged 18 years or older had obesity accounting for 650 million people [WHO, 2021] (**Figure 1**).

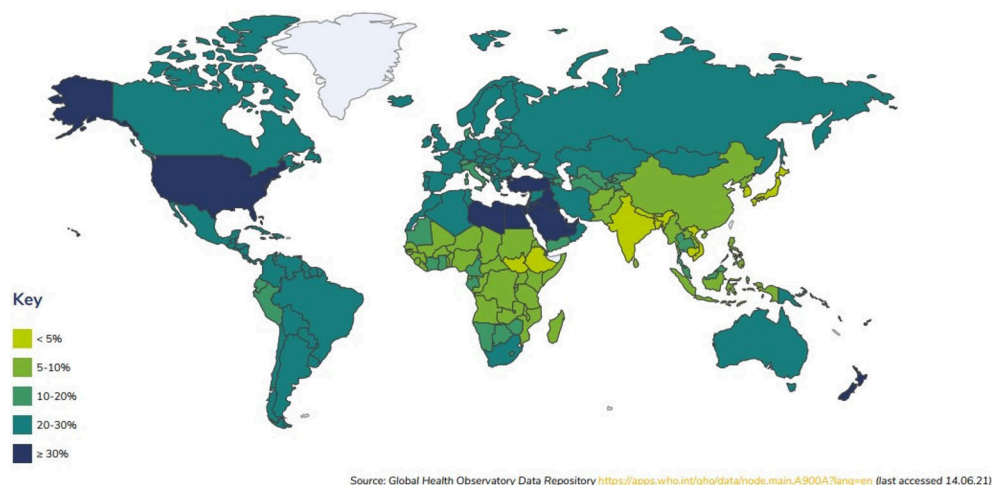


Figure 1. Estimates of prevalence of obesity ($\text{BMI} \geq 30 \text{ kg/m}^2$) in adults in 2016. The figure is reprinted with permission from World Obesity Federation, London as originally published by The World Obesity Federation.

Between 1980 and 2015, the prevalence of obesity has doubled in 73 countries, and continuously increased in most other countries. The increase has been similar between males and females in all age groups being highest during early adulthood [Afshin et al., 2017]. In Finland in 2017, 17% of men and 19% of women aged 18-29 years had obesity, while in the age group of > 30 years the prevalence of obesity was 26% for men and 28% for woman. Also, 46% of adults have abdominal obesity. [FinTerveys2017, 2018] The estimates suggest that global level of obesity will be on the rise: in 2035, 23% of men and 27% of women may be affected by obesity [World Obesity, 2023]. Country-specific data and trends in obesity and its economic impact are available at <https://www.worldobesity.org/>.

Obesity related non-communicable diseases, including type 2 diabetes (T2D), cardiovascular diseases (CVDs) and non-alcoholic fatty liver disease impairs both quality of life and life expectancy [Bray et al., 2017; Pereira-Miranda et al., 2017]. Above BMI 25 kg/m², each 5 kg/m² increasing in BMI associates with about 30% higher overall mortality, and 40% higher vascular, 120% diabetic, 60% kidney disease and 80% liver disease [Whitlock et al., 2009]. Also, abdominal adiposity, when adjusted for BMI, presents an independent risk for premature death [Pischoon et al., 2008]. Overweight and obesity are estimated to be responsible for 5.0 million deaths and 160 million disability-adjusted life-years globally in 2019 [Chong et al., 2023].

2.2 Central and peripheral regulation of energy homeostasis

Two complementary pathways, homeostatic and reward-driven pathways regulate food intake, glucose metabolism and energy expenditure. The homeostatic signals ensures that food intake meets the energy demand. The reward-driven, or hedonistic regulation in turn, drives motivation to acquire and consume calories regardless of energy requirement [Lutter & Nestler, 2009; Myers et al., 2021]. The interplay of the neural and peripheral processes and environmental and lifestyle factors is schematically presented in **Figure 2**.

Homeostatic signals encompass vagal afferent signals and circulating hormones and metabolites from the peripheral tissues and organs supplying information about nutritional status to brain centres that coordinate the adaptive changes in food intake, energy expenditure and storage [Lenard & Berthoud, 2008; Roh et al., 2016; Wilson & Enriori, 2015]. The gustatory system, gastrointestinal tract, pancreas, adipose tissue, liver and muscle are the main peripheral components participating in the energy homeostasis. They are in bidirectional communication with the brain through neural circuits, hormones and metabolites. The peripheral signals affecting energy balance include for instance leptin, insulin, amylin, ghrelin, cholecystokinin, peptide

YY, glucagon-like peptide-1 (GLP-1), somatostatin, glucose, fatty acids and amino acids [Lenard & Berthoud, 2008; Myers et al., 2021; Roh et al., 2016; Wilson & Enriori, 2015]. Leptin signalling represents long-term control mechanism, while leptin is secreted by white adipocytes in proportion to the amount of stored fat. Insulin, secreted by pancreatic β -cells in response to circulating nutrients, [Fu et al., 2013] is likewise comparable to fat stores, and also tissue insulin sensitivity [Brochu et al., 2000]. In addition, endocannabinoids participate in the regulation on appetite and food intake by modulating central neurons via activation of cannabinoid receptors. This is, at least partly mediated by feeding-regulated hormones, especially leptin and ghrelin (Silvestri, and Marzo, 2013).

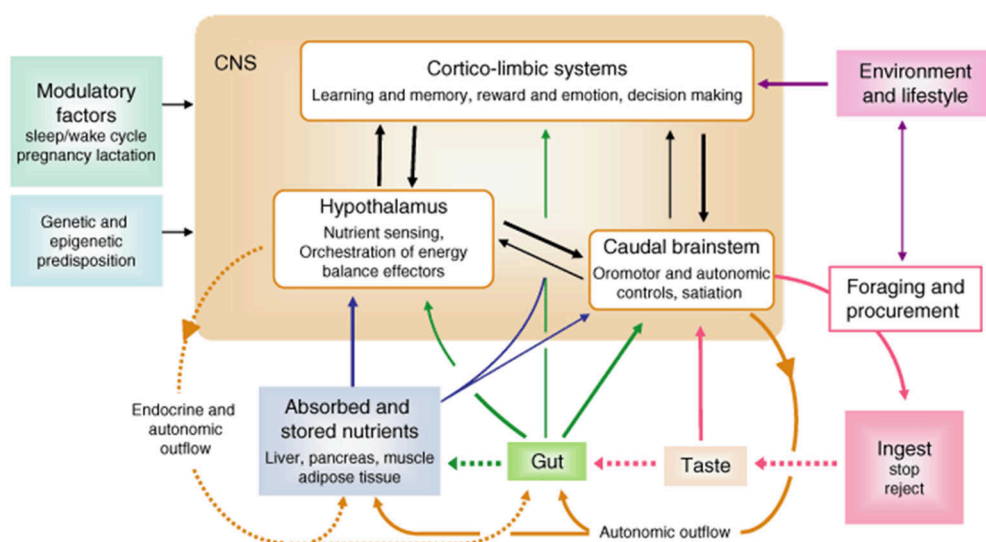


Figure 2 A schematic diagram showing major components of the peripheral and central systems involved in energy balance regulation, and control of food intake, and the interaction with environment and genes. Reprinted with permission from publisher, © Wiley, as originally published by Lenard and Berthoud, 2008.

The hindbrain is the first brain structure to receive information from the gustatory cells and gastrointestinal tract through the gustatory and vagal afferents. The hypothalamus and the specific regions within it such as arcuate (ARC) and paraventricular (PVH) nuclei in turn, has a central role in integrating information originated from peripheral organs via circulating hormones, metabolites and neural circuits. This nutritional information is then processed in the context of other internal and external information. The optimal adaptive responses are finally implemented through behavioural, autonomic and endocrine output pathways [Lenard & Berthoud, 2008].

The hypothalamic ARC contains anorexigenic (appetite-suppressing) pro-opiomelanocortin (POMC)-expressing POMC and cocaine- and amphetamine-regulated transcript (CART) neurons that promote the release of α -melanocyte-stimulating hormone (α -MSH), and the orexigenic (appetite-stimulating) neuropeptide Y (NPY) and agouti-related peptide (AgRP)-expressing NPY/AgRP neurons. These neurons project to second-order neurons in the hypothalamus and in the hindbrain resulting in a response on energy intake and expenditure [Myers et al., 2021; Timper & Brüning, 2017; Wilson & Enriori, 2015]. PVH neurons control sympathetic outflow to peripheral organs leading to increased fatty acid oxidation and lipolysis and secrete hormones having catabolic actions, including thyrotropin-releasing hormone and corticotrophin-releasing hormone, and destruction of PVH leads to hyperphagia and obesity [Roh et al., 2016]. POMC/CART and NPY/AgRP neurons express receptors for peripheral hormones, including leptin and insulin [Kleinridders et al., 2014; Timper & Brüning, 2017; Wilson & Enriori, 2015]. Other hypothalamic nuclei that are essential in energy balance regulation include dorsomedial hypothalamic (DMH), ventromedial hypothalamic (VMH) and lateral hypothalamic (LH). Destruction of the DMH and VMH results in hyperphagia, hyperglycemia and obesity [Roh et al., 2016]. Neurons within the LH links the hypothalamus with brain areas associated with reward and motivation, and with areas in brainstem associated with visceral sensory input. Destruction of LH in turn, results in hypophagia and weight loss. Hypothalamic neurons are connected to nucleus solitary tract (NTS) in the hindbrain. In addition to receiving satiety signals from periphery, NTS neurons produce appetite-regulating peptides GLP-1, NPY and POMC [Lenard & Berthoud, 2008; Roh et al., 2016; Timper & Brüning, 2017].

At fasting, low circulating and stored fuel levels are signalled to the brain by elevated ghrelin and low levels of other gut hormones, and a decrease in leptin. As a result, NPY/AgRP neurons are activated leading to feeding behaviour, a reduction in energy expenditure, energy storage, increased hepatic EGP, and release of AgRP that prevents the anorexigenic effects of POMC/CART neurons. In postprandial state, ghrelin levels decrease, leptin and insulin increase and gastrointestinal hormones secreted in response to ingested nutrients, project to ARC. This leads to inhibition of NPY/AgRP neurons and stimulation of POMC/CART neurons. POMC/CART activation results also from direct effect of glucose and fatty acids. As a result, food intake and hepatic EGP decreases while energy expenditure increases. In addition, seeing and tasting tempting foods activates POMC/CART and inhibit NPY/AgRP neurons [Timper & Brüning, 2017; Wilson & Enriori, 2015]. Hypothalamic endocannabinoid levels increase at fasting and decrease at postprandial state due to changes in the hormonal signals [Silvestri & Di Marzo, 2013]. In basal state between the meals, energy homeostasis is mostly dependent on input from leptin [Myers et al., 2010].

Cortico-limbic reward system contributes to cognitive and emotional aspect in feeding. Hedonic aspects of appetite is regulated by hunger, taste, food cues, and palatable food [Berthoud, 2004; Kleinridders & Pothos, 2019]. Opioid and endocannabinoid (ECS), as well dopamine system, are involved in the hedonic control of food intake [Berthoud, 2004; Silvestri & Di Marzo, 2013]. The homeostatic signals interact with the reward pathway. For instance, leptin suppress feeding, and insulin decreases the desire for high-fat or high-sugar food by acting on the dopaminergic neurons in the reward circuitry [Könner et al., 2009; Lutter & Nestler, 2009; Timper & Brüning, 2017].

2.3 The Pathogenesis of obesity

The constitutive cause of obesity is a long-term positive energy balance: energy intake exceeding energy expenditure [Haslam & James, 2005]. Appetite, food intake, and energy expenditure are coordinated by neural and neuroendocrine circuits at central and peripheral levels in interplay with environment and genes [Oussaada et al., 2019; Timper & Brüning, 2017; Wilson & Enriori, 2015]. This intrinsic system controlling energy balance is sensitive to disturbances that can unsettle energy homeostasis predisposing to obesity [Myers et al., 2021; Roh et al., 2016]. The overall pathogenesis of obesity is complex and not yet fully understood. Obesity involves several components regulating energy homeostasis: dysregulated interplay of brain and peripheral signals, pathological overeating and low physical activity in a genetically prone person [Oussaada et al., 2019; Timper & Brüning, 2017; Wilson & Enriori, 2015].

2.3.1 Impaired crosstalk between the brain and periphery

Altered hypothalamic function or defective sensing of peripheral signals in hypothalamic neurons, particularly leptin and insulin is associated with high-fat diet, positive energy balance, and obesity [Könner & Brüning, 2012; Kullmann et al., 2015; Roh et al., 2016]. Brain insulin resistance can result from several mechanism, for instance, decreased blood-brain-barrier (BBB) transport of insulin to the brain or impaired insulin signalling because of overfeeding and hypothalamic inflammation. Central insulin resistance in turn, further promotes increased appetite, overnutrition and weight gain [Könner & Brüning, 2012; Scherer et al., 2021]. Hypothalamic inflammation and gliosis – reactive inflammatory response of glial to cell damage – are suggested causal factors of diet-induced obesity. Obesogenic diet among genetically prone persons may induce inflammatory reaction in hypothalamic nuclei involved in energy balance regulation. This in turn, may lead to neuronal dysfunction favouring increased food intake and energy stores [Sewaybricker et al., 2023].

In addition, dysregulation of reward circuits is a hallmark of obesity. Dopamine D₂ receptor availability in subjects with obesity is proportional to their BMI [Wang et al., 2001], and increased reactivity to food reward in limbic system in subjects with obesity [Stoeckel et al., 2008]. While ECS participates in the energy balance regulation in the central and peripheral levels by modulating both homeostatic and hedonic pathways, dysregulation of this system associates with obesity. The overall action of the ECS is to promote energy intake and storage, but when energy-dense, highly palatable food is abundant, it favours development of obesity [Silvestri & Di Marzo, 2013]. The ECS is more thoroughly discussed in later chapters.

2.3.2 Environment and lifestyle

The modern environment characterized by high availability of energy dense, palatable food, increased presence of food cues with reduced level of physical activity favours weight gain. In this obesogenic environment, the hedonic regulation is prone to override the homeostatic pathway increasing the consumption of palatable food regardless of energy requirement [Lutter & Nestler, 2009; Myers et al., 2021]. In preclinical studies with rodents, gliosis and structural changes in the hypothalamic ARC, are stimulated by hypercaloric diet rich with saturated fat and simple carbohydrates, and are associated with hyperphagia and weight gain. In humans, this association is not yet proven, although neuroimaging studies and postmortem histopathological analyses have served evidence of hypothalamic gliosis associated with obesity [Sewaybricker et al., 2023].

Total body energy expenditure consists of resting metabolic rate, activity-related energy expenditure and diet-induced thermogenesis (energy dissipated in the absorption, metabolism and storage of nutrients). Studies examining energy expenditure in obesity suggest lower activity-related energy expenditure, but not resting metabolic rate or diet-induced thermogenesis, as a contributor to weight gain [Oussaada et al., 2019]. Sedentary lifestyle and low physical activity promote weight gain and ectopic fat [Jebb & Moore, 1999; Kujala et al., 2022; Leskinen et al., 2009], although conflicting results exists [Hill et al., 2012].

BMI in childhood and youth correlates positively with BMI in adulthood [Juhola et al., 2011]. Also low family income predisposes to obesity later in life [Juonala et al., 2011]. Furthermore, family history of obesity and T2D increases the risk for overweight and obesity adulthood [Anjana et al., 2009; Cederberg et al., 2015]. Other environmental and societal factors that have been linked to the development of the obesity pandemic are powerful marketing of calorie-rich food, low socioeconomic status, gut microbiota, circadian rhythm and stress [Blüher, 2019; Oussaada et al., 2019; Qayyum et al., 2009].

2.3.3 Genetic factors

Several genes associated with severe, early-onset obesity have been identified [Loos & Yeo, 2022]. These monogenic causes of obesity are however rare, accounting only approximately 7.3% of childhood-onset obesity [Kleinendorst et al., 2018]. Common, multifactorial, obesity is typically polygenic, in which the phenotype is caused by several polymorphisms, which account only a minor effect on BMI. Over 750 single-nucleotide polymorphisms have been found to be associated with BMI [Locke et al., 2015]. This genetic predisposition is not deterministic for obesity. Instead, environmental and lifestyle factors modify heritability estimates [Loos & Yeo, 2022; Silventoinen & Konttinen, 2020]. However, the monogenic and polygenic obesity share the same biology as the pathology lies in the brain neural circuits, for instance in genes coding for leptin-melanocortin pathway and pathways controlling the hedonic aspect of food intake [Loos & Yeo, 2022].

2.4 Insulin action in energy and glucose metabolism

Insulin is the main regulator of body glucose, lipid and amino acid metabolism. Following plasma glucose rise after food ingestion, insulin secretion by pancreatic β cells is stimulated. The resulting hyperinsulinemia leads to suppression of EGP and stimulation of glucose uptake (GU) and utilization in peripheral tissues. In addition, insulin stimulates energy storage by stimulating glycogen synthesis, lipogenesis, protein synthesis and by inhibiting lipolysis, glycogenolysis and protein catabolism [Norton et al., 2022; M. C. Petersen & Shulman, 2018; Saltiel & Kahn, 2001]. In the brain, insulin signalling regulates appetite, eating behaviour and whole-body energy homeostasis through several mechanisms by coordinating the organ interplay [Kullmann, Kleinridders, et al., 2020; Scherer et al., 2021].

2.4.1 Insulin secretion and signalling

High surrounding glucose concentration is the main regulator of insulin secretion from pancreatic β cells. In addition to insulin secretion, glucose increases insulin gene transcription, and translation and transcription of insulin mRNA [Weiss et al., 2000]. Amino acids, free fatty acids, and other hormones and neurotransmitters can modulate the insulin secretion too. The effect of plasma amino acids at their physiological concentrations is however small, and they only potentiate the effect of glucose. Circulating free fatty acids can exert long-term positive effects at physiological levels on the responsiveness of β cells, but at pathological levels induce β cell dysfunction [Henquin, 2021]. Incretins are peptide hormones secreted by enteroendocrine cells in the gut in response to nutrient absorption. Glucose-

dependent insulinotropic polypeptide (GIP) and glucagon-like peptide-1 (GLP-1) amplify insulin secretion initiated by hyperglycaemia [Nauck & Meier, 2018]. Somatostatin is produced in many locations in the body. Majority of circulating somatostatin originate from gastrointestinal track, and a small proportion from pancreatic δ cells. Somatostatin has an inhibitory effect on insulin secretion. Also leptin, secreted by white adipocytes, may have a long-term inhibitory effect on insulin secretion. Parasympathetic nervous system can enhance insulin secretion, while sympathetic system has an inhibitory effect. Long-term endogenic, as well exogenic hypercortisolism, may lead to hypersecretion of insulin, while as a short-term the effect is inhibitory [Henquin, 2021].

Insulin exerts its actions by binding to insulin receptors (IR), or in lesser extent to closely related insulin-like growth factor-1 (IGF-1R) receptor, on the plasma membrane of target cells (**Figure 3**). This initiates a cascade of phosphorylation events leading to activation of phosphatidylinositol 3-kinase (PI3K)/ protein kinase B (Akt) pathway. Of three Akt isoforms, Akt2 is predominant in insulin-sensitive tissues and mediates most of insulin's metabolic actions [Boucher et al., 2014; M. C. Petersen & Shulman, 2018]. The low frequency partial loss-of-function p.P50T/Akt2 variant is associated with reduced insulin sensitivity in several peripheral tissues, and also in brain [Latva-Rasku et al., 2018].

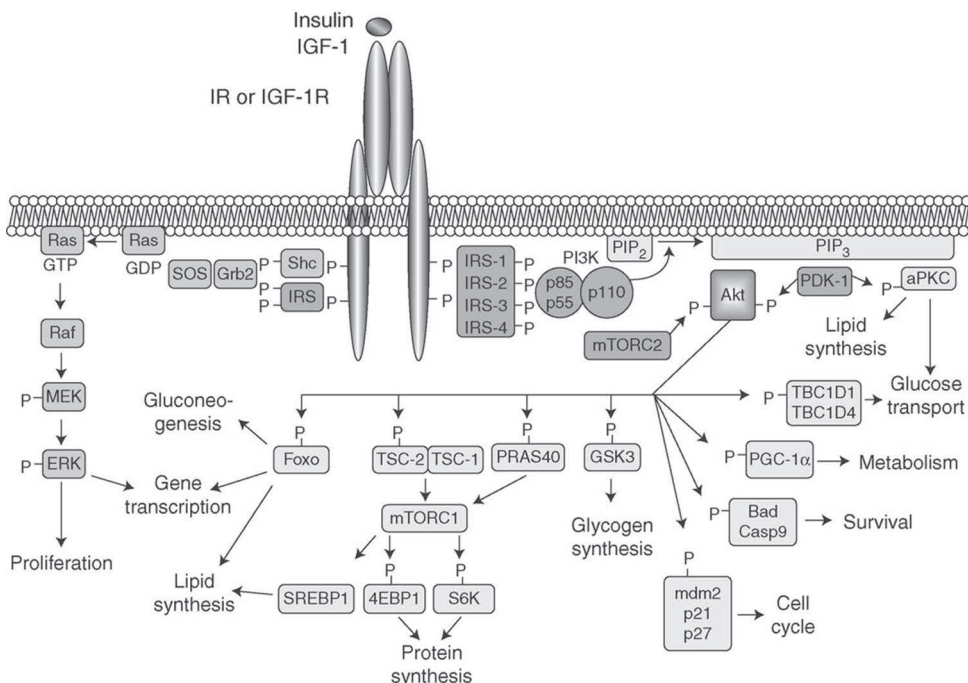


Figure 3. Insulin signalling pathways. Reprinted with permission from publisher, © Cold Spring Harbor Laboratory Press, as originally published by Boucher et al., 2014.

Activated Akt allows multiple adjacent downstream reactions that leads to insulin response in the plasma membrane. Phosphorylation of TBC1D4 and TBC1D1 by Akt mediates insulin-stimulated tissue GU by stimulating the translocation of the transporter GLUT4 from intracellular stores to the plasma membrane [Boucher et al., 2014; M. C. Petersen & Shulman, 2018; Saltiel & Kahn, 2001]. Phosphorylation of glycogen synthase kinase 3 (GSK3) in turn results in glycogen synthesis in liver. Akt induced activation of mechanistic target of rapamycin complex 1 (mTORC1) leads to enhanced protein synthesis as well as increased lipid synthesis both in liver and in white adipose tissue (WAT). Inactivation of transcription factors of the Forkhead box O (Foxo) by Akt results in decreased expression of gluconeogenic genes, and suppression of EGP in liver. Suppression of gluconeogenesis, and liver fatty acid oxidation is facilitated by phosphorylation of PGC-1 α [Boucher et al., 2014]. In addition, inactivation on Foxo results decreased expression of lipogenic genes leading to reduced hepatic very-low-density lipoprotein (VLDL) and triglyceride production [Boucher et al., 2014; M. C. Petersen & Shulman, 2018; Sparks & Dong, 2009]. Inhibition of lipolysis in WAT comprises of several Akt-dependent events as well [Norton et al., 2022].

2.4.2 Insulin action on peripheral tissue metabolism in normal physiology

2.4.2.1 Skeletal muscle

In skeletal muscle, insulin action contributes primarily to GU and glycogen synthesis. Hyperinsulinemia increases skeletal muscle GU up to 10-fold compared to fasting state [Norton et al., 2022]. In basal postprandial state, skeletal muscle is responsible for 30-40% of total systemic glucose disposal. The insulin stimulated GU is mediated via recruitment of GLUT4 to the plasma membrane of myocytes. Once entered to myocytes, glucose is phosphorylated to glucose-6-phosphate by hexokinase II. Insulin-stimulated pathway downstream to glucose-6-phosphate can either drift to glycolysis or glycogen synthesis, of which the latter predominates at postprandial state. While glycogen synthesis is allowed by GSK3 inhibition by Akt, insulin also suppresses glycogen breakdown by inhibin glycogen phosphorylase. Insulin also participates to skeletal muscle protein metabolism. Insulin suppresses proteolysis and stimulates protein synthesis [Norton et al., 2022; M. C. Petersen & Shulman, 2018].

2.4.2.2 White adipose tissue

The effect of insulin in WAT is anabolic: insulin suppresses lipolysis, stimulates GU and adipogenesis by promoting triglyceride synthesis. At postprandial state, insulin inhibits the release of non-esterified fatty acids (NEFA) into circulation and to other tissues [Norton et al., 2022]. Long-term impairment of insulin action to suppress WAT lipolysis and chronic exposure to increased level of circulating NEFAs can lead to impaired insulin action in multiple tissues and compensatory increase in insulin secretion, which is further disturbed by the “lipotoxic” effect on insulin secretion of β cells. Ultimately this can lead to development of T2D. Insulin-suppressed WAT lipolysis is indirectly involved in the suppression on hepatic EGP though reduction of substrate and energy availability for hepatic gluconeogenesis [M. C. Petersen & Shulman, 2018; Wajchenberg, 2000].

Insulin-stimulated GU into WAT is facilitated by GLUT4 [M. C. Petersen & Shulman, 2018]. At postprandial state, the GU into WAT account for 5-10% of glucose disposal [Virtanen et al., 2002]. However, fat depots largely differ according to their metabolic characteristics such as lipid composition, secreted factors, and sensitivity to sympathetic and hormonal control of lipolysis, lipogenesis and GU [Wajchenberg, 2000]. Higher metabolic activity measured as GU has been shown in visceral (VAT) than in abdominal subcutaneous (SAT) adipose tissue both *in vivo* and *in vitro* [Christen et al., 2010; Virtanen et al., 2002]. Excess amount of visceral adipose tissue associates with systemic insulin resistance and metabolic risk factors stronger than abdominal adipose tissue, while femoral subcutaneous adipose tissue can even have a protective role [Fox et al., 2007; Goodpaster et al., 2005; Zhang et al., 2015].

Insulin promotes adipogenesis in adipocytes by providing glucose for the formation of glycerol-3-phosphate (G3P) with which fatty acids esterify into acyl-CoA to be used in glycerolipid synthesis. Insulin also stimulates the activity of lipoprotein lipase (LPL), which acts on endothelium to release fatty acids from circulating triglycerides to be taken up to adipocyte. Furthermore, insulin promotes *de novo* lipogenesis, which proportion of the adipocyte lipid synthesis is however small [M. C. Petersen & Shulman, 2018].

2.4.2.3 Brown adipose tissue

Brown adipose tissue, located mainly in supraclavicular and paravertebral depots in adults, is capable to produce heat because of large number of mitochondria and expression of uncoupling protein -1 (UCP1). Although fatty acids are likely the main substrates for BAT energy utilization, glucose is an important nutrient in BAT. BAT cells express GLUT1 and insulin-responsive GLUT4 transporters, of which GLUT4 are shown to be more abundant in BAT than in WAT [Orava et al., 2011; Ramage et

al., 2016]. Under cold-exposure, BAT GU is up to eightfold higher than that of skeletal muscle accounting for 1% of whole-body glucose disposal [Carpentier et al., 2018]. Insulin can stimulate BAT GU up to fivefold independent of blood flow. It seems that cold induced thermogenesis increases BAT GU by increasing perfusion, while insulin-stimulated GU is not dependent on increased blood flow [Orava et al., 2011].

2.4.2.4 Liver

Insulin action in the liver regulates hepatic glucose and lipid metabolism via direct and indirect mechanisms. During the fasting state, low circulating insulin and high glucagon level increase hepatic EGP. Following glucose ingestion and rise in plasma insulin and decline in glucagon levels, hepatic EGP decreases, GU, glycogen and protein synthesis, and also the synthesis and storage of lipids increases [Norton et al., 2022; M. C. Petersen & Shulman, 2018; Titchenell et al., 2017].

Insulin from the pancreatic β cell is secreted into the portal vein, and liver removes 50% of the insulin secreted into circulation. Inhibition of hepatic EGP by insulin takes place rapidly, and is mediated directly through suppression of glycogenolysis. Suppression of gluconeogenesis is less sensitive to insulin. Indirect effect on insulin on gluconeogenesis is mediated through suppression of WAT lipolysis and a decrease in fatty acid availability for gluconeogenesis. Under normal physiological conditions, the direct inhibition of gluconeogenesis is most prominent and predominate in fed state, whereas the indirect insulin action predominates under fasting [Norton et al., 2022; M. C. Petersen & Shulman, 2018].

Number of inputs, such as arterial-portal vein glucose gradient, fatty acids, amino acids, insulin and neural mediators modulate the uptake of glucose into hepatocytes. Hyperinsulinemia or hyperglycaemia themselves are not sufficient to enhance hepatic GU. However, delivery of glucose to liver via oral-enteral-portal vein route, and elevated insulin concentration increases the hepatic GU [Moore et al., 2012]. Glucose enters to hepatocyte through GLUT2 transporters [Thorens, 2015]. The liver takes up approximately one third of the glucose load after a meal, thus limiting postprandial hyperglycaemia [Moore et al., 2012]. In the hepatocytes, glucose is converted to glucose-6-phosphate (G6P) by glucokinase (GCK), of which transcription insulin increases. G6P, glucose and insulin stimulate glycogen synthase leading to glycogen formation [Radziuk & Pye, 2002].

Insulin action in hepatic lipid metabolism is likewise anabolic. In postprandial state, insulin promotes lipid storage in the hepatocytes by increasing *de novo* lipogenesis, increases the uptake of triglyceride from circulation, suppresses fatty acid oxidation and decreases the export of VLDL. Insulin-stimulated protein synthesis in hepatocytes is mediated via Akt induced activation of mTORC1 activity [Norton et al., 2022; M. C. Petersen & Shulman, 2018].

2.4.3 Brain insulin signalling

2.4.3.1 Insulin transport and receptors

Insulin enters the brain across the BBB via saturable receptor-mediated transport [Banks et al., 2012; King & Johnson, 1985]. Insulin concentration in the cerebrospinal fluid (CSF) is approximately 25% of that in blood, and increases proportionally after ingestion of meal or with peripheral insulin infusion [Woods et al., 2003]. However, if serum level of insulin is high enough to result in hypoglycaemia, the CNS insulin acts in counter-regulatory manner to restrain hypoglycaemia. Several factors and conditions affect the rate of insulin transport, including brain region, hyperglycaemia, triglycerides, starvation, obesity, T2D, inflammatory conditions and neurodegenerative diseases [Banks et al., 2012; Scherer et al., 2021]. Insulin can also enter the brain via rapid, passive extravasation through the median eminence (ME), located directly below the mediobasal hypothalamus and adjacent to ARC. This route allows insulin a straight access to interact with the orexigenic and anorexigenic neurons [Beddows & Dodd, 2021].

IRs, and also IGF-1Rs, are expressed throughout the brain in most cell types. The highest density of IRs is found in the hypothalamus, olfactory bulb, hippocampus, cerebral cortex and cerebellum [Banks et al., 2012; Havrankova et al., 1978; Plum et al., 2005]. The IR density is higher in neurons than in glial cells, of which 20-40% express IRs, and the density decreases with age [Banks et al., 2012; Scherer et al., 2021]. Astrocytes, the most abundant glia cells in the brain and located between vessels and neurons, are involved in nutrient sensing and the central regulation of systemic metabolism. Astrocytic insulin signalling plays a key role in regulating hypothalamic neuronal responses in order to adequately respond to changes in systemic glucose availability. In mice, astrocyte-specific loss of IRs led to impaired neuronal glucose sensing, reduced glucose and insulin levels in CSF and decreased brain GU. The mice lacking astrocytic IRs are unable to increase or decrease feeding in response to glucose deprivation or hyperglycaemia [García-Cáceres et al., 2016]. Insulin binding to its receptor activates the PI3K/Akt signalling pathway, leads to activation of ATP-sensitive potassium (K_{ATP}) channel and modulation of synaptic plasticity, gene expression and neuronal excitability. [Beddows & Dodd, 2021; Plum et al., 2005].

2.4.3.2 The hypothalamic and extrahypothalamic targets of insulin

Hypothalamic NPY/AgRP and POMC/CART neurons in the ARC are the primarily targets of central insulin through which insulin signals in the brain. In postprandial state, IR activation in NPY/AgRP neurons results in decreased transcription of

orexigenic NPY and AgRP. Insulin binding to POMC/CART neurons on the other hand, leads upregulation of anorexigenic α -MSH and activation of melanocortin 4 receptors (MC4R) [Kleinridders et al., 2014; Plum et al., 2005]. The action of insulin in hypothalamic neurons is interconnected with leptin signalling. In addition to ARC, IR signalling in VMH and LH neurons modulates energy balance regulation [Timper & Brüning, 2017]. Hypothalamic IR activation in astrocytes controls glucose and insulin transport from circulation to brain and regulates glucose-induced activation of hypothalamic POMC neurons [García-Cáceres et al., 2016].

IRs are expressed also in the dopaminergic neurons in the reward circuit, where insulin act to decrease the motivation to consume food [Kullmann, Kleinridders, et al., 2020; Timper & Brüning, 2017]. Furthermore, intranasal (IN) administration of insulin improves the functional connectivity in dopaminergic neurons, which has found to associate with decreases in hunger and food desire. Central insulin resistance in turn, associated with increased craving of palatable food [Kullmann, Kleinridders, et al., 2020]. However, nutritional status and diet can modulate the effects of insulin on dopaminergic neurons. Food restriction has been shown to enhance and obesogenic diet decrease the dopamine release [Stouffer et al., 2015]. The effect of insulin in dopaminergic signalling might also be sex-dependent [Kullmann, Kleinridders, et al., 2020].

Insulin action is essential for synaptic plasticity and functional connectivity in the default-mode network (DMN), which participates self-referential processing and evaluation of one's internal mental and physiological state [Kleinridders et al., 2014; Kullmann et al., 2016]. The DMN comprises of precuneus/posterior cingulate cortex, lateral temporal cortex, prefrontal regions and hippocampus [Broyd et al., 2009; Kullmann, Kleinridders, et al., 2020]. The prefrontal regions receive interoceptive and exteroceptive signals stimulus via afferent input from other brain areas such as hypothalamus, striatum and limbic system, and correspond to execution of adequate behaviour. The lateral prefrontal cortex is involved in the inhibitory control of eating, while the orbitofrontal cortex and anterior cingulate cortex participates decision-making according to reward [Kullmann et al., 2016]. Hippocampal processing, important in learning and memory, is also modulated by insulin [Banks et al., 2012; Kleinridders et al., 2014; Kullmann et al., 2016]. Insulin regulates the activity of N-methyl-D-aspartate (NMDA), α -amino-3-hydroxy-5-methyl-4-isoxazolepropionic acid (AMPA) and type A γ -aminobutyric acid (GABA) receptors in the hippocampus [Kleinridders et al., 2014]. In the fusiform gyrus, a brain region nearby hippocampus within the temporal lobe, insulin suppresses the neural activity in response to visual food cues [Kullmann et al., 2016].

2.4.3.3 Brain glucose metabolism and relation to insulin signalling

The brain consumes 100-150 g glucose per day [Cahill et al., 1966] accounting for 20% of the whole-body oxygen consumption at rest [Rolfe & Brown, 1997]. Under normal physiological conditions, glucose is the main energy source for the brain. During prolonged fasting however, ketone bodies, produced by hepatic mitochondria from fatty acids, are the major energy source for brain [White & Venkatesh, 2011] along with lactate [Deitmer et al., 2019; Koepsell, 2020].

Glucose transport into central nervous system (CNS) is facilitated in non-active manner, mainly by saturable, high-affinity GLUT1 transporters in capillaries and brain cells (**Figure 4**). Additionally, GLUT3, GLUT4 and the sodium-glucose cotransporter 1 (SGLT1) in small brain capillaries may participate in local glucose transport across the BBB. The facilitated diffusion of glucose occurs independent of insulin, down the concentration gradient between glucose in blood and the brain interstitium.

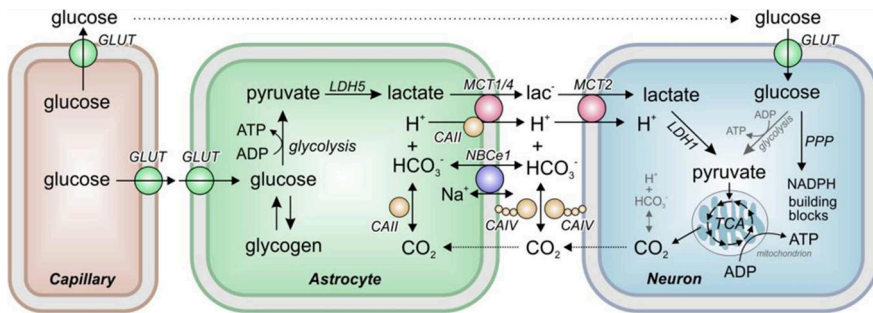


Figure 4 Glucose transport and metabolism in brain and the astrocyte-neuron lactate shuttle. GLUT1 transporters mediate glucose transport across the capillary endothelial cells to central nervous system downstream to glucose concentration gradient. The GU into astrocytes is mediated mainly by GLUT1. Inside the astrocytes, glucose is metabolized to pyruvate in glycolysis and then converted to lactate, or stored as glycogen. The lactate is shuttled from astrocytes to neurons, where it is converted to pyruvate and transferred for citric acid cycle in mitochondria for aerobic energy production. GU into neurons is facilitated mainly by high-affinity GLUT3 transporters, and in hypothalamus also by GLUT2 and insulin-responsive GLUT4 transporters. Inside the neurons glucose is utilized in the production of energy in glycolytic or pentose phosphate pathway (Deitmer et al., 2019; Koepsell, 2020). Reprinted with permission from Deitmer et al. 2019.

GU into neurons is mainly mediated by high-affinity and high-efficacy GLUT3 transporters. However, hypothalamic nuclei participating in the regulation of food intake and energy homeostasis express also low affinity GLUT2 and insulin-responsive GLUT4 transporters. It is proposed that GLUT2 are involved in the regulation of food intake and the central regulation of glucose homeostasis [Koepsell, 2020]. In rodents, reduced GLUT2 expression has been shown to link

with increased food intake and altered expression of orexigenic and anorexigenic neuropeptides [Bady et al., 2006]. In humans, genetic variation of GLUT2 associated with increased daily consumption of sugars [Eny et al., 2008].

The role of hypothalamic GLUT4 transporters in the whole-body energy and glucose homeostasis is essential, and brain GLUT4 and insulin signalling are mutually related [Koepsell, 2020; Ren et al., 2015; Reno et al., 2017]. GLUT4 is often coexpressed with IRs, and insulin, as well as leptin, stimulates GLUT4 translocation to the plasma membrane [Koepsell, 2020]. Neuronal IR knockout mice (NIRKO) have expressed significantly reduced hypothalamic GLUT4 expression, impaired hypothalamic neuronal response to hypoglycaemia, and blunted glucose-responsiveness in specific glucose-sensing neurons, but unaltered brain GU [Diggs-Andrews et al., 2010]. Mice with selective knockout of brain GLUT4 in turn were glucose intolerant, showed impaired suppression of EGP and GU into brain, and impaired response to hypoglycaemia, which was associated with reduced hypothalamic neuronal activation [Reno et al., 2017]. Likewise, mice with selective ablation of hypothalamic GLUT4 neurons also exhibited increased hepatic gluconeogenic gene expression and hepatic lipid content. In addition, the GLUT4 neuron ablated mice showed signs of negative energy balance, including decreased food intake and body weight, and increased energy expenditure [Ren et al., 2015].

In neurons, glucose is metabolized in the glycolytic pathway into pyruvate, which is further metabolized in the citric acid cycle in mitochondria, or is converted in lactate [Deitmer et al., 2019; Koepsell, 2020]. In addition, neurons receive energy in the form of lactate generated and supplied by astrocytes. This astrocyte –neuron lactate shuttle operates in accordance to neuronal activity. Lactate transferred to neurons is converted to pyruvate for aerobic energy production in mitochondria (**Figure 4.**) [Deitmer et al., 2019]. GU into astrocytes is mediated mainly by GLUT1, but also GLUT2, GLUT3 and insulin-responsive GLUT4 transporters. In addition to providing energy for neurons, astrocytes are capable to store glucose as glycogen [Deitmer et al., 2019; Koepsell, 2020].

2.4.4 Physiological effects of brain insulin action

2.4.4.1 Regulation of feeding behaviour

Insulin acts as a satiety signal for brain suppressing appetite for especially palatable foods. The primarily targets of insulin are the hypothalamic anorexigenic and orexigenic neurons, as also dopaminergic neurons in the reward system [Timper & Brüning, 2017; Wilson & Enriori, 2015]. The effect of central insulin action on food intake was first demonstrated in mice [Debons et al., 1970] and baboons [Woods & Porte, 1975] and after that with numerous other species [Kullmann et al., 2016;

Scherer et al., 2021]. In humans, IN insulin administration can be used for studying the central insulin action [Dhuria et al., 2010; Schmid et al., 2018] with only minor uptake into circulation [Born et al., 2002]. IN insulin administration increases the feeling of satiety, decreases food intake [Benedict et al., 2008; Jauch-Chara et al., 2012; Krug et al., 2018] and also body adiposity [Hallschmid et al., 2004], although conflicting findings exist [Krug et al., 2018]. Anorexigenic response to IN insulin might depend on sex, BMI and the nutritional state. In response to IN insulin administration, men has showed greater reductions in weight, adipose tissue and food intake than woman [Benedict et al., 2008; Hallschmid et al., 2004], and subjects with obesity no significant reduction in weight as compared to lean subjects [Hallschmid et al., 2008]. IN insulin administration in postprandial but not in fasted state was followed by decreased appetite and food intake [Hallschmid et al., 2012].

Furthermore, IN administered insulin enhances functional connectivity between brain areas associated with metabolic and cognitive processes, and this effect is paralleled with suppression of appetite and reduction in the amount of VAT [Kullmann, Heni, et al., 2017]. For instance, by controlling memory processes about previously eaten food and satiety signals hippocampus can inhibit subsequent food intake [Coppin, 2016]. Modification of olfaction by insulin may also affect calorie intake. Hyperinsulinemia during euglycemia [Ketterer et al., 2011] as well as intracerebroventricular [Aimé et al., 2012] and IN administration of insulin [Brünner et al., 2013] has been found to decrease olfactory detection, which associated with decreased food craving in rats [Aimé et al., 2012].

In addition, cerebral insulin may suppress appetite and food intake by increasing cerebral energy content as observed as increased levels of high-energy phosphate compounds assessed with magnetic resonance spectroscopy (MRS) after IN insulin administration [Jauch-Chara et al., 2012]. Likewise, insulin-stimulated changes in cerebral metabolites in frontal and temporal brain regions were observed with MRS, and this correlated with high whole-body insulin sensitivity. It is thus possible that low whole-body insulin sensitivity might associate with impaired neuronal metabolism [Karczewska-Kupczewska et al., 2013].

2.4.4.2 Regulation of energy expenditure and thermogenesis

The brain controls energy metabolism via adjusting basal metabolic rate, physical activity and adaptive thermogenesis [Spiegelman & Flier, 2001]. Thermogenesis occurs mainly via BAT, and also in beige adipocytes located within WAT depots, and is under central regulation and dependent on sympathetic outflow. Hypothalamus receives thermal signals from periphery and activates signalling pathway to induce BAT thermogenesis [Roh et al., 2016]. In addition, hormones and nutrients such as insulin, leptin and glucose have an influence on BAT activity

[Cannon & Nedergaard, 2004]. Data on brain insulin action on thermogenesis are mainly based on murine models. Intracerebral administration of insulin induces BAT activation [Bamshad et al., 1999; Müller et al., 1997], which was demonstrated also as increased BAT GU with positron emission tomography (PET) imaging [Sanchez-Alavez et al., 2010]. Mice lacking brain IRs in turn, displayed a decrease in body temperature under cold exposure indicating a failure in thermogenesis [Kleinridders et al., 2014]. Central administration of MC4R and melanocortin 3-receptor (MC3R) agonist had a stimulatory effect on BAT thermogenesis via enhanced sympathetic outflow, indicating the role of central melanocortin receptors in BAT thermogenesis [Brito et al., 2007]. In humans, IN insulin administration increased energy expenditure at postprandial state as measured with indirect calorimetry [Benedict et al., 2011].

2.4.4.3 White adipose tissue lipolysis and lipogenesis

In addition to direct effects, insulin controls WAT metabolism indirectly through brain insulin signalling [Scherer et al., 2021]. Insulin infused to mediobasal hypothalamus suppressed lipolysis and increased the expression of lipogenic proteins. The suppression of lipolysis is mediated via suppression of sympathetic outflow independent of peripheral insulin signalling. Also, increased lipolysis and decreased *de novo* lipogenesis have been demonstrated with mice lacking neuronal IRs [Scherer et al., 2011]. Similarly, mice with IR inactivation in all tissues, including the brain, exhibited greater loss of WAT mass and hypoleptinemia due to uncontrolled lipolysis as compared to mice with IR inactivation only in peripheral tissues demonstrating the essential role of brain insulin action in regulating adipose tissue metabolism [Koch et al., 2008]. The sympathetic nervous outflow to WAT has been shown to colocalize with MC4Rs [Song et al., 2005] and being associated with the control of WAT lipolysis [Brito et al., 2007]. Mice lacking IRs in POMC neurons, show impaired suppression on WAT lipolysis indicating an impaired indirect insulin action in WAT. The hepatic EGP however was not reduced in these mice. Deletion of IRs in AgRP neurons did not alter the rate of WAT lipolysis, but impaired the suppression of hepatic EGP [Shin et al., 2017]. Central administration of insulin stimulated fatty acid uptake into WAT under conditions of hyperinsulinemic-euglycemic clamp by activation of central K_{ATP} channels, independent of activation of insulin or leptin signalling pathways in WAT [Coomans, Geerling, et al., 2011]. In humans, IN insulin administration suppressed circulating FFA levels and the rate of appearance of deuterated glycerol, indicating suppression of lipolysis, without changes in lipolytic protein expression or changes in plasma insulin levels [Iwen et al., 2014].

2.4.4.4 Regulation of hepatic glucose and lipid metabolism

Hypothalamic insulin signalling modulates the hepatic EGP in addition to the direct insulin effect (**Figure 5**). In rodents, administration of insulin into the third cerebral ventricle suppresses hepatic EGP independent of circulating insulin or other glucoregulatory hormone levels. Also, blocking the binding of insulin to central IRs leads to impaired ability of circulating insulin to suppress EGP [Obici, Feng, et al., 2002; Obici, Zhang, et al., 2002]. While the insulin signalling cascade involves activation of K_{ATP} channel, inhibition of the channels by central infusion of sulfonylurea prevents the physiological suppression of EGP during an insulin clamp [Obici, Zhang, et al., 2002; Pocai et al., 2005].

Similarly, activation of hypothalamic K_{ATP} channels results in decreased hepatic EGP, with reduced expression of hepatic gluconeogenic enzymes [Pocai et al., 2005]. AgRP neurons in the hypothalamus and the dorsal vagal complex are recognized as an essential site of central insulin signalling regulating the hepatic EGP [Filippi et al., 2012; Könner et al., 2007]. In addition, resection of the efferent, but not afferent, hepatic branch of vagus nerve fibres abolished the effect of centrally administered insulin on hepatic EGP suggesting that efferent vagal input from brain to liver is required for the proper action of brain-liver-axis [Pocai et al., 2005]. Central insulin signalling suppresses the hepatic efferents resulting in an increase in hepatic interleukin 6 (IL-6) secretion leading to subsequent activation of transcription factor 3 (STAT3) in hepatocytes and reductions in gluconeogenic enzyme expression [Könner et al., 2007]. Indirect effect of central insulin signalling on hepatic EGP is mediated via suppression of adipose tissue lipolysis and reduced FFA and glycerol fluxes to liver [Koch et al., 2008], and possibly reduced pancreatic glucagon secretion [Paranjape et al., 2010].

Somatostatin clamp studies in dogs with insulin infused either via portal or peripheral vein and administering insulin centrally, has demonstrated the direct effect of insulin to suppress EGP to overcome that of central insulin. This finding was verified when controlling the indirect insulin effect to suppress lipolysis and glucagon secretion. Central hyperinsulinemia was shown to activate hypothalamic Akt and hepatic STAT3 accompanied by reduced gluconeogenic enzyme expression, while central administration of PI3K inhibitor reversed these actions [Ramnanan et al., 2011].

In humans, under euglycemic clamp with somatostatin, administration of IN insulin demonstrated late suppression of EGP, occurring between 180-360 min after insulin administration [Dash et al., 2015], as shown also with oral diazoxide [Esterson et al., 2016; Kishore et al., 2011]. However, earlier, 100–120 min, decreases in EGP have been reported as well [Heni et al., 2017]. Increases in the rate of glucose infusion rate 15 min after IN insulin administration (in order to maintain euglycemia during hyperinsulinemic-euglycemic clamp) as well as improvement in

the insulin sensitivity has been demonstrated [Heni, Wagner, et al., 2014]. Liver transplantation enables the study of hepatic denervation in humans. No significant difference in the glucoregulatory indices was observed between the liver transplant and control group [Schneiter et al., 2000]. It is thus assumed, that the effect of central insulin on hepatic EGP is limited, and only potentiates the action of systemic insulin [Scherer et al., 2021].

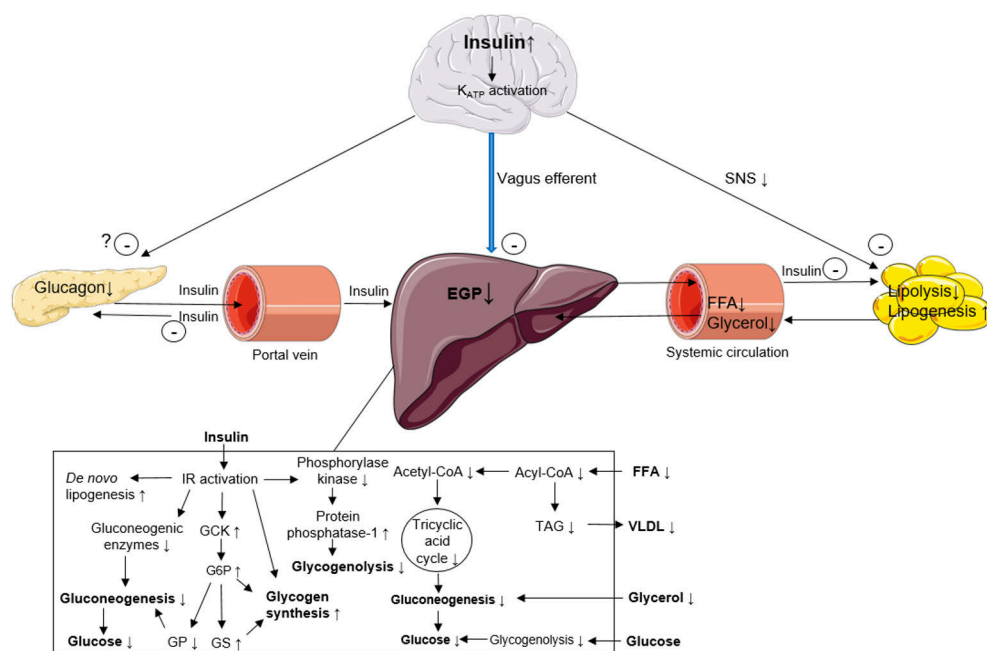


Figure 5 Direct hepatic and extrahepatic insulin suppression of hepatic endogenous glucose production (EGP). In the liver, insulin suppresses glycogenolysis and gluconeogenesis and enhance glycogen synthesis. Acute activation of hepatic IRs stimulate glycogen synthesis, whereas chronic results in downregulation of gluconeogenic enzymes, upregulation of glucokinase (GCK), and an increase in glucose-6-phosphate (G6P) and glycogen synthase (GS) levels leading to glycogen formation. G6P inhibits glycogen phosphorylase (GP) decreasing thus glucose production. Inhibition of phosphorylase kinase and activation of protein phosphatase by insulin results in suppression of glycogenolysis. Peripheral and central insulin act via decreased sympathetic nervous system (SNS) outflow to suppress WAT lipolysis and stimulate lipogenesis resulting in decreased free fatty acid (FFA) and glycerol flux to liver. Reduced FFA flux to liver inhibits intrahepatic triacylglycerol (TAG) accumulation and very-low-density lipoprotein (VLDL) secretion. Peripheral and potentially central insulin suppress pancreatic glucagon secretion, and central insulin action may suppress pancreatic insulin secretion. Activation of ATP-sensitive potassium (KATP) channels mediate central insulin action via vagal efferents to liver. Modified from Lewis et al., 2021. Based on Petersen & Shulman, 2018; Roden & Shulman, 2019 and Lewis et al., 2021. Illustrated partly using Servier Medical Art; <https://smart.servier.com/>, provided by Servier, licensed under a Creative Commons Attribution 3.0 Unported license.

Controversy exists about the effect of central insulin on adipose tissue lipolysis in humans. Suppression of lipolysis assessed by circulating FFA levels and the rate of appearance of deuterated glycerol in fasting state after IN insulin have been reported [Iwen et al., 2014] as well as transient decrease in FFA levels in postprandial state [Benedict et al., 2011]. With diazoxide during euglycemic clamp with somatostatin no changes in FFA levels were found [Esterson et al., 2016; Kishore et al., 2011]. Decreased FFA flux into the liver as a result of suppressed lipolysis and increased lipogenesis by insulin leads to decrease in hepatic triacylglycerol (TAG) content and VLDL secretion [Scherer et al., 2011]. Central insulin signalling in contrast results in enhanced hepatic VLDL secretion thus decreasing hepatic lipid content as demonstrated in rats with intracerebroventricular [Scherer et al., 2016], and in humans with IN administration of insulin [Gancheva et al., 2015]. Also, mice lacking central IRs showed decreased hepatic lipid secretion, whereas mice with peripheral loss of IRs exhibited increased hepatic lipid export [Scherer et al., 2016]. It is suggested that the opposing effect of central insulin balances the direct insulin action on liver [Scherer et al., 2021].

2.4.4.5 Brain insulin action and peripheral insulin sensitivity

Evidence points towards that brain insulin action modulates peripheral insulin sensitivity, although controversies exists. In mice, central administration of K_{ATP} channel inhibitor reduced the insulin-stimulated GU of muscle, but not heart or WAT, and reduced the inhibitory effect of insulin on hepatic EGP [Coomans, Biermasz, et al., 2011]. Central delivery of a MC4R agonist enhanced the insulin action measured as increased GU and glucose infusion rate and inhibition of EGP, while the receptor antagonist had opposing effects [Obici et al., 2001]. However, a study with centrally administered insulin antagonists, insulin or insulin agonist did not show a change in the glucose disposal, although suppression of EGP was either impaired or increased [Obici, Zhang, et al., 2002]. Also, intracerebroventricular insulin infusion [Filippi et al., 2012] and central K_{ATP} channel activation [Pocai et al., 2005] increased the glucose infusion rate needed to maintain euglycemia, which was due to suppression of EGP instead of increased GU. The different results regarding the GU has been by some authors explained by the use of differing insulin levels or duration of fast before the clamp study [Parlevliet et al., 2014].

In humans, IN insulin administration improved systemic insulin sensitivity as estimated by the homeostatic model assessment for insulin resistance (HOMA-IR), and this correlated with an increase in hypothalamic activity measured with functional magnetic resonance imaging (MRI) [Heni et al., 2012]. Improvement in whole-body insulin sensitivity after IN insulin was found also during a hyperinsulinemic-euglycemic clamp, detected as higher glucose infusion rate to

maintain euglycemia and higher insulin sensitivity index. Also these findings correlated with the change in hypothalamic activity in functional MRI [Heni, Wagner, et al., 2014].

CNS modulates pancreatic insulin, and also glucagon secretion via autonomic output according to circulating and brain interstitial fluid glucose concentration [Faber et al., 2020]. Early studies with dogs have found evidence of the central insulin action in the control on pancreatic insulin secretion, while insulin delivery into CSF was followed by an increase in peripheral insulin secretion [Chen et al., 1975]. Later studies have not found this effect consistently [Scherer et al., 2011, 2016]. In mice, maternal HFD feeding during lactation led to impaired formation of hypothalamic POMC and AgRP projections and parasympathetic innervation of pancreas in offspring, which in turn was associated with obesity and insulin resistance. POMC-specific IR inactivation in offspring prevented the impaired axonal projections and the subsequent metabolic disturbances, demonstrating the contributing effect of defective hypothalamic insulin signalling induced by maternal HFD during lactation [Vogt et al., 2014].

When hypothalamic insulin sensitivity in humans was determined as decreased hypothalamic blood flow after IN insulin delivery, the hypothalamic insulin sensitivity was found to associate with decreased pancreatic insulin secretion [Kullmann, Fritsche, et al., 2017]. [¹⁸F]FDG PET study showed a positive correlation with BGU and basal insulin secretion rate and total insulin output in non-diabetic subjects but not in subjects with T2D. Potentiation of insulin secretion associated positively with BGU in non-diabetic, but negatively in subjects with T2D. The results points towards the brain's contribution of insulin secretion independently of insulin sensitivity [Rebelos et al., 2020]. According to neuronal mapping, the glucose sensing neurons of ARC that express GCK enzyme appears to be essential for pancreatic insulin secretion. Inhibition of these neurons resulted in impaired insulin secretion and glucose intolerance [Rosario et al., 2016]. Also MC4Rs that bind α -MSH derived from POMC neurons seem to have a role in regulating insulin level. Deletion of these receptors in the dorsal vagal complex, a brainstem region integrating afferent and efferent signals, has found to result in hyperinsulinemia and insulin resistance independently of changes in weight and glucose homeostasis [Berglund et al., 2014]. In addition, perturbation of hypothalamic GLUT4 expressing neurons has found to associate with hyperglycaemia and decreased insulin secretion [Ren et al., 2015]. The brain modulates the counterregulatory responses to hypoglycaemia [Bolli & Fanelli, 1999]. Based on studies with mice, it is suggested that hypothalamic insulin signalling might modulate glucagon secretion from the pancreatic α -cells under fasting and hypoglycaemia [Paranjape et al., 2010].

2.5 Obesity and insulin resistance

2.5.1 Mechanisms of obesity-induced insulin resistance

Insulin resistance is defined as inability of target tissues to adequately respond to insulin effect [M. C. Petersen & Shulman, 2018]. Obesity-related insulin resistance contributes to both defect in IRs and insulin signal transduction. The pathophysiology of systemic insulin resistance is chronic overnutrition, which promotes ectopic lipid accumulation in skeletal muscle and liver, and adipose tissue hypertrophy and hyperplasia resulting in tissue-specific and systemic insulin resistance [M. C. Petersen & Shulman, 2018]

Skeletal muscle insulin resistance is considered to precede the hepatic and adipose tissue insulin resistance and pancreatic β -cell failure [DeFronzo & Tripathy, 2009; K. F. Petersen et al., 2007]. Because of the large proportion of postprandial glucose disposal, skeletal muscle insulin resistance has a marked significance in whole-body glucose turnover. The defect in insulin signalling cascade in myocyte has been located at the proximal level as decreased IRs and PI3K/Akt binding, GLUT4 translocation and glycogen synthesis [M. C. Petersen & Shulman, 2018]. Instead of glycogen synthesis in skeletal muscle, the ingested carbohydrates are converted to hepatic *de novo* lipogenesis resulting in increased VLDL secretion and plasma triglyceride level, and reduced plasma high-density lipoproteins [K. F. Petersen et al., 2007]. Elevated FFA and triglyceride content in myocytes favours lipid synthesis and further impairs the insulin signal transduction events and insulin-stimulated GU resulting in lipid-induced insulin resistance. Suggested mediators of lipid-induced insulin signalling impairment include fatty acid metabolite diacylglycerol (DAG), fatty acyl-coenzyme A (fatty acyl-CoA), ceramides, and incomplete mitochondrial fatty acid oxidation that produces reactive oxygen species and acylcarnitine [Kahn et al., 2006; M. C. Petersen & Shulman, 2018; Roden & Shulman, 2019].

WAT insulin resistance is associated with decreased adipocyte IR content, signalling cascade activity and decreased GU. WAT expansion due to chronic nutrient oversupply is accompanied with homeostatic stress, increased adipocyte death, macrophage recruitment and increased production of molecules including hormones and inflammatory cytokines that promote low-grade inflammation. WAT dysfunction plays a central role in the development of systemic insulin resistance. Impaired suppression of lipolysis and decreased lipogenesis stimulate increased glycerol and FFA flux to other tissues. These changes favour ectopic lipid accumulation and impairment of insulin signalling [Kahn et al., 2006; M. C. Petersen & Shulman, 2018; Roden & Shulman, 2019]. Abnormal WAT mitochondrial function associates with decreased whole-body insulin sensitivity via decreased

secretion of bioactive factors and increased production of lactate. VAT, as compared to SAT expresses higher lipolytic activity and lower rate of lipogenesis. Thus the liver is via portal delivery exposed to larger amounts of lipid metabolites than the peripheral tissues [Bódis & Roden, 2018].

Increased glycerol and FFA flux to liver stimulates hepatic gluconeogenesis, triglyceride and TAG accumulation, and formation of lipotoxic metabolites and proinflammatory mediators that inhibit insulin signalling. If continuing, these changes are associated with non-alcoholic fatty liver disease (NAFLD). Suppression of insulin-stimulated GU and glycogen synthesis results in rise in plasma glucose level. In addition, overnutrition induced ER stress stimulates hepatic *de novo* lipogenesis impairing hepatic insulin signalling. Increased lactate flux from WAT further enhances liver insulin resistance by inducing hepatic gluconeogenesis [M. C. Petersen & Shulman, 2018; Roden & Shulman, 2019].

Tissue-specific changes in insulin resistance results in postprandial and fasting hyperglycaemia followed by compensatory rise in β -cell insulin secretion and β -cell mass. Insulin secretion can increase up to fivefold to that of insulin sensitive subjects', while the β -cell mass is increased about 50% in subjects with obesity related insulin resistance. The resultant hyperinsulinemia induces downregulation of the number of IRs and the intracellular insulin signalling promoting insulin resistance. Chronic hyperglycaemia and elevated FFA levels impair the adaptive response of β -cells that results in a decline in insulin synthesis, secretion and defective intracellular insulin signalling, and ultimately the development of T2D [Kahn et al., 2006; Roden & Shulman, 2019].

2.5.2 Tissue-specific changes in insulin resistance

Insulin resistance results in tissue-specific manifestations that further modulate tissue communication. In skeletal muscle, insulin resistance is manifested as impaired insulin-stimulated GU and glycogen synthesis, increased FFA uptake derived from WAT lipolysis, and accumulation of ectopic fat. Increased skeletal muscle FFA availability impairs mitochondrial function and enhances lipotoxic signalling. In WAT, insufficient suppression of lipolysis and impaired lipogenesis with subsequent release of FFAs and glycerol, and decreased insulin-stimulated GU and low-grade inflammation takes place. Hepatic glycolysis and gluconeogenesis are enhanced, and net glycogen synthesis and GU decreased under insulin resistant conditions. Skeletal muscle insulin resistance increases glucose delivery to the liver. This, in association with hyperinsulinemia and increased FFA and glycerol flux from the unsuppressed lipolysis in WAT, promotes triglyceride and hepatic ectopic fat formation, lipotoxic signalling and impaired control of glycogen synthesis and gluconeogenesis. Upregulated *de novo* lipogenesis leads to increased VLDL

production. Obesity and HFD feeding that associates with systemic insulin resistance, leads to BAT dysfunction. This BAT “whitening” is characterized by diminished vascularity, loss of mitochondrial function and number, lipid droplet accumulation, impaired thermogenic response and decreased BAT GU (Shimizu et al., 2014). As a consequence of these dysregulated processes, insulin secretion compensatory increases restoring normoglycaemia. With persistent stimulus, and acquired and inherited factors, failure of β -cell insulin secretion and progression to T2D may occur [Roden & Shulman, 2019; Samuel & Shulman, 2016].

2.5.3 Brain insulin resistance

Mechanisms of brain insulin resistance are not fully understood. According to a theory, brain insulin resistance is a physiological adaptation to maintain systemic euglycaemia under conditions with scarce availability of nutrients and warmth; increased WAT lipolysis and hepatic EGP met the increased substrate utilization ensuring the survival. In the modern world with abundant food supply and sedentary lifestyle in turn, the brain insulin resistance is thought to serve as disadvantage response contributing in systemic insulin resistance [Scherer et al., 2021].

Accumulating evidence points to diet-induced inflammation of hypothalamus as a contributing mechanism for brain insulin resistance. This in turn leads to defective interaction with the periphery promoting dysregulation of energy homeostasis and obesity [Jais & Brüning, 2017; Kullmann et al., 2016; Seong et al., 2019]. The most examined nutrients in the pathogenesis of hypothalamic inflammation are lipids, especially long-chain saturated fatty acids (SFA). These lipid species cross the BBB and accumulate in the hypothalamus resulting in activation of inflammatory pathways and inhibition of insulin, and also leptin signalling [Jais & Brüning, 2017; Seong et al., 2019]. In rodent models, high-fat diet (HFD) feeding induces hypothalamic inflammation characterized by increased expression of proinflammatory cytokines and inflammatory response, and impaired anorexigenic insulin signalling [De Souza et al., 2005].

In rodent models, the onset of central inflammatory process is rapid. Hypothalamic inflammatory signalling is evident only after few days of HFD consuming before the onset of peripheral inflammation or substantial changes in weight [Thaler et al., 2012; Waise et al., 2015]. The effect of HFD on markers of inflammation resolves within the first few weeks suggesting a neuroprotective response. However, with prolonged HFD feeding, the hypothalamic inflammatory response and neuronal injury reappears [Thaler et al., 2012]. Accordingly, post-mortem brain tissue analysis in humans has revealed hypothalamic inflammatory changes in subjects with obesity, with the degree of changes correlating with BMI [Baufeld et al., 2016].

Various cell types are involved in the HFD-induced hypothalamic inflammation. Reactive gliosis, the recruitment, proliferation and morphological changes of astrocytes and microglia in response to injury, and subsequent impairment in the function of NPY/AgRP and POMC/CART neurons are the key events in hypothalamic inflammation. In addition, impaired BBB function in response to HFD contributes to the development of hypothalamic inflammation. Activated microglia accumulated in the hypothalamus produce proinflammatory cytokines such as TNF- α , IL-1 β and IL-6 [De Souza et al., 2005; Jais & Brüning, 2017]. Similarly, astrocytes gathered in the hypothalamus in response to HFD feeding produce inflammatory factors. The underlying molecular mechanisms recognized involve the Toll-like receptor 4 (TLR4), ceramide and protein kinase C (PKC), and ER stress pathways (**Figure 6**). The subsequent insulin resistance leads to defective activation of anorexigenic signals and suppression of orexigenic signals promoting increased food intake and positive energy balance.

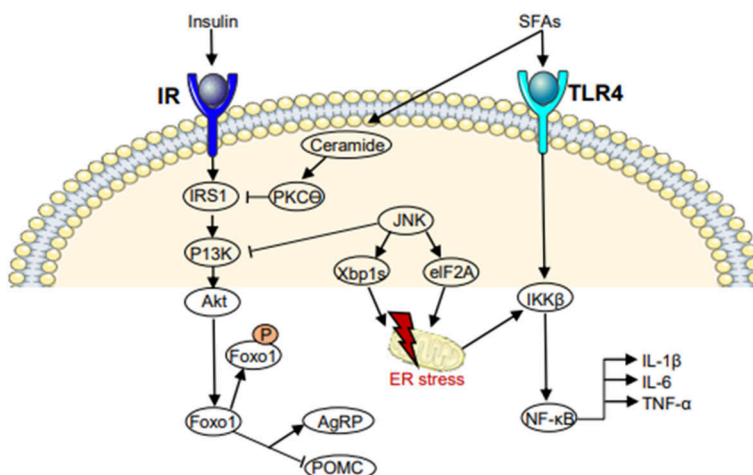


Figure 6 Molecular mechanisms inducing hypothalamic inflammation and insulin resistance. Insulin binding to insulin receptor (IR) activates PI3K/Akt signalling pathway leading to Foxo1 phosphorylation and increased anorexigenic tone via induced POMC and suppressed orexigenic NPY/AgRP gene expression. Binding of saturated fatty acids (SFA) to Toll-like receptor 4 (TLR4) activates inhibitor of kappa B kinase beta (IKK β) complex and nuclear factor kappa (NF- κ B) leading to expression of proinflammatory cytokines. TLR4 activation induces also activation of c-Jun N-terminal kinase (JNK) that inhibits insulin signalling and induces endoplasmic reticulum (ER) stress. ER stress in turn activates the IKK β and NF- κ B promoting inflammation. Induction of ceramides by palmitic acid leads to translocation of protein kinase C θ (PKC θ) to the plasma membrane of NPY/AgRP neurons, resulting in inhibition of insulin receptor substrate 1 (IRS1) and insulin signalling cascade. Based on Seong et al., 2019. Illustrated partly using Servier Medical Art; <https://smart.servier.com/>, provided by Servier, licensed under a Creative Commons Attribution 3.0 Unported license.

Other cell types involved in the neuroinflammation are pericytes, tanycytes and monocytes. Chronic HFD feeding leads to loss of hypothalamic neurons, and reductions in synaptic inputs, activity and plasticity. In addition to hypothalamus, hippocampus, various cortical regions, brainstem and amygdala have been shown to be affected by the obesity-related inflammation. In addition to HFD, the neuroinflammation in these structures is induced by a western diet rich both in fat and carbohydrates, and high intake of sucrose [Dorfman & Thaler, 2015; Guillemot-Legris & Muccioli, 2017; Jais & Brüning, 2017; Seong et al., 2019].

2.5.4 Assessing brain changes associated with obesity with neuroimaging

Neuroimaging studies have demonstrated hypothalamic inflammation also in humans with obesity. Increased gliosis was observed in the mediobasal hypothalamus in subjects with obesity as compared to normal-weight subjects in MRI analysis, and the degree of gliosis did not correlate with age or gender [Thaler et al., 2012]. Also, obesity-related low-grade systemic inflammation associated with reduced integrity of brain structures involved in feeding behaviour, and also with reduced volume of brain regions involved in reward system [Cazettes et al., 2011]. A study using diffusion tensor imaging (DTI), a MRI-based technique that provides information about brain microstructural injury, revealed a positive correlation between BMI, body fat mass, systemic insulin resistance, impaired cognitive performance and the degree of hypothalamic injury [Puig et al., 2015]. Similarly, decreased white matter integrity, which was interpreted to represent axonal loss and measured with DTI, associated with obesity-related systemic inflammation and impaired working memory [Repple et al., 2018]. Furthermore, metabolic syndrome and insulin resistance has found to associated with reduced cortical grey matter volume and thickness assessed with MRI, and the effect was due to insulin resistance per se [Lu et al., 2021]. In numerous studies obesity has found to be linked with lower grey matter volume and cortical thickness [Kullmann et al., 2016].

Further evidence on the relationship of obesity and central insulin resistance in humans has accumulated with magnetoencephalography (MEG), functional MRI (fMRI) and PET studies. MEG showed an increase in spontaneous and stimulated cerebrocortical activity during hyperinsulinemic-euglycemic clamp in lean subjects but not with subjects with obesity, and the increase in the cortical activity correlated negatively with BMI and percent body fat [Tschrirter et al., 2006]. Also, insulin-mediated cortical activity correlated negatively with VAT mass, intrahepatic lipid content and serum SFA concentrations suggesting a link between circulating SFA and defective insulin action in the brain [Tschrirter et al., 2009]. Data from fMRI

studies have revealed obesity-related changes in brain responses to food stimulus in brain areas related to food processing and reward. After food exposure, subjects with obesity showed greater brain responses than lean subjects, even when satiated [Connolly et al., 2013; Filbey et al., 2012; Heni, Kullmann, et al., 2014].

Finally, PET studies investigating brain insulin signalling have revealed increased insulin-stimulated BGU in humans and animal with obesity as compared to lean subjects [Bahri et al., 2018; Tuulari et al., 2013], and attenuation in BGU after bariatric surgery induced weight loss coupled with enhanced peripheral insulin sensitivity [Tuulari et al., 2013]. Also, subjects with impaired glucose tolerance showed increased BGU under insulin stimulation when compared to healthy subjects [Boersma et al., 2018; J. W. Eriksson et al., 2021; Hirvonen et al., 2011; Latva-Rasku et al., 2018]. Similarly, a large scale cohort analysis showed a negative correlation between the insulin-stimulated BGU and whole-body insulin sensitivity [Rebelos et al., 2021].

2.5.4.1 Brain insulin resistance and dysregulation of peripheral tissues

Brain insulin resistance has been found to associate with metabolic alterations in peripheral tissues, feeding behaviour and also in cognitive functions (**Figure 7**). Although it is unknown whether the brain insulin resistance is a cause or the consequence of these changes, it acknowledged that the brain participates in the interorgan communication regulating systemic insulin sensitivity and energy homeostasis [Kullmann, Kleinridders, et al., 2020; Scherer et al., 2021].

Overnutrition and excess dietary fat correlate with hypothalamic inflammation and resistance to circulating anorexic signals. The subsequent insulin, as well as leptin resistance results in disrupted neuronal interplay with impaired activation of POMC/CART and suppression of NPY/AgRP neurons and decreased MC4R signalling. This further promotes appetite and food intake, and decreases energy expenditure via reduced secretion of thermogenic hormones such as thyrotropin-(TRH) and corticotrophin-releasing hormone (CRH) and increased secretion of anti-thermogenic melanin-concentrating hormone (MCH) [Jais & Brüning, 2017; Seong et al., 2019]. The following positive energy balance leads to weight gain maintaining the cycle. Evidence of the association of impaired brain insulin signalling and reduced BAT metabolism has gained from studies with mice and humans [Benedict et al., 2011; Sanchez-Alavez et al., 2010]. Also, BAT activity is blunted in subjects with obesity as compared to lean subjects. This has been demonstrated as lower BAT GU rate under cold and insulin stimulation with [^{18}F]FDG PET, with the BAT GU correlating positively with whole-body insulin sensitivity [Orava et al., 2013].

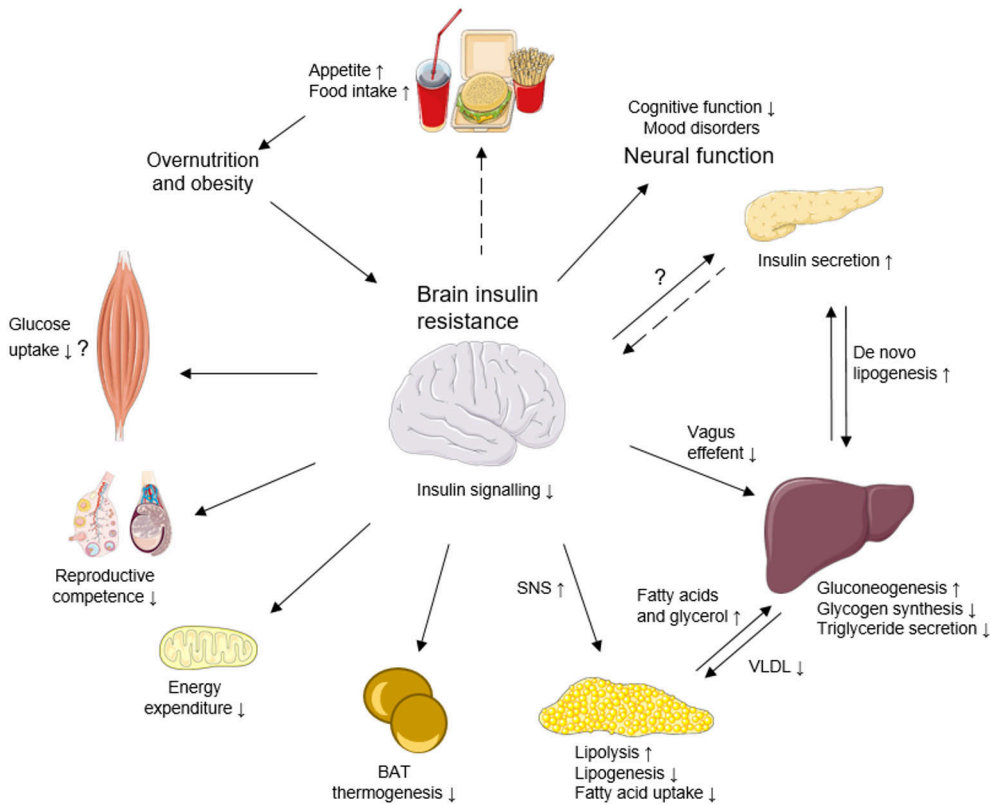


Figure 7 Brain insulin resistance and its metabolic and neural impacts. Chronic overnutrition and obesity induce brain insulin resistance leading to impaired metabolic functions in peripheral tissues, increased food intake, and a decline in cognitive functions and mood disorders. Dashed lines indicate impaired insulin effect. BAT, brown adipose tissue; SNS, sympathetic nervous system; VLDL, very-low-density lipoprotein. Based on Kullmann et al., 2016, Heni et al., 2017 and Scherer et al., 2021. Illustrated partly using Servier Medical Art; <https://smart.servier.com/>, provided by Servier, licensed under a Creative Commons Attribution 3.0 Unported license.

Brain insulin action inhibits lipolysis and promotes lipogenesis in WAT, and during brain insulin resistance, these effects are impaired, via increased sympathetic outflow to WAT. The resultant increase in FFA and glycerol flux to liver provide substrate for hepatic gluconeogenesis [Scherer et al., 2011]. Central insulin resistance results in impaired hepatic vagal nerve suppression of hepatic EGP by decreasing gluconeogenic enzyme expression and stimulating glycogen synthesis [Lewis et al., 2021]. The decreased central insulin action and simultaneous peripheral hyperinsulinemia promotes hepatic *de novo* lipogenesis, and reduces hepatic triglyceride and VLDL secretion [Scherer et al., 2016].

The relationship and potential causality between brain and skeletal muscle insulin resistance is more controversial. In a study with juvenile obese, Western diet

fed pigs, signs of impaired insulin signalling and action were detected in brain and WAT, but not in skeletal muscle, suggesting that impairments in the brain and WAT insulin signalling may precede that in skeletal muscle, or the brain might be more vulnerable to metabolic perturbations [Olver et al., 2018].

In addition, impaired brain insulin signalling has been found to associate with premature cognitive decline, Alzheimer's disease and related dementias and behavioural disorders [Kullmann et al., 2016]. Murine models have demonstrated hypogonadotropic hypogonadism and reduced fertility due to hypothalamic-pituitary-gonadotropin axis dysfunction as a result of impaired central insulin signalling [Brüning et al., 2000; Manaserh et al., 2019].

2.6 Endocannabinoid system

2.6.1 Cannabinoid receptors and their ligands

The ECS modulates appetite, food intake and energy balance, in addition to other physiological and cognitive processes [Silvestri & Di Marzo, 2013]. The ECS consists of two G-protein-coupled receptors, cannabinoid type 1 and type 2 (CB1R and CB2R, respectively), their endogenous ligands and ligand-metabolizing enzymes [Di Marzo et al., 2009]. CB1Rs are widely expressed in the CNS, including the neurons involved in the energy balance regulation. In peripheral tissues, CB1Rs are abundant in tissues controlling energy homeostasis, such as gastrointestinal tract, adipose tissue, liver, skeletal muscle, and endocrine pancreas [Silvestri & Di Marzo, 2013]. CB2Rs in turn are mostly located in immune cells, where they modulate cytokine release [Pertwee, 2006]. Although CB1Rs are considered to be the primary cannabinoid receptors responsible for metabolic regulation, CB2Rs might have a role in the energy homeostasis control [Silvestri & Di Marzo, 2013].

The most studied endogenous ligands, endocannabinoids (EC) are anandamide (AEA) and 2-arachidonoylglycerol (2-AG). All ECs are derivatives from the cell membrane long chain polyunsaturated fatty acid (PUFA) arachidonic acid. ECs are produced after cell stimulation "on demand" and released to their target cannabinoid receptor [Silvestri & Di Marzo, 2013]. Intracellular EC degradation is facilitated mainly by fatty acid amide hydrolase (FAAH) and monoacylglycerol lipase (MAGL) [Muccioli, 2010]. The precursors of the EC metabolizing enzymes derive from phospholipids, whose levels are influenced by dietary omega-3 and omega-6 PUFAs, especially arachidonic acid and docosahexaenoic acid (DHA) [Di Marzo, 2008a].

After released from the cell, ECs bind to cannabinoid receptors, and are then rapidly taken into the cell resulting in an activation of signal transduction pathway, and followed by intracellular degradation. The outcome is a modulation of

neurotransmitter release within the nervous system and multiple biological actions in peripheral tissues [Silvestri & Di Marzo, 2013].

2.6.2 Central endocannabinoid system and the regulation of energy balance

In the CNS, ECS stimulates appetite and food consumption by modulating both homeostatic and hedonic pathways. CB1Rs are widely expressed in the olfactory bulb, several cortical regions and basal ganglia, thalamic and hypothalamic nuclei, cerebellar cortex, and brainstem nuclei [Pagotto et al., 2006]. A brainstem structure outside the BBB, area postrema (AP), might be an important structure for EC signalling as well [Quarta et al., 2011]. The hypothalamic CB1Rs have been found to colocalize with neuropeptides that modulate food intake. ECs are released from the depolarized post-synaptic neuron to activate the presynaptic CB1Rs resulting in either increased stimulation of orexigenic or inhibition of anorexigenic neurons. Leptin controls negatively central ECS tone [Gatta-Cherifi & Cota, 2016], while hypothalamic insulin seems to have no effect on hypothalamic EC levels [Matias, Vergoni, et al., 2008].

Although the main effect of EC signalling in the brain is orexigenic, CB1Rs in the forebrain GABAergic neurons mediate hypophagic actions via reduced inhibitory transmission. It is proposed, that the opposing effects of the ECS in different brain structures reflects the fine-tuned control of neuronal network for the regulation of feeding behaviour [Bellocchio et al., 2010]. As the CB1R signalling may vary upon the specific brain region and presence of hormones such as leptin, ghrelin and glucocorticoids, it may depend on diet consumed as well. Accordingly, mice lacking hypothalamic VMH CB1Rs were hypophagic when exposed to food after prolonged fast, but hyperphagic when exposed to HFD [Cardinal et al., 2014].

The homeostatic pathways in the hypothalamus interact with the reward system. Activation of CB1Rs in the mesolimbic system, nucleus accumbens and ventral tegmentum area affects the hedonistic aspects of feeding by promoting the motivation to consume highly palatable food, especially high caloric food rich in fat and sugar [Tarragon & Moreno, 2017]. This takes place in interaction with the dopaminergic and opiodergic pathways [Silvestri & Di Marzo, 2013]. In addition, activation of CB1Rs in the afferent and efferent brainstem neurons are thought to modulate the vagal output to periphery and thus regulate energy metabolism according to the anorexigenic or orexigenic gastric peptides and gastrointestinal load in relation to eating or fast [Quarta et al., 2011].

Besides the control of eating behaviour, the central ECS participates in the control of thermogenesis. Hypothalamic CB1Rs are suggested to regulate neuronal input to BAT [Cota et al., 2003] and BAT thermogenesis [Richard et al., 2009].

Hypothalamic EC signalling modulates peripheral metabolism also by regulating hepatic EGP and WAT metabolism. Central CB1R activation induce hepatic insulin resistance independent of hepatic insulin signalling, whereas blockade of the central CB1Rs in HFD fed insulin resistant rats restored the hepatic insulin sensitivity. Also, central CB1R stimulation led to impaired suppression of WAT lipolysis under insulin-stimulation that was reversed by the blockage of these receptors. It was suggested that elevated central ECS tone suppresses hypothalamic insulin sensitivity, which in turn correspondence the peripheral metabolic alterations [O'Hare et al., 2011].

In addition to being located on the neuronal membrane, CB1Rs have been detected in the mitochondrial membrane, where they participate in the regulation of neuronal energy metabolism [Bénard et al., 2012]. Furthermore, CB1Rs are expressed in astrocytes on their plasma membrane and in mitochondria. ECS signalling seems to modulate several essential astrocytic functions, such as calcium signalling, which is further linked with the release of gliotransmitters and inflammation [Eraso-Pichot et al., 2023]. Interestingly, activation of mitochondrial CB1Rs in astrocytes led to decreased glycolytic production of lactate, which in turn associated with impaired neuronal metabolic state and altered social behaviour in mice. It was concluded, that mitochondrial CB1Rs regulate glycolysis and lactate production in astrocytes to ensure the metabolic homeostasis of neurons [Jimenez-Blasco et al., 2020].

2.6.3 Peripheral endocannabinoid system and energy metabolism

ECS regulates metabolic functions in several peripheral tissues, including the WAT, BAT, liver, endocrine pancreas and skeletal muscle. CB1R activation on WAT has lipogenic actions and associates with adipocyte differentiation. CB1R stimulation in WAT promotes fatty acid and glucose uptake, *de novo* lipogenesis, adipocyte differentiation, reduces lipolysis, and impairs mitochondrial biogenesis and cold-induced browning. In BAT, ECS activation results in decreased fatty acid uptake, thermogenesis and mitochondrial biogenesis. The overall effect of ECS signalling in adipose tissue is thus to favour energy storage. These actions are mediated by the direct binding of circulating ECs to adipocyte CB1Rs, central ECS signalling and modulation of sympathetic outflow to adipose tissue [Jung et al., 2022; Quarta et al., 2011]. In addition, EC biosynthesis in WAT seems to be under negative control of insulin and central leptin signalling [Matias et al., 2006].

Activation of hepatic CB1Rs promotes lipogenesis and lipid accumulation via upregulation of lipogenic enzymes and *de novo* lipogenesis [Osei-Hyiaman et al., 2005]. In addition, hepatic CB1R activation is associated with impaired glucose tolerance, presumably through inhibition of insulin signalling within hepatocytes

[Silvestri & Di Marzo, 2013]. In pancreatic β -cells, CB1R stimulation have found to enhance basal and glucose-stimulated release of insulin, as also insulin signalling [Gatta-Cherifi & Cota, 2016]. In pancreatic α -cells, stimulation of CB1Rs enhance glucagon release. It is suggested that the altered hormone secretion from the pancreas after CB1R stimulation do not however account for the alterations in plasma glucose level, which is rather affected by modulations in skeletal muscle and liver insulin sensitivity [Di Marzo, 2008b].

In myocytes, ECS seems to regulate the insulin signalling pathways downstream the IR leading to reduced translocation of GLUT4 and decreased basal and insulin-stimulated GU into myocytes. In addition, CB1R stimulation inhibits mitochondrial biogenesis and impairs skeletal muscle oxidative metabolism [Silvestri & Di Marzo, 2013].

2.6.4 Endocannabinoid system in obesity

Obesity and related metabolic disorders are characterized by dysregulation of the ECS. As a manifestation, increased EC biosynthesis and EC levels within the brain, peripheral tissues, circulation, and also altered CB1R expression has been detected in both rodents and humans [Gatta-Cherifi & Cota, 2016; Quarta et al., 2011]. Also, increased circulating EC levels are found to correlate positively with BMI, waist, body fat percentage, VAT and SAT masses, plasma triglyceride, insulin sensitivity, and negatively with high-density lipoprotein (HDL) cholesterol. Weight loss in turn is followed by a decrease in the EC levels. As the EC levels are increased in tissues, including the VAT, in subjects with obesity, they show decreased EC levels in SAT. This is suggest to reflect an imbalance of the ECS tone favouring fat accumulation to VAT depots [Quarta et al., 2011]. It is also observed that the circulating EC levels change according to the phase of eating in both lean subjects and subjects with obesity [Gatta-Cherifi & Cota, 2016] and the content of food consumed, especially the amount and quality of fat, and the duration of HFD [Matias, Petrosino, et al., 2008].

Some discrepancy exists regarding the CB1R expression rate in obesity. HFD fed [Yan et al., 2007] and obese rats [Bensaid et al., 2003] showed increased CB1R expression in WAT, while in humans with obesity, a trend toward a decreased CB1R levels with increased EC levels in VAT were observed [Matias et al., 2006]. Similarly, subjects with obesity displayed lower CB1R gene expression in abdominal SAT and VAT than lean subjects [Bennetzen et al., 2011; Blüher et al., 2006; Engeli, 2008; Sarzani et al., 2009], and weight loss was followed by an increase in the CB1R expression rate [Bennetzen et al., 2011]. EC degrading enzyme and CB1R expression in abdominal SAT both has been found to correlate negatively with circulating EC levels suggesting a negative feedback loop regulation [Engeli et al., 2005]. HFD consumption alters skeletal muscle CB1R expression in rodent

models of obesity, and the altered ECS tone might promote muscle insulin resistance [Silvestri & Di Marzo, 2013]. Accordingly, pharmacological blockade of skeletal muscle CB1Rs lead to an increase in the muscle GU [Liu et al., 2005]. Similarly, in diet-induced obese (DIO) rats, downregulation of central CB1Rs in several extrahypothalamic regions but not in the hypothalamus has been shown. Interestingly, especially intake of highly palatable food associated with the CB1R density in these extrahypothalamic regions, suggesting a link between these receptors and diet-induced obesity [Harrold et al., 2002]. Varying results of the relation of EC metabolizing enzymes in obesity has been found, expression the enzymes being differently affected depending also the WAT depot [Bennetzen et al., 2011; Blüher et al., 2006; Engeli et al., 2005].

Whether the deregulated ECS tone is a cause or the consequence of obesity has not been established [Gatta-Cherifi & Cota, 2016]. As obesity is characterized by insulin and leptin resistance, it seems that these disturbances are linked with the elevated ECS tone in both central and peripheral tissues [D'Eon et al., 2008; Di Marzo, 2008c; Di Marzo et al., 2001; Matias et al., 2006; Tam et al., 2012]. Impaired hypothalamic leptin signalling in obesity associates with elevated hypothalamic EC levels, which in turn might contribute to peripheral metabolic dysregulations including excess fat accumulation [Di Marzo et al., 2001]. Likewise, it is suggested that the central ECS upregulation hinders hypothalamic insulin sensitivity and the insulin effect on peripheral tissue metabolism, which can predispose to systemic metabolic dysregulation and obesity [Quarta et al., 2011]. Obesity-related ECS activation associates with increased expression of TNF- α , which in turn drives ECS activation, and thus creates a potential cycle between adipose tissue inflammation, ECS overactivity and weight gain [Kempf et al., 2007]. Impaired WAT and BAT mitochondrial oxidative activity due to ECS overactivity may in part contribute to decreased whole-body energy metabolism and favour weight gain [Quarta et al., 2011]. In addition, genetic variability in the CB1R coding gene, the CNR1 in humans has found to associate with BMI, insulin resistance and dyslipidaemia [Baye et al., 2008] and also visceral adiposity [Bordicchia et al., 2010]. Similarly, AEA degrading enzyme polymorphism is linked with obesity phenotype related to cardiometabolic risk with higher levels of circulating AEA [Martins et al., 2015], and interestingly, increased reward-related brain activity [Hariri et al., 2009].

2.6.5 Endocannabinoid system as a target to treat obesity

While the ECS regulates energy balance at several levels it provides a potential target to treat obesity and associated metabolic disturbances. Initial studies with rodents demonstrated that the first selective CB1R inverse agonist Rimonabant (SR141716) [Rinaldi-Carmona et al., 1994] reduced food intake and weight [Colombo et al.,

1998]. Accordingly, clinical trials revealed reductions in body weight and adiposity, as also improvements in lipid and glucose homeostasis in humans. Severe neuropsychiatric side effects forced the Rimonabant to be withdrawn from clinical use [Sam et al., 2011], and since then approaches to modulate the peripheral ECS has been investigated [Simon & Cota, 2017].

Peripherally restricted CB1R inverse agonist JD5037 was shown to reduce appetite, body weight, insulin resistance and hepatic steatosis in DIO mice, and the appetite and weight reduction were mediated by reversion of hypothalamic leptin resistance by the JD5037 [Tam et al., 2012, 2017]. Also, DIO mice treated with peripherally restricted CB1R antagonist AM6545 was found to be hypophagic and showed sustained weight loss and improvements in glucose homeostasis, plasma lipid profile and hepatic lipid content [Cluny et al., 2010; Tam et al., 2010]. Peripheral CB1R antagonist BPR0912 induced weight loss irrespective of food intake in DIO mice. In addition, chronic treatment with BPR0912 resulted in an activation of hormone-sensitive lipase (HSL), the key lipolytic enzyme in WAT, and induced upregulation of lipolytic and lipid oxidation promoting genes in DIO mice. Also, BPR0912 induced upregulation of mitochondrial UCP1 in BAT and WAT, and enhanced thermogenesis. As in previous studies, an increase in leptin sensitivity was suggested the underlying mechanism in these effects. Upregulation of β 2-adrenoreceptor in both WAT and BAT observed in DIO mice treated with BPR0912 was suggested to explain the observed improvements in insulin sensitivity and in part the loss in body weight, as β 2-adrenoreceptor activation stimulates mitochondrial function, insulin-dependent GU and GLUT4 translocation. [Hsiao et al., 2015].

As the neuropsychiatric adverse effects of Rimonabant were suggested to result from the inverse agonism of the compound [Meye et al., 2013], CB1R neutral antagonist, such as AM4113, has been found to induce weight loss without increases in anxiety and depressive-like behaviour in mice [Gueye et al., 2016]. Several studies in rodents have demonstrated AM4113 treatment induced suppression of appetite and food intake accompanied with reduction in body weight [Chambers et al., 2007; Cluny et al., 2011; Sink et al., 2008], which was primarily contributed by reduced fat mass, but unaltered circulating glucose and lipid levels [Cluny et al., 2011]. In addition, endogenous allosteric ligands such as the steroid hormone pregnenolone, hemopressin, and an urea derivative PSNCBAM-1 have shown to reduce food intake and body weight in animal studies [Simon & Cota, 2017].

Inhibition of the biosynthesis of ECs by modulating the dietary lipid composition has provided promising results both in animals and humans. Diet enriched in omega-3 and limited with omega-6 PUFAs has shown improvements in lipid profile, body composition accompanied with reduced circulating EC levels in subjects with obesity and dyslipidaemia [Berge et al., 2013; Naughton et al., 2016].

3 Aims

The aim of the thesis was to investigate whether alterations in brain and peripheral tissue insulin sensitivity and endocannabinoid system associates with obesity risk in the early adulthood. It is widely acknowledged that obesity is associated with brain insulin resistance manifested as increased insulin-stimulated brain glucose uptake, and alterations in the endocannabinoid system tone. It remains unresolved whether the alterations are present already in the pre-obese state, and whether they link with risk factors for obesity.

The specific questions addressed in this thesis were:

- I. Is cerebral glucose uptake increased in healthy young subjects in pre-obese state?
- II. Is brain glucose uptake associated with whole-body and peripheral tissue insulin sensitivity already in early adulthood?
- III. Are central and peripheral CB1R availabilities associated with obesity risk factors including overweight and increased body adiposity, insulin resistance, low physical activity and familial risk factors?

4 Materials and Methods

The study protocol was reviewed and approved by the Ethics Committee of the Hospital District of Southwest Finland. All participants provided their written informed consent prior to participating in the clinical study (NCT03106688). The studies were conducted in accordance with the principles of the Declaration of Helsinki. Volunteers were recruited via newspaper advertisements, university-hosted email lists and bulletin boards.

4.1 Study subjects

A group of 19 healthy subjects were recruited to the high-risk (HR) and 22 to the low-risk (LR) group according to common obesity risk factors (BMI, leisure time physical exercise and parental risk factors). Inclusion criteria to the HR group was male sex, age of 20–35 years, BMI 25–30 kg/m², leisure time physical exercise < 4 hours per week and maternal or paternal overweight or obesity or T2D. Inclusion criteria for LR group were male sex, age 20–35 years, BMI 18.5–24.9 kg/m², leisure time physical exercise > 4 hours per week and no parental overweight or obesity or T2D. Exclusion criteria for both groups were any chronic disease or medication that could affect glucose metabolism or neurotransmission, eating disorder, smoking tobacco, abusive use of alcohol or narcotics, and prior participation in PET studies or other significant prior exposure to radiation.

Clinical screening, consisting of physical examination, anthropometric measurements, electrocardiography (ECG), routine laboratory tests, a 2-hour oral 75-g glucose tolerance test, urine drug screening and medical history inquiry were performed before inclusion to the study. In study I and II, the sample consisted of 19 HR and 22 LR subjects, and in study III, 16 HR and 21 LR subjects. The basic characteristics of the subjects' are described in **Table 1**.

The familial obesity risk scoring applied in study I, consisted of subject's report of parental overweight, obesity and T2D; one point from such condition in one parent and two point from both parents, total score ranging from 0 to 4.

Table 1 Basic characteristics of the study subjects. HR, high-risk; LR, low-risk. Data presented as mean \pm SD.

Study	Risk group	n	Age (years)	BMI (kg/m ²)	Radiotracer
I	HR	19	27 \pm 4	27.1 \pm 1.9	[¹¹ C]carfentanil [¹⁸ F]FMPEP- <i>d</i> ₂ [¹⁸ F]FDG
	LR	22	23 \pm 3	21.9 \pm 2.0	
II	HR	19	27 \pm 4	27.1 \pm 1.9	
	LR	22	23 \pm 3	21.9 \pm 2.0	[¹⁸ F]FDG
III	HR	16	28 \pm 4	27.3 \pm 1.9	[¹⁸ F]FMPEP- <i>d</i> ₂ [¹⁸ F]FDG
	LR	21	23 \pm 3	22.1 \pm 2.0	

4.2 PET studies

4.2.1 Principles of PET

PET is a non-invasive imaging technique which allows quantitative in vivo measurement of physiological and biochemical processes such as metabolism, blood flow and neurotransmitter systems. PET is based on a positron decay of radionuclides that are used to label compounds of special biological interest

PET uses of cyclotron-produced, short half-life and positron rich radionuclides that decay by positron emission. The emitted positrons rapidly lose their kinetic energy in tissue, and subsequently annihilate with a nearby electron. The annihilation process results in two photons that are emitted in opposite directions, both carrying energy of 511 keV. The photons emitted are recorded in coincidence detection by a PET scanner containing an imaging ring of radiation detectors (**Figure 8**). The line between the two detectors is called the line of response (LOR), and during a PET scan, data from numerous LORs at different angles are collected. The number of counts measured by a detector is proportional to the radioactivity along the LOR. The raw data, consisting of coincidence events of all angles, is represented as sinogram, which is ultimately reconstructed into cross-sectional images. The PET data can be collected as dynamic or static sequence. The dynamic time frames provide information about the changes in tissue activity concentration over time course, and enables modelling and calculations of the rates of radiotracer transportation between blood and tissue compartments. Static data acquisition comprises of a single frame, scanned usually later after tracer injection, and can be used when the radiotracer concentration in circulation and tissues are expected to be more stable [Cherry & Dahlbom, 2006; Turkington, 2001].

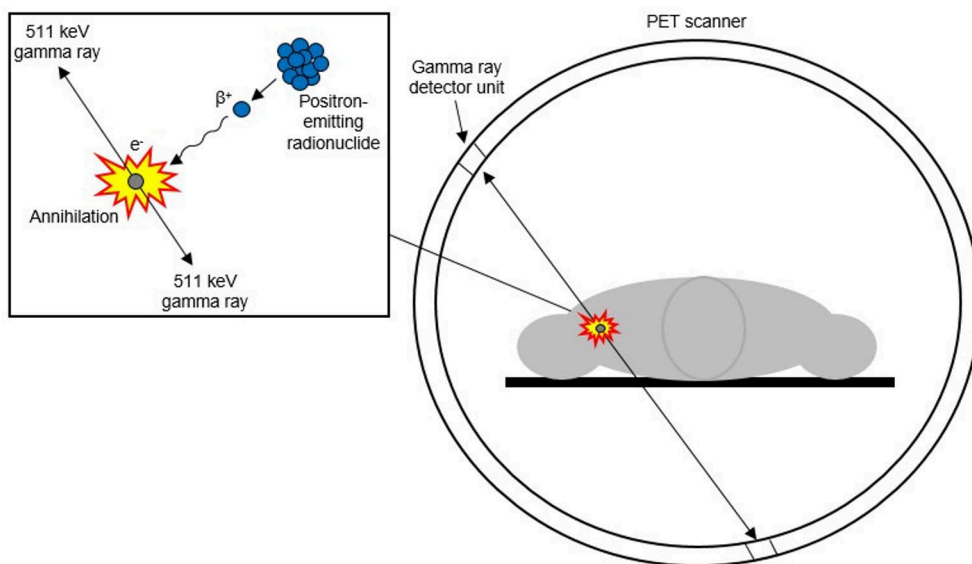


Figure 8 A schematic illustration of positron-electron annihilation producing two 511 keV photons leaving in opposite directions, and detection of the coincidence event by the PET scanner. Modified from van der Veld et al., 2013.

While the quality of images is degraded by such factors as dead time (missing photon detection due to increased rate of photons hitting a detector), decay (the decay of the radionuclide after radioligand injection, and the decrease of radioactivity during the PET scan) and photon attenuation (the loss of detection of coincidence due to photon absorption in the body), they should be corrected before or during image reconstruction. Correction for decay and dead time can be done automatically, while the attenuation correction is performed by modelling using low-dose CT images acquired before the start of PET scans. [Cherry & Dahlbom, 2006; Turkington, 2001].

4.2.2 Radiochemistry

Radionuclides were produced in the cyclotrons of Åbo Akademi University and Turku PET Centre, and radiotracers were synthesized in the Radiopharmaceutical Chemistry Laboratory of the Turku PET Centre.

[^{18}F]FDG was used to quantify tissue glucose uptake in Studies I-III. [^{18}F]FDG is a glucose analogue, with a hydroxyl group at the C-2- position in the glucose molecule substituted by a fluorine-18 (half-life 109.8 min) radionuclide. [^{18}F]FDG is widely used in the determination of regional glucose utilization by tissues and organs. As glucose, [^{18}F]FDG enters the cell via GLUT transporters, and then either rapidly undergoes a phosphorylation by hexokinase into [^{18}F]FDG-6-phosphate ([^{18}F]FDG-

6-P) [Bessell et al., 1972] or is transported back to circulation. Further metabolites such as 2- ^{18}F -fluoro-2-deoxy-6-phosphogluconate (^{18}F FDG-6-PG1) and 2- ^{18}F -Fluoro-2-deoxy-6-phospho-d-gluconolactone (^{18}F FDG-6-PGL) appears later, 90 min after ^{18}F FDG injection with extent varying from tissue to tissue. Likewise, these metabolites accumulate inside the cell [Bender et al., 2001]. Because of the fluorine-18 substituting the hydroxyl group in the C-2 position, the ^{18}F FDG-6-P does not enter the glycolytic pathway [Horton et al., 1973] nor glycogen synthesis [Bender et al., 2001], and is not transported back to blood. Because of low expression of glucose-6P-phosphatase in other tissues than liver and kidney [van Schaftingen & Gerin, 2002], dephosphorylation of ^{18}F FDG-6-P is limited, and the ^{18}F FDG-6-P gets trapped in inside the cell until the positron decay of fluorine-18. This forms the basis of the measurement of the glucose consumption of a tissue by modelling ^{18}F FDG uptake with PET data [Phelps et al., 1979]. Comparing hyperinsulinemic-euglycemic clamp with ^{18}F FDG PET study, tissue-specific GU rates can be assessed *in vivo* [Nuutila et al., 1992]. ^{18}F FDG was produced using FASTlab synthesis platform (GE Healthcare) according to a modified method of Hamacher et al [Hamacher et al., 1986] and Lemaire et al [Lemaire et al., 2002]. Radiochemical purity was $> 98\%$.

^{18}F FMPEP- d_2 was used to measure tissue CB1R availability in studies I and III. ^{18}F FMPEP- d_2 is an inverse agonist of CB1Rs, and has high affinity and selectivity for CB1Rs [Donohue et al., 2008]. ^{18}F FMPEP- d_2 passes the BBB, and demonstrates high uptake in brain making it suitable for the measurement of brain CB1R availability [Hirvonen, 2015; Terry, Hirvonen, Liow, Zoghbi, et al., 2010]. In a dosimetry study, of the peripheral organs that were visually identified from the PET images, the uptake of ^{18}F FMPEP- d_2 was highest in the liver, followed by the lungs, small intestine, kidneys, heart and spleen, gallbladder, lumbar vertebrae and urinary bladder. While ^{18}F FMPEP- d_2 is excreted in urine and bile, it is not applicable for the measurement of CB1R availability in the liver, intestine or urinary bladder [Terry, Hirvonen, Liow, Seneca, et al., 2010]. Binding of ^{18}F FMPEP- d_2 to CB1Rs in BAT but not in WAT was detected in rats [O. Eriksson et al., 2015]. In humans, CB1R availability in BAT under cold exposure was upregulated as detected with ^{18}F FMPEP- d_2 PET imaging, and the binding of ^{18}F FMPEP- d_2 in WAT, and also in brain, was lower in subjects with obesity as compared to lean participants [Lahesmaa et al., 2018] suggesting that ^{18}F FMPEP- d_2 is eligible for quantifying the availability of peripheral CB1Rs. The binding of ^{18}F FMPEP- d_2 to its receptors may depend on the level of the natural ligands endocannabinoids competing the receptor binding [Takkinen et al., 2018]. The radiotracer was produced as described previously [Lahdenpohja et al., 2020]. Radiochemical purity was $> 95\%$.

4.2.3 PET image acquisition

The PET studies were performed at the Turku PET Centre on separate days. The subjects were instructed to abstain from caffeine, alcohol and physical exercise on the PET scan days and the day before each scan. All studies were done in room temperature. During all the PET scans, the subjects were positioned in a supine position with their heads strapped to the scan table to prevent head movement. To obtain arterialized venous blood samples, the arm used for blood sampling was heated with a hot water bottle. Plasma radioactivity was measured with an automatic γ -counter (Wizard 1480 3", Wallac, Turku, Finland). The subjects were clinically monitored by physician throughout the scans.

4.2.3.1 [^{18}F]FDG PET scan with hyperinsulinemic–euglycemic clamp

The [^{18}F]FDG scans were performed with the GE Discovery (Discovery 690 PET/CT, GE Healthcare) PET camera after a 12-h overnight fast. Hyperinsulinemic–euglycemic clamp was applied along with the PET imaging to measure whole-body insulin sensitivity (**Figure 9**) [DeFronzo et al., 1979; Nuutila et al., 1992].

Subjects laid in a supine position and one cannula was inserted in an antecubital vein for insulin and glucose infusion and for radiotracer injection, and one in the contralateral antecubital vein for blood sampling. After collecting fasting laboratory samples, the clamp was started. Insulin (Actrapid, Novo Nordisk A/S, Bagsvaerd, Denmark) was administered in a primed continuous manner at the rate of 40 mU/m²/min after first 7 min of priming with higher doses. Euglycemia, (plasma glucose level 5.0 ± 0.5 mmol/L) was maintained with a variable rate of 20% glucose infusion based on plasma glucose measurements taken every 5 to 10 minutes. Plasma insulin was measured at fasting and every 30 min to ascertain adequate insulin level during the clamp, and serum FFA at fasting and every 60 min to study the suppression on lipolysis. Whole-body insulin sensitivity, indexed by the M value was calculated as the average of 20-min intervals between 60–160 min during steady euglycemia using following formula:

$$M = GIR - UC - SC \quad (1)$$

where GIR is the glucose infusion rate expressed in μmol per kg of body weight or per kg fat-free mass (kg_{FFM}) UC is the urinary glucose excretion rate, and SC is the space correction accounting for the changes in the glucose level in the glucose space [DeFronzo et al., 1979].

The subjects were transferred to the PET/CT scanner. A scout CT was acquired for attenuation correction. After reaching steady euglycemia (80 ± 13 min from the start of the insulin infusion), a single bolus of 156 ± 10 MBq of [^{18}F]FDG was injected intravenously and dynamic PET scanning was started with the clamp

ongoing. Dynamic scans of thoracic region (0–40 min using 4×15 , 6×20 , 2×60 , 2×150 and 6×300 s frames), upper abdomen (40–55 min; 3×300 s) and thighs (55–70 min; 3×300 s) and static data of the neck (10 min; 1×600 s) and brain (10 min; 1×600 s) were collected. Short low-dose CT scans were obtained before the emission scan of every region. To measure plasma activity, arterialized venous blood samples were taken at 4.5, 7.5, 10, 20 and 30 min from the [^{18}F]FDG injection, and in the middle time points of the upper abdomen, thigh, neck and brain scans. The amount of [^{18}F]FDG lost to urine was determined from a urine collected at the end of the scan and during the scan when necessary, and measured with an isotope dose calibrator (Model VDC-205; Comcer Netherlands, Joure, Netherlands)

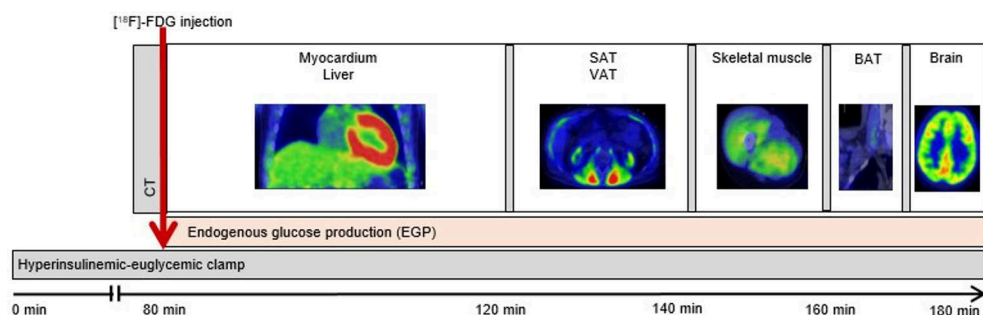


Figure 9 Clinical [^{18}F]FDG PET study design during hyperinsulinemic–euglycemic clamp. BAT, brown adipose tissue; SAT, subcutaneous adipose tissue; VAT, visceral adipose tissue.

4.2.3.2 [^{18}F]FMPEP- d_2 scan

The [^{18}F]FMPEP- d_2 scans were performed with PET/CT (GE Discovery VCT PET/CT, GE Healthcare) after a 6–12 hour fast. Two cannulas were inserted in veins of opposite forearms, one for blood sampling and one for [^{18}F]FMPEP- d_2 injection. Before the scan, fasting blood samples were collected to measure hematocrit and serum endocannabinoid levels. A scout CT was acquired for attenuation correction. 147–215 MBq of [^{18}F]FMPEP- d_2 was injected as an intravenous bolus and dynamic scans of the brain (60 min using 3×60 s, 5×180 s and 7×360 s frames), neck (12 min; 4×180 s frames), abdomen (9 min; 3×180 s) and a late scan of the brain (9 min; 3×180 s) were conducted. Before each scanning region, CT scans were acquired for photon attenuation and anatomical reference. Arterialized venous blood samples to measure plasma activity were collected at 0.25, 0.5, 0.75, 1, 1.25, 1.5, 1.75, 2, 2.5, 3, 4.5, 7.5, 11, 15, 20, 25, 30, 35, 40, 45, 50 and 60 min from the [^{18}F]FMPEP- d_2 injection, and at following time points (min from the regional scan start): neck (2 and 6 min), abdomen (4.5 min) and late brain scan (4.5 min). Additional blood samples for [^{18}F]FMPEP- d_2 metabolite analysis were taken before the scan and at 4.5, 11, 15, 20, 30, 45 and 60 min from the radiotracer injection, and

at following time points (min from the regional scan start): neck (2 and 6 min), abdomen (4.5 min) (**Figure 10**).

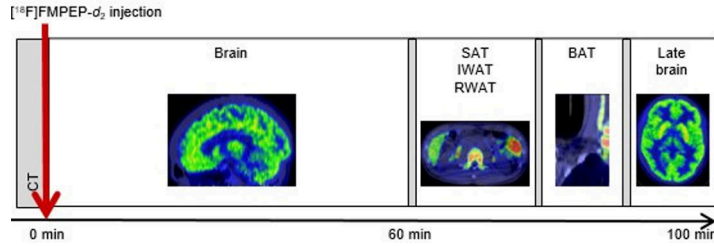


Figure 10 Clinical $[^{18}\text{F}]\text{FMPEP-}d_2$ PET study design. BAT, brown adipose tissue; IWAT, intraperitoneal white adipose tissue; RWAT, retroperitoneal adipose tissue; SAT, subcutaneous adipose tissue.

4.2.4 PET image analysis

4.2.4.1 Quantification of glucose uptake with $[^{18}\text{F}]\text{FDG}$

Quantification of tissue GU with $[^{18}\text{F}]\text{FDG}$ is commonly based on three-compartmental model. In this model, $[^{18}\text{F}]\text{FDG}$ in plasma, $[^{18}\text{F}]\text{FDG}$ in extracellular space and $[^{18}\text{F}]\text{FDG-6-P}$ inside the cells are considered as compartments [Phelps et al., 1979] (**Figure 11**).

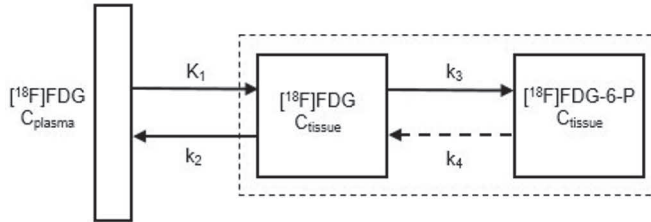


Figure 11 Three-compartment model of $[^{18}\text{F}]\text{FDG}$ kinetic modelling. K_1 and k_2 are rates of $[^{18}\text{F}]\text{FDG}$ transportation, k_3 is the rate of $[^{18}\text{F}]\text{FDG}$ phosphorylation, and k_4 the rate of $[^{18}\text{F}]\text{FDG-6-P}$ dephosphorylation. Modified from Gunn et al., 2001.

Metabolic rate of glucose ($\text{MR}_{\text{glucose}}$) can be calculated using following formula:

$$\text{MR}_{\text{glucose}} = \frac{C_{\text{glucose}}}{LC} \times \frac{K_1^* \times k_3^*}{k_2^* + k_3^*} \quad (2)$$

where C_{glucose} is the average plasma glucose concentration from the $[^{18}\text{F}]\text{FDG}$ injection until the end of the PET scan, LC is a lumped constant that accounts for the differences in transport and phosphorylation rates between $[^{18}\text{F}]\text{FDG}$ and glucose of

the studied tissue, K_1^* is the rate of $[^{18}\text{F}]\text{FDG}$ membrane transport forward, k_2^* is the rate of $[^{18}\text{F}]\text{FDG}$ membrane transport backward, and k_3^* is the rate constant of $[^{18}\text{F}]\text{FDG}$ phosphorylation.

A direct estimation of the combination of the rate constants can be derived using a graphical method, the Patlak plot [Patlak & Blasberg, 1985], that combines the rate of constants (K_1^* , k_2^* , k_3^*) as the net uptake rate (K_i) for $[^{18}\text{F}]\text{FDG}$ for the further calculation of $\text{MR}_{\text{glucose}}$:

$$K_i^* = \frac{K_1^* \times k_3^*}{k_2^* + k_3^*} \quad (3)$$

$$\text{MR}_{\text{glucose}} = \frac{C_{\text{glucose}}}{LC} \times K_i^* \quad (4)$$

The principle of the Patlak plot is that the accumulation of radiotracer in the irreversible compartment in relation to the radiotracer that has been available in plasma reflects the net uptake rate of the radiotracer in the tissue. This takes place when the concentration of the radiotracer in the reversible tissue compartments and in plasma are in dynamic equilibrium. This happens after the early sharp rise in plasma concentration when the radiotracer concentration in reversible tissue compartments start to follow that in plasma. The Patlak plot is useful in other tissues than in brain, where the endothelial wall is very permeable for glucose and $[^{18}\text{F}]\text{FDG}$ as compared to the BBB. The following equation describes the Patlak plot:

$$\frac{C_{\text{tissue}}(T)}{C_{\text{plasma}}(T)} = K_i \times \frac{\int_0^T C_{\text{plasma}}(t) dt}{C_{\text{plasma}}(T)} + \text{Int} \quad (5)$$

where the tissue concentration of radiotracer in relation to the radiotracer availability in plasma in certain time is calculated by multiplying the net uptake rate (K_i) by integral of plasma radiotracer concentration from injection to the middle of the selected time frame divided by plasma concentration during the frame and added with the intercept (Int) of the slope with the y-axis (**Figure 12**) [Oikonen, 2023].

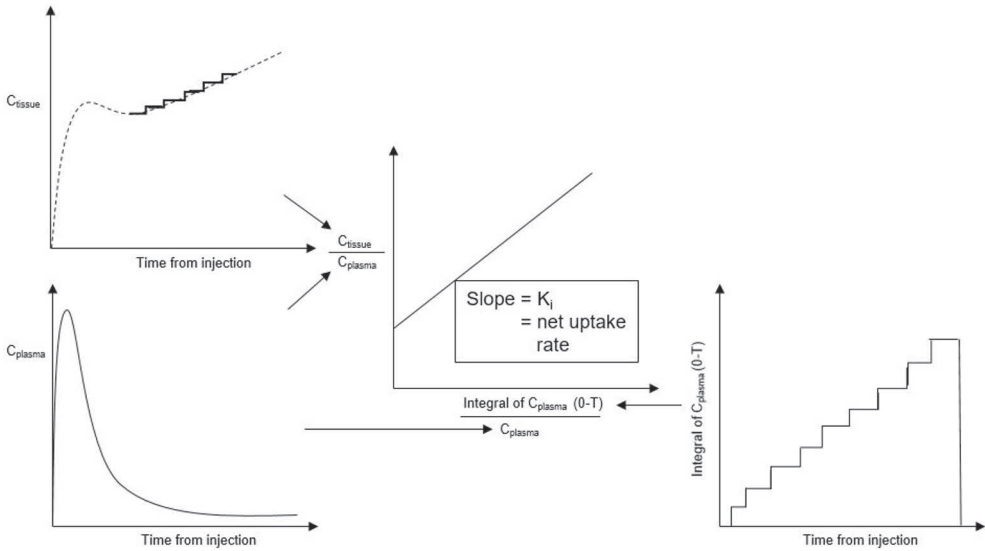


Figure 12 The Patlak plot becomes linear when the equilibrium between the radiotracer concentrations in the reversible compartments and plasma is achieved. The y-axis of the plot comprises of the ratio of concentrations of radiotracer in tissue region of interest and plasma as function of time. The x-axis is the ratio of the integral of plasma radiotracer concentration and the plasma concentration. The slope of the plot's linear phase represents the tissue net uptake rate of the radiotracer. Based on Oikonen, 2023.

Concentration of [^{18}F]FDG in plasma is measured from blood samples collected during the scan, and can be combined with the PET image-derived activity to form the input function for the analysis of [^{18}F]FDG uptake. Conversion of tissue [^{18}F]FDG uptake to GU is performed multiplying the K_i with the average plasma glucose concentration from [^{18}F]FDG injection to the end of the scanned tissue and divided by tissue density and LC as described in chapter 4.2.5.2.

The Patlak plot is suitable only for dynamic PET scans. For static scans in which activity is measured only in one timepoint, calculation of fractional uptake rate (FUR) of [^{18}F]FDG is preferred. FUR can be calculated with the following equation:

$$FUR = \frac{C_{tissue}(T)}{\int_0^T C_{plasma}(t)dt} \quad (6)$$

FUR is a simple estimate of the Patlak plot slope K_i , with the extension that the distribution volume of [^{18}F]FDG is no longer important at late time after [^{18}F]FDG injection [Thie, 1995]. Tissue GU is obtained by multiplying FUR with the average plasma glucose concentration and dividing by LC. FUR overestimates the net uptake rate of the radiotracer, but at late timepoints (over 60 min after injection) the bias is less than 5%, making FUR a suitable alternative for the Patlak plot [Oikonen, 2021].

4.2.4.2 Quantification of peripheral tissue glucose uptake (II, III)

Carimas software (version 2.9, Turku PET Centre, downloadable at <https://turkupetcentre.fi/software/>) was used for PET image analyses. Tissue [^{18}F]FDG activity was measured by manually drawing regions of interest (ROI) or volume of interest (VOI) to both quadriceps femoris and hamstrings muscles, right lobe of the liver, supraclavicular BAT depots and several volumes of abdominal SAT and VAT on the fused PET/CT images. Several ROIs and VOIs in several slices of images were drawn avoiding large vessels to minimize the spill over effect due to partial volume effect and motion. In the analysis of myocardium, a segmenting tool implemented in Carimas software was used to include the left ventricular walls and septum in the analysis.

Input function for [^{18}F]FDG was determined by combining PET image derived data from left ventricle from 0 to 4.5 min to the arterialized plasma sampling from 4.5 min to the end of the scan. Dynamic tissue time-activity curves and input functions were then used to determine the fractional uptake (K_i) of [^{18}F]FDG using the Patlat plot or its approximation fractional uptake rate (FUR). Tissue-specific GU was calculated using the following formula:

$$\text{Tissue GU} = \frac{K_i \times \text{plasma glucose}}{\text{tissue density} \times \text{LC}} \times 1000 \quad (7)$$

where K_i (or FUR) is the fractional uptake of [^{18}F]FDG (l/min), plasma glucose is the average glucose concentration from [^{18}F]FDG injection to the end of the scanned tissue (mmol/L), tissue density (kg/L) and LC is 1.2 for skeletal muscle, 1.0 for liver and myocardium, and 1.14 for adipose tissue [Bøtker et al., 1997; Iozzo et al., 2007; Kelley et al., 1999; Peltoniemi et al., 2000; Virtanen et al., 2001].

4.2.4.3 Quantification of brain glucose uptake (I, II)

Automated PET image processing pipeline Magia [Karjalainen et al., 2020] (<https://github.com/tkkarjal/magia>), running on MATLAB (The MathWorks, Inc., Natick, MA, USA), was used for preprocessing and modelling of the PET data. [^{18}F]FDG PET images were first corrected for motion and then coregistered with the MRI images. To define ROIs, Magia uses FreeSurfer (<https://surfer.nmr.mgh.harvard.edu/>). The ROI-wise kinetic modelling was based on extraction of ROI-wise time-activity curves. Parametric images were spatially normalized to Montreal Neurobiological Institute (MNI) space and then smoothed using a Gaussian kernel (full width at half maximum; FWHM = 8 mm). Insulin-stimulated BGU was quantified using FUR. To quantify the FUR values, the tissue radioactivity values were averaged over the time frames after 40 minutes from [^{18}F]FDG injection (late scan). The input function for [^{18}F]FDG was obtained in the

same manner as in peripheral tissues. The FUR estimates were converted into BGU ($\mu\text{mol}/\text{min}/100\text{g}$) with the following equation:

$$BGU = 100 \times \frac{\text{avg}_{\text{plasma glucose}} \times \text{FUR}}{LC \times \text{density}} \quad (8)$$

where $\text{avg}_{\text{plasma glucose}}$ is the average plasma glucose concentration (mmol/L) from the time of [^{18}F]FDG injection to the end of brain scan, LC is lumped constant (0.65) [Wu et al., 2003] and density is grey matter relative density in the brain (1.04) [Snyder et al., 1975].

4.2.4.4 Measurement of endogenous glucose production (EGP) (II, III)

EGP was calculated by subtracting the exogenous glucose infusion rate (GIR) from the rate of disappearance of glucose (Rd) during the hyperinsulinemic-euglycemic clamp using the following formula:

$$EGP = R_d + V_{\text{glucose}} \times \frac{\Delta_{\text{glucose}}}{\Delta_T} - \text{GIR} \quad (9)$$

GIR is corrected by a space correction [DeFronzo et al., 1979], where V_{glucose} is the estimated constant for glucose distribution volume (0.19 l/kg), Δ_{glucose} is the change in glucose concentration from [^{18}F]FDG injection to the end of sampling (mmol/L), Δ_T is the time from [^{18}F]FDG injection to the end of sampling (min) and GIR is the total amount of infused glucose during the scan (mg/kg).

Glucose disappearance rate (Rd) ($\mu\text{mol}/\text{min}/\text{kg}$) was calculated using the following equation:

$$R_d = \frac{\text{MCR}_{\text{FDG}} \times \text{avg}_{\text{plasma glucose}}}{\text{weight}} \quad (10)$$

where MCR_{FDG} (ml/min) is the metabolic clearance rate of [^{18}F]FDG, $\text{avg}_{\text{plasma glucose}}$ is the average plasma glucose concentration (mmol/L) from the time of [^{18}F]FDG injection to the end of sampling, and weight is the subject's weight (kg).

MCR_{FDG} was calculated with the following formula:

$$\text{MCR}_{\text{FDG}} = \frac{\text{dose}_{\text{FDG}} - \text{urine}_{\text{FDG}}}{\text{AUC}_{\text{FDG}}} \quad (11)$$

where dose_{FDG} is the injected [^{18}F]FDG dose (kBq), $\text{urine}_{\text{FDG}}$ is the amount of radiotracer lost to urine ($\mu\text{mol}/\text{min}/\text{kg}$) during the entire scan (kBq), and AUC_{FDG} is the area under the curve representing [^{18}F]FDG from the radiotracer injection to infinity.

4.2.4.5 Quantification of cannabinoid receptor availability in peripheral tissues (III)

CB1R availability in peripheral tissues was quantified both as FUR and volume of distribution (V_T) of the [^{18}F]FMPEP- d_2 . Radiometabolite corrected plasma input for image analysis was determined by correcting the plasma time-activity curve (TAC) for the fraction of nonmetabolized radioligand measured using thin layer chromatography and digital autoradiography as previously described elsewhere [Laheesmaa et al., 2018].

To determine the FUR of [^{18}F]FMPEP- d_2 , Carimas 2.9 Software was used for the image analysis of abdominal SAT, intraperitoneal (IWAT) and retroperitoneal white adipose tissue (RWAT), BAT and muscle. ROIs of each abdominal adipose tissue depots were manually drawn on the fused PET/CT images to several volumes. BAT ROIs were drawn bilaterally in supraclavicular adipose tissue depots. Only voxels with CT Hounsfield units (HU) within the adipose tissue range -50 to -250 were included. ROIs in the skeletal muscle were drawn bilaterally in the deltoideus muscle. Several ROIs in several slices of images for each tissue were drawn avoiding large vessels, and the average of the ROIs was analysed. FUR in each peripheral tissue was calculated by dividing the tissue radioactivity concentration at time X by the AUC_{0-X} of the radiometabolite corrected plasma TAC. Only FUR estimation was possible in peripheral tissue, since the PET acquisition of those areas did not start directly after radiotracer injection.

V_T ($\text{mL}\cdot\text{cm}^{-3}$) is defined as the ratio of the radioligand concentration in tissue target region to the plasma radioligand concentration at the equilibrium state (Innis et al., 2007). V_T of each peripheral tissue was calculated by dividing the radioactivity concentration in tissue by radiometabolite corrected plasma activity at the time interval of the scanned tissue. The V_T and FUR of [^{18}F]FMPEP- d_2 in peripheral tissues were reciprocally related indicating that the V_T may be suitable for estimating CB1R availability also in the late PET scans.

4.2.4.6 Quantification of cannabinoid receptor availability in brain (I, III)

CB1R availability in the brain was quantified as V_T in 21 bilateral ROIs involved in emotion and food reward processing (Study I), and as V_T in the whole brain (Study III). To process the [^{18}F]FMPEP- d_2 PET data, Magia pipeline was used as described above. The PET images were first smoothed using Gaussian kernel (FWHM = 6 mm) to increase signal-to-noise ratio before model fitting. Then, calculated parametric images were spatially normalized to MNI-space and further smoothed using a Gaussian kernel (FWHM = 6 mm). In study I, V_T was determined using multiple-time graphical analysis for reversible radiotracer uptake described by Logan [Logan, 2000]. In this method, activity concentration-time curves for the tissue and plasma

are combined to form a single Logan plot, where linearity is achieved after intercept is effectively constant, and the slope can be estimated as V_T . Image frames starting at 36 minutes and later after the radiotracer injection were used in the modelling, since Logan plots became linear after 36 minutes. Following equation for the Logan plot and V_T calculation can be presented:

$$\frac{\int_0^T C_{ROI}(t)dt}{C_{ROI}(T)} = V_T \times \frac{\int_0^T C_p(t)dt}{C_{ROI}(T)} + Int \quad (12)$$

where $C_{ROI}(T)$ is the activity concentration in tissue at the time T , C_p is the activity concentration in the plasma, and Int is the intercept. Detailed modelling information is provided at Turku PET Centre webpages: http://www.turkupetcentre.net/petanalysis/model_mtga.html#logan

In study II, mean V_T of the whole brain was calculated as the average of all white and grey matter voxels within the MNI space template.

4.3 Anthropometric measurements

Height and weight of the subjects were measured at the Turku PET Centre. Weight was measured in underwear or light hospital clothes in fasting state after urinating. Waist circumference was measured at the midpoint between the lowest ribs and the top of iliac crest, and hip circumference around the largest lateral extension of the hip. Body fat percentage was assessed with an air displacement plethysmograph (the Bod Pod system, software version 5.4.0, COSMED, Inc., Concord, CA, USA) after at least four hours of fasting. Blood pressure was measured in sitting position from upper arm with a digital blood pressure monitor. Two measurements in relaxed state were done and the mean value was used.

4.4 Biochemical analysis (I-III)

Plasma glucose during the clamp was determined in the laboratory of the Turku PET Centre in duplicates using the glucose oxidate method (Analox GM9; Analox Instruments, London, UK). Plasma insulin at fasting and during the clamp were measured using an automated electrochemiluminescence immunoassay (Cobas 8000; Roche Diagnostics), serum free fatty acid (FFA) with an enzymatic colorimetric method (NEFA-HR2, ACS-ACOD; Wako Chemicals, Neuss, Germany; Cobas 8000 c502 and Cobas 800 c702 Analyzer, Roche Diagnostics), plasma glucose at fasting and in oral glucose tolerance test (OGTT) with an enzymatic photometry/hexokinase reaction (Cobas 8000 c 702; Roche Diagnostics) and HbA1c with immunoturbidimetry (Cobas 6000 c 501, Roche Diagnostics) at the Turku University Hospital laboratory. Total plasma cholesterol and HDL and LDL

cholesterol were measured with a direct photometric enzymatic assay (Cobas 8000 c 702, Roche Diagnostics) and plasma triglycerides with a photometric enzymatic assay (GPO-PAP; Cobas 8000 c 702, Roche Diagnostics). Plasma creatinine was measured with a photometric enzymatic assay (Cobas 8000 c 702, Roche Diagnostics) and serum high-sensitivity C-reactive protein (hs-CRP) with immunonefelometry (BN ProSpec System; Siemens Healthineers). Plasma alanine aminotransferase, alkaline phosphatase and gamma-glutamyltransferase (GGT) in fasting state were assessed using a kinetic photometry according to IFCC recommendation (Cobas 8000 c 702, Roche Diagnostics) also at the Turku University Hospital laboratory.

4.5 Metabolomic analysis (II, III)

Metabolic biomarkers were quantified from serum samples at fasting state using high-throughput proton NMR metabolomics (Nightingale Health Oyj, Helsinki, Finland). The method affords simultaneous quantification of routine lipids, fatty acids, amino acids, glycolysis related metabolites, ketone bodies, fluid balance and inflammation markers well as lipoprotein subclass profiling with lipid concentrations within 14 subclasses. The experimentation and applications of the NMR metabolomics have been detailed discussed previously [Soininen et al., 2015].

4.6 Measurement of tissue masses (II, III)

The abdominal subcutaneous (SAT) and visceral (VAT) adipose tissue volumes were analyzed from MRI images using sliceOmatic® (Tomovision, Montreal, Quebec, Canada). A whole-body MRI was performed at 3T after a 12-hour fasting using the MRI part of a clinical PET-MRI system (Philips Ingenuity TF PET/MR, Philips, Amsterdam, Netherlands). The abdominal SAT compartment was defined as the fat depot between the skin and the above the abdominal musculature. The abdominal VAT volume was quantified from the combination of the intraperitoneal and retroperitoneal fat compartments [Hung et al., 2014].

The femoral SAT and skeletal muscle mass were analyzed from CT images acquired with PET/CT (GE Discovery VCT PET/CT, GE Healthcare) while performing the [^{18}F]FDG -PET/CT-study, because of artefacts in the MRI images in the femoral region. The tissue volume analysis were performed with Carimas software. A total of 47 slices of CT-derived images covering the length of 15 cm, the height of the scanned femoral area, in the mid-section of the thighs of both lower limbs were used for the analysis. To define the tissue regions, attenuation threshold value of -300 to -10 HU for adipose tissue [Martinez-Tellez et al., 2020] and -29 to +150 HU for skeletal muscle [Aubrey et al., 2014] was used. The MRI and CT

derived tissue volumes were converted to masses using densities of 0.9196 kg/L for adipose tissue [Abate et al., 1994] and 1.0597 kg/L for skeletal muscle [Segal et al., 1986]. Brain volumes were determined from MRI images and converted to mass using a density of 1.04 kg/L [Snyder et al., 1975].

4.7 Statistical analysis

In study I, BGU quantified with [^{18}F]FDG and [^{18}F]FMPEP- d_2 , V_T were compared between groups using two-sample t-test. Full-volume data were analyzed with nonparametric testing using SnPM13 (<http://www.nisox.org/Software/SnPM13/>). $P < 0.05$ was considered as the cluster-defining threshold, and only clusters large enough to be statistically significant (False Discovery rate, FDR $P < 0.05$) were reported. Bayesian hierarchical modelling was applied to estimate effect of the obesity risk factors (BMI, physical exercise and parental risk factors) to BGU, V_T and BP_{ND} in a ROI-level. The modelling was performed with the R package BRMS (<https://cran.r-project.org/web/packages/brms/index.html>), which uses the efficient Markov chain Monte Carlo sampling tools of RStan (<https://mc-stan.org/users/interfaces/rstan>). To improve model fit, BGU, V_T and BP_{ND} were log-transformed. Associations between serum endocannabinoids and [^{18}F]FMPEP- d_2 V_T were tested in separate full-volume models. Eight endocannabinoid compounds were analysed, so the results were confirmed with Bonferroni-corrected P value as the cluster-defining threshold ($0.05/8 = 0.00625$). In all analysis, the age was included as a covariate.

In study II, data are presented as mean \pm SD. Differences between groups were studied using independent samples t-test or Wilcoxon rank-sum test as appropriate. Categorical variables were compared with the χ^2 test. SPSS statistical software, version 27 was used in statistical analysis. Associations between BGU and distinct predictor variables were examined with a general linear model and SPM12 (<https://www.fil.ion.ucl.ac.uk/spm/software/spm12/>). The comparison of correlation coefficients between the groups was performed using two-sample independent t-test. The statistical threshold in SPM analysis was set at a cluster level and corrected with false discovery rate (FDR) with $P < 0.05$. Age was controlled for in the SPM analysis.

In study III, the statistical analyses were performed using IBM SPSS statistical software, version 28.0. All data are presented as mean \pm SD. An independent samples t-test or Wilcoxon rank-sum test were used as appropriate, to study between-groups comparisons. Categorical variables were compared with χ^2 test. Correlations between distinct variables were studied using the Pearson or Spearman correlation tests. $P < 0.05$ was considered statistically significant.

5 Results

5.1 Obesity risk associates with increased brain glucose uptake already in early adulthood

5.1.1 Study I-II: Increased brain glucose uptake in subjects with high versus low obesity risk

Insulin-stimulated BGU was globally higher in subjects with high (HR) versus low (LR) obesity risk (**Figure 13**).

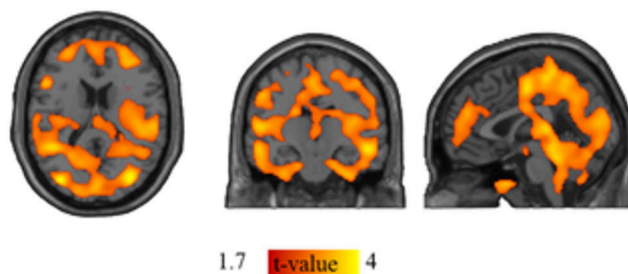


Figure 13 A Statistical parametric mapping (SPM) results from two-sample t test between the HR and the LR group. Colouring show cerebral regions with significantly higher BGU in the high than in the low obesity risk group. Higher T values denote larger differences between the groups. Data are thresholded at $P < 0.05$ and false discovery rate (FDR) corrected at cluster level. Modified from the original publication II.

5.1.2 Study I: Familial obesity risk associates with increased brain glucose uptake

When analysed the association between the three distinct obesity risk factors (BMI, leisure time physical activity and familial obesity risk, including parental overweight, obesity or T2D) and BGU, increased familial obesity risk had the strongest association with increased BGU (**Figure 14**), while the effect of BMI was weaker.

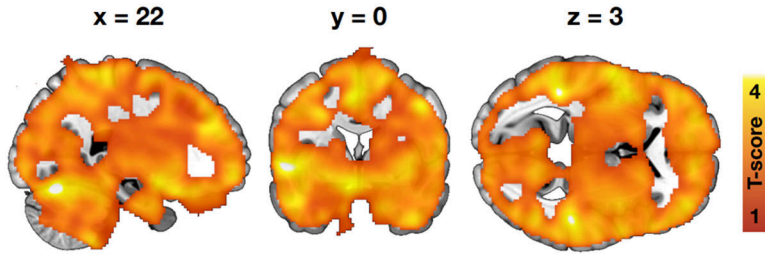


Figure 14 Brain regions (as defined by FDR-corrected SPM one-sample *t* test) where higher familial obesity risk score was associated with increased BGU in the whole study group. Data are thresholded at $P < 0.05$ and false discovery rate (FDR) corrected at cluster level. Modified from the original publication I.

5.1.3 Study II: Whole-body insulin sensitivity associates negatively with brain glucose uptake

During the clamp, plasma glucose levels were steady with no differences between the groups (5.3 ± 0.3 mmol/L in HR vs. 5.3 ± 0.2 mmol/L in LR group, $P = 0.5$). Steady-state insulin levels were higher (581.7 ± 94.9 pmol/L in HR vs. 510.5 ± 76.8 in LR pmol/L, $P = 0.01$) and FFA suppression was smaller (0.05 ± 0.03 mmol/L in HR vs. 0.03 ± 0.01 mmol/L in LR, $P = 0.03$) in the HR as compared to the LR group, and these two measurements were also correlated ($r = -0.41$, $P = 0.009$).

Whole-body insulin sensitivity indexed by the M value and the rate of glucose disappearance (Rd) were lower in the HR than in the LR group (**Figure 15A**).

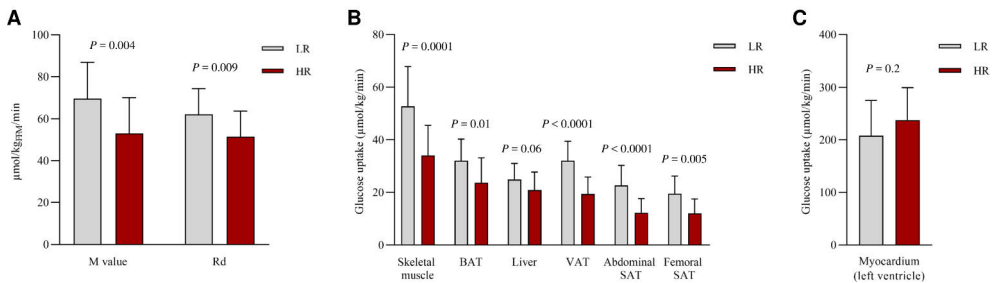


Figure 15 Whole-body and tissue-specific glucose uptake (GU) rates. **(A)** Whole-body insulin sensitivity indexed by the M value and the rate of glucose disappearance (Rd) calculated with the fat-free mass in the low-risk (LR) and in the high-risk (HR) group. **(B)** GU rates in skeletal muscle, brown adipose tissue (BAT), liver, visceral adipose tissue (VAT) and abdominal and femoral subcutaneous adipose tissue (SAT) and **(C)** myocardium in the LR and in the HR group. Bar heights represent sample means and vertical lines sample SD. P values for comparison of LR vs HR group. Reproduced from the original publication II.

Similarly, the HR group exhibited lower rates of GU in skeletal muscle, liver, VAT, abdominal and femoral SAT and BAT than the LR group (**Figure 15B**).

Myocardial left ventricle GU rates did not differ between the groups (**Figure 15C**). Insulin-suppressed EGP ($-0.6 \pm 8.9 \mu\text{mol/kg}_{\text{FFM}}/\text{min}$ in HR vs. $-2.2 \pm 8.9 \mu\text{mol/kg}_{\text{FFM}}/\text{min}$ in LR, $P = 0.6$) did not significantly differ between the groups. M value and Rd correlated negatively with insulin-suppressed FFA levels, and M value positively with Rd and negatively with EGP in both groups and in the whole dataset (**Figure 16**).

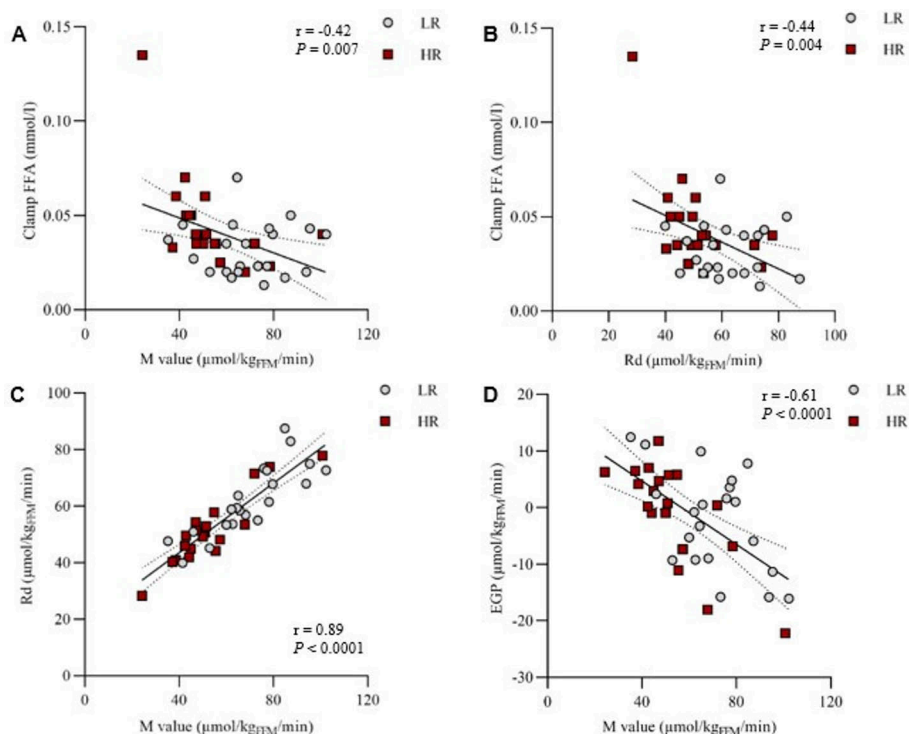


Figure 16 Association between the whole-body insulin sensitivity indexes. (A) Association between the M value and free fatty acid (FFA) levels and (B) the rate of glucose disappearance (Rd) and FFA levels during the hyperinsulinemic-euclycemic clamp, (C) M value and Rd, (D) M value and endogenous glucose production (EGP). Modified from the original publication II.

BGU correlated negatively with M value, and the association was driven by the HR group (**Figure 17A**). Furthermore, BGU correlated positively with 2-h plasma glucose level in OGTT among all study subjects and negatively with insulin sensitivity index by Matsuda (Matsuda-ISI) in the HR group (**Figure 17B-C**). BGU in the HR group correlated negatively with skeletal muscle GU and showed a trend toward a negative correlation with BAT GU, whereas no association was found between BGU and liver, VAT or abdominal and femoral SAT GU.

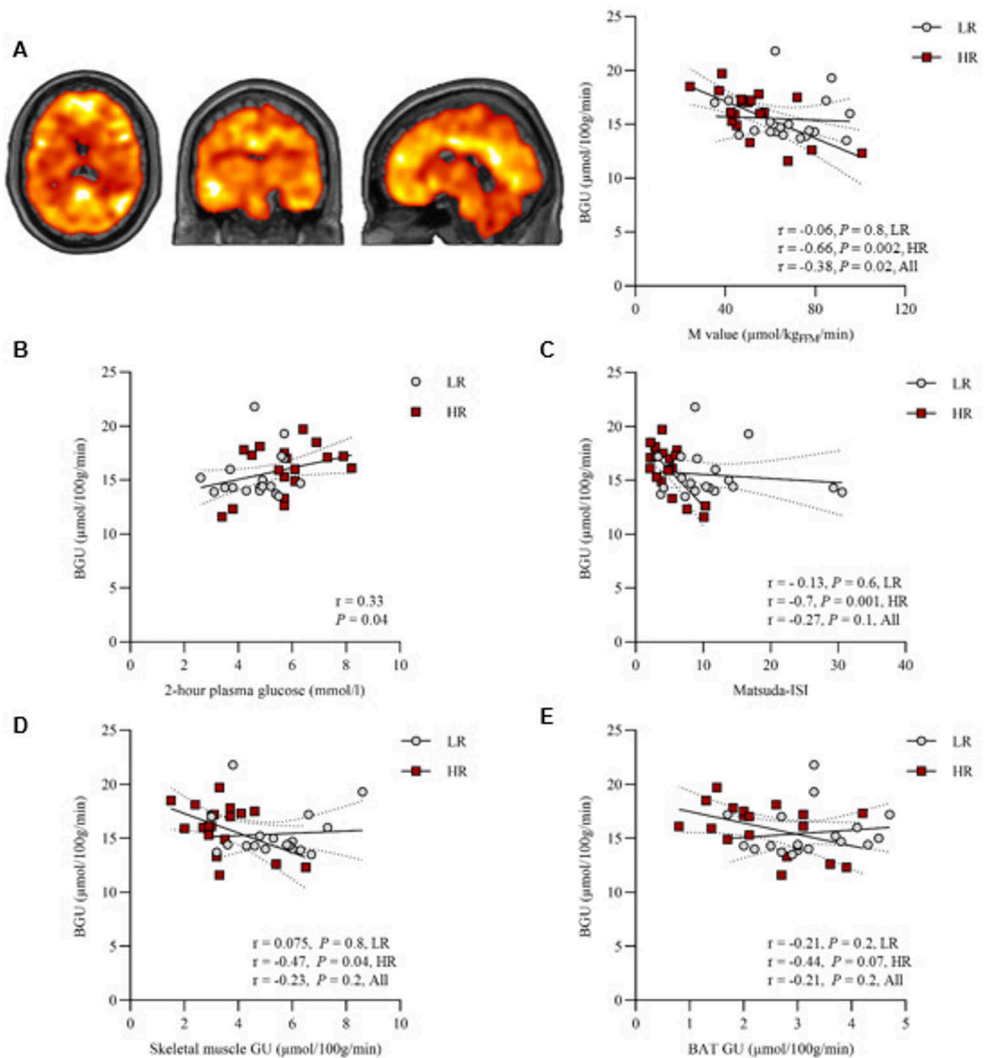


Figure 17 Brain glucose uptake (BGU) in the high-risk (HR) and the low-risk (LR) group. **(A)** Brain clusters (as defined by false discovery rate (FDR) corrected Statistical parametric mapping (SPM) one-sample t test) for the association between BGU and M value and the corresponding scatterplot. Higher T values denote larger differences between the groups **(B)** Association between the BGU and 2-hour plasma glucose level in oral glucose tolerance test, **(C)** BGU and insulin sensitivity index by Matsuda (Matsuda-ISI), **(D)** BGU and skeletal muscle glucose uptake (GU) and **(E)** BGU and brown adipose tissue (BAT) GU in the LR and in the HR group. Scatterplots show global cerebral GU. Modified from the original publication II.

Insulin-suppressed FFA correlated positively with BGU in the ROI level and the association was driven by the HR group (**Table 2**).

Table 2 Associations (Pearson correlations) between the regional insulin-stimulated brain glucose uptake rates and insulin-suppressed free fatty acid (FFA) levels. Associations are shown separately for all study subjects, the low-risk (LR) and the high-risk (HR) group. Significant associations are indicated by bold font. * $P < 0.05$, ** $P < 0.001$. Modified from original publication II.

ROI	All	LR	HR
Amygdala	0.36*	-0.02	0.47*
Caudate	0.36*	0.05	0.50*
Cerebellum	0.34*	0.15	0.38
Dorsal anterior cingulate cortex	0.34*	0.06	0.43
Hippocampus	0.28*	-0.004	0.40
Inferior temporal gyrus	0.33*	0.03	0.39
Insula	0.30	0.04	0.37
Medulla	0.22	-0.064	0.30
Midbrain	0.25	-0.02	0.33
Middle temporal gyrus	0.35*	0.06	0.41
Nucleus accumbens	0.34*	0.02	0.53*
Orbitofrontal cortex	0.37*	0.12	0.44
Pars opercularis	0.35*	0.07	0.41
Posterior cingulate cortex	0.43*	0.21	0.47*
Pons	0.24	-0.06	0.37
Putamen	0.32*	-0.005	0.42
Rostral anterior cingulate cortex	0.36*	0.08	0.49*
Superior frontal gyrus	0.40*	0.11	0.47*
Superior temporal gyrus	0.27	-0.0005	0.33
Temporal pole	0.32*	0.08	0.40
Thalamus	0.33*	0.18	0.37

5.1.4 Study II: EGP associates positively with brain glucose uptake

Higher insulin-suppressed EGP associated with insulin-stimulated BGU in the whole dataset. The association was driven by the HR group (**Figure 18**).

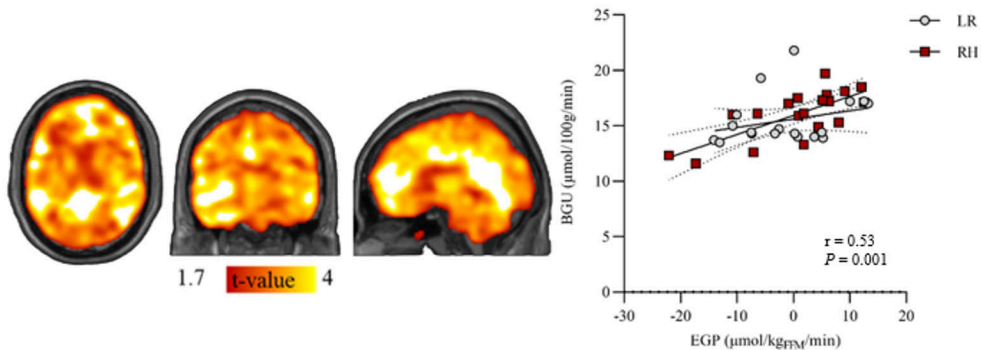


Figure 18 Brain regions (as defined by FDR-corrected SPM one-sample t test) where BGU was associated with EGP in the whole study group. Data are thresholded at $P < 0.05$ and false discovery rate (FDR) corrected at cluster level. Scatterplot shows the association between EGP and global BGU separately for the high-risk (HR) and the low-risk (LR) groups. Modified from the original publication II.

5.2 Obesity risk associates with lower abdominal adipose tissue CB1 receptor availability

5.2.1 Study III: Lower abdominal adipose tissue CB1 receptor availability in subjects with high as compared to low obesity risk

CB1R availability was quantified with [^{18}F]FMPEP- d_2 PET in peripheral tissues including abdominal SAT, IWAT and RWAT, BAT and muscle. CB1R availability, determined as the V_T and FUR of [^{18}F]FMPEP- d_2 , of the each abdominal adipose tissue depot was lower in the HR versus LR group. CB1R availability of muscle was numerically lower in HR than in the LR group but did not reach statistical significance. No difference was found in CB1R availability of BAT between the groups (**Figure 19**). Tissue-wise V_T and FUR values were positively associated ($r = 0.80$, $P < 0.0001$ for abdominal SAT; $r = 0.72$, $P < 0.0001$ for IWAT; $r = 0.78$, $P < 0.0001$ for RWAT; $r = 0.87$, $P < 0.0001$ for BAT; $r = 0.58$, $P = 0.0002$ for muscle).

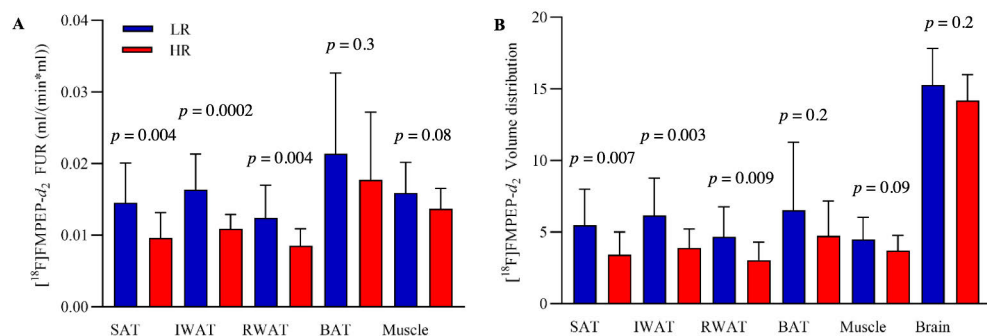


Figure 19 Lower CB1R availability in abdominal SAT, IWAT and RWAT in the high-risk (HR) as compared to the low-risk (LR) group. **(A)** The FUR of [¹⁸F]FMPEP-d₂ in abdominal subcutaneous (SAT), intraperitoneal (IWAT) and retroperitoneal white adipose tissue (RWAT), brown adipose tissue (BAT) and muscle in the LR and in the HR group. **(B)** [¹⁸F]FMPEP-d₂ VT of SAT, IWAT, RWAT, BAT, muscle and the whole brain in the LR and in the HR group. Modified from the original publication III.

5.2.2 Study III: Lower CB1 receptor availability is associated with decreased insulin sensitivity, higher body adiposity, unfavourable lipid profile and inflammatory markers

CB1R availability of each abdominal adipose tissue depot was positively associated with abdominal adipose tissue insulin sensitivity assessed as tissue-specific GU (**Figure 20A-C** and **Table 3**). CB1R availability of the RWAT also correlated positively also with whole-body insulin sensitivity (M value and Rd), and the CB1R availability of IWAT with Rd. Furthermore, CB1R availability of each abdominal adipose tissue depot correlated negatively with serum insulin-suppressed FFA level (**Table 3**).

CB1R availability of the abdominal adipose tissue correlated negatively with body weight, BMI, total fat and abdominal adipose tissue masses (**Table 3** and **Figure 20D-F**) CB1R availability of muscle correlated negatively with weight, BMI and visceral adipose tissue mass, while CB1R availability of BAT did not correlate with any of these measures (**Table 3**).

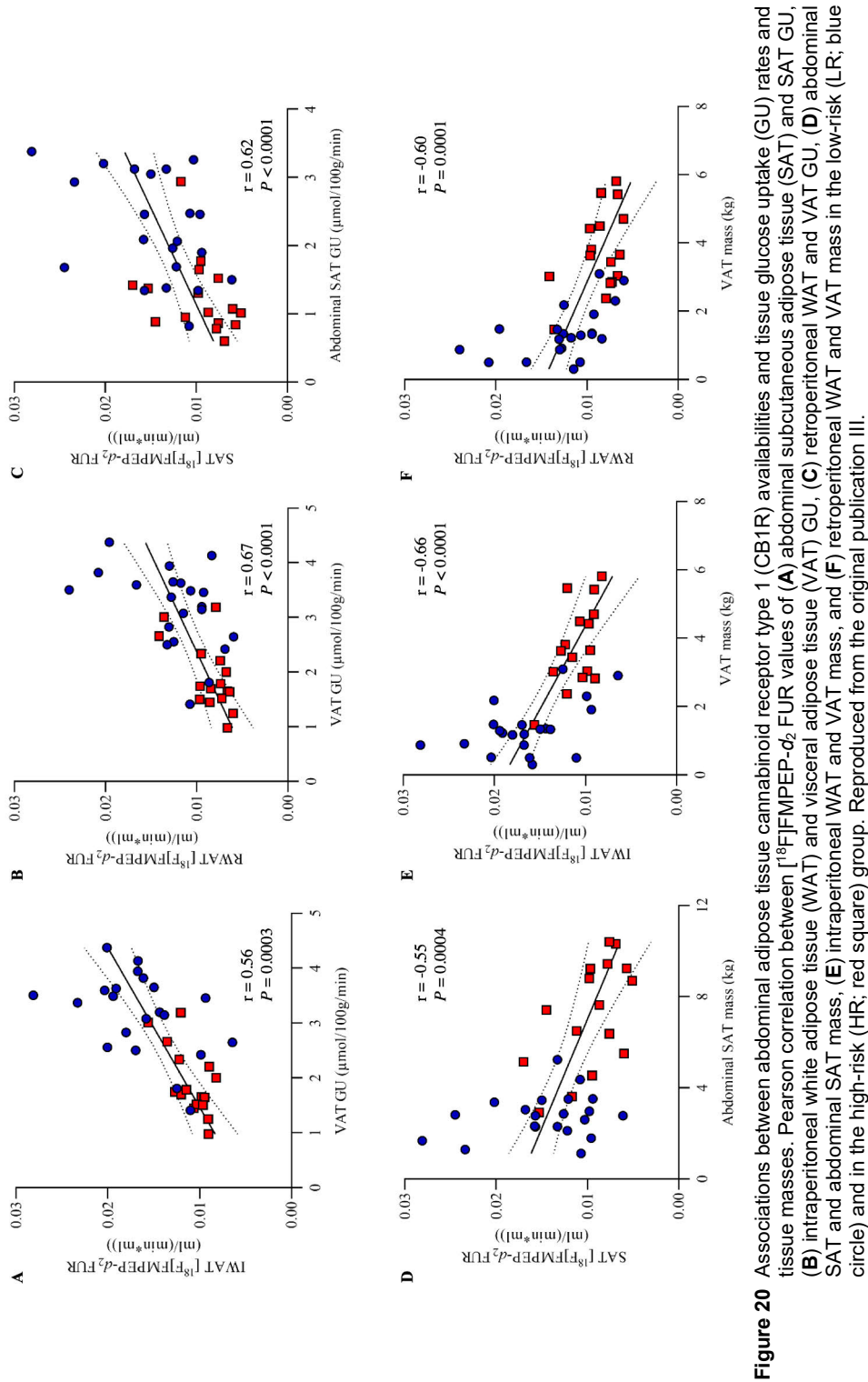


Figure 20 Associations between abdominal adipose tissue cannabinoid receptor type 1 (CB1R) availabilities and tissue glucose uptake (GU) rates and tissue masses. Pearson correlation between $[^{18}\text{F}]\text{FMPEP-d}_2\text{FUR}$ values of (A) abdominal subcutaneous adipose tissue (SAT) and SAT GU, (B) intraperitoneal white adipose tissue (WAT) and visceral adipose tissue (VAT) GU, (C) retroperitoneal WAT and VAT GU, (D) abdominal SAT and abdominal SAT mass, (E) intraperitoneal WAT and VAT mass, and (F) retroperitoneal WAT and VAT mass in the low-risk (L; blue circle) and in the high-risk (R; red square) group. Reproduced from the original publication III.

Table 3 Associations (Pearson correlations) between [^{18}F]FMPEP- d_2 FUR values of abdominal subcutaneous (SAT), intraperitoneal (IWAT) and retroperitoneal white adipose tissue (RWAT), brown adipose tissue (BAT) and muscle, and V_T of the whole brain and anthropometric and metabolic characters, and insulin-stimulated tissue-specific glucose uptake rates. Statistically significant associations are indicated by bold font. * $P < 0.05$; ** $P < 0.01$; *** $P < 0.001$; **** $P < 0.0001$.

^aAssociations with the LR (n = 20) and HR (n = 16) subjects who gave an urine sample.

^bAssociations with the LR (n = 20) and HR (n = 16) subjects who completed the [^{18}F]FDG scan successfully.

^cAssociations with the LR (n = 19) and HR (n = 16) subjects who completed the [^{18}F]FDG scan successfully. Modified from original publication III.

	FUR (ml/(min*ml))			V_T		
	SAT	IWAT	RWAT	BAT	MUSCLE	BRAIN
Age (years)	-0.49**	-0.42**	-0.42**	-0.16	-0.33*	-0.24
Weight (kg)	-0.49**	-0.59***	0.57***	-0.25	-0.40*	-0.39*
BMI (kg/m ²)	-0.49**	-0.57***	-0.59***	-0.29	-0.40*	-0.44**
Body fat (kg)	-0.56***	-0.63****	-0.65****	-0.13	-0.31	-0.36*
Body fat (%)	-0.53***	-0.63****	-0.68****	-0.07	-0.25	-0.36*
Fat free mass (kg)	-0.15	-0.16	-0.09	-0.32	-0.35*	-0.08
Abdominal SAT mass (kg)	-0.55***	-0.60***	-0.59***	-0.09	-0.29	-0.28
VAT mass (kg)	-0.50**	-0.66****	-0.60****	-0.10	-0.33*	-0.37*
Systolic blood pressure (mmHg)	-0.19	-0.34*	-0.35*	0.11	-0.10	-0.50**
Diastolic blood pressure (mmHg)	-0.07	-0.23	-0.22	0.15	-0.17	-0.42**
HbA _{1c} (mmol/mol)	-0.23	-0.37*	-0.20	-0.004	0.09	-0.10
hs-CRP (mg/l)	-0.32	-0.31	-0.26	-0.07	-0.17	-0.28
Fasting serum FFA (mmol/l)	0.078	-0.04	-0.10	0.14	-0.02	-0.25
Clamp serum FFA (mmol/l)	-0.39*	-0.39*	-0.38*	-0.007	-0.13	-0.31
M value ($\mu\text{mol/kg/min}$)	0.28	-0.27	0.39*	0.17	0.19	0.38*
M value ($\mu\text{mol/kg}_{\text{FFM}}/\text{min}$)	0.16	0.14	0.24	0.17	0.16	0.35*
Rd ($\mu\text{mol/kg/min}$)	0.26	0.36*	0.42*	0.14	0.20	0.23
Rd ($\mu\text{mol/kg}_{\text{FFM}}/\text{min}$)	0.15	0.20	0.28	0.14	0.18	0.24
EGP ($\mu\text{mol/kg/min}$) ^a	-0.05	0.08	0.02	0.10	0.06	-0.33
EGP ($\mu\text{mol/kg}_{\text{FFM}}/\text{min}$) ^a	-0.12	-0.01	-0.08	0.08	0.05	-0.43*
GU ($\mu\text{mol}/100\text{g/min}$)						
Abdominal SAT	0.56***	0.64****	0.60****	0.31	0.24	0.30
VAT	0.57***	0.67****	0.62****	0.37*	0.32	0.32
BAT ^b	0.33	0.43*	0.50**	0.03	0.34*	0.34*
Muscle ^c	0.25	0.34*	0.41*	0.18	0.21	0.20
Femoral SAT ^c	0.41*	0.45**	0.51**	0.03	0.11	0.34
Liver	0.15	-0.002	0.02	0.09	-0.02	-0.23

Lower CB1R availability of each abdominal adipose tissue depot associated with unfavourable lipid profile including higher levels of total, non-HDL, remnant, VLDL and LDL cholesterol, triglycerides, free cholesterol, ratio of triglycerides to phosphoglycerides, ApoB and ApoB/ApoA1 ratio. CB1R availability of IWAT and RWAT also correlated negatively with serum fatty acid levels, including omega-6 fatty acids and linoleic acid. CB1R availability of the abdominal SAT correlated positively with HDL cholesterol. Lower CB1R availability of the abdominal adipose tissue associated with higher serum concentration of glycoprotein acetyls (GlycA), a biomarker of systemic inflammation. Lower CB1R availability of muscle associated with higher levels of total, non-HDL, remnant, VLDL and LDL cholesterol, ApoB, ApoB/ApoA1 ratio, and fatty acids. CB1R availability of BAT did not correlate with serum metabolomics (**Figure 21**).

There were no significant association between peripheral tissue CB1R availabilities and serum EC levels. Higher serum EC levels were associated with decreased whole-body insulin sensitivity (M value and Rd) and insulin-suppressed EGP. Higher levels of circulating AA and AEA were associated with lower M value adjusted with fat-free mass (M value_{FFM}), and higher AEA concentration also with lower M value, Rd and Rd_{FFM}. Higher serum AG (1+2) and DEA levels were associated with higher insulin-suppressed EGP and EGP_{FFM}. Serum γ -LEA correlated positively with abdominal SAT GU. (**Table 4**).

Serum AG (1+2) level correlated positively with BMI, while no significant correlations were found between serum EC levels and body weight or adipose tissue masses (**Table 4**).

Higher circulating AG (1+2) level associated with unfavourable lipid profile and higher serum inflammatory markers, including higher total, non-HDL, remnant, VLDL and LDL cholesterol, triglycerides, ApoB, ApoB/apoA1 ratio and fatty acids and GlycA, whereas serum γ -LEA level correlated positively with HDL cholesterol and ApoA1 (**Figure 22**).

Linoleic acid, a precursor for ECs was found to correlate positively with abdominal SAT ($r = 0.40$, $P = 0.004$), VAT ($r = 0.60$, $P = 0.0001$) and total body fat ($r = 0.53$, $P = 0.001$) masses, weight ($r = 0.57$, $P = 0.0003$), and also with BMI ($r = 0.53$, $P = 0.001$).

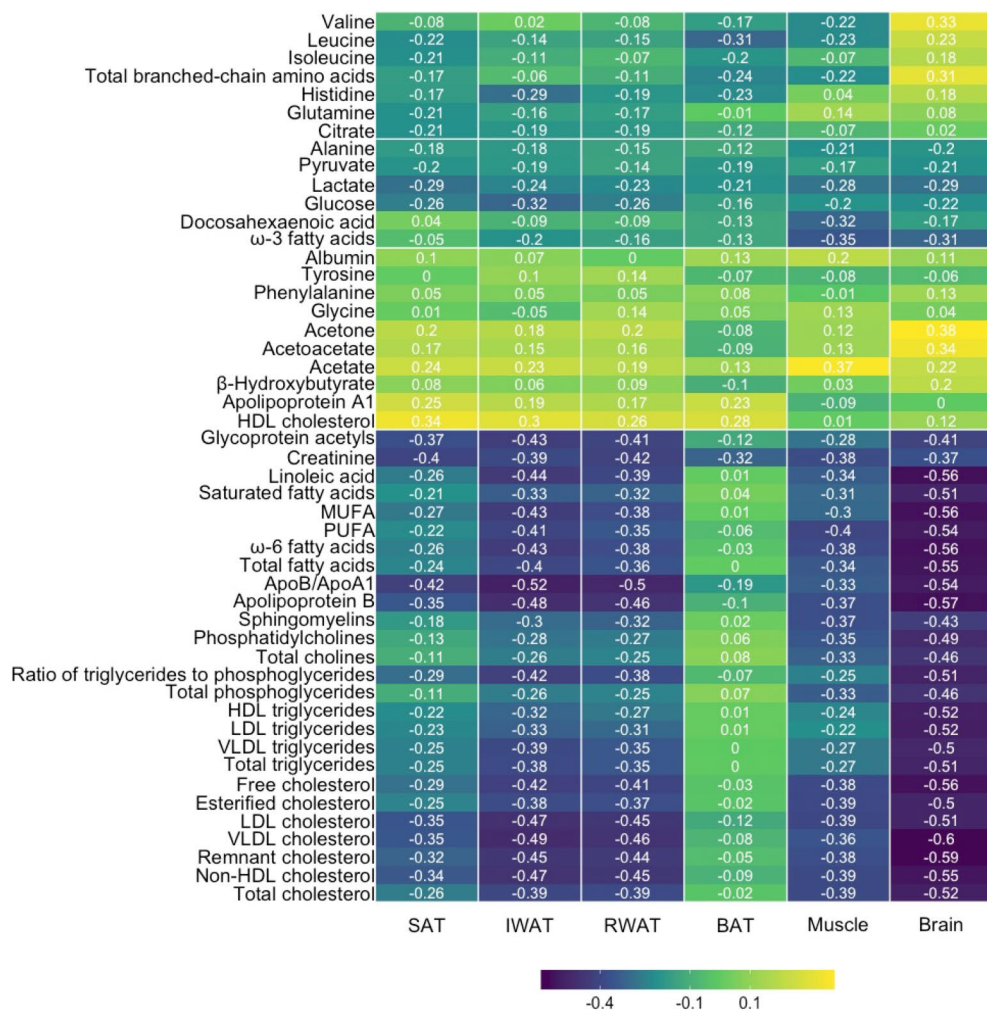


Figure 21 Correlation heatmap between CB1R availabilities of abdominal subcutaneous (SAT), intraperitoneal (IWAT) and retroperitoneal white adipose tissue (RWAT), brown adipose tissue (BAT), muscle and the whole brain with serum metabolomics across the whole study sample size. Reproduced from the original publication III.

Table 4 Associations (Pearson correlations) between circulating endocannabinoid concentrations and selective variables of body composition, insulin sensitivity, [^{18}F]FMPEP- d_2 FUR values of abdominal subcutaneous (SAT), intraperitoneal (IWAT) and retroperitoneal white adipose tissue (RWAT), brown adipose tissue (BAT) and muscle, and [^{18}F]FMPEP- d_2 V_T of the whole brain. Statistically significant associations are indicated by bold font. * $P < 0.05$; ** $P < 0.01$.

^aAssociations with the LR ($n = 20$) and HR ($n = 16$) subjects who gave an urine sample.

^bAssociations with the LR ($n = 20$) and HR ($n = 16$) subjects who completed the [^{18}F]FDG scan successfully.

^cAssociations with the LR ($n = 19$) and HR ($n = 16$) subjects who completed the [^{18}F]FDG scan successfully.

^dAssociations with the LR ($n = 20$) and HR ($n = 16$) subjects whose [^{18}F]FMPEP- d_2 image analysis was able to conduct.

Modified from original publication III.

	AA	AEA	AG (1+2)	A-LEA	Y-LEA	DEA	NALS	OEA
Weight (kg)	0.04	0.23	0.26	0.16	0.14	0.09	-0.09	-0.06
BMI (kg/m^2)	0.16	0.22	0.36*	0.07	0.03	0.10	-0.08	-0.09
Body fat (kg)	0.06	0.24	0.23	0.02	-0.01	0.23	-0.08	0.02
Abdominal SAT mass (kg)	0.05	0.21	0.16	0.02	-0.04	0.24	-0.14	0.04
VAT mass (kg)	0.13	0.26	0.26	-0.02	-0.05	0.24	-0.06	0.09
M value ($\mu\text{mol}/\text{kg}/\text{min}$)	-0.31	-0.43**	-0.24	-0.16	-0.13	-0.33	-0.14	-0.26
M value ($\mu\text{mol}/\text{kg}_{\text{FFM}}/\text{min}$)	-0.34*	-0.44**	-0.23	-0.22	-0.20	-0.29	-0.18	-0.29
Rd ($\mu\text{mol}/\text{kg}/\text{min}$)	-0.25	-0.37*	-0.12	-0.02	-0.03	-0.22	-0.10	-0.19
Rd ($\mu\text{mol}/\text{kg}_{\text{FFM}}/\text{min}$)	-0.24	-0.43**	-0.03	-0.11	-0.12	-0.19	-0.06	-0.19
EGP ($\mu\text{mol}/\text{kg}/\text{min}$) ^a	0.28	0.24	0.40*	0.29	0.25	0.35*	0.29	0.26
EGP ($\mu\text{mol}/\text{kg}_{\text{FFM}}/\text{min}$) ^a	0.33	0.28	0.39*	0.22	0.22	0.41*	0.30	0.30
Clamp serum FFA (mmol/l)	0.03	0.02	0.02	-0.20	-0.15	0.04	-0.18	-0.10
GU ($\mu\text{mol}/100\text{g}/\text{min}$)								
Abdominal SAT	0.04	-0.10	-0.01	0.29	0.37*	-0.17	0.28	0.10
VAT	0.02	-0.12	-0.08	0.23	0.28	-0.26	0.14	-0.04
BAT ^b	-0.14	-0.33	0.10	0.08	0.08	-0.31	-0.03	-0.10
Muscle ^c	-0.19	-0.24	-0.06	-0.03	-0.01	-0.17	0.07	0.03
Femoral SAT ^c	0.00	0.01	-0.05	0.26	0.30	-0.05	0.22	0.22
Liver	0.23	0.01	0.23	-0.25	-0.13	-0.05	0.11	0.03

	AA	AEA	AG (1+2)	A-LEA	γ-LEA	DEA	NALS	OEA
[¹⁸ F]FMPEP-d ₂ FUR (ml/(min*ml))								
SAT	0.24	-0.11	-0.15	0.25	0.32	-0.19	0.23	0.16
IWAT	0.19	-0.12	-0.22	0.26	0.22	-0.21	0.18	0.12
RWAT	0.19	-0.19	-0.20	0.25	0.25	-0.20	0.22	0.14
BAT ^d	-0.004	-0.07	-0.02	0.08	0.15	-0.06	-0.10	0.07
Muscle	-0.01	-0.26	-0.29	0.03	0.03	-0.11	0.09	-0.05
[¹⁸ F]FMPEP-d ₂ V _T of the whole brain	-0.28	-0.20	-0.34*	0.03	-0.05	-0.03	-0.11	-0.03

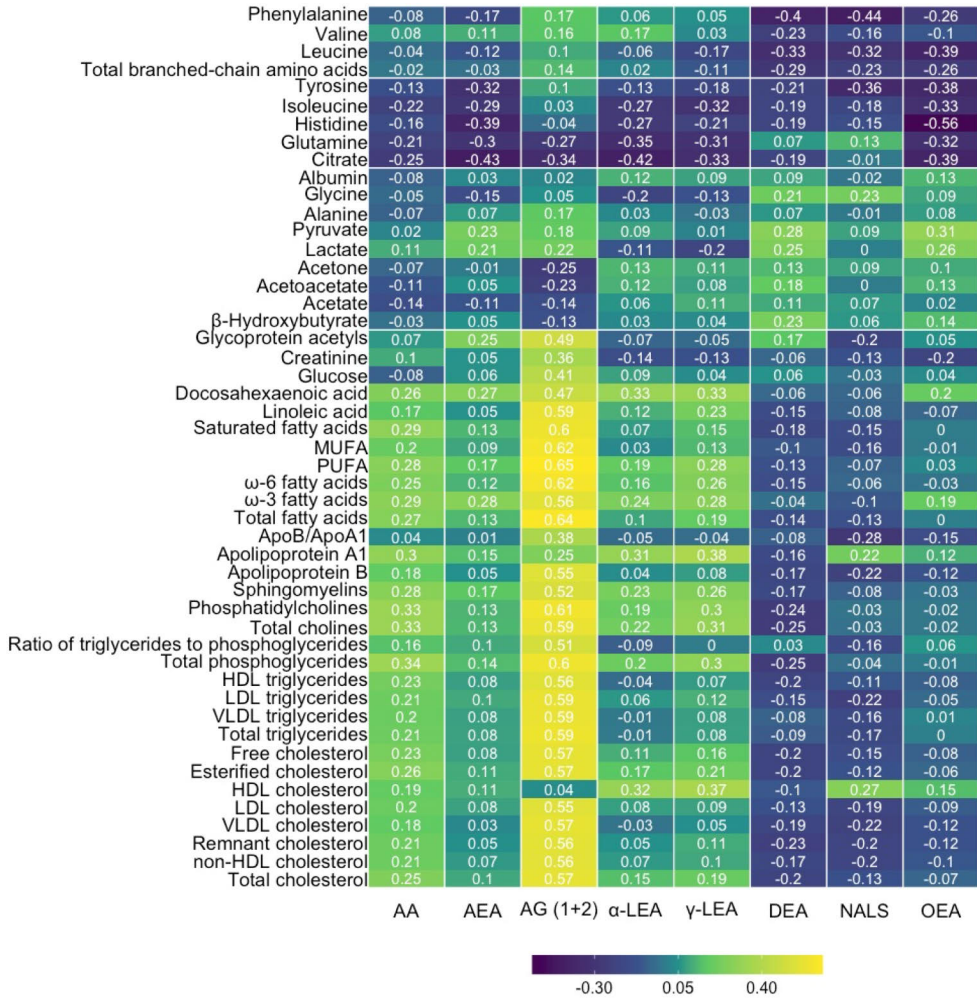


Figure 22 Correlation heatmap between serum endocannabinoid levels and serum metabolomics across the whole study sample size. AA = arachidonic acid; AEA = anandamide; AG (1+2) = arachidonoyl glycerol (1 + 2); α-LEA = α-linolenic acid; γ-LEA = γ-linolenic acid; DEA = docosatetraenoyl ethanolamide; NALS = N-arachidonoyl-L-serine; OEA = oleyl ethanolamide. Reproduced from the original publication III.

5.3 Obesity risk associates with central CB1 receptor availability

5.3.1 Study I: Familial obesity risk is associated with lower brain CB1 receptor availability

CB1R availability in brain, analysed in 21 bilateral regions involved in emotion and food reward processing, did not statistically differ between the HR and LR group. Higher familial obesity risk and BMI was associated with lower CB1R availability in the brain (**Figure 23**). Higher serum AEA level was associated with lower CB1R availability in ventral striatum (**Figure 24**), while no significant associations were found between the other seven studied circulating ECs and brain CB1R availability.

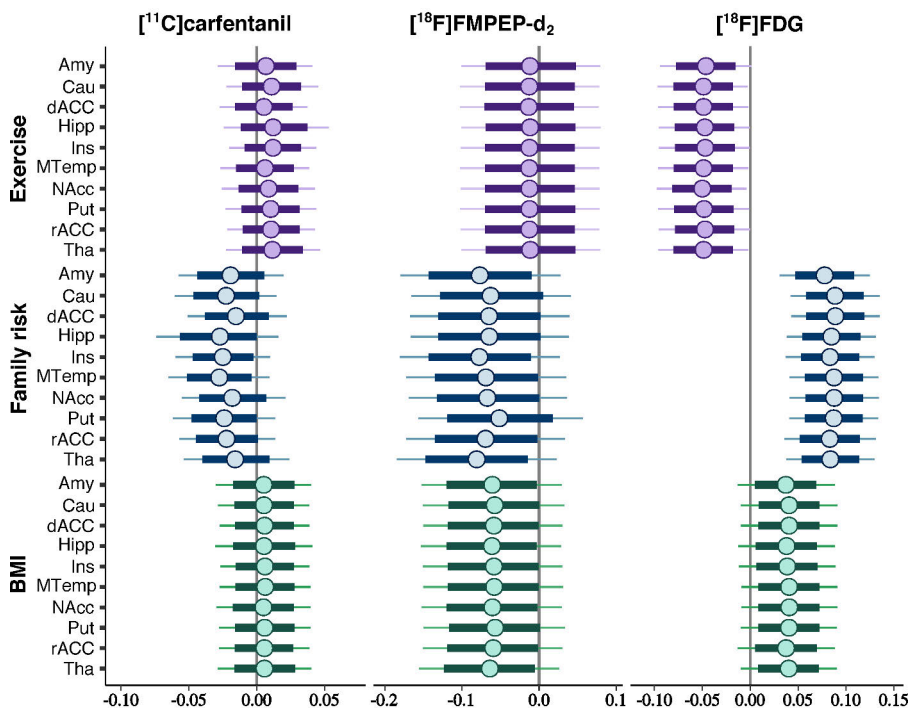


Figure 23 Effects of the obesity risk factors on brain CB1R availability. Posterior distributions of the regression coefficients for exercise, family risk and body mass index (BMI) on log-transformed volume of distribution V_T of the $[^{18}\text{F}]$ FMPEP- d_2 in representative regions of interest, with age as a covariate. The colored circles represent posterior means, the thick horizontal bars 80% posterior intervals, and the thin bars 95% posterior intervals. The width of posterior intervals expresses the level of uncertainty of the estimate. Shown are also the effects of the obesity risk factors on binding potential of the $[^{18}\text{F}]$ Carfentanil and brain glucose uptake quantified with the $[^{18}\text{F}]$ FDG. Amy, amygdala; Cau, caudate; dACC, dorsal anterior cingulate cortex; Hipp, hippocampus; Ins, insula; MTemp, middle temporal gyrus; NAcc, nucleus accumbens; Put, putamen; rACC rostral anterior cingulate cortex; Tha, thalamus. Reproduced from the original publication I.

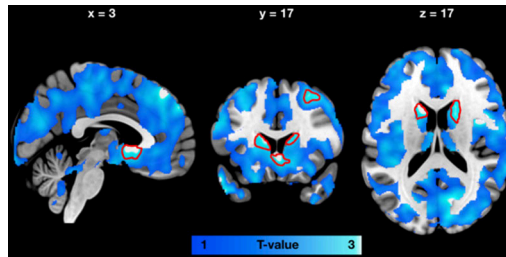


Figure 24 Brain regions (as defined by FDR-corrected SPM one-sample t test) where circulating anandamide (AEA) level was associated with lowered CB1R availability in the whole study group. Data are thresholded at $P < 0.05$ and false discovery rate (FDR) corrected at cluster level. The areas marked with red indicate clusters significant with Bonferroni-corrected cluster-defining P value ($0.05/8 = 0.00625$). Reproduced from the original publication I.

5.3.2 Study III: Lower whole-body insulin sensitivity, higher body adiposity and unfavourable lipid profile is associated with lower whole-brain CB1 receptor availability

Mean CB1R availability in the whole-brain did not differ statistically between the HR and the LR group (**Figure 25**). Lower CB1R availability of the whole brain associated with decreased whole-body insulin sensitivity indexed by M value and higher insulin-suppressed EGP adjusted with fat-free mass (**Figure 26**). Lower CB1R availability of the whole brain associated also with higher body weight, BMI, total body fat mass and visceral adipose tissue mass (**Table 3**).

Lower CB1R availability in the whole brain was associated with unfavourable lipid profile including higher levels of with total, non-HDL, remnant, VLDL and LDL cholesterol, triglycerides, free cholesterol, ratio of triglycerides to phosphoglycerides, ApoB and ApoB/ApoA1 ratio (**Figure 21**).

Serum AG (1+2) concentration associated negatively with the whole-brain CB1R availability ($r = -0.34$, $P = 0.04$).

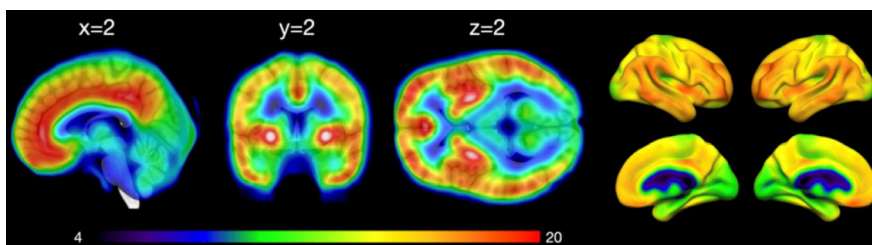


Figure 25 Mean volume of distribution (V_T) for the $[^{18}\text{F}]$ FMPEP- d_2 scans in the brain in the whole study population. Modified from the original publication III.

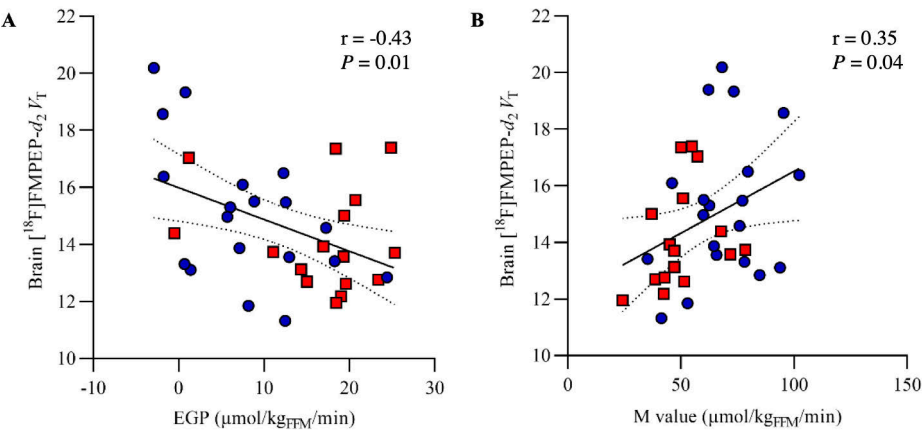


Figure 26 Association between the mean cannabinoid receptor type 1 (CB1R) availability in the whole-brain and insulin-suppressed hepatic endogenous glucose production (EGP) and whole-body insulin sensitivity indexed by M value adjusted with fat-free-mass (FFM). Pearson correlation between [¹⁸F]FMPEP-d₂ V_T values of the whole-brain and (A) EGP and (B) M value. Reproduced from the original publication III.

6 Discussion

6.1 Impaired brain insulin sensitivity in the pre-obese state

The aim of this thesis was to examine brain and peripheral tissue insulin signalling and ECS in healthy non-obese young men. We showed that altered brain insulin action and crosstalk between periphery, as well as ECS deregulation may precede obesity.

In Study I, we showed increased insulin-stimulated BGU in subjects with high as compared to low obesity risk. Whole-body and peripheral tissue GU rates in turn were lower in high versus low obesity risk subjects, and there was a negative correlation between insulin-stimulated BGU and whole-body GU (Study II). Our results are in line with previous published data in animals and humans with obesity [Bahri et al., 2018; Rebelos et al., 2021; Tuulari et al., 2013]. In addition to obesity, other insulin resistant states including impaired glucose tolerance and T2D are associated with higher insulin-stimulated BGU when compared with healthy populations [J. W. Eriksson et al., 2021; Hirvonen et al., 2011; Latva-Rasku et al., 2018]. It is thus suggested that the increased BGU is a manifestation of brain insulin resistance. Brain insulin signalling has several pivotal effects on the regulation of body energy homeostasis at central and peripheral levels, including feeding behaviour, energy expenditure and thermogenesis, WAT and hepatic lipid metabolism, and whole-body insulin sensitivity via suppression of hepatic EGP and stimulation of peripheral tissue GU. In the presence of brain insulin resistance, the physiological brain insulin actions are attenuated or even diminished, predisposing to increased homeostatic and hedonic food intake, further weight gain, as well as altered lipid and glucose fluxes. Accumulating evidence suggest that overnutrition and diet-induced hypothalamic inflammation are constitutive factors for the development of brain insulin resistance [Kullmann, Kleinridders, et al., 2020; Scherer et al., 2021]. Especially diet rich with SFAs associate with impaired insulin effect in the brain [Tschritter et al., 2009]. In addition, genetic background, maternal metabolism during pregnancy and advancing age are known to affect brain insulin sensitivity [Heni et al., 2015]. Interestingly, in Study I, we also found an association between higher familial obesity risk and increased insulin-simulated BGU.

Concerning the pre-obese and otherwise healthy state of our young subjects, we suggest our findings indicate that alterations in brain insulin signalling are relatively early events in metabolic disturbances.

Study II revealed associations between enlarged body fat mass, particularly accumulation of fat in abdominal but not femoral WAT depots, and increased BGU under insulin stimulation. Whereas visceral adiposity has long been acknowledged as a consistent indicator for metabolic diseases [Després & Lemieux, 2006], femoral SAT seems to have a protective role [Goodpaster et al., 2005; Goss & Gower, 2012]. A previous study showed an association between brain insulin sensitivity, adiposity and body fat distribution; hypothalamic insulin sensitivity correlated negatively with the ratio of VAT to SAT mass [Kullmann, Valenta, et al., 2020]. It however remains unsolved, whether the increased visceral adiposity plays a role in the pathogenesis of brain insulin resistance or is it a consequence of impaired brain insulin action.

As a potential manifestation of dysregulated organ crosstalk, we observed positive correlation between insulin-suppressed hepatic EGP as well as serum FFA levels and BGU (Study II). Preclinical and clinical studies have demonstrated that insulin action in the brain modulates both hepatic and WAT metabolism [Lewis et al., 2021; Scherer et al., 2021]. Central insulin action has direct effect on hepatic EGP by reducing gluconeogenic enzyme expression and indirect effects by suppressing WAT lipolysis and thus substrate fluxes to liver [Lewis et al., 2021]. It has been shown an association between increased insulin-stimulated BGU and insulin-suppressed EGP in subjects with morbid obesity [Rebelos et al., 2019] and AKT2 gene variant [Latva-Rasku et al., 2018], but not in lean subjects. We suggest our result to accord the view of defective organ crosstalk and reflect early metabolic dysregulation.

6.2 Lower Abdominal adipose tissue CB1 receptor availability associates with metabolic dysregulation in the pre-obese state

In Study III, young healthy subjects with overweight and risk for obesity exhibited lower abdominal adipose tissue CB1R availability as compared to subjects with low obesity risk. Accordingly, lower CB1R availability was associated with decreased insulin sensitivity, higher body adiposity, unfavourable lipid profile and inflammatory markers. Accumulating evidence indicates that ECS is dysregulated in obesity and associated metabolic disorders. It is suggested that the dysregulated ECS might even contribute to the development of obesity, while it modulates the body energy homeostasis at multiple sites [Gatta-Cherifi & Cota, 2016; Quarta et al., 2011].

ECS in WAT, and also in other tissues, has been studied mainly by assessing the tissue EC levels and the gene expression of CB1R and the main EC metabolizing enzymes. Higher levels of ECs in VAT has been found in both rodents and humans with obesity [D'Eon et al., 2008; Matias et al., 2006]. Reduced EC levels in SAT depots in obesity [Bennetzen et al., 2011; Matias et al., 2006] have been argued to reflect the differing nature of the SAT and VAT depots [You et al., 2011]. Lower expression of CB1R in VAT and SAT has been measured in subjects with obesity as compared to lean subjects [Bennetzen et al., 2011; Blüher et al., 2006; Engeli et al., 2005; Kempf et al., 2007], and increases in the CB1R expression followed by weight loss [Bennetzen et al., 2011]. However, there are also contradictory findings [You et al., 2011]. Some studies have reported obesity-related increases in CB1R as well as FAAH expression levels in both VAT and SAT [Bensaid et al., 2003; Pagano et al., 2007; Yan et al., 2007] or a positive correlation between the VAT CB1R expression and VAT area or adipocyte hypertrophy [Bordicchia et al., 2010; Yan et al., 2007]. The expression of EC degrading enzymes, especially the key enzyme FAAH, are differently affected by obesity, adipose tissue depot, and weight loss [Bennetzen et al., 2011; Blüher et al., 2006; Bordicchia et al., 2010; Engeli et al., 2005; Sarzani et al., 2009; You et al., 2011]. Despite mixed results, it is generally agreed that the biological action of activation of the ECS in WAT is to promote adipocyte differentiation, fatty acid *de novo* lipogenesis, triglyceride accumulation, and to reduce lipolysis and mitochondrial function, favouring thus white instead of beige or brown adipocytes, and inhibition of CB1Rs reverses these actions [Silvestri & Di Marzo, 2013]. ECS overactivity in WAT in turn is one hallmark of obesity [Quarta et al., 2011; Simon & Cota, 2017].

Thus far, only few studies have quantified peripheral tissue CB1R availability in humans using [^{18}F]FMPEP- d_2 PET. Unlike measuring CB1R expression in tissue biopsies, [^{18}F]FMPEP- d_2 PET does not display the total amount of CB1Rs in the tissue. Instead, [^{18}F]FMPEP- d_2 binds to CB1Rs that are not occupied with their natural ligands ECs. A previous study showed lower [^{18}F]FMPEP- d_2 binding, that is lower availability of unoccupied CB1Rs in abdominal VAT and SAT in healthy males with obesity (BMI: $32.9 \pm 4.6 \text{ kg/m}^2$) as compared with lean (BMI: $24.9 \pm 1.7 \text{ kg/m}^2$) males [Lahesmaa et al., 2018]. We observed convergent results; lower CB1R availability in abdominal WAT depots in healthy overweight subjects with obesity risk as compared to lean subjects with no obesity risk. This might be explained by lower total count of CB1Rs, increased WAT EC levels due to increased EC biosynthesis and/or decreased degradation. Indeed, EC production and degradation in white adipocytes appears to be negatively regulated by insulin and leptin. Insulin and leptin resistance, as observed in overweight and prolonged consumption of HFD, are associated with upregulated EC biosynthesis that in turn may predispose to

further accumulation of WAT and weight gain and a cycle promoting overactive ECS tone [Silvestri & Di Marzo, 2013].

Consistent with current understanding, the lower CB1R availability in abdominal WAT depots in the HR subjects we found, likely reflecting dysregulated ECS tone, correlated negatively with weight, BMI, total body fat and VAT and abdominal SAT masses. Although the skeletal muscle CB1R availability did not reach statistical difference between the HR and LR group, it correlated negatively with weight, BMI and VAT mass as well. Abdominal adipose tissue and skeletal muscle CB1R availability associated with unfavourable lipid profile. Abdominal SAT CB1R availability correlated positively with HDL cholesterol, which may represent the metabolic difference of distinct WAT depots. Interestingly, adipose tissue CB1R availability correlated negatively with fatty acids, including omega-6 PUFAs and linoleic acid. Excessive dietary linoleic acid has been implicated in the pathogenesis of weight gain and obesity in which one presented mechanism is an increased synthesis one ECs from linoleic acid leading to ECS overactivation [Naughton et al., 2016]. As a further indication of metabolic disturbance, we observed a negative correlation between WAT CB1R availabilities and GlycA, a composite biomarker of systemic inflammation and cardiometabolic risk [Connelly et al., 2017]. In previous studies, obesity-related ECS activation has been found to accompany WAT inflammation [Kempf et al., 2007]. Also HFD consumption and obesity initiate WAT inflammation manifested with secretion of inflammatory cytokines [Kawai et al., 2021].

CB1R availability in abdominal WAT depots correlated positively with the VAT and SAT insulin sensitivity assessed as insulin-stimulated GU and serum insulin-suppressed FFA levels, and the CB1R availability in intraperitoneal and retroperitoneal WAT depots also with the whole-body insulin sensitivity. This accords with the previous studies in which pharmacological blockade of CB1Rs in DIO mice induced correction of insulin resistance via enhanced expression of GLUT4 and glycolytic enzymes [Jbilo et al., 2005]. Concerning the skeletal muscle, we did not find associations between the tissue CB1R availability and insulin sensitivity. As WAT is a metabolically highly active and insulin sensitive tissue, it might be that the observed association between WAT ECS tone and insulin sensitivity reflect relatively early alterations in the pathogenesis and of obesity [Roden & Shulman, 2019].

The level of circulating ECs, especially 2-AG, are increased in obesity and particularly with excess VAT. Although the pathological role and the origin of circulating ECs remains unsolved, they are thought to express the overactivity of peripheral ECS, increased synthesis and/or decreased degradation of ECs, which might be modulated also by insulin sensitivity, genetic factors and the gender [Silvestri & Di Marzo, 2013]. According to previous studies, it is suggested that the

circulating level of 2-AG might apply as a biomarker of VAT rather than abdominal SAT, whereas AEA would reflect insulin resistance in SAT. We found positive correlation with AG (1+2) and BMI, but not WAT masses. AG (1+2) and AEA both associated with indices of systemic (M value, Rd and EGP), but not tissue-specific insulin sensitivity. In addition, according to previous studies, higher circulating AG (1+2) level associated with unfavourable lipid profile as well as higher GlycA level. Blocking CB1Rs with the inverse agonist Rimonabant showed an increase in HDL cholesterol, decrease in triglyceride level and ApoB/ApoA1 ratio, a shift towards larger LDL particles and a decrease in C-reactive protein in subjects with obesity, and it was suggested that the improvements would not be only secondary to weight loss [Després et al., 2005]. In sum, our results reflect metabolic dysregulation already in the pre-obese state.

6.3 Central CB1 receptor availability associates with metabolic dysregulation in the pre-obese state

In Study I, we investigated the CB1R availability in 21 bilateral brain regions involved in emotion and food reward based on previous studies [Hirvonen et al., 2012; Tuominen et al., 2014; Tuulari et al., 2013]. In Study III, the CB1R availability of the whole brain were assessed. The risk-group comparison showed no significance difference in the brain CB1R availability in either studies. However, the familial obesity risk, comprising of parental overweight/obesity/T2D, correlated negatively with the brain CB1R availability in Study I. Furthermore, higher BMI (Study I and III), total body fat mass and VAT mass (Study III) associated with lower brain CB1R availability.

Previous [^{18}F]FMPEP- d_2 PET study showed lower brain, as well as abdominal VAT and SAT CB1R availability in subjects with obesity as compared to lean subjects [Lahesmaa et al., 2018]. Other studies have shown negative correlation with BMI and brain CB1R availability [Ceccarini et al., 2016; Hirvonen et al., 2012]. Interestingly, the link between the lower CB1R availability and higher BMI was observed in brain areas involved in homeostatic energy balance regulation including the hypothalamus and brainstem. In subjects with eating disorders, such as anorexia or bulimia nervosa, the negative correlation between the CB1R availability and BMI has also been observed in the mesolimbic reward system [Ceccarini et al., 2016]. Subjects with anorexia nervosa have however increased overall cerebral CB1R availability as compared to healthy subjects [Gérard et al., 2011]. Earlier autoradiography studies have found lower CB1R availability in several extrahypothalamic brain regions in DIO mice than in lean mice, and the CB1R availability correlated negatively with total calorie intake and consumption of highly

palatable food [Harrold et al., 2002]. As upregulated EC levels are measured in several brain regions, including the hypothalamus [Higuchi et al., 2011] and hippocampus [Massa et al., 2010] in rodent models of obesity and prolonged HFD consumption, it is suggested that the lower cerebral CB1R availability results from increased cerebral EC levels due to overactive ECS [Engeli, 2008]. A HFD, typically rich in omega-6 and poor in omega-3 PUFAs, increased AEA [Berger et al., 2001] and 2-AG [Watanabe et al., 2003] levels in animal models. When considering the pre-obese state of our participants, our results indicate comparable effects.

Of the studied serum ECs, AEA level correlated negatively with CB1R availability in the ventral striatum (Study I), while AG (1+2) level had negative relationship with the CB1R availability in the whole brain (Study III). A recent study showed likewise negative correlation between serum EC levels, including AEA and AG (1+2), and central CB1R availability in healthy subjects with mild overweight (BMI 25.3 ± 3.7 kg/m²) [Dickens et al., 2020]. Our result confirm that ECS is dysregulated already in the pre-obese state. Circulating EC levels might reflect the peripheral ECS tone, or even be a causative factor of metabolic deregulation [Silvestri & Di Marzo, 2013]. Accordingly, when studied the metabolomics, unfavourable lipid profile and higher levels of circulating fatty acids, including omega-6 PUFAs and linoleic acid associated with decreased brain CB1R availability (Study III).

Whole-body insulin sensitivity (M value) correlated positively and insulin-suppressed EGP negatively with the whole brain CB1R availability (Study III). It has been proposed that insulin downregulates ECS, whereas in conditions of insulin resistance, such as obesity, sustained hyperinsulinemia and hyperglycaemia results in an increase in adipocyte size and number and hypertrophic pancreatic β -cells, and ECS upregulation. It is suggested that this modulation of ECS by insulin might concern other tissues as well [Matias & Di Marzo, 2007]. As insulin resistance is a common feature of obesity, it might be that insulin resistance promotes or worsens ECS deregulation that in turn further enhances weight gain [Matias & Di Marzo, 2007; Quarta et al., 2011]. A link between cerebral EC signalling and hepatic insulin sensitivity was found in a study, where central CB1R activation led to impaired insulin-induced suppression of hepatic EGP without alterations in hepatic insulin signalling [O'Hare et al., 2011]. Furthermore, when exposed rats for three day HFD, a model of early insulin resistance characterized by hepatic and hypothalamic insulin resistance [Ono et al., 2008], blocking the brain CB1Rs restored the hepatic insulin sensitivity [O'Hare et al., 2011]. The study demonstrates that upregulated cerebral ECS tone may induce hepatic insulin resistance. We suggest our result to be in line with the presented preclinical data demonstrating the crosstalk between the brain and peripheral ECS and insulin action.

6.4 Strengths and limitations

The strength of the current study is the application of the dynamic multi-tracer PET imaging that enables quantification of the brain and peripheral tissue metabolism and receptor binding *in vivo*. Combining PET with hyperinsulinemic–euglycemic clamp, the golden standard method for assessing whole-body insulin sensitivity, allows simultaneous assessment of hepatic EGP. In addition to PET and clamp studies, the characteristics of the subjects' were carefully determined using MRI and CT imaging, as well as air displacement plethysmograph (the Bod Pod system) for quantifying body adiposity, and blood sampling to measure several metabolic biomarkers and circulating ECs. These comprehensive measurements allow modelling of the brain-periphery interactions. The new whole-body PET scanner Quadra in Turku PET Centre enables simultaneous dynamic imaging of the whole-body, and using Quadra in further studies would allow even more precise studying of the brain-periphery interactions.

As a limitation, our studies comprised only males. Therefore, the results may not be directly generalized to females. There have been divergent results concerning the effects of sex on brain glucose metabolism and insulin sensitivity [Feng et al., 2022; Gur et al., 1995]. Also, studies applying IN insulin administration have suggested sex-dependent differences in the effects of central insulin on appetite and body weight, although the feeding states in those studies differed [Flint et al., 2007; Hallschmid et al., 2004, 2012; Jauch-Chara et al., 2012]. According to previous large-scale cohort study however, insulin-stimulated BGU was not significantly affected by sex [Rebelos et al., 2021]. According to ECS, it seems that estrogen negatively modulates CB1R-induced changes in appetite, body temperature and activity of POMC neurons [Kellert et al., 2009]. Furthermore, there is a bidirectional interaction between the ECS and gonadal hormones. EC signalling in the hypothalamus and anterior pituitary reduces the release of gonadal hormones, which in turn, particularly estrogen, alter ECS-related protein expression and response to ECs [Gorzalka & Dang, 2012]. Whether this interaction has an impact on feeding behaviour or results in sex-dependent differences on ECS function apparently needs further investigation.

The subjects in the high obesity risk group were older than the low-risk subjects. Age is known to be a predictor of brain insulin sensitivity; cerebral insulin signalling decreases with advancing age, as happens in the periphery as well [Kullmann et al., 2016]. However, the effects of age were controlled in the statistical analyses whenever possible. Again, in the study consisting of subjects with wide age range (women 23–80 and men 20–69 years), showed that although the whole-body insulin sensitivity was the best predictor of insulin-stimulated BGU, age associated negatively with BGU. The association was strongest in the limbic and temporal lobes, a trend toward a negative correlation was found in the frontal and parietal

lobes, while no correlation in occipital lobes [Rebelos et al., 2021]. In BGU analysis in Study I and II, the age was used as a covariate with unchanged results.

Hepatic EGP values in Study II and III were mainly negative in both high and low-risk group indicating EGP suppression under insulin stimulation. Wide range, and also negative EGP values has been shown in previous study in subjects without diabetes, reflecting the amount of lean body mass [Natali et al., 2000]. Similarly, one previous study presented a progressive decline in insulin suppression of hepatic EGP with increasing VAT mass and hepatic lipid content (HLC) [Gastaldelli et al., 2007]. A recent study comprising of lean non-Asian Indian subjects, showed 95% percentile of HLC to be 1.85%, lower than the previously determined upper normal level 5.56% [Szczepaniak et al., 2005]. Although we did not measure the HLC, we assume it under 1.85% in our subjects thus explaining the effective suppression of EGP.

PET has a limited spatial resolution, typically 4–5 mm resulting in partial volume effect (PVE) that limits studying very small regions, such as hypothalamus, with PET. Motion artefact is another concern when scanning moving structures with PET [Cherry & Dahlbom, 2006]. To limit the effect of spillover due to PVE and motion we carefully draw several ROIs and VOIs in several slices of images avoiding large vessels. In [^{18}F]FDG analysis, the mean K_i values were then extracted from each tissue and used in the analysis.

In study I and II, we investigated CB1R binding with PET and CB1R inverse agonist [^{18}F]FMPEP- d_2 . As the method quantifies the amount of available CB1Rs that are not occupied with their natural ligands, it is not possible to measure the total amount and density of CB1Rs or their affinity. Therefore, changes in the CB1R availability may result from alterations in EC levels, receptor density or affinity, or mixture of them. A previous study in mice model of Alzheimer's disease demonstrated altered brain CB1R availability with unchanged CB1R availability [Takkinen et al., 2018] suggesting that the altered receptor availability represent alterations in EC levels or receptor affinity. Rodent models of obesity have detected reduced CB1R and EC degrading enzyme gene expression in WAT accompanied with increased circulating EC levels indicating a negative feedback loop regulation [Engeli et al., 2005].

Importantly, as our study design is cross-sectional, we cannot ascertain the causality of the observed effects; whether the detected metabolic differences and receptor availabilities between the two risk groups are a cause or a consequence of obesity risk and how do they interact.

6.5 Clinical implications and future aspects

Obesity is a complex disease, characterized by defective interactions between the brain and periphery, altered interorgan substrate fluxes and handling, and deregulated neural signalling pathways. Our results show that these alterations are already present in non-obese subjects with overweight. Concerning the obesity epidemic, understanding the pathogenic pathways predisposing to weight gain is essential, as it would enable launching early interventions and discovering new and maybe more individualized therapeutic targets to treat obesity.

Previous studies from our centre and others have discussed the methods investigating brain insulin sensitivity, and the term brain insulin resistance [Kullmann, Kleinridders, et al., 2020; Latva-Rasku, 2020; Rebelos, 2020]. By applying different methods distinct study groups have gained evidence of disturbances in central insulin action in metabolic diseases, and the term brain insulin resistance has been approved. Available imaging methods for investigating brain insulin action in humans include [^{18}F]FDG PET, MEG and fMRI. Hyperinsulinemic-euglycemic clamp enables assessing of brain glucose handling under insulin-stimulation in relation to other tissues, while intranasal insulin administration allows more selective evaluation of the central and peripheral effects of insulin within the CNS. IN administered insulin spreads throughout the brain and only small proportion is absorbed into circulation, while during the clamp, the insulin effect is systemic [Kullmann, Kleinridders, et al., 2020]. Combining these different approaches would allow building comprehensive understanding of brain insulin action, but this approach is precluded by the methodological complexity and necessity of highly trained personnel and adequate equipment.

The studies of this thesis are part of PROSPECT research project (Clinicaltrials.gov, NCT03106688), in which we have studied the brain and whole-body insulin sensitivity, central u-opioid (MOR) receptor, as well as CB1R availability in brain and peripheral tissues. Radiation exposure limits the further PET studies in the same population. However, fMRI with IN insulin administration would provide complementary information about the effects of insulin on certain brain regions as compared to insulin-stimulated BGU acquired with [^{18}F]FDG PET during clamp. It would be interesting to test whether the effect of insulin in specific brain regions' activity is weaker in subjects with high as compared to low obesity risk, and does the effect associate with VAT mass, as in previous study in subjects with obesity [Kullmann et al., 2015]. Considering the better resolution of MRI than PET/CT, the assessment of insulin action within the hypothalamus would be of special interest, as this structure cannot be accurately delineated and quantified with PET. Simultaneous hyperinsulinemic-euglycemic clamp would allow assessment of potential improvements in the whole-body insulin sensitive and risk-group differences, as well as confirm the association of central insulin action and whole-

body insulin sensitivity that we found in Study II. Investigating the relationship between central insulin and hepatic EGP, that we also found in Study II, with IN insulin application would be interesting but would require exposing the subjects to radiation when using [^{18}F]FDG PET. Follow-up study within the ongoing PROSPECT project will determine the change in BMI and body composition and their relation to the baseline results in PET studies. Moreover, further studies and effort is needed to resolve the causality between defects in brain insulin signalling and obesity and associated metabolic diseases.

According to ECS, the next interesting step would be determining CB1R and EC expression from tissue, particularly WAT biopsies to determine whether the lower CB1R availability in high as compared to low obesity risk subjects we found in Study III, results from altered CBR1 density or EC level. For such a study, it would be reasonable to recruit a new sample of participants, both male and female subjects with and without obesity, perform [^{18}F]FMPEP- d_2 PET study, and obtain the tissue biopsies at the same visit before the scan, so that the tissue CB1R and EC levels would represent the same metabolic state. Quantifying circulating ECs would offer a chance to compare the serum and tissue EC levels as well. Better understanding of the contribution of WAT CB1Rs in the regulation of whole-body energy metabolism would also profit targeting treatment of obesity. Concerning the brain CB1Rs, and their interaction with central insulin signalling, and other neural signal networks, requires further investigations too.

7 Conclusions

The thesis aimed to investigate obesity risk factors focusing in brain and peripheral tissue insulin sensitivity and endocannabinoid system applying PET imaging. The main findings of the thesis were the following:

1. Brain insulin sensitivity, quantified as insulin-simulated brain glucose uptake, is decreased already in non-obese state, in the presence of overweight. Decreased brain insulin sensitivity associates with decreased whole-body and skeletal muscle insulin sensitivity, and decreased suppression of hepatic EGP and white adipose tissue lipolysis. Familial obesity risk, including parental overweight/obesity/T2D, associates with decreased brain insulin sensitivity. These results add to the current knowledge on the development of obesity, suggesting that altered brain insulin signalling and impaired crosstalk between the brain and peripheral organs may exist already in subjects with overweight and risk factors for obesity.
2. Subjects with overweight and risk factors for developing obesity have lower abdominal adipose tissue CB1R availability as compared to lean subjects. The lower CB1R availability in abdominal adipose tissue depots associates with decreased adipose tissue insulin sensitivity, enlarged body fat mass, unfavorable lipid profile and higher inflammatory markers. Of the circulating endocannabinoids and related structures, the levels of arachidonic acid, anandamide and arachidonoyl glycerol correlated negatively with whole-body insulin sensitivity. Serum arachidonoyl glycerol level associated also with reduced suppression of hepatic EGP, higher BMI, unfavorable lipid profile and higher levels of systemic inflammatory markers. These results indicate that endocannabinoid system dysregulation in white adipose tissue may be an early manifestation of metabolic disorders, including dyslipidemia, insulin resistance and abdominal obesity.
3. Lower cerebral CB1R availability associates with decreased whole-body insulin sensitivity, decreased suppression of hepatic EGP, as well as higher weight, BMI, enlarged visceral adipose tissue mass and unfavorable lipid

profile. Reduced CB1R availability in cerebral pathways regulating food intake associates with higher level of circulating anandamide, whereas globally decreased brain CB1R availability associates with higher serum arachidonoyl glycerol level. These findings suggest that alterations in brain endocannabinoid signaling take place early, and may even represent the pathological process in the development of obesity comprising of defective crosstalk between the brain and peripheral endocannabinoid and insulin signalling.

Acknowledgements

This study was carried out at the Turku PET Centre, and within the Finnish Centre of Excellence in Cardiovascular and Metabolic Diseases, supported by Academy of Finland, University of Turku, Turku University Hospital and Åbo Akademi University during the years 2017–2023. For financial support I wish to thank Jalmari and Rauha Ahokas Foundation, Turunmaa Duodecim Society, Turku University Hospital Foundation for Education and Research, The Diabetes Research Foundation, Orion Research Foundation and The State Research Funding.

I express my sincerely gratitude to my supervisors Professor Pirjo Nuutila and Professor Lauri Nummenmaa for the opportunity to conduct my doctoral thesis work under your guidance. Pirjo, I admire your knowledge and groundbreaking work in the field of metabolic research and PET imaging. I have felt privileged to be involved in your research group. Lauri, I am grateful for your excellent guidance and encouraging attitude, as well as careful language check of this thesis. You both have had trust on the PROSPECT project and encouraged me to accomplish this challenging journey.

I wish a warm thank to Docent Kirsi Timonen for accepting the invitation to be my opponent. I'm very much looking forward to meeting you. I appreciate the work of Professor Hubert Preissl and Docent Sanni Söderlund for reviewing this thesis and giving me valuable feedback. I acknowledge Professor Kirsi Pietiläinen and Docent Marco Bucci for being in my doctoral follow-up group and Marco Bucci also for the expertise in brain modelling and being one of my co-authors.

I express the warmest thanks to Tatu Kantonen, with whom I have shared the PROSPECT project. Thank you for your companionship, precise work and determined attitude. Despite some setbacks we encountered, I have had a strong trust that together we would manage the early mornings and long days with the PET studies. I am remarkably thankful for the study participants. This thesis would not have been possible without your commitment. I wish to thank all the co-authors that I have had an opportunity to work with. Thank you Eleni Rebelos, Aino Latva-Rasku, Prince Dadson, Tomi Karjalainen, Kari Kalliokoski, Kirsi Laitinen, Noora Houttu, Merja Haaparanta-Solin, Richard Aarnio, Vesa Oikonen, Alex Dickens, Annie von Eyken, Anna K. Kirjavainen, Semi Helin, Jussi Hirvonen, Johan Rajander

and Tapani Rönnemaa. A special thanks to Sanna Laurila, Minna Lahesmaa-Hatting, Aino Latva-Rasku and Miikka Honka for teaching me the basics of the PET image analysis. Eleni, I wish to thank you also for the great collaboration and guidance in so many practical issues. Aino, I appreciate your support and experience that you have shared as well. Prince, I wish to thank you for your encouragement and positivity.

I thank docent Jarna Hannukainen and study nurse Mia Koutu for getting me started with the clamp studies, Heikki Laurikainen for guiding me and Tatu with [^{18}F]FMPEP- d_2 studies and Lihua Sun for the help with PROSPECT's fMRI studies. I wish to thank study nurse Sanna Himanen for the precious help with the PROSPECT's follow-up visits as well as the inspiring ideas that you have shared. I want to thank also all the other people with whom I have shared the PET analysis room during these years and the whole Nummenmaa lab team.

I have had a privilege to work in the Turku PET Centre that is extremely innovative place to conduct research. I express my gratitude to Professor Juhani Knuuti for allowing this possibility. Heartfelt thanks to the wonderful staff of the PET Centre. Minna Aatsinki, Sanna Suominen, Heidi Partanen, Eija Salo, Anne-Mari Jokinen, Hannele Lehtinen, Virva Saunavaara, Tuula Tolvanen, Mika Teräs as well as all the other great laboratory technicians, radiochemists, radiographers and physicians. Thank you all for your excellent and dedicated work, guidance and kindness. It has been pleasure to work with you. I am extremely thankful to Vesa Oikonen for the help with data analysis and modelling. I wish my warm thank also to Rami Mikkola and Marko Tättäläinen for helping with IT issues, Sauli Piirola and Timo Laitinen for providing PET software tools and support with them, and Lenita Saloranta and Minna Kangasperko for the assistance with administrative matters.

I wish to thank my superiors in the clinics for granting me time of for research. Thank you Markus Juonala and Minna Soinio in Turku and Tuula Pekkarinen in Pori. I wish my warmest thanks to my colleagues in the department of endocrinology in Turku and Pori. Thank you for your support Minna Soinio, Pia Hakanen, Lassi Nelimarkka, Heidi Immonen, Antti Autere, Nelli Tuomola, Aku Virta, Aino Latva-Rasku, Matti Vuori, Tyko Hellsten, Tuula Pekkarinen, Pirkko Korsoff and Hanna Laine.

Finally, I wish to thank my dear parents and my dear sister for your endless love and support. I am grateful for your encouragement over these years. I know I can always turn to you.

Turku, December 2023
Laura Pekkarinen

References

- Abate, N., Burns, D., Peshock, R. M., Garg, A., & Grundy, S. M. (1994). Estimation of adipose tissue mass by magnetic resonance imaging: Validation against dissection in human cadavers. *Journal of Lipid Research*, 35(8), 1490–1496. [https://doi.org/10.1016/s0022-2275\(20\)40090-2](https://doi.org/10.1016/s0022-2275(20)40090-2)
- Afshin, A., Forouzanfar, M. H., Reitsma, M. B., Sur, P., Estep, K., Lee, A., Marczak, L., Mokdad, A. H., Moradi-Lakeh, M., Naghavi, M., Salama, J. S., Vos, T., Abate, K. H., Abbafati, C., Ahmed, M. B., Al-Aly, Z., Alkerwi, A., Al-Raddadi, R., Amare, A. T., ... Murray, C. J. L. (2017). Health Effects of Overweight and Obesity in 195 Countries over 25 Years. *The New England Journal of Medicine*, 377(1), 13–27. <https://doi.org/10.1056/NEJMoa1614362>
- Aimé, P., Hegoburu, C., Jaillard, T., Degletagne, C., Garcia, S., Messaoudi, B., Thevenet, M., Lorsignol, A., Duchamp, C., Mouly, A.-M., & Julliard, A. K. (2012). A physiological increase of insulin in the olfactory bulb decreases detection of a learned aversive odor and abolishes food odor-induced sniffing behavior in rats. *PloS One*, 7(12), e51227. <https://doi.org/10.1371/journal.pone.0051227>
- Anjana, R. M., Lakshminarayanan, S., Deepa, M., Farooq, S., Pradeepa, R., & Mohan, V. (2009). Parental history of type 2 diabetes mellitus, metabolic syndrome, and cardiometabolic risk factors in Asian Indian adolescents. *Metabolism*, 58(3), 344–350. <https://doi.org/https://doi.org/10.1016/j.metabol.2008.10.006>
- Aubrey, J., Esfandiari, N., Baracos, V. E., Buteau, F. A., Frenette, J., Putman, C. T., & Mazurak, V. C. (2014). Measurement of skeletal muscle radiation attenuation and basis of its biological variation. *Acta Physiologica (Oxford, England)*, 210(3), 489–497. <https://doi.org/10.1111/apha.12224>
- Bady, I., Marty, N., Dallaporta, M., Emery, M., Gyger, J., Tarussio, D., Foretz, M., & Thorens, B. (2006). Evidence from glut2-null mice that glucose is a critical physiological regulator of feeding. *Diabetes*, 55(4), 988–995. <https://doi.org/10.2337/diabetes.55.04.06.db05-1386>
- Bahri, S., Horowitz, M., & Malbert, C. H. (2018). Inward Glucose Transfer Accounts for Insulin-Dependent Increase in Brain Glucose Metabolism Associated with Diet-Induced Obesity. *Obesity*, 26(8), 1322–1331. <https://doi.org/10.1002/oby.22243>
- Bamshad, M., Song, C. K., & Bartness, T. J. (1999). CNS origins of the sympathetic nervous system outflow to brown adipose tissue. *The American Journal of Physiology*, 276(6), R1569-78. <https://doi.org/10.1152/ajpregu.1999.276.6.R1569>
- Banks, W. A., Owen, J. B., & Erickson, M. A. (2012). Insulin in the brain: There and back again. In *Pharmacology and Therapeutics* (Vol. 136, Issue 1, pp. 82–93). <https://doi.org/10.1016/j.pharmthera.2012.07.006>
- Baufeld, C., Osterloh, A., Prokop, S., Miller, K. R., & Heppner, F. L. (2016). High-fat diet-induced brain region-specific phenotypic spectrum of CNS resident microglia. *Acta Neuropathologica*, 132(3), 361–375. <https://doi.org/10.1007/s00401-016-1595-4>
- Baye, T. M., Zhang, Y., Smith, E., Hillard, C. J., Gunnell, J., Myklebust, J., James, R., Kissebah, A. H., Olivier, M., & Wilke, R. A. (2008). Genetic variation in cannabinoid receptor 1 (CNR1) is associated with derangements in lipid homeostasis, independent of body mass index. *Pharmacogenomics*, 9(11), 1647–1656. <https://doi.org/10.2217/14622416.9.11.1647>

- Beddows, C. A., & Dodd, G. T. (2021). Insulin on the brain: The role of central insulin signalling in energy and glucose homeostasis. *Journal of Neuroendocrinology*, 33(4), e12947. <https://doi.org/10.1111/jne.12947>
- Bellocchio, L., Lafenêtre, P., Cannich, A., Cota, D., Puente, N., Grandes, P., Chaouloff, F., Piazza, P. V., & Marsicano, G. (2010). Bimodal control of stimulated food intake by the endocannabinoid system. *Nature Neuroscience*, 13(3), 281–283. <https://doi.org/10.1038/nn.2494>
- Bénard, G., Massa, F., Puente, N., Lourenço, J., Bellocchio, L., Soria-Gómez, E., Matias, I., Delamarre, A., Metna-Laurent, M., Cannich, A., Hebert-Chatelain, E., Mulle, C., Ortega-Gutiérrez, S., Martín-Fontecha, M., Klugmann, M., Guggenhuber, S., Lutz, B., Gertsch, J., Chaouloff, F., ... Marsicano, G. (2012). Mitochondrial CB₁ receptors regulate neuronal energy metabolism. *Nature Neuroscience*, 15(4), 558–564. <https://doi.org/10.1038/nn.3053>
- Bender, D., Munk, O. L., Feng, H. Q., & Keiding, S. (2001). Metabolites of (18)F-FDG and 3-O-(11)C-methylglucose in pig liver. *Journal of Nuclear Medicine : Official Publication, Society of Nuclear Medicine*, 42(11), 1673–1678.
- Benedict, C., Brede, S., Schiöth, H. B., Lehnert, H., Schultes, B., Born, J., & Hallschmid, M. (2011). Intranasal insulin enhances postprandial thermogenesis and lowers postprandial serum insulin levels in healthy men. *Diabetes*, 60(1), 114–118. <https://doi.org/10.2337/db10-0329>
- Benedict, C., Kern, W., Schultes, B., Born, J., & Hallschmid, M. (2008). Differential sensitivity of men and women to anorexigenic and memory-improving effects of intranasal insulin. *The Journal of Clinical Endocrinology and Metabolism*, 93(4), 1339–1344. <https://doi.org/10.1210/jc.2007-2606>
- Bennetzen, M. F., Wellner, N., Ahmed, S. S., Ahmed, S. M., Diep, T. A., Hansen, H. S., Richelsen, B., & Pedersen, S. B. (2011). Investigations of the human endocannabinoid system in two subcutaneous adipose tissue depots in lean subjects and in obese subjects before and after weight loss. *International Journal of Obesity (2005)*, 35(11), 1377–1384. <https://doi.org/10.1038/ijo.2011.8>
- Bensaid, M., Gary-Bobo, M., Esclangon, A., Maffrand, J. P., Le Fur, G., Oury-Donat, F., & Soubrié, P. (2003). The cannabinoid CB₁ receptor antagonist SR141716 increases Acrp30 mRNA expression in adipose tissue of obese fa/fa rats and in cultured adipocyte cells. *Molecular Pharmacology*, 63(4), 908–914. <https://doi.org/10.1124/mol.63.4.908>
- Berge, K., Piscitelli, F., Hoem, N., Silvestri, C., Meyer, I., Banni, S., & Di Marzo, V. (2013). Chronic treatment with krill powder reduces plasma triglyceride and anandamide levels in mildly obese men. *Lipids in Health and Disease*, 12, 78. <https://doi.org/10.1186/1476-511X-12-78>
- Berger, A., Crozier, G., Bisogno, T., Cavaliere, P., Innis, S., & Di Marzo, V. (2001). Anandamide and diet: inclusion of dietary arachidonate and docosahexaenoate leads to increased brain levels of the corresponding N-acyl ethanolamines in piglets. *Proceedings of the National Academy of Sciences of the United States of America*, 98(11), 6402–6406. <https://doi.org/10.1073/pnas.101119098>
- Berglund, E. D., Liu, T., Kong, X., Sohn, J.-W., Vong, L., Deng, Z., Lee, C. E., Lee, S., Williams, K. W., Olson, D. P., Scherer, P. E., Lowell, B. B., & Elmquist, J. K. (2014). Melanocortin 4 receptors in autonomic neurons regulate thermogenesis and glycemia. *Nature Neuroscience*, 17(7), 911–913. <https://doi.org/10.1038/nn.3737>
- Berthoud, H.-R. (2004). Mind versus metabolism in the control of food intake and energy balance. *Physiology & Behavior*, 81(5), 781–793. <https://doi.org/10.1016/j.physbeh.2004.04.034>
- Bessell, E. M., Foster, A. B., & Westwood, J. H. (1972). The use of deoxyfluoro-D-glucopyranoses and related compounds in a study of yeast hexokinase specificity. *The Biochemical Journal*, 128(2), 199–204. <https://doi.org/10.1042/bj1280199>
- Blüher, M. (2019). Obesity: global epidemiology and pathogenesis. *Nature Reviews. Endocrinology*, 15(5), 288–298. <https://doi.org/10.1038/s41574-019-0176-8>
- Blüher, M., Engeli, S., Klöting, N., Berndt, J., Fasshauer, M., Bátkai, S., Pacher, P., Schön, M. R., Jordan, J., & Stumvoll, M. (2006). Dysregulation of the peripheral and adipose tissue endocannabinoid system in human abdominal obesity. *Diabetes*, 55(11), 3053–3060. <https://doi.org/10.2337/db06-0812>

- Bódis, K., & Roden, M. (2018). Energy metabolism of white adipose tissue and insulin resistance in humans. *European Journal of Clinical Investigation*, 48(11), e13017. <https://doi.org/10.1111/eci.13017>
- Boersma, G. J., Johansson, E., Pereira, M. J., Heurling, K., Skrtic, S., Lau, J., Katsogiannos, P., Panagiotou, G., Lubberink, M., Kullberg, J., Ahlström, H., & Eriksson, J. W. (2018). Altered Glucose Uptake in Muscle, Visceral Adipose Tissue, and Brain Predict Whole-Body Insulin Resistance and may Contribute to the Development of Type 2 Diabetes: A Combined PET/MR Study. *Hormone and Metabolic Research = Hormon- Und Stoffwechselforschung = Hormones et Metabolisme*, 50(8), 627–639. <https://doi.org/10.1055/a-0643-4739>
- Bolli, G. B., & Fanelli, C. G. (1999). Physiology of glucose counterregulation to hypoglycemia. *Endocrinology and Metabolism Clinics of North America*, 28(3), 467–493, v. [https://doi.org/10.1016/s0889-8529\(05\)70083-9](https://doi.org/10.1016/s0889-8529(05)70083-9)
- Bordicchia, M., Battistoni, I., Mancinelli, L., Giannini, E., Refi, G., Minardi, D., Muzzonigro, G., Mazzucchelli, R., Montironi, R., Piscitelli, F., Petrosino, S., Dessi-Fulgheri, P., Rappelli, A., Di Marzo, V., & Sarzani, R. (2010). Cannabinoid CB1 receptor expression in relation to visceral adipose depots, endocannabinoid levels, microvascular damage, and the presence of the Cnr1 A3813G variant in humans. *Metabolism: Clinical and Experimental*, 59(5), 734–741. <https://doi.org/10.1016/j.metabol.2009.09.018>
- Born, J., Lange, T., Kern, W., McGregor, G. P., Bickel, U., & Fehm, H. L. (2002). Sniffing neuropeptides: a transnasal approach to the human brain. *Nature Neuroscience*, 5(6), 514–516. <https://doi.org/10.1038/nn849>
- Bøtker, H. E., Böttcher, M., Schmitz, O., Gee, A., Hansen, S. B., Cold, G. E., Nielsen, T. T., & Gjedde, A. (1997). Glucose uptake and lumped constant variability in normal human hearts determined with [18F]fluorodeoxyglucose. *Journal of Nuclear Cardiology: Official Publication of the American Society of Nuclear Cardiology*, 4(2 Pt 1), 125–132. [https://doi.org/10.1016/s1071-3581\(97\)90061-1](https://doi.org/10.1016/s1071-3581(97)90061-1)
- Boucher, J., Kleinriders, A., & Kahn, C. R. (2014). Insulin receptor signaling in normal and insulin-resistant states. *Cold Spring Harbor Perspectives in Biology*, 6(1). <https://doi.org/10.1101/cshperspect.a009191>
- Bray, G. A., Kim, K. K., & Wilding, J. P. H. (2017). Obesity: a chronic relapsing progressive disease process. A position statement of the World Obesity Federation. In *Obesity reviews: an official journal of the International Association for the Study of Obesity* (Vol. 18, Issue 7, pp. 715–723). <https://doi.org/10.1111/obr.12551>
- Brito, M. N., Brito, N. A., Baro, D. J., Song, C. K., & Bartness, T. J. (2007). Differential activation of the sympathetic innervation of adipose tissues by melanocortin receptor stimulation. *Endocrinology*, 148(11), 5339–5347. <https://doi.org/10.1210/en.2007-0621>
- Brochu, M., Starling, R. D., Tchernof, A., Matthews, D. E., Garcia-Rubi, E., & Poehlman, E. T. (2000). Visceral adipose tissue is an independent correlate of glucose disposal in older obese postmenopausal women. *The Journal of Clinical Endocrinology and Metabolism*, 85(7), 2378–2384. <https://doi.org/10.1210/jcem.85.7.6685>
- Broyd, S. J., Demanuele, C., Debener, S., Helps, S. K., James, C. J., & Sonuga-Barke, E. J. S. (2009). Default-mode brain dysfunction in mental disorders: a systematic review. *Neuroscience and Biobehavioral Reviews*, 33(3), 279–296. <https://doi.org/10.1016/j.neubiorev.2008.09.002>
- Brüning, J. C., Gautam, D., Burks, D. J., Gillette, J., Schubert, M., Orban, P. C., Klein, R., Krone, W., Müller-Wieland, D., & Kahn, C. R. (2000). Role of brain insulin receptor in control of body weight and reproduction. *Science (New York, N.Y.)*, 289(5487), 2122–2125. <https://doi.org/10.1126/science.289.5487.2122>
- Brünner, Y. F., Benedict, C., & Freiherr, J. (2013). Intranasal insulin reduces olfactory sensitivity in normosmic humans. *The Journal of Clinical Endocrinology and Metabolism*, 98(10), E1626–30. <https://doi.org/10.1210/jc.2013-2061>

- Cahill, G. F. J., Herrera, M. G., Morgan, A. P., Soeldner, J. S., Steinke, J., Levy, P. L., Reichard, G. A. J., & Kipnis, D. M. (1966). Hormone-fuel interrelationships during fasting. *The Journal of Clinical Investigation*, 45(11), 1751–1769. <https://doi.org/10.1172/JCI105481>
- Cannon, B., & Nedergaard, J. (2004). Brown adipose tissue: function and physiological significance. *Physiological Reviews*, 84(1), 277–359. <https://doi.org/10.1152/physrev.00015.2003>
- Cardinal, P., André, C., Quarta, C., Bellocchio, L., Clark, S., Elie, M., Leste-Lasserre, T., Maitre, M., Gonzales, D., Cannich, A., Pagotto, U., Marsicano, G., & Cota, D. (2014). CB1 cannabinoid receptor in SF1-expressing neurons of the ventromedial hypothalamus determines metabolic responses to diet and leptin. *Molecular Metabolism*, 3(7), 705–716. <https://doi.org/10.1016/j.molmet.2014.07.004>
- Carpentier, A. C., Blondin, D. P., Virtanen, K. A., Richard, D., Haman, F., & Turcotte, É. E. (2018). Brown Adipose Tissue Energy Metabolism in Humans. *Frontiers in Endocrinology*, 9, 447. <https://doi.org/10.3389/fendo.2018.00447>
- Cazettes, F., Cohen, J. I., Yau, P. L., Talbot, H., & Convit, A. (2011). Obesity-mediated inflammation may damage the brain circuit that regulates food intake. *Brain Research*, 1373, 101–109. <https://doi.org/10.1016/j.brainres.2010.12.008>
- Ceccarini, J., Weltens, N., Ly, H. G., Tack, J., Van Oudenhove, L., & Van Laere, K. (2016). Association between cerebral cannabinoid 1 receptor availability and body mass index in patients with food intake disorders and healthy subjects: a [(18)F]MK-9470 PET study. *Translational Psychiatry*, 6(7), e853. <https://doi.org/10.1038/tp.2016.118>
- Cederberg, H., Stančáková, A., Kuusisto, J., Laakso, M., & Smith, U. (2015). Family history of type 2 diabetes increases the risk of both obesity and its complications: is type 2 diabetes a disease of inappropriate lipid storage? *Journal of Internal Medicine*, 277(5), 540–551. <https://doi.org/https://doi.org/10.1111/joim.12289>
- Chambers, A. P., Vemuri, V. K., Peng, Y., Wood, J. T., Olszewska, T., Pittman, Q. J., Makriyannis, A., & Sharkey, K. A. (2007). A neutral CB1 receptor antagonist reduces weight gain in rat. *American Journal of Physiology. Regulatory, Integrative and Comparative Physiology*, 293(6), R2185-93. <https://doi.org/10.1152/ajpregu.00663.2007>
- Chen, M., Woods, S. C., & Porte, D. J. (1975). Effect of cerebral intraventricular insulin on pancreatic insulin secretion in the dog. *Diabetes*, 24(10), 910–914. <https://doi.org/10.2337/diab.24.10.910>
- Cherry, S. ., & Dahlbom, M. (2006). *PET: Physics, Instrumentation, and Scanners*. Springer New York.
- Chong, B., Jayabaskaran, J., Kong, G., Chan, Y. H., Chin, Y. H., Goh, R., Kannan, S., Ng, C. H., Loong, S., Kueh, M. T. W., Lin, C., Anand, V. V., Lee, E. C. Z., Chew, H. S. J., Tan, D. J. H., Chan, K. E., Wang, J.-W., Muthiah, M., Dimitriadis, G. K., ... Chew, N. W. S. (2023). Trends and predictions of malnutrition and obesity in 204 countries and territories: an analysis of the Global Burden of Disease Study 2019. *EClinicalMedicine*, 57, 101850. <https://doi.org/10.1016/j.eclinm.2023.101850>
- Christen, T., Sheikine, Y., Rocha, V. Z., Hurwitz, S., Goldfine, A. B., Di Carli, M., & Libby, P. (2010). Increased glucose uptake in visceral versus subcutaneous adipose tissue revealed by PET imaging. *JACC: Cardiovascular Imaging*, 3(8), 843–851. <https://doi.org/10.1016/j.jcmg.2010.06.004>
- Cluny, N. L., Chambers, A. P., Vemuri, V. K., Wood, J. T., Eller, L. K., Freni, C., Reimer, R. A., Makriyannis, A., & Sharkey, K. A. (2011). The neutral cannabinoid CB1 receptor antagonist AM4113 regulates body weight through changes in energy intake in the rat. *Pharmacology, Biochemistry, and Behavior*, 97(3), 537–543. <https://doi.org/10.1016/j.pbb.2010.10.013>
- Cluny, N. L., Vemuri, V. K., Chambers, A. P., Limebeer, C. L., Bedard, H., Wood, J. T., Lutz, B., Zimmer, A., Parker, L. A., Makriyannis, A., & Sharkey, K. A. (2010). A novel peripherally restricted cannabinoid receptor antagonist, AM6545, reduces food intake and body weight, but does not cause malaise, in rodents. *British Journal of Pharmacology*, 161(3), 629–642. <https://doi.org/10.1111/j.1476-5381.2010.00908.x>

- Colombo, G., Agabio, R., Diaz, G., Lobina, C., Reali, R., & Gessa, G. L. (1998). Appetite suppression and weight loss after the cannabinoid antagonist SR 141716. *Life Sciences*, 63(8), PL113-7. [https://doi.org/10.1016/s0024-3205\(98\)00322-1](https://doi.org/10.1016/s0024-3205(98)00322-1)
- Connelly, M. A., Otvos, J. D., Shalauova, I., Playford, M. P., & Mehta, N. N. (2017). GlycA, a novel biomarker of systemic inflammation and cardiovascular disease risk. *Journal of Translational Medicine*, 15(1), 219. <https://doi.org/10.1186/s12967-017-1321-6>
- Connolly, L., Coveleskie, K., Kilpatrick, L. A., Labus, J. S., Ebrat, B., Stains, J., Jiang, Z., Tillisch, K., Raybould, H. E., & Mayer, E. A. (2013). Differences in brain responses between lean and obese women to a sweetened drink. *Neurogastroenterology and Motility*, 25(7), 579-e460. <https://doi.org/10.1111/nmo.12125>
- Coomans, C. P., Biermasz, N. R., Geerling, J. J., Guigas, B., Rensen, P. C. N., Havekes, L. M., & Romijn, J. A. (2011). Stimulatory effect of insulin on glucose uptake by muscle involves the central nervous system in insulin-sensitive mice. *Diabetes*, 60(12), 3132–3140. <https://doi.org/10.2337/db10-1100>
- Coomans, C. P., Geerling, J. J., Guigas, B., van den Hoek, A. M., Parlevliet, E. T., Ouwens, D. M., Pijl, H., Voshol, P. J., Rensen, P. C. N., Havekes, L. M., & Romijn, J. A. (2011). Circulating insulin stimulates fatty acid retention in white adipose tissue via KATP channel activation in the central nervous system only in insulin-sensitive mice. *Journal of Lipid Research*, 52(9), 1712–1722. <https://doi.org/10.1194/jlr.M015396>
- Coppin, G. (2016). The anterior medial temporal lobes: Their role in food intake and body weight regulation. *Physiology & Behavior*, 167, 60–70. <https://doi.org/10.1016/j.physbeh.2016.08.028>
- Cota, D., Marsicano, G., Tschöp, M., Grübler, Y., Flachskamm, C., Schubert, M., Auer, D., Yassouridis, A., Thöne-Reineke, C., Ortman, S., Tomassoni, F., Cervino, C., Nisoli, E., Linthorst, A. C. E., Pasquali, R., Lutz, B., Stalla, G. K., & Pagotto, U. (2003). The endogenous cannabinoid system affects energy balance via central orexigenic drive and peripheral lipogenesis. *The Journal of Clinical Investigation*, 112(3), 423–431. <https://doi.org/10.1172/JCI17725>
- D'Eon, T. M., Pierce, K. A., Roix, J. J., Tyler, A., Chen, H., & Teixeira, S. R. (2008). The role of adipocyte insulin resistance in the pathogenesis of obesity-related elevations in endocannabinoids. *Diabetes*, 57(5), 1262–1268. <https://doi.org/10.2337/db07-1186>
- Dash, S., Xiao, C., Morgantini, C., Koulajian, K., & Lewis, G. F. (2015). Intranasal insulin suppresses endogenous glucose production in humans compared with placebo in the presence of similar venous insulin concentrations. *Diabetes*, 64(3), 766–774. <https://doi.org/10.2337/db14-0685>
- De Souza, C. T., Araujo, E. P., Bordin, S., Ashimine, R., Zollner, R. L., Boschero, A. C., Saad, M. J. A., & Velloso, L. A. (2005). Consumption of a fat-rich diet activates a proinflammatory response and induces insulin resistance in the hypothalamus. *Endocrinology*, 146(10), 4192–4199. <https://doi.org/10.1210/en.2004-1520>
- Debons, A. F., Krimsky, I., & From, A. (1970). A direct action of insulin on the hypothalamic satiety center. *The American Journal of Physiology*, 219(4), 938–943. <https://doi.org/10.1152/ajplegacy.1970.219.4.938>
- DeFronzo, R. A., Tobin, J. D., & Andres, R. (1979). Glucose clamp technique: a method for quantifying insulin secretion and resistance. *The American Journal of Physiology*, 237(3), E214-23. <https://doi.org/10.1152/ajpendo.1979.237.3.E214>
- DeFronzo, R. A., & Tripathy, D. (2009). Skeletal muscle insulin resistance is the primary defect in type 2 diabetes. *Diabetes Care*, 32 Suppl 2(Suppl 2), S157-63. <https://doi.org/10.2337/dc09-S302>
- Deitmer, J. W., Theparambil, S. M., Ruminot, I., Noor, S. I., & Becker, H. M. (2019). Energy Dynamics in the Brain: Contributions of Astrocytes to Metabolism and pH Homeostasis. *Frontiers in Neuroscience*, 13, 1301. <https://doi.org/10.3389/fnins.2019.01301>
- Després, J.-P., Golay, A., & Sjöström, L. (2005). Effects of rimonabant on metabolic risk factors in overweight patients with dyslipidemia. *The New England Journal of Medicine*, 353(20), 2121–2134. <https://doi.org/10.1056/NEJMoa044537>

- Després, J.-P., & Lemieux, I. (2006). Abdominal obesity and metabolic syndrome. *Nature*, 444(7121), 881–887. <https://doi.org/10.1038/nature05488>
- Dhuria, S. V, Hanson, L. R., & Frey, W. H. 2nd. (2010). Intranasal delivery to the central nervous system: mechanisms and experimental considerations. *Journal of Pharmaceutical Sciences*, 99(4), 1654–1673. <https://doi.org/10.1002/jps.21924>
- Di Marzo, V. (2008a). Endocannabinoids: synthesis and degradation. *Reviews of Physiology, Biochemistry and Pharmacology*, 160, 1–24. https://doi.org/10.1007/112_0505
- Di Marzo, V. (2008b). The endocannabinoid system in obesity and type 2 diabetes. In *Diabetologia* (Vol. 51, Issue 8, pp. 1356–1367). <https://doi.org/10.1007/s00125-008-1048-2>
- Di Marzo, V. (2008c). The endocannabinoid system in obesity and type 2 diabetes. *Diabetologia*, 51(8), 1356–1367. <https://doi.org/10.1007/s00125-008-1048-2>
- Di Marzo, V., Goparaju, S. K., Wang, L., Liu, J., Bátkai, S., Járαι, Z., Fezza, F., Miura, G. I., Palmiter, R. D., Sugiura, T., & Kunos, G. (2001). Leptin-regulated endocannabinoids are involved in maintaining food intake. *Nature*, 410(6830), 822–825. <https://doi.org/10.1038/35071088>
- Di Marzo, V., Ligresti, A., & Cristino, L. (2009). The endocannabinoid system as a link between homeostatic and hedonic pathways involved in energy balance regulation. *International Journal of Obesity* (2005), 33 Suppl 2, S18-24. <https://doi.org/10.1038/ijo.2009.67>
- Dickens, A. M., Borgan, F., Laurikainen, H., Lamichhane, S., Marques, T., Rönkkö, T., Veronese, M., Lindeman, T., Hyötyläinen, T., Howes, O., Hietala, J., & Orešič, M. (2020). Links between central CB1-receptor availability and peripheral endocannabinoids in patients with first episode psychosis. *NPJ Schizophrenia*, 6(1), 21. <https://doi.org/10.1038/s41537-020-00110-7>
- Diggs-Andrews, K. A., Zhang, X., Song, Z., Daphna-Iken, D., Routh, V. H., & Fisher, S. J. (2010). Brain insulin action regulates hypothalamic glucose sensing and the counterregulatory response to hypoglycemia. *Diabetes*, 59(9), 2271–2280. <https://doi.org/10.2337/db10-0401>
- Donohue, S. R., Krushinski, J. H., Pike, V. W., Chernet, E., Phebus, L., Chesterfield, A. K., Felder, C. C., Halldin, C., & Schaus, J. M. (2008). Synthesis, ex vivo evaluation, and radiolabeling of potent 1,5-diphenylpyrrolidin-2-one cannabinoid subtype-1 receptor ligands as candidates for in vivo imaging. *Journal of Medicinal Chemistry*, 51(18), 5833–5842. <https://doi.org/10.1021/jm800416m>
- Dorfman, M. D., & Thaler, J. P. (2015). Hypothalamic inflammation and gliosis in obesity. *Current Opinion in Endocrinology, Diabetes, and Obesity*, 22(5), 325–330. <https://doi.org/10.1097/MED.0000000000000182>
- Dutta, B. J., Singh, S., Seksaria, S., Das Gupta, G., & Singh, A. (2022). Inside the diabetic brain: Insulin resistance and molecular mechanism associated with cognitive impairment and its possible therapeutic strategies. *Pharmacological Research*, 182, 106358. <https://doi.org/10.1016/j.phrs.2022.106358>
- EASO. (2015). The European Association for the Study of Obesity (EASO). 2015 Milan Declaration. A Call to Action on Obesity. <https://easo.org/2015-milan-declaration-a-call-to-action-on-obesity/>
- Engeli, S. (2008). Peripheral Metabolic Effects of Endocannabinoids and Cannabinoid Receptor Blockade. *Obesity Facts*, 1(1), 8–15. <https://doi.org/10.1159/000114255>
- Engeli, S., Böhnke, J., Feldpausch, M., Gorzelniak, K., Janke, J., Bátkai, S., Pacher, P., Harvey-White, J., Luft, F. C., Sharma, A. M., & Jordan, J. (2005). Activation of the peripheral endocannabinoid system in human obesity. *Diabetes*, 54(10), 2838–2843. <https://doi.org/10.2337/diabetes.54.10.2838>
- Eny, K. M., Wolever, T. M. S., Fontaine-Bisson, B., & El-Sohemy, A. (2008). Genetic variant in the glucose transporter type 2 is associated with higher intakes of sugars in two distinct populations. *Physiological Genomics*, 33(3), 355–360. <https://doi.org/10.1152/physiolgenomics.00148.2007>
- Eraso-Pichot, A., Pouvreau, S., Olivera-Pinto, A., Gomez-Sotres, P., Skupio, U., & Marsicano, G. (2023). Endocannabinoid signaling in astrocytes. *Glia*, 71(1), 44–59. <https://doi.org/10.1002/glia.24246>

- Eriksson, J. W., Visvanathar, R., Kullberg, J., Strand, R., Skrtic, S., Ekström, S., Lubberink, M., Lundqvist, M. H., Katsogiannos, P., Pereira, M. J., & Ahlström, H. (2021). Tissue-specific glucose partitioning and fat content in prediabetes and type 2 diabetes: Whole-body PET/MRI during hyperinsulinemia. *European Journal of Endocrinology*. <https://doi.org/10.1530/EJE-20-1359>
- Eriksson, O., Mikkola, K., Espes, D., Tuominen, L., Virtanen, K., Forsbäck, S., Haaparanta-Solin, M., Hietala, J., Solin, O., & Nuutila, P. (2015). The Cannabinoid Receptor-1 Is an Imaging Biomarker of Brown Adipose Tissue. *Journal of Nuclear Medicine*, 56(12), 1937 LP – 1941. <https://doi.org/10.2967/jnumed.115.156422>
- Esterson, Y. B., Carey, M., Boucai, L., Goyal, A., Raghavan, P., Zhang, K., Mehta, D., Feng, D., Wu, L., Kehlenbrink, S., Koppaka, S., Kishore, P., & Hawkins, M. (2016). Central Regulation of Glucose Production May Be Impaired in Type 2 Diabetes. *Diabetes*, 65(9), 2569–2579. <https://doi.org/10.2337/db15-1465>
- Faber, C. L., Deem, J. D., Campos, C. A., Taborsky, G. J. J., & Morton, G. J. (2020). CNS control of the endocrine pancreas. *Diabetologia*, 63(10), 2086–2094. <https://doi.org/10.1007/s00125-020-05204-6>
- Feng, B., Cao, J., Yu, Y., Yang, H., Jiang, Y., Liu, Y., Wang, R., & Zhao, Q. (2022). Gender-Related Differences in Regional Cerebral Glucose Metabolism in Normal Aging Brain. *Frontiers in Aging Neuroscience*, 14, 809767. <https://doi.org/10.3389/fnagi.2022.809767>
- Filbey, F. M., Myers, U. S., & Dewitt, S. (2012). Reward circuit function in high BMI individuals with compulsive overeating: similarities with addiction. *NeuroImage*, 63(4), 1800–1806. <https://doi.org/10.1016/j.neuroimage.2012.08.073>
- Filippi, B. M., Yang, C. S., Tang, C., & Lam, T. K. T. (2012). Insulin activates Erk1/2 signaling in the dorsal vagal complex to inhibit glucose production. *Cell Metabolism*, 16(4), 500–510. <https://doi.org/10.1016/j.cmet.2012.09.005>
- FinTerveys2017*. (2018). Terveys, Toimintakyky Ja Hyvinvointi Suomessa: FinTerveys 2017 - Tutkimus. <https://urn.fi/URN:ISBN:978-952-343-105-8>
- Flint, A., Gregersen, N. T., Gluud, L. L., Møller, B. K., Raben, A., Tetens, I., Verdich, C., & Astrup, A. (2007). Associations between postprandial insulin and blood glucose responses, appetite sensations and energy intake in normal weight and overweight individuals: a meta-analysis of test meal studies. *The British Journal of Nutrition*, 98(1), 17–25. <https://doi.org/10.1017/S000711450768297X>
- Fox, C. S., Massaro, J. M., Hoffmann, U., Pou, K. M., Maurovich-Horvat, P., Liu, C.-Y., Vasan, R. S., Murabito, J. M., Meigs, J. B., Cupples, L. A., D’Agostino, R. B. S., & O’Donnell, C. J. (2007). Abdominal visceral and subcutaneous adipose tissue compartments: association with metabolic risk factors in the Framingham Heart Study. *Circulation*, 116(1), 39–48. <https://doi.org/10.1161/CIRCULATIONAHA.106.675355>
- Fu, Z., Gilbert, E. R., & Liu, D. (2013). Regulation of insulin synthesis and secretion and pancreatic Beta-cell dysfunction in diabetes. *Current Diabetes Reviews*, 9(1), 25–53.
- Gancheva, S., Koliaki, C., Bierwagen, A., Nowotny, P., Heni, M., Fritsche, A., Häring, H.-U., Szendroedi, J., & Roden, M. (2015). Effects of intranasal insulin on hepatic fat accumulation and energy metabolism in humans. *Diabetes*, 64(6), 1966–1975. <https://doi.org/10.2337/db14-0892>
- García-Cáceres, C., Quarta, C., Varela, L., Gao, Y., Gruber, T., Legutko, B., Jastroch, M., Johansson, P., Ninkovic, J., Yi, C. X., Le Thuc, O., Szigeti-Buck, K., Cai, W., Meyer, C. W., Pfluger, P. T., Fernandez, A. M., Luquet, S., Woods, S. C., Torres-Alemán, I., ... Tschöp, M. H. (2016). Astrocytic Insulin Signaling Couples Brain Glucose Uptake with Nutrient Availability. *Cell*, 166(4), 867–880. <https://doi.org/10.1016/j.cell.2016.07.028>
- Gastaldelli, A., Cusi, K., Pettiti, M., Hardies, J., Miyazaki, Y., Berria, R., Buzzigoli, E., Sironi, A. M., Cersosimo, E., Ferrannini, E., & DeFronzo, R. A. (2007). Relationship between hepatic/visceral fat and hepatic insulin resistance in nondiabetic and type 2 diabetic subjects. *Gastroenterology*, 133(2), 496–506. <https://doi.org/10.1053/j.gastro.2007.04.068>

- Gatta-Cherifi, B., & Cota, D. (2016). New insights on the role of the endocannabinoid system in the regulation of energy balance. *International Journal of Obesity*, 40(2), 210–219. <https://doi.org/10.1038/ijo.2015.179>
- Gérard, N., Pieters, G., Goffin, K., Bormans, G., & Van Laere, K. (2011). Brain type 1 cannabinoid receptor availability in patients with anorexia and bulimia nervosa. *Biological Psychiatry*, 70(8), 777–784. <https://doi.org/10.1016/j.biopsych.2011.05.010>
- Goodpaster, B. H., Krishnaswami, S., Harris, T. B., Katsiaras, A., Kritchevsky, S. B., Simonsick, E. M., Nevitt, M., Holvoet, P., & Newman, A. B. (2005). Obesity, regional body fat distribution, and the metabolic syndrome in older men and women. *Archives of Internal Medicine*, 165(7), 777–783. <https://doi.org/10.1001/archinte.165.7.777>
- Gorzalka, B. B., & Dang, S. S. (2012). Minireview: Endocannabinoids and gonadal hormones: bidirectional interactions in physiology and behavior. *Endocrinology*, 153(3), 1016–1024. <https://doi.org/10.1210/en.2011-1643>
- Goss, A. M., & Gower, B. A. (2012). Insulin sensitivity is associated with thigh adipose tissue distribution in healthy postmenopausal women. *Metabolism: Clinical and Experimental*, 61(12), 1817–1823. <https://doi.org/10.1016/j.metabol.2012.05.016>
- Gueye, A. B., Pryslawsky, Y., Trigo, J. M., Pouliat, N., Delis, F., Antoniou, K., Loureiro, M., Laviolette, S. R., Vemuri, K., Makriyannis, A., & Le Foll, B. (2016). The CB1 Neutral Antagonist AM4113 Retains the Therapeutic Efficacy of the Inverse Agonist Rimonabant for Nicotine Dependence and Weight Loss with Better Psychiatric Tolerability. *The International Journal of Neuropsychopharmacology*, 19(12). <https://doi.org/10.1093/ijnp/pyw068>
- Guillemot-Legrès, O., & Muccioli, G. G. (2017). Obesity-Induced Neuroinflammation: Beyond the Hypothalamus. *Trends in Neurosciences*, 40(4), 237–253. <https://doi.org/10.1016/j.tins.2017.02.005>
- Gur, R. C., Mozley, L. H., Mozley, P. D., Resnick, S. M., Karp, J. S., Alavi, A., Arnold, S. E., & Gur, R. E. (1995). Sex differences in regional cerebral glucose metabolism during a resting state. *Science (New York, N.Y.)*, 267(5197), 528–531. <https://doi.org/10.1126/science.7824953>
- Hallschmid, M., Benedict, C., Schultes, B., Born, J., & Kern, W. (2008). Obese men respond to cognitive but not to catabolic brain insulin signaling. *International Journal of Obesity* (2005), 32(2), 275–282. <https://doi.org/10.1038/sj.ijo.0803722>
- Hallschmid, M., Benedict, C., Schultes, B., Fehm, H.-L., Born, J., & Kern, W. (2004). Intranasal insulin reduces body fat in men but not in women. *Diabetes*, 53(11), 3024–3029. <https://doi.org/10.2337/diabetes.53.11.3024>
- Hallschmid, M., Higgs, S., Thienel, M., Ott, V., & Lehnert, H. (2012). Postprandial administration of intranasal insulin intensifies satiety and reduces intake of palatable snacks in women. *Diabetes*, 61(4), 782–789. <https://doi.org/10.2337/db11-1390>
- Hamacher, K., Coenen, H. H., & Stöcklin, G. (1986). Efficient stereospecific synthesis of no-carrier-added 2-[18F]-fluoro-2-deoxy-D-glucose using aminopolyether supported nucleophilic substitution. *Journal of Nuclear Medicine: Official Publication, Society of Nuclear Medicine*, 27(2), 235–238.
- Hariri, A. R., Gorka, A., Hyde, L. W., Kimak, M., Halder, I., Ducci, F., Ferrell, R. E., Goldman, D., & Manuck, S. B. (2009). Divergent effects of genetic variation in endocannabinoid signaling on human threat- and reward-related brain function. *Biological Psychiatry*, 66(1), 9–16. <https://doi.org/10.1016/j.biopsych.2008.10.047>
- Harrold, J. A., Elliott, J. C., King, P. J., Widdowson, P. S., & Williams, G. (2002). Down-regulation of cannabinoid-1 (CB-1) receptors in specific extrahypothalamic regions of rats with dietary obesity: a role for endogenous cannabinoids in driving appetite for palatable food? *Brain Research*, 952(2), 232–238. [https://doi.org/10.1016/s0006-8993\(02\)03245-6](https://doi.org/10.1016/s0006-8993(02)03245-6)
- Haslam, D. W., & James, W. P. T. (2005). Obesity. *Lancet (London, England)*, 366(9492), 1197–1209. [https://doi.org/10.1016/S0140-6736\(05\)67483-1](https://doi.org/10.1016/S0140-6736(05)67483-1)

- Havrankova, J., Roth, J., & Brownstein, M. (1978). Insulin receptors are widely distributed in the central nervous system of the rat. *Nature*, 272(5656), 827–829. <https://doi.org/10.1038/272827a0>
- Heni, M., Kullmann, S., Ketterer, C., Guthoff, M., Bayer, M., Staiger, H., Machicao, F., Häring, H.-U., Preissl, H., Veit, R., & Fritsche, A. (2014). Differential effect of glucose ingestion on the neural processing of food stimuli in lean and overweight adults. *Human Brain Mapping*, 35(3), 918–928. <https://doi.org/10.1002/hbm.22223>
- Heni, M., Kullmann, S., Ketterer, C., Guthoff, M., Linder, K., Wagner, R., Stingl, K. T., Veit, R., Staiger, H., Häring, H.-U., Preissl, H., & Fritsche, A. (2012). Nasal insulin changes peripheral insulin sensitivity simultaneously with altered activity in homeostatic and reward-related human brain regions. *Diabetologia*, 55(6), 1773–1782. <https://doi.org/10.1007/s00125-012-2528-y>
- Heni, M., Kullmann, S., Preissl, H., Fritsche, A., & Häring, H.-U. (2015). Impaired insulin action in the human brain: causes and metabolic consequences. *Nature Reviews. Endocrinology*, 11(12), 701–711. <https://doi.org/10.1038/nrendo.2015.173>
- Heni, M., Wagner, R., Kullmann, S., Gancheva, S., Roden, M., Peter, A., Stefan, N., Preissl, H., Häring, H. U., & Fritsche, A. (2017). Hypothalamic and striatal insulin action suppresses endogenous glucose production and may stimulate glucose uptake during hyperinsulinemia in lean but not in overweight men. *Diabetes*, 66(7). <https://doi.org/10.2337/db16-1380>
- Heni, M., Wagner, R., Kullmann, S., Veit, R., Mat Husin, H., Linder, K., Benkendorff, C., Peter, A., Stefan, N., Häring, H.-U., Preissl, H., & Fritsche, A. (2014). Central insulin administration improves whole-body insulin sensitivity via hypothalamus and parasympathetic outputs in men. *Diabetes*, 63(12), 4083–4088. <https://doi.org/10.2337/db14-0477>
- Henquin, J.-C. (2021). Non-glucose modulators of insulin secretion in healthy humans: (dis)similarities between islet and in vivo studies. *Metabolism: Clinical and Experimental*, 122, 154821. <https://doi.org/10.1016/j.metabol.2021.154821>
- Higuchi, S., Ohji, M., Araki, M., Furuta, R., Katsuki, M., Yamaguchi, R., Akitake, Y., Matsuyama, K., Irie, K., Mishima, K., Mishima, K., Iwasaki, K., & Fujiwara, M. (2011). Increment of hypothalamic 2-arachidonoylglycerol induces the preference for a high-fat diet via activation of cannabinoid 1 receptors. *Behavioural Brain Research*, 216(1), 477–480. <https://doi.org/10.1016/j.bbr.2010.08.042>
- Hill, J. O., Wyatt, H. R., & Peters, J. C. (2012). Energy balance and obesity. *Circulation*, 126(1), 126–132. <https://doi.org/10.1161/CIRCULATIONAHA.111.087213>
- Hirvonen, J. (2015). In vivo imaging of the cannabinoid CB1 receptor with positron emission tomography. *Clinical Pharmacology and Therapeutics*, 97(6), 565–567. <https://doi.org/10.1002/cpt.116>
- Hirvonen, J., Goodwin, R. S., Li, C.-T., Terry, G. E., Zoghbi, S. S., Morse, C., Pike, V. W., Volkow, N. D., Huestis, M. A., & Innis, R. B. (2012). Reversible and regionally selective downregulation of brain cannabinoid CB1 receptors in chronic daily cannabis smokers. *Molecular Psychiatry*, 17(6), 642–649. <https://doi.org/10.1038/mp.2011.82>
- Hirvonen, J., Virtanen, K. A., Nummenmaa, L., Hannukainen, J. C., Honka, M. J., Bucci, M., Nesterov, S. V., Parkkola, R., Rinne, J., Iozzo, P., & Nuutila, P. (2011). Effects of insulin on brain glucose metabolism in impaired glucose tolerance. *Diabetes*. <https://doi.org/10.2337/db10-0940>
- Horton, R. W., Meldrum, B. S., & Bachelard, H. S. (1973). Enzymic and cerebral metabolic effects of 2-deoxy-D-glucose. *Journal of Neurochemistry*, 21(3), 507–520. <https://doi.org/10.1111/j.1471-4159.1973.tb05996.x>
- Hsiao, W.-C., Shia, K.-S., Wang, Y.-T., Yeh, Y.-N., Chang, C.-P., Lin, Y., Chen, P.-H., Wu, C.-H., Chao, Y.-S., & Hung, M.-S. (2015). A novel peripheral cannabinoid receptor 1 antagonist, BPR0912, reduces weight independently of food intake and modulates thermogenesis. *Diabetes, Obesity & Metabolism*, 17(5), 495–504. <https://doi.org/10.1111/dom.12447>
- Hung, C.-S., Lee, J.-K., Yang, C.-Y., Hsieh, H.-R., Ma, W.-Y., Lin, M.-S., Liu, P.-H., Shih, S.-R., Liou, J.-M., Chuang, L.-M., Chen, M.-F., Lin, J.-W., Wei, J.-N., & Li, H.-Y. (2014). Measurement of

- visceral fat: should we include retroperitoneal fat? *PLoS One*, 9(11), e112355. <https://doi.org/10.1371/journal.pone.0112355>
- Iozzo, P., Jarvisalo, M. J., Kiss, J., Borra, R., Naum, G. A., Viljanen, A., Viljanen, T., Gastaldelli, A., Buzzigoli, E., Guiducci, L., Barsotti, E., Savunen, T., Knuuti, J., Haaparanta-Solin, M., Ferrannini, E., & Nuutila, P. (2007). Quantification of liver glucose metabolism by positron emission tomography: validation study in pigs. *Gastroenterology*, 132(2), 531–542. <https://doi.org/10.1053/j.gastro.2006.12.040>
- Iwen, K. A., Scherer, T., Heni, M., Sayk, F., Wellnitz, T., Machleidt, F., Preissl, H., Häring, H.-U., Fritsche, A., Lehnert, H., Buettner, C., & Hallschmid, M. (2014). Intranasal insulin suppresses systemic but not subcutaneous lipolysis in healthy humans. *The Journal of Clinical Endocrinology and Metabolism*, 99(2), E246–51. <https://doi.org/10.1210/jc.2013-3169>
- Jais, A., & Brüning, J. C. (2017). Hypothalamic inflammation in obesity and metabolic disease. *The Journal of Clinical Investigation*, 127(1), 24–32. <https://doi.org/10.1172/JCI88878>
- Jastreboff, A. M., Kotz, C. M., Kahan, S., Kelly, A. S., & Heymsfield, S. B. (2019). Obesity as a Disease: The Obesity Society 2018 Position Statement. *Obesity (Silver Spring, Md.)*, 27(1), 7–9. <https://doi.org/10.1002/oby.22378>
- Jauch-Chara, K., Friedrich, A., Rezmer, M., Melchert, U. H., G Scholand-Engler, H., Hallschmid, M., & Oltmanns, K. M. (2012). Intranasal insulin suppresses food intake via enhancement of brain energy levels in humans. *Diabetes*, 61(9), 2261–2268. <https://doi.org/10.2337/db12-0025>
- Jbilo, O., Ravinet-Trillou, C., Arnone, M., Buisson, I., Bribes, E., Péleraux, A., Pénarier, G., Soubrié, P., Le Fur, G., Galiègue, S., & Casellas, P. (2005). The CB1 receptor antagonist rimonabant reverses the diet-induced obesity phenotype through the regulation of lipolysis and energy balance. *FASEB Journal: Official Publication of the Federation of American Societies for Experimental Biology*, 19(11), 1567–1569. <https://doi.org/10.1096/fj.04-3177fje>
- Jebb, S. A., & Moore, M. S. (1999). Contribution of a sedentary lifestyle and inactivity to the etiology of overweight and obesity: current evidence and research issues. *Medicine and Science in Sports and Exercise*, 31(11 Suppl), S534–41. <https://doi.org/10.1097/00005768-199911001-00008>
- Jensen, M. D., Ryan, D. H., Apovian, C. M., Ard, J. D., Comuzzie, A. G., Donato, K. A., Hu, F. B., Hubbard, V. S., Jakicic, J. M., Kushner, R. F., Loria, C. M., Millen, B. E., Nonas, C. A., Pi-Sunyer, F. X., Stevens, J., Stevens, V. J., Wadden, T. A., Wolfe, B. M., Yanovski, S. Z., ... Tomaselli, G. F. (2014). 2013 AHA/ACC/TOS guideline for the management of overweight and obesity in adults: a report of the American College of Cardiology/American Heart Association Task Force on Practice Guidelines and The Obesity Society. *Circulation*, 129(25 Suppl 2), S102–38. <https://doi.org/10.1161/01.cir.0000437739.71477.ee>
- Jimenez-Blasco, D., Busquets-Garcia, A., Hebert-Chatelain, E., Serrat, R., Vicente-Gutierrez, C., Ioannidou, C., Gómez-Sotres, P., Lopez-Fabuel, I., Resch-Beusher, M., Resel, E., Arnouil, D., Saraswat, D., Varilh, M., Cannich, A., Julio-Kalajic, F., Bonilla-Del Río, I., Almeida, A., Puente, N., Achicallende, S., ... Marsicano, G. (2020). Glucose metabolism links astroglial mitochondria to cannabinoid effects. *Nature*, 583(7817), 603–608. <https://doi.org/10.1038/s41586-020-2470-y>
- Juhola, J., Magnussen, C. G., Viikari, J. S. A., Kähönen, M., Hutri-Kähönen, N., Jula, A., Lehtimäki, T., Åkerblom, H. K., Pietikäinen, M., Laitinen, T., Jokinen, E., Taittonen, L., Raitakari, O. T., & Juonala, M. (2011). Tracking of serum lipid levels, blood pressure, and body mass index from childhood to adulthood: the Cardiovascular Risk in Young Finns Study. *The Journal of Pediatrics*, 159(4), 584–590. <https://doi.org/10.1016/j.jpeds.2011.03.021>
- Jung, K.-M., Lin, L., & Piomelli, D. (2022). The endocannabinoid system in the adipose organ. *Reviews in Endocrine & Metabolic Disorders*, 23(1), 51–60. <https://doi.org/10.1007/s1154-020-09623-z>
- Juonala, M., Juhola, J., Magnussen, C. G., Würtz, P., Viikari, J. S. A., Thomson, R., Seppälä, I., Hernesniemi, J., Kähönen, M., Lehtimäki, T., Hurme, M., Telama, R., Mikkilä, V., Eklund, C., Räsänen, L., Hintsanen, M., Keltikangas-Järvinen, L., Kivimäki, M., & Raitakari, O. T. (2011). Childhood environmental and genetic predictors of adulthood obesity: the cardiovascular risk in

- young Finns study. *The Journal of Clinical Endocrinology and Metabolism*, 96(9), E1542-9. <https://doi.org/10.1210/jc.2011-1243>
- Kahn, S. E., Hull, R. L., & Utzschneider, K. M. (2006). Mechanisms linking obesity to insulin resistance and type 2 diabetes. *Nature*, 444(7121), 840–846. <https://doi.org/10.1038/nature05482>
- Karczewska-Kupczewska, M., Tarasów, E., Nikolajuk, A., Stefanowicz, M., Matulewicz, N., Oziomek, E., Górska, M., Strackowski, M., & Kowalska, I. (2013). The effect of insulin infusion on the metabolites in cerebral tissues assessed with proton magnetic resonance spectroscopy in young healthy subjects with high and low insulin sensitivity. *Diabetes Care*, 36(9), 2787–2793. <https://doi.org/10.2337/dc12-1437>
- Karjalainen, T., Tuisku, J., Santavirta, S., Kantonen, T., Bucci, M., Tuominen, L., Hirvonen, J., Hietala, J., Rinne, J. O., & Nummenmaa, L. (2020). Magia: Robust Automated Image Processing and Kinetic Modeling Toolbox for PET Neuroinformatics. In *Frontiers in Neuroinformatics* (Vol. 14, p. 3). <https://www.frontiersin.org/article/10.3389/fninf.2020.00003>
- Kawai, T., Autieri, M. V., & Scalia, R. (2021). Adipose tissue inflammation and metabolic dysfunction in obesity. *American Journal of Physiology. Cell Physiology*, 320(3), C375–C391. <https://doi.org/10.1152/ajpcell.00379.2020>
- Kellert, B. A., Nguyen, M. C., Nguyen, C., Nguyen, Q. H., & Wagner, E. J. (2009). Estrogen rapidly attenuates cannabinoid-induced changes in energy homeostasis. *European Journal of Pharmacology*, 622(1–3), 15–24. <https://doi.org/10.1016/j.ejphar.2009.09.001>
- Kelley, D. E., Williams, K. V., Price, J. C., & Goodpaster, B. (1999). Determination of the lumped constant for [18F] fluorodeoxyglucose in human skeletal muscle. *Journal of Nuclear Medicine : Official Publication, Society of Nuclear Medicine*, 40(11), 1798–1804.
- Kempf, K., Hector, J., Strate, T., Schwarzloh, B., Rose, B., Herder, C., Martin, S., & Algenstaedt, P. (2007). Immune-mediated Activation of the Endocannabinoid System in Visceral Adipose Tissue in Obesity. *Hormone and Metabolic Research*, 39(8), 596–600. <https://doi.org/10.1055/s-2007-984459>
- Ketterer, C., Tschritter, O., Preissl, H., Heni, M., Häring, H.-U., & Fritsche, A. (2011). *Insulin sensitivity of the human brain*.
- King, G. L., & Johnson, S. M. (1985). Receptor-mediated transport of insulin across endothelial cells. *Science (New York, N.Y.)*, 227(4694), 1583–1586. <https://doi.org/10.1126/science.3883490>
- Kishore, P., Boucai, L., Zhang, K., Li, W., Koppaka, S., Kehlenbrink, S., Schiwek, A., Esterson, Y. B., Mehta, D., Bursheh, S., Su, Y., Gutierrez-Juarez, R., Muzumdar, R., Schwartz, G. J., & Hawkins, M. (2011). Activation of K(ATP) channels suppresses glucose production in humans. *The Journal of Clinical Investigation*, 121(12), 4916–4920. <https://doi.org/10.1172/JCI58035>
- Kleinendorst, L., Massink, M. P. G., Cooman, M. I., Savas, M., van der Baan-Slootweg, O. H., Roelants, R. J., Janssen, I. C. M., Meijers-Heijboer, H. J., Knoers, N. V. A. M., Ploos van Amstel, H. K., van Rossum, E. F. C., van den Akker, E. L. T., van Haften, G., van der Zwaag, B., & van Haelst, M. M. (2018). Genetic obesity: next-generation sequencing results of 1230 patients with obesity. *Journal of Medical Genetics*, 55(9), 578–586. <https://doi.org/10.1136/jmedgenet-2018-105315>
- Kleinridders, A., Ferris, H. A., Cai, W., & Kahn, C. R. (2014). Insulin action in brain regulates systemic metabolism and brain function. *Diabetes*, 63(7), 2232–2243. <https://doi.org/10.2337/db14-0568>
- Kleinridders, A., & Pothos, E. N. (2019). Impact of Brain Insulin Signaling on Dopamine Function, Food Intake, Reward, and Emotional Behavior. *Current Nutrition Reports*, 8(2), 83–91. <https://doi.org/10.1007/s13668-019-0276-z>
- Koch, L., Wunderlich, F. T., Seibler, J., Könnner, A. C., Hampel, B., Irlenbusch, S., Brabant, G., Kahn, C. R., Schwenk, F., & Brüning, J. C. (2008). Central insulin action regulates peripheral glucose and fat metabolism in mice. *The Journal of Clinical Investigation*, 118(6), 2132–2147. <https://doi.org/10.1172/JCI31073>

- Koepsell, H. (2020). Glucose transporters in brain in health and disease. In *Pflugers Archiv European Journal of Physiology* (Vol. 472, Issue 9, pp. 1299–1343). Springer. <https://doi.org/10.1007/s00424-020-02441-x>
- Könnner, A. C., & Brüning, J. C. (2012). Selective insulin and leptin resistance in metabolic disorders. *Cell Metabolism*, 16(2), 144–152. <https://doi.org/10.1016/j.cmet.2012.07.004>
- Könnner, A. C., Janoschek, R., Plum, L., Jordan, S. D., Rother, E., Ma, X., Xu, C., Enriori, P., Hampel, B., Barsh, G. S., Kahn, C. R., Cowley, M. A., Ashcroft, F. M., & Brüning, J. C. (2007). Insulin action in AgRP-expressing neurons is required for suppression of hepatic glucose production. *Cell Metabolism*, 5(6), 438–449. <https://doi.org/10.1016/j.cmet.2007.05.004>
- Könnner, A. C., Klöckener, T., & Brüning, J. C. (2009). Control of energy homeostasis by insulin and leptin: targeting the arcuate nucleus and beyond. *Physiology & Behavior*, 97(5), 632–638. <https://doi.org/10.1016/j.physbeh.2009.03.027>
- Krug, R., Mohwinkel, L., Drotleff, B., Born, J., & Hallschmid, M. (2018). Insulin and Estrogen Independently and Differentially Reduce Macronutrient Intake in Healthy Men. *The Journal of Clinical Endocrinology and Metabolism*, 103(4), 1393–1401. <https://doi.org/10.1210/jc.2017-01835>
- Kujala, U. M., Leskinen, T., Rottensteiner, M., Aaltonen, S., Ala-Korpela, M., Waller, K., & Kaprio, J. (2022). Physical activity and health: Findings from Finnish monozygotic twin pairs discordant for physical activity. *Scandinavian Journal of Medicine & Science in Sports*, 32(9), 1316–1323. <https://doi.org/10.1111/sms.14205>
- Kullmann, S., Fritsche, A., Wagner, R., Schwab, S., Häring, H.-U., Preissl, H., & Heni, M. (2017). Hypothalamic insulin responsiveness is associated with pancreatic insulin secretion in humans. *Physiology & Behavior*, 176, 134–138. <https://doi.org/10.1016/j.physbeh.2017.03.036>
- Kullmann, S., Heni, M., Hallschmid, M., Fritsche, A., Preissl, H., & Häring, H. U. (2016). Brain insulin resistance at the crossroads of metabolic and cognitive disorders in humans. *Physiological Reviews*, 96(4), 1169–1209. <https://doi.org/10.1152/physrev.00032.2015>
- Kullmann, S., Heni, M., Veit, R., Scheffler, K., Machann, J., Häring, H.-U., Fritsche, A., & Preissl, H. (2015). Selective insulin resistance in homeostatic and cognitive control brain areas in overweight and obese adults. *Diabetes Care*, 38(6), 1044–1050. <https://doi.org/10.2337/dc14-2319>
- Kullmann, S., Heni, M., Veit, R., Scheffler, K., Machann, J., Häring, H.-U., Fritsche, A., & Preissl, H. (2017). Intranasal insulin enhances brain functional connectivity mediating the relationship between adiposity and subjective feeling of hunger. *Scientific Reports*, 7(1), 1627. <https://doi.org/10.1038/s41598-017-01907-w>
- Kullmann, S., Kleinridders, A., Small, D. M., Fritsche, A., Häring, H.-U., Preissl, H., & Heni, M. (2020). Central nervous pathways of insulin action in the control of metabolism and food intake. *The Lancet. Diabetes & Endocrinology*, 8(6), 524–534. [https://doi.org/10.1016/S2213-8587\(20\)30113-3](https://doi.org/10.1016/S2213-8587(20)30113-3)
- Kullmann, S., Valenta, V., Wagner, R., Tschrirter, O., Machann, J., Häring, H.-U., Preissl, H., Fritsche, A., & Heni, M. (2020). Brain insulin sensitivity is linked to adiposity and body fat distribution. *Nature Communications*, 11(1), 1841. <https://doi.org/10.1038/s41467-020-15686-y>
- Lahdenpohja, S., Keller, T., Forsback, S., Viljanen, T., Kokkomäki, E., Kivelä, R. V., Bergman, J., Solin, O., & Kirjavainen, A. K. (2020). Automated GMP production and long-term experience in radiosynthesis of CB(1) tracer [(18) F]FMPEP-d(2). *Journal of Labelled Compounds & Radiopharmaceuticals*, 63(9), 408–418. <https://doi.org/10.1002/jlcr.3845>
- Lahesmaa, M., Eriksson, O., Gnad, T., Oikonen, V., Bucci, M., Hirvonen, J., Koskensalo, K., Teuho, J., Niemi, T., Taittonen, M., Lahdenpohja, S., U Din, M., Haaparanta-Solin, M., Pfeifer, A., Virtanen, K. A., & Nuutila, P. (2018). Cannabinoid Type 1 Receptors Are Upregulated During Acute Activation of Brown Adipose Tissue. *Diabetes*, 67(7), 1226–1236. <https://doi.org/10.2337/db17-1366>
- Latva-Rasku, A. (2020). *Regulators of central and peripheral insulin sensitivity in humans*. <https://urn.fi/URN:ISBN:978-951-29-8112-0>

- Latva-Rasku, A., Honka, M.-J., Stančáková, A., Koistinen, H. A., Kuusisto, J., Guan, L., Manning, A. K., Stringham, H., Gloyn, A. L., Lindgren, C. M., Collins, F. S., Mohlke, K. L., Scott, L. J., Karjalainen, T., Nummenmaa, L., Boehnke, M., Nuutila, P., & Laakso, M. (2018). A Partial Loss-of-Function Variant in AKT2 Is Associated With Reduced Insulin-Mediated Glucose Uptake in Multiple Insulin-Sensitive Tissues: A Genotype-Based Callback Positron Emission Tomography Study. *Diabetes*, 67(2), 334–342. <https://doi.org/10.2337/db17-1142>
- Lemaire, C., Damhaut, P., Lauricella, B., Mosdzianowski, C., Morelle, J. L., Monclus, M., Van Naemen, J., Mulleneers, E., Aerts, J., Plenevaux, A., Brihaye, C., & Luxen, A. (2002). Fast F-18 FDG synthesis by alkaline hydrolysis on a low polarity solid phase supports. *Journal of Labelled Compounds and Radiopharmaceuticals*, 45(5). <https://doi.org/10.1002/jlcr.572>
- Lenard, N. R., & Berthoud, H.-R. (2008). Central and peripheral regulation of food intake and physical activity: pathways and genes. *Obesity (Silver Spring, Md.)*, 16 Suppl 3(Suppl 3), S11–22. <https://doi.org/10.1038/oby.2008.511>
- Leskinen, T., Sipilä, S., Alen, M., Cheng, S., Pietiläinen, K. H., Usenius, J.-P., Suominen, H., Kovanen, V., Kainulainen, H., Kaprio, J., & Kujala, U. M. (2009). Leisure-time physical activity and high-risk fat: a longitudinal population-based twin study. *International Journal of Obesity (2005)*, 33(11), 1211–1218. <https://doi.org/10.1038/ijo.2009.170>
- Lewis, G. F., Carpentier, A. C., Pereira, S., Hahn, M., & Giacca, A. (2021). Direct and indirect control of hepatic glucose production by insulin. *Cell Metabolism*, 33(4), 709–720. <https://doi.org/10.1016/j.cmet.2021.03.007>
- Liu, Y. L., Connoley, I. P., Wilson, C. A., & Stock, M. J. (2005). Effects of the cannabinoid CB1 receptor antagonist SR141716 on oxygen consumption and soleus muscle glucose uptake in Lep(ob)/Lep(ob) mice. *International Journal of Obesity (2005)*, 29(2), 183–187. <https://doi.org/10.1038/sj.ijo.0802847>
- Locke, A. E., Kahali, B., Berndt, S. I., Justice, A. E., Pers, T. H., Day, F. R., Powell, C., Vedantam, S., Buchkovich, M. L., Yang, J., Croteau-Chonka, D. C., Esko, T., Fall, T., Ferreira, T., Gustafsson, S., Kutalik, Z., Luan, J., Mägi, R., Randall, J. C., ... Speliotes, E. K. (2015). Genetic studies of body mass index yield new insights for obesity biology. *Nature*, 518(7538), 197–206. <https://doi.org/10.1038/nature14177>
- Logan, J. (2000). Graphical analysis of PET data applied to reversible and irreversible tracers. *Nuclear Medicine and Biology*, 27(7), 661–670. [https://doi.org/10.1016/s0969-8051\(00\)00137-2](https://doi.org/10.1016/s0969-8051(00)00137-2)
- Loos, R. J. F., & Yeo, G. S. H. (2022). The genetics of obesity: from discovery to biology. *Nature Reviews. Genetics*, 23(2), 120–133. <https://doi.org/10.1038/s41576-021-00414-z>
- Lu, R., Aziz, N. A., Diers, K., Stöcker, T., Reuter, M., & Breteler, M. M. B. (2021). Insulin resistance accounts for metabolic syndrome-related alterations in brain structure. *Human Brain Mapping*, 42(8), 2434–2444. <https://doi.org/10.1002/hbm.25377>
- Lutter, M., & Nestler, E. J. (2009). Homeostatic and hedonic signals interact in the regulation of food intake. *The Journal of Nutrition*, 139(3), 629–632. <https://doi.org/10.3945/jn.108.097618>
- Manaserh, I. H., Chikkamenahalli, L., Ravi, S., Dube, P. R., Park, J. J., & Hill, J. W. (2019). Ablating astrocyte insulin receptors leads to delayed puberty and hypogonadism in mice. *PLoS Biology*, 17(3), e3000189. <https://doi.org/10.1371/journal.pbio.3000189>
- Martinez-Tellez, B., Sanchez-Delgado, G., Boon, M. R., Rensen, P. C. N., Llamas-Elvira, J. M., & Ruiz, J. R. (2020). Distribution of Brown Adipose Tissue Radiodensity in Young Adults: Implications for Cold [18F]FDG-PET/CT Analyses. *Molecular Imaging and Biology*, 22(2), 425–433. <https://doi.org/10.1007/s11307-019-01381-y>
- Martins, C. J. de M., Genelhu, V., Pimentel, M. M. G., Celoria, B. M. J., Mangia, R. F., Aveta, T., Silvestri, C., Di Marzo, V., & Francischetti, E. A. (2015). Circulating Endocannabinoids and the Polymorphism 385C>A in Fatty Acid Amide Hydrolase (FAAH) Gene May Identify the Obesity Phenotype Related to Cardiometabolic Risk: A Study Conducted in a Brazilian Population of Complex Interethnic Admixture. *PloS One*, 10(11), e0142728. <https://doi.org/10.1371/journal.pone.0142728>

- Massa, F., Mancini, G., Schmidt, H., Steindel, F., Mackie, K., Angioni, C., Oliet, S. H. R., Geisslinger, G., & Lutz, B. (2010). Alterations in the hippocampal endocannabinoid system in diet-induced obese mice. *The Journal of Neuroscience : The Official Journal of the Society for Neuroscience*, 30(18), 6273–6281. <https://doi.org/10.1523/JNEUROSCI.2648-09.2010>
- Matias, I., & Di Marzo, V. (2007). Endocannabinoids and the control of energy balance. *Trends in Endocrinology & Metabolism*, 18(1), 27–37. <https://doi.org/https://doi.org/10.1016/j.tem.2006.11.006>
- Matias, I., Gonthier, M.-P., Orlando, P., Martiadis, V., De Petrocellis, L., Cervino, C., Petrosino, S., Hoareau, L., Festy, F., Pasquali, R., Roche, R., Maj, M., Pagotto, U., Monteleone, P., & Di Marzo, V. (2006). Regulation, function, and dysregulation of endocannabinoids in models of adipose and beta-pancreatic cells and in obesity and hyperglycemia. *The Journal of Clinical Endocrinology and Metabolism*, 91(8), 3171–3180. <https://doi.org/10.1210/jc.2005-2679>
- Matias, I., Petrosino, S., Racioppi, A., Capasso, R., Izzo, A. A., & Di Marzo, V. (2008). Dysregulation of peripheral endocannabinoid levels in hyperglycemia and obesity: Effect of high fat diets. *Molecular and Cellular Endocrinology*, 286(1-2 Suppl 1), S66-78. <https://doi.org/10.1016/j.mce.2008.01.026>
- Matias, I., Vergoni, A. V., Petrosino, S., Ottani, A., Pocai, A., Bertolini, A., & Di Marzo, V. (2008). Regulation of hypothalamic endocannabinoid levels by neuropeptides and hormones involved in food intake and metabolism: insulin and melanocortins. *Neuropharmacology*, 54(1), 206–212. <https://doi.org/10.1016/j.neuropharm.2007.06.011>
- Meye, F. J., Trezza, V., Vanderschuren, L. J. M. J., Ramakers, G. M. J., & Adan, R. A. H. (2013). Neutral antagonism at the cannabinoid 1 receptor: a safer treatment for obesity. *Molecular Psychiatry*, 18(12), 1294–1301. <https://doi.org/10.1038/mp.2012.145>
- Moore, M. C., Coate, K. C., Winnick, J. J., An, Z., & Cherrington, A. D. (2012). Regulation of hepatic glucose uptake and storage in vivo. *Advances in Nutrition (Bethesda, Md.)*, 3(3), 286–294. <https://doi.org/10.3945/an.112.002089>
- Muccioli, G. G. (2010). Endocannabinoid biosynthesis and inactivation, from simple to complex. *Drug Discovery Today*, 15(11–12), 474–483. <https://doi.org/10.1016/j.drudis.2010.03.007>
- Müller, C., Voirol, M. J., Stefanoni, N., Surmely, J. F., Jéquier, E., Gaillard, R. C., & Tappy, L. (1997). Effect of chronic intracerebroventricular infusion of insulin on brown adipose tissue activity in fed and fasted rats. *International Journal of Obesity and Related Metabolic Disorders : Journal of the International Association for the Study of Obesity*, 21(7), 562–566. <https://doi.org/10.1038/sj.ijo.0800441>
- Myers, M. G. J., Affinati, A. H., Richardson, N., & Schwartz, M. W. (2021). Central nervous system regulation of organismal energy and glucose homeostasis. *Nature Metabolism*, 3(6), 737–750. <https://doi.org/10.1038/s42255-021-00408-5>
- Myers, M. G. J., Leibel, R. L., Seeley, R. J., & Schwartz, M. W. (2010). Obesity and leptin resistance: distinguishing cause from effect. *Trends in Endocrinology and Metabolism: TEM*, 21(11), 643–651. <https://doi.org/10.1016/j.tem.2010.08.002>
- Natali, A., Toschi, E., Camastra, S., Gastaldelli, A., Groop, L., & Ferrannini, E. (2000). Determinants of postabsorptive endogenous glucose output in non-diabetic subjects. European Group for the Study of Insulin Resistance (EGIR). *Diabetologia*, 43(10), 1266–1272. <https://doi.org/10.1007/s001250051522>
- Nauck, M. A., & Meier, J. J. (2018). Incretin hormones: Their role in health and disease. *Diabetes, Obesity & Metabolism*, 20 Suppl 1, 5–21. <https://doi.org/10.1111/dom.13129>
- Naughton, S. S., Mathai, M. L., Hryciw, D. H., & McAinch, A. J. (2016). Linoleic acid and the pathogenesis of obesity. *Prostaglandins & Other Lipid Mediators*, 125, 90–99. <https://doi.org/10.1016/j.prostaglandins.2016.06.003>
- Norton, L., Shannon, C., Gastaldelli, A., & DeFronzo, R. A. (2022). Insulin: The master regulator of glucose metabolism. *Metabolism: Clinical and Experimental*, 129, 155142. <https://doi.org/10.1016/j.metabol.2022.155142>

- Nuutila, P., Koivisto, V. A., Knuuti, J., Ruotsalainen, U., Teräs, M., Haaparanta, M., Bergman, J., Solin, O., Voipio-Pulkki, L. M., & Wegelius, U. (1992). Glucose-free fatty acid cycle operates in human heart and skeletal muscle in vivo. *The Journal of Clinical Investigation*, 89(6), 1767–1774. <https://doi.org/10.1172/JCI115780>
- O'Hare, J. D., Zielinski, E., Cheng, B., Scherer, T., & Buettner, C. (2011). Central endocannabinoid signaling regulates hepatic glucose production and systemic lipolysis. *Diabetes*, 60(4), 1055–1062. <https://doi.org/10.2337/db10-0962>
- Obici, S., Feng, Z., Karkanias, G., Baskin, D. G., & Rossetti, L. (2002). Decreasing hypothalamic insulin receptors causes hyperphagia and insulin resistance in rats. *Nature Neuroscience*, 5(6), 566–572. <https://doi.org/10.1038/nn0602-861>
- Obici, S., Feng, Z., Tan, J., Liu, L., Karkanias, G., & Rossetti, L. (2001). Central melanocortin receptors regulate insulin action. *The Journal of Clinical Investigation*, 108(7), 1079–1085. <https://doi.org/10.1172/JCI12954>
- Obici, S., Zhang, B. B., Karkanias, G., & Rossetti, L. (2002). Hypothalamic insulin signaling is required for inhibition of glucose production. *Nature Medicine*, 8(12), 1376–1382. <https://doi.org/10.1038/nm798>
- Oikonen, V. (2021). *Fractional uptake rate (FUR)*. http://www.turkupetcentre.net/petanalysis/model_fur.html
- Oikonen, V. (2023). *Multiple Time Graphical Analysis (MTGA)*. http://www.turkupetcentre.net/petanalysis/model_mtga.html
- Olver, T. D., Grunewald, Z. I., Jurrissen, T. J., MacPherson, R. E. K., LeBlanc, P. J., Schnurbusch, T. R., Czajkowski, A. M., Laughlin, M. H., Rector, R. S., Bender, S. B., Walters, E. M., Emter, C. A., & Padilla, J. (2018). Microvascular insulin resistance in skeletal muscle and brain occurs early in the development of juvenile obesity in pigs. *American Journal of Physiology. Regulatory, Integrative and Comparative Physiology*, 314(2), R252–R264. <https://doi.org/10.1152/ajpregu.00213.2017>
- Ono, H., Pocai, A., Wang, Y., Sakoda, H., Asano, T., Backer, J. M., Schwartz, G. J., & Rossetti, L. (2008). Activation of hypothalamic S6 kinase mediates diet-induced hepatic insulin resistance in rats. *The Journal of Clinical Investigation*, 118(8), 2959–2968. <https://doi.org/10.1172/JCI34277>
- Orava, J., Nuutila, P., Lidell, M. E., Oikonen, V., Noponen, T., Viljanen, T., Scheinin, M., Taittonen, M., Niemi, T., Enerbäck, S., & Virtanen, K. A. (2011). Different metabolic responses of human brown adipose tissue to activation by cold and insulin. *Cell Metabolism*, 14(2), 272–279. <https://doi.org/10.1016/j.cmet.2011.06.012>
- Orava, J., Nuutila, P., Noponen, T., Parkkola, R., Viljanen, T., Enerbäck, S., Rissanen, A., Pietiläinen, K. H., & Virtanen, K. A. (2013). Blunted metabolic responses to cold and insulin stimulation in brown adipose tissue of obese humans. *Obesity (Silver Spring, Md.)*, 21(11), 2279–2287. <https://doi.org/10.1002/oby.20456>
- Osei-Hyiaman, D., DePetrillo, M., Pacher, P., Liu, J., Radaeva, S., Bátkai, S., Harvey-White, J., Mackie, K., Offertáler, L., Wang, L., & Kunos, G. (2005). Endocannabinoid activation at hepatic CB1 receptors stimulates fatty acid synthesis and contributes to diet-induced obesity. *The Journal of Clinical Investigation*, 115(5), 1298–1305. <https://doi.org/10.1172/JCI23057>
- Oussaada, S. M., van Galen, K. A., Cooman, M. I., Kleinendorst, L., Hazebroek, E. J., van Haelst, M. M., Ter Horst, K. W., & Serlie, M. J. (2019). The pathogenesis of obesity. *Metabolism: Clinical and Experimental*, 92, 26–36. <https://doi.org/10.1016/j.metabol.2018.12.012>
- Pagano, C., Pilon, C., Calcagno, A., Urbanet, R., Rossato, M., Milan, G., Bianchi, K., Rizzuto, R., Bernante, P., Federspil, G., & Vettor, R. (2007). The endogenous cannabinoid system stimulates glucose uptake in human fat cells via phosphatidylinositol 3-kinase and calcium-dependent mechanisms. *The Journal of Clinical Endocrinology and Metabolism*, 92(12), 4810–4819. <https://doi.org/10.1210/jc.2007-0768>

- Pagotto, U., Marsicano, G., Cota, D., Lutz, B., & Pasquali, R. (2006). The emerging role of the endocannabinoid system in endocrine regulation and energy balance. *Endocrine Reviews*, 27(1), 73–100. <https://doi.org/10.1210/er.2005-0009>
- Paranjape, S. A., Chan, O., Zhu, W., Horblitt, A. M., McNay, E. C., Cresswell, J. A., Bogan, J. S., McCrimmon, R. J., & Sherwin, R. S. (2010). Influence of insulin in the ventromedial hypothalamus on pancreatic glucagon secretion in vivo. *Diabetes*, 59(6), 1521–1527. <https://doi.org/10.2337/db10-0014>
- Parlevliet, E. T., Coomans, C. P., Rensen, P. C. N., & Romijn, J. A. (2014). The Brain Modulates Insulin Sensitivity in Multiple Tissues. In P. J. D. Delhanty & A. J. van der Lely (Eds.), *How Gut and Brain Control Metabolism* (Vol. 42, p. 0). S.Karger AG. <https://doi.org/10.1159/000358314>
- Patlak, C. S., & Blasberg, R. G. (1985). Graphical evaluation of blood-to-brain transfer constants from multiple-time uptake data. Generalizations. *Journal of Cerebral Blood Flow and Metabolism : Official Journal of the International Society of Cerebral Blood Flow and Metabolism*, 5(4), 584–590. <https://doi.org/10.1038/jcbfm.1985.87>
- Peltoniemi, P., Lönnroth, P., Laine, H., Oikonen, V., Tolvanen, T., Grönroos, T., Strindberg, L., Knuuti, J., & Nuutila, P. (2000). Lumped constant for [(18)F]fluorodeoxyglucose in skeletal muscles of obese and nonobese humans. *American Journal of Physiology. Endocrinology and Metabolism*, 279(5), E1122–30. <https://doi.org/10.1152/ajpendo.2000.279.5.E1122>
- Pereira-Miranda, E., Costa, P. R. F., Queiroz, V. A. O., Pereira-Santos, M., & Santana, M. L. P. (2017). Overweight and Obesity Associated with Higher Depression Prevalence in Adults: A Systematic Review and Meta-Analysis. *Journal of the American College of Nutrition*, 36(3), 223–233. <https://doi.org/10.1080/07315724.2016.1261053>
- Pertwee, R. G. (2006). The pharmacology of cannabinoid receptors and their ligands: an overview. *International Journal of Obesity (2005)*, 30 Suppl 1, S13–8. <https://doi.org/10.1038/sj.ijo.0803272>
- Petersen, K. F., Dufour, S., Savage, D. B., Bilz, S., Solomon, G., Yonemitsu, S., Cline, G. W., Befroy, D., Zeman, L., Kahn, B. B., Papademetris, X., Rothman, D. L., & Shulman, G. I. (2007). The role of skeletal muscle insulin resistance in the pathogenesis of the metabolic syndrome. *Proceedings of the National Academy of Sciences of the United States of America*, 104(31), 12587–12594. <https://doi.org/10.1073/pnas.0705408104>
- Petersen, M. C., & Shulman, G. I. (2018). Mechanisms of Insulin Action and Insulin Resistance. *Physiological Reviews*, 98(4), 2133–2223. <https://doi.org/10.1152/physrev.00063.2017>
- Phelps, M. E., Huang, S. C., Hoffman, E. J., Selin, C., Sokoloff, L., & Kuhl, D. E. (1979). Tomographic measurement of local cerebral glucose metabolic rate in humans with (F-18)2-fluoro-2-deoxy-D-glucose: validation of method. *Annals of Neurology*, 6(5), 371–388. <https://doi.org/10.1002/ana.410060502>
- Pischon, T., Boeing, H., Hoffmann, K., Bergmann, M., Schulze, M. B., Overvad, K., van der Schouw, Y. T., Spencer, E., Moons, K. G. M., Tjønneland, A., Halkjaer, J., Jensen, M. K., Stegger, J., Clavel-Chapelon, F., Boutron-Ruault, M.-C., Chajes, V., Linseisen, J., Kaaks, R., Trichopoulou, A., ... Riboli, E. (2008). General and abdominal adiposity and risk of death in Europe. *The New England Journal of Medicine*, 359(20), 2105–2120. <https://doi.org/10.1056/NEJMoa0801891>
- Plum, L., Schubert, M., & Brüning, J. C. (2005). The role of insulin receptor signaling in the brain. In *Trends in Endocrinology and Metabolism* (Vol. 16, Issue 2, pp. 59–65). Elsevier Inc. <https://doi.org/10.1016/j.tem.2005.01.008>
- Pocai, A., Lam, T. K. T., Gutierrez-Juarez, R., Obici, S., Schwartz, G. J., Bryan, J., Aguilar-Bryan, L., & Rossetti, L. (2005). Hypothalamic K(ATP) channels control hepatic glucose production. *Nature*, 434(7036), 1026–1031. <https://doi.org/10.1038/nature03439>
- Puig, J., Blasco, G., Daunis-I-Estadella, J., Molina, X., Xifra, G., Ricart, W., Pedraza, S., Fernández-Aranda, F., & Fernández-Real, J. M. (2015). Hypothalamic damage is associated with inflammatory markers and worse cognitive performance in obese subjects. *The Journal of Clinical Endocrinology and Metabolism*, 100(2), E276–81. <https://doi.org/10.1210/jc.2014-2682>

- Qayyum, A., Chen, D. M., Breiman, R. S., Westphalen, A. C., Yeh, B. M., Jones, K. D., Lu, Y., Coakley, F. V., & Callen, P. W. (2009). Evaluation of diffuse liver steatosis by ultrasound, computed tomography, and magnetic resonance imaging: which modality is best? *Clinical Imaging*, 33(2), 110–115. <https://doi.org/10.1016/j.clinimag.2008.06.036>
- Quarta, C., Mazza, R., Obici, S., Pasquali, R., & Pagotto, U. (2011). Energy balance regulation by endocannabinoids at central and peripheral levels. *Trends in Molecular Medicine*, 17(9), 518–526. <https://doi.org/10.1016/j.molmed.2011.05.002>
- Radziuk, J., & Pye, S. (2002). Quantitation of basal endogenous glucose production in Type II diabetes: Importance of the volume of distribution. In *Diabetologia*. <https://doi.org/10.1007/s00125-002-0841-6>
- Ramage, L. E., Akyol, M., Fletcher, A. M., Forsythe, J., Nixon, M., Carter, R. N., van Beek, E. J. R., Morton, N. M., Walker, B. R., & Stimson, R. H. (2016). Glucocorticoids Acutely Increase Brown Adipose Tissue Activity in Humans, Revealing Species-Specific Differences in UCP-1 Regulation. *Cell Metabolism*, 24(1), 130–141. <https://doi.org/10.1016/j.cmet.2016.06.011>
- Ramnanan, C. J., Saraswathi, V., Smith, M. S., Donahue, E. P., Farmer, B., Farmer, T. D., Neal, D., Williams, P. E., Lautz, M., Mari, A., Cherrington, A. D., & Edgerton, D. S. (2011). Brain insulin action augments hepatic glycogen synthesis without suppressing glucose production or gluconeogenesis in dogs. *The Journal of Clinical Investigation*, 121(9), 3713–3723. <https://doi.org/10.1172/JCI45472>
- Rebelos, E. (2020). *Novel aspects of insulin resistance: focus on the brain. Studies using positron emission tomography*. <https://urn.fi/URN:ISBN:978-951-29-8151-9>
- Rebelos, E., Bucci, M., Karjalainen, T., Oikonen, V., Bertoldo, A., Hannukainen, J. C., Virtanen, K. A., Latva-Rasku, A., Hirvonen, J., Heinonen, I., Parkkola, R., Laakso, M., Ferrannini, E., Iozzo, P., Nummenmaa, L., & Nuutila, P. (2021). Insulin Resistance Is Associated With Enhanced Brain Glucose Uptake During Euglycemic Hyperinsulinemia: A Large-Scale PET Cohort. *Diabetes Care*, 44(3), 788–794. <https://doi.org/10.2337/dc20-1549>
- Rebelos, E., Immonen, H., Bucci, M., Hannukainen, J. C., Nummenmaa, L., Honka, M. J., Soinio, M., Salminen, P., Ferrannini, E., Iozzo, P., & Nuutila, P. (2019). Brain glucose uptake is associated with endogenous glucose production in obese patients before and after bariatric surgery and predicts metabolic outcome at follow-up. *Diabetes, Obesity and Metabolism*, 21(2), 218–226. <https://doi.org/10.1111/dom.13501>
- Rebelos, E., Mari, A., Bucci, M., Honka, M.-J., Hannukainen, J. C., Virtanen, K. A., Hirvonen, J., Nummenmaa, L., Heni, M., Iozzo, P., Ferrannini, E., & Nuutila, P. (2020). Brain substrate metabolism and β -cell function in humans: A positron emission tomography study. *Endocrinology, Diabetes & Metabolism*, 3(3), e00136. <https://doi.org/10.1002/edm2.136>
- Ren, H., Lu, T. Y., McGraw, T. E., & Accili, D. (2015). Anorexia and impaired glucose metabolism in mice with hypothalamic ablation of Glut4 neurons. *Diabetes*, 64(2), 405–417. <https://doi.org/10.2337/db14-0752>
- Reno, C. M., Puente, E. C., Sheng, Z., Daphna-Iken, D., Bree, A. J., Routh, V. H., Kahn, B. B., & Fisher, S. J. (2017). Brain GLUT4 Knockout Mice Have Impaired Glucose Tolerance, Decreased Insulin Sensitivity, and Impaired Hypoglycemic Counterregulation. *Diabetes*, 66(3), 587–597. <https://doi.org/10.2337/db16-0917>
- Repple, J., Opel, N., Meinert, S., Redlich, R., Hahn, T., Winter, N. R., Kaehler, C., Emden, D., Leenings, R., Grotegerd, D., Zaremba, D., Bürger, C., Förster, K., Dohm, K., Enneking, V., Leehr, E. J., Böhnlein, J., Karliczek, G., Heindel, W., ... Dannlowski, U. (2018). Elevated body-mass index is associated with reduced white matter integrity in two large independent cohorts. *Psychoneuroendocrinology*, 91, 179–185. <https://doi.org/10.1016/j.psyneuen.2018.03.007>
- Richard, D., Guesdon, B., & Timofeeva, E. (2009). The brain endocannabinoid system in the regulation of energy balance. *Best Practice & Research. Clinical Endocrinology & Metabolism*, 23(1), 17–32. <https://doi.org/10.1016/j.beem.2008.10.007>

- Rinaldi-Carmona, M., Barth, F., Héaulme, M., Shire, D., Calandra, B., Congy, C., Martinez, S., Maruani, J., Néliat, G., & Caput, D. (1994). SR141716A, a potent and selective antagonist of the brain cannabinoid receptor. *FEBS Letters*, 350(2–3), 240–244. [https://doi.org/10.1016/0014-5793\(94\)00773-x](https://doi.org/10.1016/0014-5793(94)00773-x)
- Roden, M., & Shulman, G. I. (2019). The integrative biology of type 2 diabetes. *Nature*, 576(7785), 51–60. <https://doi.org/10.1038/s41586-019-1797-8>
- Roh, E., Song, D. K., & Kim, M.-S. (2016). Emerging role of the brain in the homeostatic regulation of energy and glucose metabolism. *Experimental & Molecular Medicine*, 48(3), e216. <https://doi.org/10.1038/emm.2016.4>
- Rolfe, D. F., & Brown, G. C. (1997). Cellular energy utilization and molecular origin of standard metabolic rate in mammals. *Physiological Reviews*, 77(3), 731–758. <https://doi.org/10.1152/physrev.1997.77.3.731>
- Rosario, W., Singh, I., Wautlet, A., Patterson, C., Flak, J., Becker, T. C., Ali, A., Tamarina, N., Philipson, L. H., Enquist, L. W., Myers, M. G. J., & Rhodes, C. J. (2016). The Brain-to-Pancreatic Islet Neuronal Map Reveals Differential Glucose Regulation From Distinct Hypothalamic Regions. *Diabetes*, 65(9), 2711–2723. <https://doi.org/10.2337/db15-0629>
- Saltiel, A. R., & Kahn, C. R. (2001). Insulin signalling and the regulation of glucose and lipid metabolism. *Nature*, 414(6865), 799–806. <https://doi.org/10.1038/414799a>
- Sam, A. H., Salem, V., & Ghatge, M. A. (2011). Rimobabant: From RIO to Ban. *Journal of Obesity*, 2011, 432607. <https://doi.org/10.1155/2011/432607>
- Samuel, V. T., & Shulman, G. I. (2016). The pathogenesis of insulin resistance: integrating signaling pathways and substrate flux. *The Journal of Clinical Investigation*, 126(1), 12–22. <https://doi.org/10.1172/JCI77812>
- Sanchez-Alavez, M., Tabarean, I. V., Osborn, O., Mitsukawa, K., Schaefer, J., Dubins, J., Holmberg, K. H., Klein, I., Klaus, J., Gomez, L. F., Kolb, H., Secrest, J., Jochems, J., Myashiro, K., Buckley, P., Hadcock, J. R., Eberwine, J., Conti, B., & Bartfai, T. (2010). Insulin causes hyperthermia by direct inhibition of warm-sensitive neurons. *Diabetes*, 59(1), 43–50. <https://doi.org/10.2337/db09-1128>
- Sarzani, R., Bordicchia, M., Marcucci, P., Bedetta, S., Santini, S., Giovagnoli, A., Scappini, L., Minardi, D., Muzzonigro, G., Dessi-Fulgheri, P., & Rappelli, A. (2009). Altered pattern of cannabinoid type 1 receptor expression in adipose tissue of dysmetabolic and overweight patients. *Metabolism: Clinical and Experimental*, 58(3), 361–367. <https://doi.org/10.1016/j.metabol.2008.10.009>
- Scherer, T., Lindtner, C., O’Hare, J., Hackl, M., Zielinski, E., Freudenthaler, A., Baumgartner-Parzer, S., Tödter, K., Heeren, J., Krššák, M., Scheja, L., Fürsinn, C., & Buettner, C. (2016). Insulin Regulates Hepatic Triglyceride Secretion and Lipid Content via Signaling in the Brain. *Diabetes*, 65(6), 1511–1520. <https://doi.org/10.2337/db15-1552>
- Scherer, T., O’Hare, J., Diggs-Andrews, K., Schweiger, M., Cheng, B., Lindtner, C., Zielinski, E., Vempati, P., Su, K., Dighe, S., Milsom, T., Puchowicz, M., Scheja, L., Zechner, R., Fisher, S. J., Previs, S. F., & Buettner, C. (2011). Brain insulin controls adipose tissue lipolysis and lipogenesis. *Cell Metabolism*, 13(2), 183–194. <https://doi.org/10.1016/j.cmet.2011.01.008>
- Scherer, T., Sakamoto, K., & Buettner, C. (2021). Brain insulin signalling in metabolic homeostasis and disease. *Nature Reviews. Endocrinology*, 17(8), 468–483. <https://doi.org/10.1038/s41574-021-00498-x>
- Schmid, V., Kullmann, S., Gfrörer, W., Hund, V., Hallschmid, M., Lipp, H.-P., Häring, H.-U., Preissl, H., Fritsche, A., & Heni, M. (2018). Safety of intranasal human insulin: A review. *Diabetes, Obesity & Metabolism*, 20(7), 1563–1577. <https://doi.org/10.1111/dom.13279>
- Schneiter, P., Gillet, M., Chioloro, R., Wauters, J. P., Berger, M., & Tappy, L. (2000). Postprandial hepatic glycogen synthesis in liver transplant recipients. *Transplantation*, 69(5), 978–981. <https://doi.org/10.1097/00007890-200003150-00052>

- Segal, S. S., White, T. P., & Faulkner, J. A. (1986). Architecture, composition, and contractile properties of rat soleus muscle grafts. *The American Journal of Physiology*, 250(3 Pt 1), C474-9. <https://doi.org/10.1152/ajpcell.1986.250.3.C474>
- Seong, J., Kang, J. Y., Sun, J. S., & Kim, K. W. (2019). Hypothalamic inflammation and obesity: a mechanistic review. *Archives of Pharmacal Research*, 42(5), 383–392. <https://doi.org/10.1007/s12272-019-01138-9>
- Sewaybricker, L. E., Huang, A., Chandrasekaran, S., Melhorn, S. J., & Schur, E. A. (2023). The Significance of Hypothalamic Inflammation and Gliosis for the Pathogenesis of Obesity in Humans. *Endocrine Reviews*, 44(2), 281–296. <https://doi.org/10.1210/endrev/bnac023>
- Shin, A. C., Filatova, N., Lindtner, C., Chi, T., Degann, S., Oberlin, D., & Buettner, C. (2017). Insulin Receptor Signaling in POMC, but Not AgRP, Neurons Controls Adipose Tissue Insulin Action. *Diabetes*, 66(6), 1560–1571. <https://doi.org/10.2337/db16-1238>
- Silventoinen, K., & Konttinen, H. (2020). Obesity and eating behavior from the perspective of twin and genetic research. *Neuroscience and Biobehavioral Reviews*, 109, 150–165. <https://doi.org/10.1016/j.neubiorev.2019.12.012>
- Silvestri, C., & Di Marzo, V. (2013). The endocannabinoid system in energy homeostasis and the etiopathology of metabolic disorders. *Cell Metabolism*, 17(4), 475–490. <https://doi.org/10.1016/j.cmet.2013.03.001>
- Simon, V., & Cota, D. (2017). MECHANISMS IN ENDOCRINOLOGY: Endocannabinoids and metabolism: past, present and future. *European Journal of Endocrinology*, 176(6), R309–R324. <https://doi.org/10.1530/EJE-16-1044>
- Sink, K. S., McLaughlin, P. J., Wood, J. A. T., Brown, C., Fan, P., Vemuri, V. K., Peng, Y., Olszewska, T., Thakur, G. A., Makriyannis, A., Parker, L. A., & Salamone, J. D. (2008). The novel cannabinoid CB1 receptor neutral antagonist AM4113 suppresses food intake and food-reinforced behavior but does not induce signs of nausea in rats. *Neuropsychopharmacology: Official Publication of the American College of Neuropsychopharmacology*, 33(4), 946–955. <https://doi.org/10.1038/sj.npp.1301476>
- Snyder, W., Cook, M., Nasset, E., Karhausen, L., Howells, G., & Tipton, I. (1975). *Report of the Task Group on Reference Man. A report prepared by a task group of committee 2 of the international commission on radiological protection*. Pergamon Press.
- Soininen, P., Kangas, A. J., Würtz, P., Suna, T., & Ala-Korpela, M. (2015). Quantitative serum nuclear magnetic resonance metabolomics in cardiovascular epidemiology and genetics. *Circulation. Cardiovascular Genetics*, 8(1), 192–206. <https://doi.org/10.1161/CIRCGENETICS.114.000216>
- Song, C. K., Jackson, R. M., Harris, R. B. S., Richard, D., & Bartness, T. J. (2005). Melanocortin-4 receptor mRNA is expressed in sympathetic nervous system outflow neurons to white adipose tissue. *American Journal of Physiology. Regulatory, Integrative and Comparative Physiology*, 289(5), R1467-76. <https://doi.org/10.1152/ajpregu.00348.2005>
- Sparks, J. D., & Dong, H. H. (2009). FoxO1 and hepatic lipid metabolism. *Current Opinion in Lipidology*, 20(3), 217–226. <https://doi.org/10.1097/MOL.0b013e32832b3f4c>
- Spiegelman, B. M., & Flier, J. S. (2001). Obesity and the regulation of energy balance. *Cell*, 104(4), 531–543. [https://doi.org/10.1016/s0092-8674\(01\)00240-9](https://doi.org/10.1016/s0092-8674(01)00240-9)
- Stoeckel, L. E., Weller, R. E., Cook, E. W. 3rd, Twieg, D. B., Knowlton, R. C., & Cox, J. E. (2008). Widespread reward-system activation in obese women in response to pictures of high-calorie foods. *NeuroImage*, 41(2), 636–647. <https://doi.org/10.1016/j.neuroimage.2008.02.031>
- Stouffer, M. A., Woods, C. A., Patel, J. C., Lee, C. R., Witkovsky, P., Bao, L., Machold, R. P., Jones, K. T., de Vaca, S. C., Reith, M. E. A., Carr, K. D., & Rice, M. E. (2015). Insulin enhances striatal dopamine release by activating cholinergic interneurons and thereby signals reward. *Nature Communications*, 6, 8543. <https://doi.org/10.1038/ncomms9543>
- Szczepaniak, L. S., Nurenberg, P., Leonard, D., Browning, J. D., Reingold, J. S., Grundy, S., Hobbs, H. H., & Dobbins, R. L. (2005). Magnetic resonance spectroscopy to measure hepatic triglyceride

- content: prevalence of hepatic steatosis in the general population. *American Journal of Physiology. Endocrinology and Metabolism*, 288(2), E462–8. <https://doi.org/10.1152/ajpendo.00064.2004>
- Takkinen, J. S., López-Picón, F. R., Kirjavainen, A. K., Pihlaja, R., Snellman, A., Ishizu, T., Löyttyniemi, E., Solin, O., Rinne, J. O., & Haaparanta-Solin, M. (2018). [(18)F]FMPEP-d(2) PET imaging shows age- and genotype-dependent impairments in the availability of cannabinoid receptor 1 in a mouse model of Alzheimer's disease. *Neurobiology of Aging*, 69, 199–208. <https://doi.org/10.1016/j.neurobiolaging.2018.05.013>
- Tam, J., Cinar, R., Liu, J., Godlewski, G., Wesley, D., Jourdan, T., Szanda, G., Mukhopadhyay, B., Chedester, L., Liow, J.-S., Innis, R. B., Cheng, K., Rice, K. C., Deschamps, J. R., Chorvat, R. J., McElroy, J. F., & Kunos, G. (2012). Peripheral cannabinoid-1 receptor inverse agonism reduces obesity by reversing leptin resistance. *Cell Metabolism*, 16(2), 167–179. <https://doi.org/10.1016/j.cmet.2012.07.002>
- Tam, J., Szanda, G., Drori, A., Liu, Z., Cinar, R., Kashiwaya, Y., Reitman, M. L., & Kunos, G. (2017). Peripheral cannabinoid-1 receptor blockade restores hypothalamic leptin signaling. *Molecular Metabolism*, 6(10), 1113–1125. <https://doi.org/10.1016/j.molmet.2017.06.010>
- Tam, J., Vemuri, V. K., Liu, J., Bátka, S., Mukhopadhyay, B., Godlewski, G., Osei-Hyiaman, D., Ohnuma, S., Ambudkar, S. V., Pickel, J., Makriyannis, A., & Kunos, G. (2010). Peripheral CB1 cannabinoid receptor blockade improves cardiometabolic risk in mouse models of obesity. *The Journal of Clinical Investigation*, 120(8), 2953–2966. <https://doi.org/10.1172/JCI42551>
- Tarragon, E., & Moreno, J. J. (2017). Role of Endocannabinoids on Sweet Taste Perception, Food Preference, and Obesity-related Disorders. *Chemical Senses*, 43(1), 3–16. <https://doi.org/10.1093/chemse/bjx062>
- Terry, G. E., Hirvonen, J., Liow, J.-S., Seneca, N., Tauscher, J. T., Schaus, J. M., Phebus, L., Felder, C. C., Morse, C. L., Pike, V. W., Halldin, C., & Innis, R. B. (2010). Biodistribution and dosimetry in humans of two inverse agonists to image cannabinoid CB1 receptors using positron emission tomography. *European Journal of Nuclear Medicine and Molecular Imaging*, 37(8), 1499–1506. <https://doi.org/10.1007/s00259-010-1411-7>
- Terry, G. E., Hirvonen, J., Liow, J.-S., Zoghbi, S. S., Gladding, R., Tauscher, J. T., Schaus, J. M., Phebus, L., Felder, C. C., Morse, C. L., Donohue, S. R., Pike, V. W., Halldin, C., & Innis, R. B. (2010). Imaging and quantitation of cannabinoid CB1 receptors in human and monkey brains using (18)F-labeled inverse agonist radioligands. *Journal of Nuclear Medicine: Official Publication, Society of Nuclear Medicine*, 51(1), 112–120. <https://doi.org/10.2967/jnumed.109.067074>
- Thaler, J. P., Yi, C.-X., Schur, E. A., Guyenet, S. J., Hwang, B. H., Dietrich, M. O., Zhao, X., Sarruf, D. A., Izgur, V., Maravilla, K. R., Nguyen, H. T., Fischer, J. D., Matsen, M. E., Wisse, B. E., Morton, G. J., Horvath, T. L., Baskin, D. G., Tschöp, M. H., & Schwartz, M. W. (2012). Obesity is associated with hypothalamic injury in rodents and humans. *The Journal of Clinical Investigation*, 122(1), 153–162. <https://doi.org/10.1172/JCI59660>
- Thie, J. A. (1995). Clarification of a fractional uptake concept. In *Journal of nuclear medicine: official publication, Society of Nuclear Medicine* (Vol. 36, Issue 4, pp. 711–712).
- Thorens, B. (2015). GLUT2, glucose sensing and glucose homeostasis. *Diabetologia*, 58(2), 221–232. <https://doi.org/10.1007/s00125-014-3451-1>
- Timper, K., & Brüning, J. C. (2017). Hypothalamic circuits regulating appetite and energy homeostasis: pathways to obesity. *Disease Models & Mechanisms*, 10(6), 679–689. <https://doi.org/10.1242/dmm.026609>
- Titchenell, P. M., Lazar, M. A., & Birnbaum, M. J. (2017). Unraveling the Regulation of Hepatic Metabolism by Insulin. *Trends in Endocrinology and Metabolism: TEM*, 28(7), 497–505. <https://doi.org/10.1016/j.tem.2017.03.003>
- Tschritter, O., Preissl, H., Hennige, A. M., Sartorius, T., Grichisch, Y., Stefan, N., Guthoff, M., Düsing, S., Machann, J., Schleicher, E., Cegan, A., Birbaumer, N., Fritsche, A., & Häring, H.-U. (2009). The insulin effect on cerebrocortical theta activity is associated with serum concentrations of

- saturated nonesterified Fatty acids. *The Journal of Clinical Endocrinology and Metabolism*, 94(11), 4600–4607. <https://doi.org/10.1210/jc.2009-0469>
- Tschritter, O., Preissl, H., Hennige, A. M., Stumvoll, M., Porubska, K., Frost, R., Marx, H., Klösel, B., Lutzenberger, W., Birbaumer, N., Häring, H.-U., & Fritsche, A. (2006). The cerebrocortical response to hyperinsulinemia is reduced in overweight humans: a magnetoencephalographic study. *Proceedings of the National Academy of Sciences of the United States of America*, 103(32), 12103–12108. <https://doi.org/10.1073/pnas.0604404103>
- Tuominen, L., Nummenmaa, L., Keltikangas-Järvinen, L., Raitakari, O., & Hietala, J. (2014). Mapping neurotransmitter networks with PET: an example on serotonin and opioid systems. *Human Brain Mapping*, 35(5), 1875–1884. <https://doi.org/10.1002/hbm.22298>
- Turkington, T. G. (2001). Introduction to PET instrumentation. *Journal of Nuclear Medicine Technology*, 29(1), 4–11.
- Tuulari, J. J., Karlsson, H. K., Hirvonen, J., Hannukainen, J. C., Bucci, M., Helmiö, M., Ovaska, J., Soinio, M., Salminen, P., Savisto, N., Nummenmaa, L., & Nuutila, P. (2013). Weight loss after bariatric surgery reverses insulin-induced increases in brain glucose metabolism of the morbidly obese. *Diabetes*, 62(8), 2747–2751. <https://doi.org/10.2337/db12-1460>
- van Schaftingen, E., & Gerin, I. (2002). The glucose-6-phosphatase system. *The Biochemical Journal*, 362(Pt 3), 513–532. <https://doi.org/10.1042/0264-6021:3620513>
- Virtanen, K. A., Lönnroth, P., Parkkola, R., Peltoniemi, P., Asola, M., Viljanen, T., Tolvanen, T., Knuuti, J., Rönnemaa, T., Huupponen, R., & Nuutila, P. (2002). Glucose uptake and perfusion in subcutaneous and visceral adipose tissue during insulin stimulation in nonobese and obese humans. *The Journal of Clinical Endocrinology and Metabolism*, 87(8), 3902–3910. <https://doi.org/10.1210/jcem.87.8.8761>
- Virtanen, K. A., Peltoniemi, P., Marjamäki, P., Asola, M., Strindberg, L., Parkkola, R., Huupponen, R., Knuuti, J., Lönnroth, P., & Nuutila, P. (2001). Human adipose tissue glucose uptake determined using [¹⁸F]-fluoro-deoxy-glucose ([¹⁸F]FDG) and PET in combination with microdialysis. In *Diabetologia* (Vol. 44).
- Vogt, M. C., Paeger, L., Hess, S., Steculorum, S. M., Awazawa, M., Hampel, B., Neupert, S., Nicholls, H. T., Mauer, J., Hausen, A. C., Predel, R., Kloppenburg, P., Horvath, T. L., & Brüning, J. C. (2014). Neonatal insulin action impairs hypothalamic neurocircuit formation in response to maternal high-fat feeding. *Cell*, 156(3), 495–509. <https://doi.org/10.1016/j.cell.2014.01.008>
- Waise, T. M. Z., Toshinai, K., Naznin, F., NamKoong, C., Md Moin, A. S., Sakoda, H., & Nakazato, M. (2015). One-day high-fat diet induces inflammation in the nodose ganglion and hypothalamus of mice. *Biochemical and Biophysical Research Communications*, 464(4), 1157–1162. <https://doi.org/10.1016/j.bbrc.2015.07.097>
- Wajchenberg, B. L. (2000). Subcutaneous and visceral adipose tissue: their relation to the metabolic syndrome. *Endocrine Reviews*, 21(6), 697–738. <https://doi.org/10.1210/edrv.21.6.0415>
- Wang, G. J., Volkow, N. D., Logan, J., Pappas, N. R., Wong, C. T., Zhu, W., Netusil, N., & Fowler, J. S. (2001). Brain dopamine and obesity. *Lancet (London, England)*, 357(9253), 354–357. [https://doi.org/10.1016/s0140-6736\(00\)03643-6](https://doi.org/10.1016/s0140-6736(00)03643-6)
- Watanabe, S., Doshi, M., & Hamazaki, T. (2003). n-3 Polyunsaturated fatty acid (PUFA) deficiency elevates and n-3 PUFA enrichment reduces brain 2-arachidonoylglycerol level in mice. *Prostaglandins, Leukotrienes, and Essential Fatty Acids*, 69(1), 51–59. [https://doi.org/10.1016/s0952-3278\(03\)00056-5](https://doi.org/10.1016/s0952-3278(03)00056-5)
- Weiss, M., Steiner, D. F., & Philipson, L. H. (2000). *Insulin Biosynthesis, Secretion, Structure, and Structure-Activity Relationships*. (K. R. Feingold, B. Anawalt, M. R. Blackman, A. Boyce, G. Chrousos, E. Corpas, W. W. de Herder, K. Dhatriya, K. Dungan, J. Hofland, S. Kalra, G. Kaltsas, N. Kapoor, C. Koch, P. Kopp, M. Korbonits, C. S. Kovacs, W. Kuohung, B. Laferrère, ... D. P. Wilson (Eds.)).
- White, H., & Venkatesh, B. (2011). Clinical review: ketones and brain injury. *Critical Care (London, England)*, 15(2), 219. <https://doi.org/10.1186/cc10020>

- Whitlock, G., Lewington, S., Sherliker, P., Clarke, R., Emberson, J., Halsey, J., Qizilbash, N., Collins, R., & Peto, R. (2009). Body-mass index and cause-specific mortality in 900 000 adults: collaborative analyses of 57 prospective studies. *Lancet (London, England)*, 373(9669), 1083–1096. [https://doi.org/10.1016/S0140-6736\(09\)60318-4](https://doi.org/10.1016/S0140-6736(09)60318-4)
- WHO. (2021). World Health Organization (WHO), Obesity and Overweight. <https://www.who.int/news-room/fact-sheets/detail/obesity-and-overweight>
- Wilson, J. L., & Enriori, P. J. (2015). A talk between fat tissue, gut, pancreas and brain to control body weight. *Molecular and Cellular Endocrinology*, 418 Pt 2, 108–119. <https://doi.org/10.1016/j.mce.2015.08.022>
- Woods, S. C., & Porte, D. J. (1975). Effect of intracisternal insulin on plasma glucose and insulin in the dog. *Diabetes*, 24(10), 905–909. <https://doi.org/10.2337/diab.24.10.905>
- Woods, S. C., Seeley, R. J., Baskin, D. G., & Schwartz, M. W. (2003). Insulin and the blood-brain barrier. *Current Pharmaceutical Design*, 9(10), 795–800. <https://doi.org/10.2174/1381612033455323>
- World Obesity. (2023). The World Obesity Federation (World Obesity), World Obesity Atlas 2023. <https://data.worldobesity.org/publications/?cat=19>
- Wu, H.-M., Bergsneider, M., Glenn, T. C., Yeh, E., Hovda, D. A., Phelps, M. E., & Huang, S.-C. (2003). Measurement of the global lumped constant for 2-deoxy-2-[18F]fluoro-D-glucose in normal human brain using [15O]water and 2-deoxy-2-[18F]fluoro-D-glucose positron emission tomography imaging. A method with validation based on multiple methodologies. *Molecular Imaging and Biology*, 5(1), 32–41. [https://doi.org/10.1016/s1536-1632\(02\)00122-1](https://doi.org/10.1016/s1536-1632(02)00122-1)
- Yan, Z. C., Liu, D. Y., Zhang, L. L., Shen, C. Y., Ma, Q. L., Cao, T. B., Wang, L. J., Nie, H., Zidek, W., Tepel, M., & Zhu, Z. M. (2007). Exercise reduces adipose tissue via cannabinoid receptor type 1 which is regulated by peroxisome proliferator-activated receptor-delta. *Biochemical and Biophysical Research Communications*, 354(2), 427–433. <https://doi.org/10.1016/j.bbrc.2006.12.213>
- You, T., Disanzo, B. L., Wang, X., Yang, R., & Gong, D. (2011). Adipose tissue endocannabinoid system gene expression: depot differences and effects of diet and exercise. *Lipids in Health and Disease*, 10, 194. <https://doi.org/10.1186/1476-511X-10-194>
- Zhang, M., Hu, T., Zhang, S., & Zhou, L. (2015). Associations of Different Adipose Tissue Depots with Insulin Resistance: A Systematic Review and Meta-analysis of Observational Studies. *Scientific Reports*, 5, 18495. <https://doi.org/10.1038/srep18495>

Original Publications

**Kantonen, T., Pekkarinen, L., Karjalainen, T., Bucci, M., Kalliokoski, K.,
Haaparanta-Solin, M., Aarnio, R., Dickens, A. M., von Eyken, A.,
Laitinen, K., Houttu, N., Kirjavainen, A. K., Helin, S., Hirvonen, J.,
Rönnemaa, T., Nuutila, P., & Nummenmaa, L. (2022)
Obesity risk is associated with altered cerebral glucose metabolism
and decreased μ -opioid and CB1 receptor availability.
International Journal of Obesity**

ARTICLE

OPEN



Molecular Biology

Obesity risk is associated with altered cerebral glucose metabolism and decreased μ -opioid and CB₁ receptor availability

Tatu Kantonen^{1,2}, Laura Pekkarinen^{1,3}, Tomi Karjalainen^{1,4}, Marco Bucci^{1,5}, Kari Kalliokoski¹, Merja Haaparanta-Solin^{1,6}, Richard Aarnio¹, Alex M. Dickens⁷, Annie von Eyken⁷, Kirsi Laitinen^{1,8}, Noora Houlttu⁸, Anna K. Kirjavainen¹, Semi Helin¹, Jussi Hirvonen^{1,9}, Tapani Rönnemaa^{3,10}, Pirjo Nuutila^{1,3} and Lauri Nummenmaa^{1,11}

© The Author(s) 2021

BACKGROUND: Obesity is a pressing public health concern worldwide. Novel pharmacological means are urgently needed to combat the increase of obesity and accompanying type 2 diabetes (T2D). Although fully established obesity is associated with neuromolecular alterations and insulin resistance in the brain, potential obesity-promoting mechanisms in the central nervous system have remained elusive. In this triple-tracer positron emission tomography study, we investigated whether brain insulin signaling, μ -opioid receptors (MORs) and cannabinoid CB₁ receptors (CB₁Rs) are associated with risk for developing obesity.

METHODS: Subjects were 41 young non-obese males with variable obesity risk profiles. Obesity risk was assessed by subjects' physical exercise habits, body mass index and familial risk factors, including parental obesity and T2D. Brain glucose uptake was quantified with [¹⁸F]FDG during hyperinsulinemic euglycemic clamp, MORs were quantified with [¹¹C]carfentanil and CB₁Rs with [¹⁸F]FMPEP-d₂.

RESULTS: Subjects with higher obesity risk had globally increased insulin-stimulated brain glucose uptake (19 high-risk subjects versus 19 low-risk subjects), and familial obesity risk factors were associated with increased brain glucose uptake (38 subjects) but decreased availability of MORs (41 subjects) and CB₁Rs (36 subjects).

CONCLUSIONS: These results suggest that the hereditary mechanisms promoting obesity may be partly mediated via insulin, opioid and endocannabinoid messaging systems in the brain.

International Journal of Obesity (2022) 46:400–407; <https://doi.org/10.1038/s41366-021-00996-y>

INTRODUCTION

Prevalence of obesity has more than doubled from 1975 to date, and in 2016, there were over 600 million obese adults globally [1]. Obesity is a major cause of mortality and morbidity worldwide because it is accompanied with conditions such as type 2 diabetes (T2D), cardiovascular disease and neurodegeneration [2, 3]. Epidemiological studies have indicated overweight, physical inactivity, low socioeconomic status, parental obesity and parental T2D to be key risk factors for future obesity [4–9]. Energy balance regulation is a complex process controlled by both central and peripheral neurohumoral mechanisms, and brain's reward and appetite circuits play a key role in maintenance of obesity [10]. Yet, it is not known if alterations in these systems predispose to subsequent development of obesity.

Among the peripherally produced metabolic hormones, insulin regulates pleasure-driven feeding in mesolimbic pathways, interacting with opioidergic reward systems [11]. In morbidly obese subjects, increasing the plasma insulin concentration to supra-physiological levels results in acceleration of central glucose metabolism [12]. One human positron emission tomography (PET) study with [¹⁸F]FDG found that middle-aged subjects with peripheral insulin resistance have blunted glucose metabolism response to insulin also in brain, especially in appetite-controlling regions such as ventral striatum [13]. These studies suggest that cerebral insulin resistance is a pathophysiological trait in developed obesity, but it is unknown whether alterations in brain's insulin signaling could increase the risk of future weight gain in the non-obese state.

¹Turku PET Centre, University of Turku, Turku FI-20521, Finland. ²Clinical Neurosciences, Turku University Hospital, Turku FI-20521, Finland. ³Department of Endocrinology, Turku University Hospital, Turku FI-20521, Finland. ⁴Turku PET Centre, Turku University Hospital, Turku FI-20521, Finland. ⁵Turku PET Centre, Åbo Akademi University, Turku FI-20500, Finland. ⁶MediCity Research Laboratory, University of Turku, Turku FI-20500, Finland. ⁷Turku Bioscience Centre, University of Turku and Åbo Akademi University, Turku FI-20500, Finland. ⁸Institute of Biomedicine, Research Centre for Integrative Physiology and Pharmacology, University of Turku, Turku FI-20500, Finland. ⁹Department of Radiology, University of Turku and Turku University Hospital, Turku FI-20500, Finland. ¹⁰Department of Medicine, University of Turku, Turku FI-20500, Finland. ¹¹Department of Psychology, University of Turku, Turku FI-20500, Finland. [✉]email: taskan@utu.fi

Received: 10 December 2020 Revised: 6 July 2021 Accepted: 12 October 2021
Published online: 2 November 2021

Table 1. The principles of familial obesity risk (Family Risk) scoring, total score ranging from 0 to 4. Gestational diabetes (one subject) was scored as type 2 diabetes.

Parent overweight or obesity	No	One parent	Both parents
	0	1	2
Parent type 2 diabetes	No	One parent	Both parents
	0	1	2

Endogenous opioids and particularly μ -opioid receptor (MOR) ligands mediate reward and are involved in the control of food intake [14]. Opioid receptor agonists stimulate and antagonists reduce food intake in rodents and humans [15]. PET studies have found global MOR downregulation in morbidly obese humans, and shown that this downregulation recovers after weight loss following bariatric surgery [16]. However, it is not known whether the initial MOR downregulation is caused by obesity, or whether it reflects a vulnerable endophenotype for excessive eating and weight gain.

In addition to opioids, endocannabinoids influence feeding through hypothalamic and cortico-limbic circuits [17]. CB₁ receptor (CB₁R) is the most abundant endocannabinoid receptor in the brain, modulating central effects of endogenous and exogenous cannabinoids [18]. In rats, CB₁-agonist administration to nucleus accumbens shell increases food intake [19], whereas CB₁R knockout mice are immune to diet-induced obesity [20] and have dampened sensitivity to food reward [21]. Furthermore, central CB₁R density is reduced in obese rodents [22]. Lowered central CB₁R density could thus also constitute a risk factor for developing obesity.

In this triple-tracer PET study, we investigated whether risk factors for obesity are associated with insulin-stimulated brain glucose uptake (BGU) and central MOR and CB₁R availability in a sample of healthy, non-obese young males ($n = 41$). Obesity risk was indexed by parental obesity and T2D and participant's physical exercise and actual BMI. The work was a part of PROSPECT project which was preregistered to Clinicaltrials.gov (Neuromolecular Risk Factors for Obesity, PROSPECT, NCT03106688). Based on prior clinical studies on obesity, we hypothesized that higher obesity risk would be associated with increased BGU during hyperinsulinemia [12]. We also hypothesized that higher obesity risk would associate with reduced MOR and CB₁R availability [22, 23].

SUBJECTS AND METHODS

The study was conducted in accordance with the Declaration of Helsinki. The Ethical Committee (EC) of the Hospital District of South-Western Finland approved the study, and all participants signed EC-approved written informed consent forms before data gathering.

Subjects

We recruited 43 men with low or high risk for developing obesity via Internet discussion forums, traditional bulletin boards, university-hosted email lists and newspaper advertisements. Clinical screening was done by a physician (TaK or LP), and it involved medical history checkup, physical examination, 2-h oral 75 g glucose tolerance test (OGTT), urine drug-screening and blood tests. None of the subjects had detectable levels of 11-Nor-9-carboxy- Δ^9 -tetrahydrocannabinol in their blood (a marker of cannabis consumption).

Exclusion criteria were poor compliance with the study schedule, smoking or use of nicotine products, abusive use of alcohol, use of illicit drugs, any chronic disease or medication that could affect glucose metabolism or neurotransmission, neurological or psychiatric disease, eating disorder, any contraindication to magnetic resonance imaging (MRI) and prior participation in PET studies or other significant exposure to radiation. Inclusion criteria for the high-risk (HR) group were male sex, age of 20–35 years, overweight i.e., body mass index (BMI) of 25–30 kg/m², leisure time physical exercise <4 h/week, maternal / paternal

overweight or obesity or maternal/paternal T2D. Inclusion criteria for the low-risk (LR) group were male sex, age of 20–35 years, normal weight i.e., BMI of 18.5–24.9 kg/m², leisure time physical exercise ≥ 4 h/week, and no maternal / paternal T2D.

Risk grouping was based on previously established risk factors for future obesity: BMI [4], leisure time physical exercise (hours/week) [8] and familial obesity risk (Family Risk i.e., current parental overweight / obesity and T2D; [7, 9] Table 1). Altogether 19 men were recruited to the HR group and 24 men to the LR group. Subjects' body fat percentage was measured with air displacement plethysmograph (the Bod Pod system, software version 5.4.0, COSMED, Inc., Concord, CA, USA). Sample size was determined by a priori power analysis based on our prior neuroreceptor PET studies on obesity [23], which suggested that a sample size of 16 + 16 would be sufficient for establishing the predicted effects at $p < 0.05$ with actual power exceeding 0.95, assuming regional effect size of $r = 0.5$.

Two LR subjects were excluded after the screening because they did not respond to further contact attempts. The final sample ($n = 41$) consisted of 19 HR individuals and 22 LR individuals, who were scanned with [¹¹C]carfentanil and MRI. One LR subject discontinued the [¹⁸F]FDG-PET study before the brain scan, because the cannulas felt unpleasant. Two LR subjects' [¹⁸F]FDG scan had to be discontinued before the brain scan because of scheduling problems. A total of 19 LR and 19 HR subjects thus completed the brain [¹⁸F]FDG study. Due to scheduling problems and technical issues, 36 subjects (16 HR and 20 LR individuals) completed the [¹⁸F]FMPEP-*d*₂ scan successfully. One HR subject did not arrive to the body composition analysis. Basic characteristics of the sample are summarized in Table 2.

Radiochemistry

BGU was quantified with [¹⁸F]FDG, which was produced using FASTlab synthesis platform (GE Healthcare) according to a modified method of Hamacher et al. [24] and Lemaire et al. [25]. Radiochemical purity was >98%.

MOR availability was measured with radioligand [¹¹C]carfentanil [26], which was synthesized using [¹¹C]methyl triflate, where cyclotron-produced [¹¹C]methane was halogenated by gas phase reaction into [¹¹C]methyl iodide [27] and converted online into [¹¹C]methyl triflate [28]. The [¹¹C]methane was produced at the Accelerator Laboratory of the Åbo Akademi University, using the ¹⁴N(p, α)¹¹C nuclear reaction in a N₂-H₂ target gas (10 % H₂). [¹¹C]methyl triflate was bubbled into a solution containing acetone (200 μ l), O-desmethyl precursor (0.3–0.4 mg, 0.79–1.05 μ mol) and tetrabutylammonium hydroxide (aq) (4 μ l, 0.2 M) at 0°C. The reaction mixture was diluted and loaded into a solid phase extraction cartridge (C18 Sep-Pak® Light, Waters Corp., Milford, MA) and the cartridge was washed. Dilution and washing were done using 25% ethanol in sterile water solution, 10 mL each step. The [¹¹C]carfentanil was extracted with ethanol from the cartridge, diluted with 0.1 M phosphate buffer solution into <10% ethanol level and finally sterile filtered (Millex GV, 0.22 μ m polyvinylidene fluoride membrane, 33 mm, Merck Millipore). Analytical HPLC column (Phenomenex Luna® 5 μ m C8(2) 100 Å, 4.6 \times 100 mm), acetonitrile (32.5%) in 50 mM H₃PO₄ mobile phase, 1 mL/min flow rate, 7 min run time and detectors in series for UV absorption (210 nm) and radioactivity were used for determination of identity, radiochemical purity and mass concentration. Radiochemical purity of the produced [¹¹C]carfentanil batches was 98.5 \pm 0.3% (mean \pm SD). The injected [¹¹C]carfentanil radioactivity was 248 \pm 11 MBq and molar radioactivity at time of injection 290 \pm 110 MBq/nmol corresponding to an injected mass of 0.40 \pm 0.23 μ g.

CB₁R availability was measured with [¹⁸F]FMPEP-*d*₂, which was produced as described previously [29]. The radiochemical purity was >95% and the molar activity >500 GBq/ μ mol at the end of synthesis.

Image acquisition

Subjects had a 12-h overnight fast before the [¹⁸F]FDG scan, and fasted 6–12 h before the [¹¹C]carfentanil and [¹⁸F]FMPEP-*d*₂ scans. The PET scans were done on separate days. The subjects were advised to abstain from physical exercise in the PET scan days and the day before. Detailed scan protocols and hyperinsulinemic euglycemic clamp execution are described in Supplementary Text 1. The [¹⁸F]FDG scans were done with GE Discovery (Discovery 690 PET/CT, GE Healthcare), and the [¹¹C]carfentanil and [¹⁸F]FMPEP-*d*₂ PET images were acquired with PET/CT (GE Discovery VCT PET/CT, GE Healthcare). The tracer was administered in a catheter placed in subject's antecubital vein. Subject's head was strapped to the scan table to prevent excessive head movement. Computed tomography scans were

Table 2 Characteristics of the final sample ($n = 41$). p value is for two-tailed independent samples t test between the two groups. 34 subjects (18 low-risk and 16 high-risk subjects) had no data points missing. The missing data are denoted and specified^{a,c,d}.

	Low-risk males ($n = 22$)		High-risk males ($n = 19$)		p value
	mean	SD	mean	SD	
Age (years)	23.0	2.9	27.1	4.3	<0.001
BMI (kg/m^2)	22.0	1.9	27.2	1.9	<0.001
Body fat (%) ^a	16.4	5.5	29.1	7.8	<0.001
Physical exercise (hours/week)	6.2	2.8	2.7	1.0	<0.001
Family Risk score (0–4)	0.1	0.3	1.4	0.9	<0.001
Homeostatic Model Assessment for Insulin Resistance (HOMA-IR) ^b	1.2	0.7	2.2	0.8	<0.001
Fasting plasma glucose (mmol/l)	4.9	0.5	5.5	0.4	<0.001
2-h plasma glucose in oral glucose tolerance test (mmol/l)	4.8	1.0	5.9	1.4	0.004
Injected activity of [^{11}C]carfentanil (MBq)	244.5	10.7	252.6	10.7	0.02
Injected activity of [^{18}F]FDG (MBq) ^c	153.7	10.3	159.4	8.9	0.08
Injected activity of [^{18}F]FMPEP- d_2 (MBq) ^d	188.2	11.0	187.6	14.8	0.88

^aBody fat percentage for high-risk subjects is computed with $n = 18$, since one high-risk subject didn't complete the body composition analysis.

^bHOMA-IR indexes body insulin resistance and is quantified from fasting blood values with the equation: $\text{HOMA-IR} = (\text{fP-Glucose} \times \text{fP-Insulin})/22.5$.

^cMean and SD for the low-risk ($n = 19$) and high-risk subjects ($n = 19$) that completed the [^{18}F]FDG scan successfully.

^dMean and SD for the low-risk ($n = 20$) and high-risk subjects ($n = 16$) that completed the [^{18}F]FMPEP- d_2 scan successfully.

acquired before PET scans for attenuation correction. The subjects were clinically monitored by physician throughout the scans. In the [^{18}F]FDG and [^{18}F]FMPEP- d_2 scans, the plasma radioactivity was measured from arterialized blood samples in fixed time intervals using automatic γ -counter (Wizard 1480 3", Wallac, Turku, Finland). Anatomical T1-weighted MR images (TR, 8.1 ms; TE, 3.7 ms; flip angle, 7°; scan time, 263 s; 1 mm³ isotropic voxels) were obtained with PET/MR (Ingenuity TF PET/MR, Philips) for anatomical normalization and reference. Hyperinsulinemic euglycemic clamp was applied during the [^{18}F]FDG scans as previously described [30].

Image processing and modeling

Automated processing tool Magia [31] (<https://github.com/tkjarjal/magia>) was used to process the PET data. Processing began with motion-correction of the PET data followed by coregistration of the PET and MR images. Magia uses FreeSurfer (<http://surfer.nmr.mgh.harvard.edu/>) to define the regions of interest (ROIs) as well as the reference regions (here applicable to [^{11}C]carfentanil data). The ROI-wise kinetic modeling was based on extraction of ROI-wise time-activity curves. Prior to calculation of parametric images, the [^{18}F]FMPEP- d_2 and [^{11}C]carfentanil PET images were smoothed using Gaussian kernel to increase signal-to-noise ratio before model fitting (FWHM = 6 mm for [^{18}F]FMPEP- d_2 , 2 mm for [^{11}C]carfentanil). Parametric images were spatially normalized to MNI-space and finally smoothed using a Gaussian kernel (FWHM = 8 mm for [^{18}F]FDG, 6 mm for [^{11}C]carfentanil and [^{18}F]FMPEP- d_2). BGU-estimates ($\mu\text{mol}/\text{min}/100\text{g}$) obtained from the [^{18}F]FDG PET data are based on fractional uptake rate [32]. [^{11}C]carfentanil binding was quantified by binding potential (BP_{ND}), which is the ratio of specific binding to nondisplaceable binding in the tissue [33]. Occipital cortex was used as the reference region [34]. CB₁R availability was quantified as [^{18}F]FMPEP- d_2 volume of distribution (V_T) using graphical analysis (Logan) [35]. The starting point of 36 min was used, since Logan plots became linear after 36 min from injection [35]. Detailed description about the modeling of each tracer is presented in Supplementary Text 1.

Analysis of serum endocannabinoids

Circulating endocannabinoids might affect central CB₁R availability [36]. Serum endocannabinoids and related fatty acids were analyzed from fasting-state blood samples drawn in [^{18}F]FMPEP- d_2 scan day as described previously [36], with slight modifications (see Supplementary Text 2 for the full description). Serum endocannabinoid levels are shown in Supplementary Table 1.

Experimental design and statistical analysis

Primary analyses. The primary outcome variables in the analyses were BGU measured with [^{18}F]FDG, [^{11}C]carfentanil BP_{ND} and [^{18}F]FMPEP- d_2

V_T . The primary study question was whether these outcome variables differ between the LR and HR groups. Full-volume data were analyzed with nonparametric testing using SnPM13 (<http://niso.org/Software/SnPM13/>). We used $p < 0.05$ as the cluster-defining threshold, and only report clusters large enough to be statistically significant (FWE $p < 0.05$). A total of 5000 permutations were used to estimate the null distribution. LR and HR groups were compared using two-sample t -test. Age was included as a covariate in all full-volume models, since age is known to affect at least [^{11}C]carfentanil binding [37, 38] and [^{18}F]FDG uptake [39].

Secondary analyses. Additionally, we analyzed the associations of individual risk factors (BMI, physical exercise and Family Risk) to the PET outcome variables (BGU, BP_{ND} , and V_T) in a priori ROIs with Bayesian approach. Based on previous studies [12, 40, 41], FreeSurfer (<http://surfer.nmr.mgh.harvard.edu/>) was used to extract 21 bilateral ROIs involved in emotion and food reward processing: amygdala, caudate, cerebellum, dorsal anterior cingulate cortex, hippocampus, inferior temporal gyrus, insula, medulla, midbrain, middle temporal gyrus, nucleus accumbens, orbitofrontal cortex, pars opercularis, posterior cingulate cortex, pons, putamen, rostral anterior cingulate cortex, superior frontal gyrus, superior temporal gyrus, temporal pole, and thalamus. We used varying (random) slopes and intercepts for the ROIs, and thus the results do not require separate correction for multiple ROIs [42]. We used regularizing priors (zero-mean normal distribution with unit-variance) for the regression coefficients to reduce overfitting. Bayesian hierarchical modeling was done with the R package BRMS (<https://cran.r-project.org/package=brms>) that uses the efficient Markov chain Monte Carlo sampling tools of RStan (<https://mc-stan.org/users/interfaces/rstan>). We fitted the models separately for body mass index, familial obesity risk, and physical exercise. All models also included age as a nuisance covariate. We used weakly informative priors: For intercepts, we used the default of BRMS, i.e., Student's t distribution with scale 3 and 10 degrees of freedom. For predictors, a Gaussian distribution with standard deviation of 1 was used to provide weak regularization. The BRMS default prior half Student's t distribution with 3 degrees of freedom was used for standard deviations of group-level effects; BRMS automatically selects the scale parameter to improve convergence and sampling efficiency. The BRMS default prior LKJ (1) was used for correlations of group-level random effects. The ROI-level models were estimated using five chains, each of which had 1000 warmup samples and 4000 post-warmup samples, thus totaling 20000 post-warmup samples. The sampling parameters were slightly modified to facilitate convergence (adapt_delta = 0.99; max_treedepth = 20). The sampling produced no divergent iterations and the Rhats were all 1.0, suggesting that the chains converged successfully. Before model estimation, continuous predictors were standardized to have zero mean and unit variance, thus making the regression coefficients comparable across the

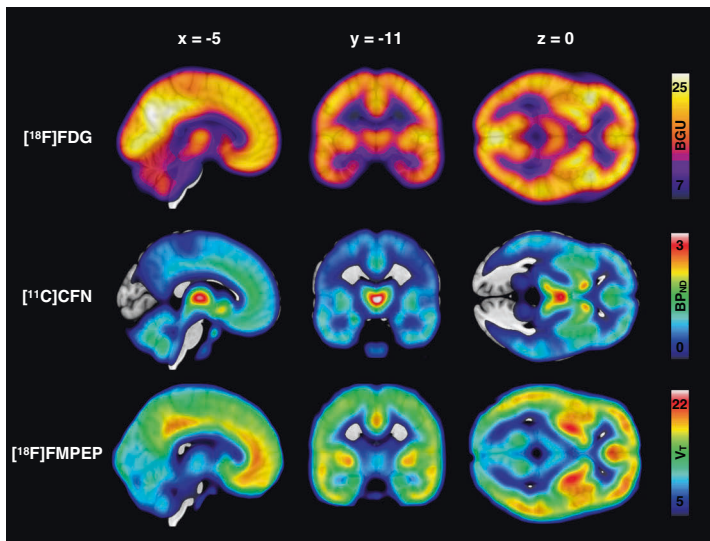


Fig. 1 Mean distribution of brain glucose uptake, μ -opioid receptor availability and CB_1 receptor availability in the whole study sample. Top: Mean brain glucose uptake (BGU) of the 38 $[^{18}F]$ FDG scans (19 low-risk and 19 high-risk subjects). Middle: Mean binding potential (BP_{ND}) of the 41 $[^{11}C]$ carfentanil scans (22 low-risk and 19 high-risk subjects). Bottom: Mean volume of distribution (V_T) of the 36 $[^{18}F]$ FMPEP- d_2 scans (20 low-risk and 16 high-risk subjects).

predictors. All outcome variables ($[^{11}C]$ carfentanil BP_{ND} , $[^{18}F]$ FMPEP- d_2 V_T and BGU) were log-transformed to improve model fit [37]. Since all three outcome variables had associations with the Family Risk score, we created *post hoc* Bayesian linear regression model with age-adjusted BGU, BP_{ND} and V_T values as the predictors of Family Risk to assess the relative effects of the outcome variables.

In addition, serum endocannabinoids were studied in separate full volume models of $[^{18}F]$ FMPEP- d_2 V_T . Since eight distinct endocannabinoid compounds were analyzed, we confirmed the results with Bonferroni-corrected p value as the cluster-defining threshold ($0.05/8 = 0.00625$).

RESULTS

Mean distribution of BGU, MOR availability and CB_1 R availability are shown in Fig. 1. Descriptive Pearson correlations of the sample are presented in the Supplementary Fig. 1 and Supplementary Table 2.

Risk group comparisons

HR group had increased BGU compared to the LR group in multiple brain regions. Prominent associations were found in frontotemporal and cingulate cortices, hypothalamus, and bilaterally in insula and putamen (Fig. 2). MOR or CB_1 R availabilities did not have statistically significant differences between the two groups.

Effects of distinct risk factors

Brain glucose uptake. Increase in Family Risk was associated with globally increased in BGU (Fig. 3, all ROIs in Supplementary Fig. 2). BMI had a moderate positive association with BGU, while increased physical exercise associated with lower BGU (Fig. 3). Full volume visualization of the Family Risk associations is presented in Fig. 4.

μ -opioid receptor availability. Higher Family Risk was associated with lower BP_{ND} in frontotemporal cortex, insula and striatum (Figs. 3 and 4, all ROIs in Supplementary Fig. 2), while the effects of BMI and physical exercise markedly overlapped with zero.

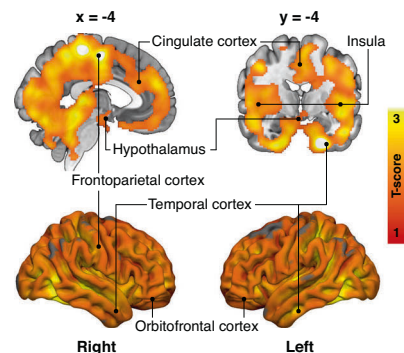


Fig. 2 Obesity risk and brain glucose uptake. Brain regions where the high-risk subjects ($n = 19$) had increased brain glucose uptake (BGU) compared with the low-risk subjects ($n = 19$) while controlling for age. The data are thresholded at $p < 0.05$, FWE corrected at cluster level. T-score from the two-sample t-test is shown in red-to-yellow scale.

CB_1 receptor availability. Family Risk and BMI had negative association with V_T (Fig. 3, all ROIs in Supplementary Fig. 2). Anandamide (AEA) was the only endocannabinoid to exhibit significant effects to V_T . Increase in serum AEA was associated with lower V_T in frontal striatum (Supplementary Fig. 3).

Linear regression analysis of family risk with three tracers. Finally, we pooled the data across the three radioligands in a reversed analysis to test which cerebral alterations are the best predictors of familial obesity risk. Increased BGU explained the higher Family Risk score in every ROI. The posterior distributions of $[^{11}C]$ carfentanil BP_{ND} and $[^{18}F]$ FMPEP- d_2 V_T mostly overlapped with

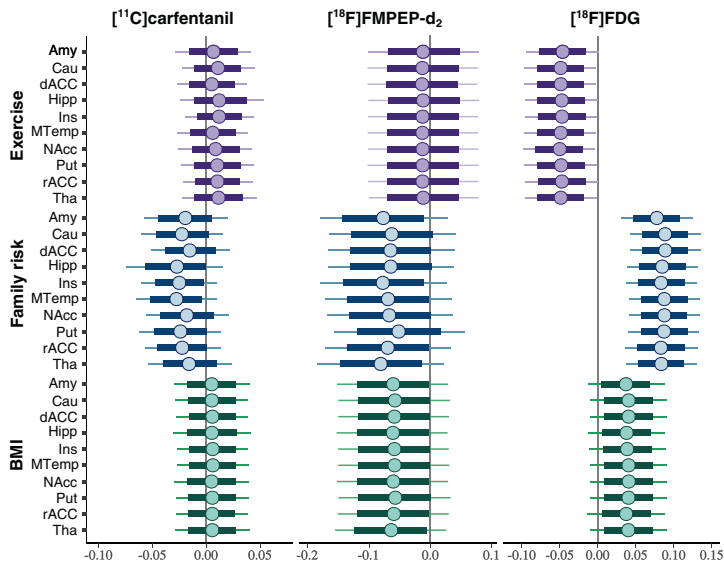


Fig. 3 Effects of obesity risk factors on brain glucose uptake and neuroreceptor availability in ten representative regions of interest. Posterior distributions of the regression coefficients for exercise, family risk and body mass index (BMI) on log-transformed binding potential (BP_{ND}) of the [^{11}C]carfentanil, volume of distribution (V_T) of the [^{18}F]FMPEP- d_2 and brain glucose uptake (BGU) quantified with [^{18}F]FDG in representative regions of interest, age as a covariate. The colored circles represent posterior means, the thick horizontal bars 80% posterior intervals, and the thin horizontal bars 95% posterior intervals. The width of posterior intervals illustrates the level of uncertainty of the estimate. Abbreviations: Amy = amygdala, Cau = caudate, dACC = dorsal anterior cingulate cortex, Hipp = hippocampus, Ins = insula, MTemp = middle temporal gyrus, NAcc = nucleus accumbens, Put = putamen, rACC = rostral anterior cingulate cortex, Tha = thalamus.

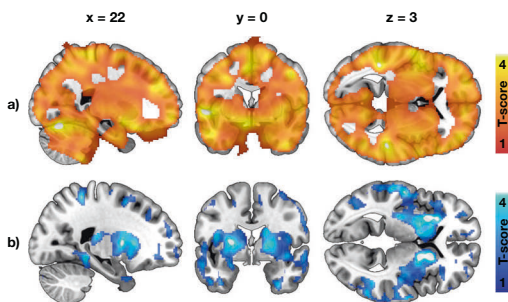


Fig. 4 Effects of familial obesity risk to central glucose uptake and μ -opioid receptor availability. **a** Brain regions where higher Family Risk score associated with increased brain glucose uptake in the 38 individuals studied with [^{18}F]FDG. **b** Brain regions where higher Family Risk score associated with lower μ -opioid receptor availability in the 41 individuals studied with [^{11}C]carfentanil. The effects of familial obesity risk we global for brain glucose uptake, whereas the associations were most prominent in striatum and insula for μ -opioid receptors. The images show results from SnPM13 linear regression, with age and other risk factors (BMI, physical exercise) as covariates. The data are thresholded at $p < 0.05$, FWE corrected at cluster level.

zero, and the directions of the associations were negative (Supplementary Fig. 4).

DISCUSSION

Our main finding was that non-obese young males with high risk for future obesity had increased insulin-stimulated brain glucose

uptake. Furthermore, the increased familial obesity risk (i.e., parental obesity and T2D prevalence) was associated with lowered μ -opioid and CB_1 receptor density in addition to the globally altered glucose metabolism in the brain. Brain glucose uptake had the strongest and most consistent association with familial obesity risk among the three examined PET variables.

Sedentary lifestyle combined to readily available high-calorie food has been proposed to be core issue for obesity epidemic [43], yet hereditary factors play a key role in individual obesity risk. Multiple genes contribute to susceptibility for obesity and T2D, and a first-degree relative with obesity raises individual's obesity risk two- to threefold [44]. Our results highlight that molecular and metabolic alterations in the brain are also associated with individual obesity risk. The present findings complement those previously reported in middle-aged obese subjects, suggesting that alterations in brain's insulin signaling and MOR and CB_1R neurotransmission might contribute to elevated risk for gaining weight.

Brain glucose uptake and obesity risk

The non-obese subjects with high risk for developing obesity showed widespread increase in brain glucose uptake during hyperinsulinemia—a phenomenon that has been previously reported in morbidly obese individuals [12]. It has been suggested that central inflammation, impaired insulin transport regulation in the blood-brain barrier and diminished neuronal responses to insulin might promote these changes in fully developed obesity [12, 45, 46]. The present results show that these pathophysiological processes are active already in non-obese subjects with risk factors for obesity: HR group had globally increased BGU compared to the LR group, and a familial history of obesity and T2D were strongly linked to increased BGU. Central insulin resistance has been proposed to underlie the pathogenesis of

obesity and T2D [47]. Disturbances in brain insulin action and impaired signaling between the brain and peripheral organs may contribute to pathological energy homeostasis and weight gain. Familial obesity risk had positive correlation with BGU extensively in the brain, also in cingulate cortex, striatum and nucleus accumbens that have important role in the central regulation of food intake and reward [48]. Impaired insulin action in these brain regions, together with altered neuroreceptor signaling, could potentially predispose to increased food intake and weight gain.

Central μ -opioid receptor downregulation as an obesity-promoting mechanism

Parental obesity and T2D were associated with lower MOR availability in non-obese state in multiple brain areas, including frontal cortex, striatum, and insula. Previously MOR downregulation in same brain areas has been found in patients with morbid obesity [23] and binge eating disorder (BED) [49]. These alterations accord with genetic studies suggesting that variability in MOR-coding gene OPRM1 is linked with MOR function and eating behavior. Variation in OPRM1 (SNP rs1799971, prevalence in Finland ~19% [50]) reduces MOR availability [51] and is over-represented in patients with BED [52]. MOR system mediates feeding and reward [14], and prior studies have found that MOR downregulation makes an individual more sensitive to environment's rewarding food cues [53]. Individuals with hereditary predisposition towards downregulated MORs may thus be more sensitive to respond to the anticipatory food cues in the environment, leading to excess feeding [54]. Alternatively, they might also compensate the reduced MOR availability by excessive food intake to get sufficient reward response and incentive to halt food intake. These proposed mechanisms could possibly lead to vicious cycle in feeding behavior, where excessive endogenous opioid stimulation by feeding [55] would cause further MOR downregulation and vice versa [16].

CB₁ receptor availability and endogenous cannabinoids

Our results suggest that higher familial obesity risk and higher body mass are associated with lower CB₁R availability in the brain. Our findings are in line with a prior PET study that has linked increase in BMI to lower CB₁R availability [41]. In a recent PET study, serum endocannabinoid peptides (including AEA) had negative relationship with central CB₁R availability [36]. Our results add support to these earlier findings: we found that serum AEA concentration had negative relationship with CB₁R in ventral striatum already in the non-obese state. In animal studies, AEA has been shown to stimulate food intake via activation of central CB₁Rs [56] and to amplify hedonic reward responses to sweet taste [57]. In obese humans, serum AEA is increased and associates with decreased CB₁R gene expression [58]. The elevated systemic AEA concentration might thus be a pathophysiological trait promoting CB₁R downregulation, and possibly weight gain.

Limitations and future directions

First, since we studied only males, the conclusions may not be generalizable to females. Second, there was a small age-difference between the two risk groups. Age was however included in all analyses as a nuisance covariate. By study design, the BMI of HR group was higher than the BMI in LR group, since overweight in early adulthood is a predictive factor for future obesity [4]. However, compared to BMI, familial obesity risk had generally stronger and independent effects to the brain glucose uptake and neuroreceptor availability (Figs. 3 and 4). Also in healthy males, BMI in the range of 18–34 does not affect central MOR availability [37]. Third, we did not have the information about genetic profile of the subjects, and were therefore not able to directly assess the genetic obesity risk. Fourth, the information about physical exercise and parental risk factors were acquired by interview by licensed physician with a standardized medical history checkup,

rather than by direct measurement. Finally, as a cross-sectional work this study cannot differentiate whether the detected cerebral alterations are the cause or the effect of increasing obesity risk or whether one receptor system's alteration would serve as the primal cause for the detected changes in the other systems. In a single PET scan, it is also not possible to demonstrate the exact molecule-level mechanism for altered receptor availability [37]. Follow-up studies with assessment of eating behavior are needed to confirm the proposed effects of these brain signaling alterations to future weight gain.

CONCLUSIONS

Individuals with well-established risk factors for obesity have alterations in the brain's insulin responsivity and opioid and endocannabinoid signaling that resemble those observed in obesity. History of parental obesity and T2D is manifested as altered cerebral insulin sensitivity and reduced MOR and CB₁R availability. The detected neurochemical alterations emphasize the hereditary and centrally mediated mechanisms in obesity development. Disturbance of these integrative food intake control systems in the brain may potentially predispose to weight gain and obesity.

CODE AVAILABILITY

The code for preprocessing of the PET data (Magia) is available at <https://github.com/tkkarjal/magia>.

REFERENCES

1. Abarca-Gómez L, Abdeen ZA, Hamid ZA, Abu-Rmeileh NM, Acosta-Cazares B, Acuin C, et al. Worldwide trends in body-mass index, underweight, overweight, and obesity from 1975 to 2016: a pooled analysis of 2416 population-based measurement studies in 128.9 million children, adolescents, and adults. *Lancet*. 2017;390:2627–42.
2. Van Gaal LF, Mertens IL, De Block CE. Mechanisms linking obesity with cardiovascular disease. *Nature*. 2006;444:875–80.
3. Kivipelto M, Ngandu T, Fratiglioni L, Viitanen M, Kareholt I, Winblad B, et al. Obesity and vascular risk factors at midlife and the risk of dementia and Alzheimer disease. *Arch Neurol*. 2005;62:1556–60.
4. Juhola J, Magnussen CG, Viikari JSA, Kähönen M, Hutri-Kähönen N, Jula A, et al. Tracking of serum lipid levels, blood pressure, and body mass index from childhood to adulthood: the cardiovascular risk in Young Finns study. *J Pediatr*. 2011;159:584–90.
5. Parsons TJ, Power C, Logan S, Summerbell CD. Childhood predictors of adult obesity: a systematic review. *Int J Obes Relat Metab Disord*. 1999;23:S1–S107.
6. Haffner SM, Stern MP, Hazuda HP, Mitchell BD, Patterson JK, Ferrannini E. Parental history of diabetes is associated with increased cardiovascular risk factors. *Arteriosclerosis*. 1989;9:928–33.
7. Anjana RM, Lakshminarayanan S, Deepa M, Farooq S, Pradeepa R, Mohan V. Parental history of type 2 diabetes mellitus, metabolic syndrome, and cardio-metabolic risk factors in Asian Indian adolescents. *Metabolism*. 2009;58:344–50.
8. Yang X, Telama R, Leskinen E, Mansikkaniemi K, Viikari J, Raitakari OT. Testing a model of physical activity and obesity tracking from youth to adulthood: the cardiovascular risk in young Finns study. *Int J Obes*. 2007;31:521–7.
9. Juonala M, Juhola J, Magnussen CG, Würtz P, Viikari JSA, Thomson R, et al. Childhood environmental and genetic predictors of adulthood obesity: the cardiovascular risk in Young Finns study. *J Clin Endocrinol Metab*. 2011;96:E1542–9.
10. Guyenet SJ, Schwartz MW. Regulation of food intake, energy balance, and body fat mass: implications for the pathogenesis and treatment of obesity. *J Clin Endocrinol Metab*. 2012;97:745–55.
11. Davis JF, Choi DL, Benoit SC. Insulin, leptin and reward. *Trends Endocrinol Metabol*. 2010;21:68–74.
12. Tuulari JJ, Karlsson HK, Hirvonen J, Hannukainen JC, Buccini M, Helmiö M, et al. Weight loss after bariatric surgery reverses insulin-induced increases in brain glucose metabolism of the morbidly obese. *Diabetes*. 2013;62:2747–51.
13. Anthony K, Reed LJ, Dunn JT, Bingham E, Hopkins D, Marsden PK, et al. Attenuation of insulin-evoked responses in brain networks controlling appetite and reward in insulin resistance: the cerebral basis for impaired control of food intake in metabolic syndrome? *Diabetes*. 2006;55:2986–92.

14. Gosnell BA, Levine AS. Reward systems and food intake: role of opioids. *Int J Obes*. 2009;33:554–8.
15. Yeomans MR, Gray RW. Opioid peptides and the control of human ingestive behaviour. *Neurosci Biobehav Rev*. 2002;26:713–28.
16. Karlsson HK, Tuuluri JJ, Tuominen L, Hirvonen J, Honka H, Parkkola R, et al. Weight loss after bariatric surgery normalizes brain opioid receptors in morbid obesity. *Mol Psychiatry*. 2016;21:1057–62.
17. Bermudez-Silva FJ, Cardinal P, Cota D. The role of the endocannabinoid system in the neuroendocrine regulation of energy balance. *J Psychopharmacol*. 2012;26:114–24.
18. Mechoulam R, Parker LA. The endocannabinoid system and the brain. *Annu Rev Psychol*. 2013;64:21–47.
19. Kirkham TC, Williams CM, Fezza F, Marzo VD. Endocannabinoid levels in rat limbic forebrain and hypothalamus in relation to fasting, feeding and satiation: stimulation of eating by 2-arachidonoyl glycerol. *Br J Pharmacol*. 2002;136:550–7.
20. Ravinet Trillou C, Delgorge C, Menet C, Arnone M, Soubrie P. CB1 cannabinoid receptor knockout in mice leads to leanness, resistance to diet-induced obesity and enhanced leptin sensitivity. *Int J Obes*. 2004;28:640–8.
21. Sanchis-Segura C, Cline BH, Marsicano G, Lutz B, Spanagel R. Reduced sensitivity to reward in CB1 knockout mice. *Psychopharmacology*. 2004;176:223–32.
22. Harrold JA, Elliott JC, King PJ, Widdowson PS, Williams G. Down-regulation of cannabinoid-1 (CB1) receptors in specific extrahypothalamic regions of rats with dietary obesity: a role for endogenous cannabinoids in driving appetite for palatable food? *Brain Res*. 2002;952:232–8.
23. Karlsson HK, Tuominen L, Tuuluri JJ, Hirvonen J, Parkkola R, Helin S, et al. Obesity is associated with decreased mu-opioid but unaltered dopamine D2 receptor availability in the brain. *J Neurosci*. 2015;35:3959–65.
24. Hamacher K, Coenen HH, Stöcklin G. Efficient stereospecific synthesis of no-carrier-added 2-[¹⁸F]-fluoro-2-deoxy-D-glucose using aminopolyether supported nucleophilic substitution. *J Nucl Med*. 1986;27:235–8.
25. Lemaire C, Damhaut P, Lauricella B, Mosdzianowski C, Morelle JL, Monclus M, et al. Fast [¹⁸F]FDG synthesis by alkaline hydrolysis on a low polarity solid phase support. *J Label Compd Radiopharm*. 2002;45:435–47.
26. Eriksson O, Antoni G. [¹¹C]Carfentanil binds preferentially to mu-opioid receptor subtype 1 compared to subtype 2. *Mol Imaging*. 2015;14:476–83.
27. Larsen P, Ulin J, Dahlström K, Jensen M. Synthesis of [¹¹C] iodomethane by iodination of [¹¹C] methane. *Appl Radiat Isot*. 1997;48:153–7.
28. Jewett DM. A simple synthesis of [¹¹C] methyl triflate. *Int J Radiat Appl Instrum*. 1992;43:1383–5.
29. Lahdenpohja S, Keller T, Forsback S, Viljanen T, Kokkonmäki E, Kivelä RV, et al. Automated GMP production and long-term experience in radiosynthesis of CB1 tracer [¹⁸F] FMPEP-d2. *J Label Compd Radiopharm*. 2020;63:408–18.
30. DeFronzo RA, Tobin JD, Andres R. Glucose clamp technique: a method for quantifying insulin secretion and resistance. *Am J Physiol-Endocrinol Metab*. 1979;237:E214.
31. Karjalainen T, Tuisku J, Santavirta S, Kantonen T, Bucci M, Tuominen L, et al. Magia: robust automated image processing and kinetic modeling toolbox for PET neuroinformatics. *Front Neuroinform*. 2020;14:3.
32. Thie JA. Clarification of a fractional uptake concept. *J Nucl Med*. 1995;36:711–2.
33. Innis RB, Cunningham VJ, Delforge J, Fujita M, Gjedde A, Gunn RN, et al. Consensus nomenclature for in vivo imaging of reversibly binding radioligands. *J Cereb Blood Flow Metab*. 2007;27:1533–9.
34. Frost JJ, Douglass KH, Mayberg HS, Dannals RF, Links JM, Wilson AA, et al. Multicompartmental analysis of [¹¹C]-Carfentanil binding to opiate receptors in humans measured by positron emission tomography. *J Cereb Blood Flow Metab*. 1989;9:398–409.
35. Logan J. Graphical analysis of PET data applied to reversible and irreversible tracers. *Nuclear Med Biol*. 2000;27:661–70.
36. Dickens AM, Borgan F, Laurikainen H, Lamichhane S, Marques T, Rönkkö T, et al. Links between central CB1-receptor availability and peripheral endocannabinoids in patients with first episode psychosis. *npj Schizophr*. 2020;6:1–10.
37. Kantonen T, Karjalainen T, Isojärvi J, Nuutila P, Tuisku J, Rinne J, et al. Inter-individual variability and lateralization of μ -opioid receptors in the human brain. *NeuroImage*. 2020;217:116922.
38. Zubieta JK, Dannals RF, Frost JJ. Gender and age influences on human brain μ -opioid receptor binding measured by PET. *Am J Psychiatry*. 1999;156:842–8.
39. Loessner A, Alavi A, Lewandrowski K-U, Mozley D, Souder E, Gur R. Regional cerebral function determined by FDG-PET in healthy volunteers: normal patterns and changes with age. *J Nucl Med*. 1995;36:1141–9.
40. Tuominen L, Nummenmaa L, Keltikangas-Järvinen L, Raitakari O, Hietala J. Mapping neurotransmitter networks with PET: an example on serotonin and opioid systems. *Hum Brain Mapp*. 2014;35:1875–84.
41. Hirvonen J, Goodwin RS, Li CT, Terry GE, Zoghbi SS, Morse C, et al. Reversible and regionally selective downregulation of brain cannabinoid CB1 receptors in chronic daily cannabis smokers. *Mol Psychiatry*. 2012;17:642–9.
42. Gelman A, Hill J, Yajima M. Why we (usually) don't have to worry about multiple comparisons. *J Res Educ Effect*. 2012;5:189–211.
43. Hill JO, Peters JC. Environmental contributions to the obesity epidemic. *Science*. 1998;280:1371–4.
44. Loos RJ, Bouchard C. Obesity—is it a genetic disorder? *J Intern Med*. 2003;254:401–25.
45. Hallschmid M, Schultes B. Central nervous insulin resistance: a promising target in the treatment of metabolic and cognitive disorders? *Diabetologia*. 2009;52:2264–9.
46. Rebelos E, Rinne JO, Nuutila P, Ekblad LL. Brain glucose metabolism in health, obesity, and cognitive decline—does insulin have anything to do with it? A narrative review. *J Clin Med*. 2021;10:1532.
47. Kullmann S, Heni M, Hallschmid M, Fritsche A, Preissl H, Haring HU. Brain insulin resistance at the crossroads of metabolic and cognitive disorders in humans. *Physiol Rev*. 2016;96:1169–209.
48. Stoeckel LE, Weller RE, Cook EW 3rd, Twieg DB, Knowlton RC, Cox JE. Widespread reward-system activation in obese women in response to pictures of high-calorie foods. *Neuroimage*. 2008;41:636–47.
49. Majuri J, Joutsa J, Johansson J, Voon V, Alakurtti K, Parkkola R, et al. Dopamine and opioid neurotransmission in behavioral addictions: a comparative PET study in pathological gambling and binge eating. *Neuropsychopharmacology*. 2017;42:1169–77.
50. Rouvinen-Lagerström N, Lahti J, Alho H, Kovanen L, Aalto M, Partonen T, et al. μ -Opioid receptor gene (OPRM1) polymorphism A118G: lack of association in Finnish populations with alcohol dependence or alcohol consumption. *Alcohol Alcohol*. 2013;48:519–25.
51. Weerts EM, McCaul ME, Kuwabara H, Yang X, Xu X, Dannals RF, et al. Influence of OPRM1 Asn40Asp variant (A118G) on [¹¹C]carfentanil binding potential: preliminary findings in human subjects. *Int J Neuropsychopharmacol*. 2013;16:47–53.
52. Davis CA, Levitan RD, Reid C, Carter JC, Kaplan AS, Patte KA, et al. Dopamine for “wanting” and opioids for “liking”: a comparison of obese adults with and without binge eating. *Obesity*. 2009;17:1220–5.
53. Nummenmaa L, Saanijoki T, Tuominen L, Hirvonen J, Tuuluri JJ, Nuutila P, et al. μ -opioid receptor system mediates reward processing in humans. *Nat Commun*. 2018;9:1500.
54. Kantonen T, Karjalainen T, Pekkarinen L, Isojärvi J, Kallioikoski K, Kaasinen V, et al. Cerebral μ -opioid and CB1 receptor systems have distinct roles in human feeding behavior. *Transl Psychiatry*. 2021;11:442.
55. Tuuluri JJ, Tuominen L, de Boer FE, Hirvonen J, Helin S, Nuutila P, et al. Feeding releases endogenous opioids in humans. *J Neurosci*. 2017;37:8284–91.
56. Jamshidi N, Taylor DA. Anandamide administration into the ventromedial hypothalamus stimulates appetite in rats. *Br J Pharmacol*. 2001;134:1151–4.
57. Mahler SV, Smith KS, Berridge KC. Endocannabinoid hedonic hotspot for sensory pleasure: anandamide in nucleus accumbens shell enhances “liking” of a sweet reward. *Neuropsychopharmacology*. 2007;32:2267–78.
58. Engeli S, Böhnke J, Feldpausch M, Gorzelski K, Janke J, Bätke S, et al. Activation of the peripheral endocannabinoid system in human obesity. *Diabetes*. 2005;54:2838.

ACKNOWLEDGEMENTS

We would like to acknowledge the Turku Metabolomics Centre and Biocenter Finland for their contribution to the circulating endocannabinoid analyses. We thank Vesa Oikonen and Jouni Tuisku for valuable comments on the manuscript.

AUTHOR CONTRIBUTIONS

TaK: Corresponding and first author, study design, study coordination, data acquisition, data modeling, statistical analysis, interpretation of the results, tables and figures, main writer of the manuscript. LP: Study design, study coordination, data acquisition, data modeling, statistical analysis, interpretation of the results, writing of the manuscript. ToK: Study design, data modeling, statistical analysis, interpretation of the results, figures, writing of the manuscript. MB: Data modeling, statistical analysis, interpretation of the results, writing of the manuscript. KK: Study design, interpretation of the results, writing of the manuscript. MH: Data modeling, interpretation of the results, writing of the manuscript. RA: Data acquisition, data modeling, interpretation of the results, writing of the manuscript. AMD: Endocannabinoid measurements, interpretation of the results, writing of the manuscript. AE: Endocannabinoid measurements, interpretation of the results, writing of the manuscript. KL: Data acquisition, interpretation of the results, writing of the manuscript. NH: Data acquisition, interpretation of the results, writing of the manuscript. AKK: Radiotracer production, interpretation of the results, writing of the manuscript. SH: Radiotracer production, interpretation of the results, writing of the manuscript. JH: Data modeling, interpretation of the results, writing of the manuscript. TR: Study design, interpretation

of the results, writing of the manuscript. PN: Study design, study coordination, interpretation of the results, writing of the manuscript, supervision of the study. LN: Study design, study coordination, statistical analysis, interpretation of the results, figures, writing of the manuscript, supervision of the study.

FUNDING

This study was supported by Academy of Finland grants #294897# to LN and Center of Excellence funding #307402# to PN, and Sigrid Juselius Foundation. We thank Finnish Cultural Foundation (Southwest Finland Fund), Emil Aaltonen Foundation and Jenny and Antti Wihuri Foundation for personal grants to TaK. We also thank Jalmari and Rauha Ahokas Foundation, Turunmaa Duodecim Society and Turku University Hospital Foundation for Education and Research for personal grants to LP. Open Access funding provided by University of Turku (UTU) including Turku University Central Hospital.

COMPETING INTERESTS

The authors declare no conflict of interest.

ADDITIONAL INFORMATION

Supplementary information The online version contains supplementary material available at <https://doi.org/10.1038/s41366-021-00996-y>.

Correspondence and requests for materials should be addressed to Tatu Kantonen.

Reprints and permission information is available at <http://www.nature.com/reprints>

Publisher's note Springer Nature remains neutral with regard to jurisdictional claims in published maps and institutional affiliations.



Open Access This article is licensed under a Creative Commons Attribution 4.0 International License, which permits use, sharing, adaptation, distribution and reproduction in any medium or format, as long as you give appropriate credit to the original author(s) and the source, provide a link to the Creative Commons license, and indicate if changes were made. The images or other third party material in this article are included in the article's Creative Commons license, unless indicated otherwise in a credit line to the material. If material is not included in the article's Creative Commons license and your intended use is not permitted by statutory regulation or exceeds the permitted use, you will need to obtain permission directly from the copyright holder. To view a copy of this license, visit <http://creativecommons.org/licenses/by/4.0/>.

© The Author(s) 2021

**Pekkarinen, L., Kantonen, T., Rebelos, E., Latva-Rasku, A., Dadson, P.,
Karjalainen, T., Bucci, M., Kalliokoski, K., Laitinen, K., Houttu, N.,
Kirjavainen, A. K., Rajander, J., Rönnemaa, T., Nummenmaa, L., &
Nuutila, P. (2022)**

**Obesity risk is associated with brain glucose uptake and insulin
resistance.**

European Journal of Endocrinology

Obesity risk is associated with brain glucose uptake and insulin resistance

Laura Pekkarinen^{1,2}, Tatu Kantonen^{1,3}, Eleni Rebelos¹, Aino Latva-Rasku¹, Prince Dadson¹, Tomi Karjalainen¹, Marco Bucci^{1,4}, Kari Kalliokoski¹, Kirsi Laitinen⁵, Noora Houlttu⁵, Anna K Kirjavainen¹, Johan Rajander⁴, Tapani Rönnemaa^{2,6}, Lauri Nummenmaa^{1,7} and Pirjo Nuutila^{1,2}

¹Turku PET Centre, University of Turku, Turku, Finland, ²Department of Endocrinology, Turku University Hospital, Turku, Finland, ³Clinical Neurosciences, Turku University Hospital, Turku, Finland, ⁴Turku PET Centre, Åbo Akademi University, Turku, Finland, ⁵Institute of Biomedicine, Research Centre for Integrative Physiology and Pharmacology, University of Turku, Turku, Finland, ⁶Department of Medicine, University of Turku, Turku, Finland, and ⁷Department of Psychology, University of Turku, Turku, Finland

Correspondence should be addressed to P Nuutila
Email
pirjo.nuutila@utu.fi

Abstract

Objective: To investigate whether alterations in brain glucose uptake (BGU), insulin action in the brain–liver axis and whole-body insulin sensitivity occur in young adults in pre-obese state.

Methods: Healthy males with either high risk (HR; $n = 19$) or low risk (LR; $n = 22$) for developing obesity were studied with [¹⁸F]fluoro-D-glucose ([¹⁸F]FDG)–positron emission tomography during hyperinsulinemic–euglycemic clamp. Obesity risk was assessed according to BMI, physical activity and parental overweight/obesity and type 2 diabetes. Brain, skeletal muscle, brown adipose tissue (BAT), visceral adipose tissue (VAT) and abdominal and femoral s.c. adipose tissue (SAT) glucose uptake (GU) rates were measured. Endogenous glucose production (EGP) was calculated by subtracting the exogenous glucose infusion rate from the rate of disappearance of [¹⁸F]FDG. BGU was analyzed using statistical parametric mapping, and peripheral tissue activity was determined using Carimas Software imaging processing platform.

Results: BGU was higher in the HR vs LR group and correlated inversely with whole-body insulin sensitivity (M value) in the HR group but not in the LR group. Insulin-suppressed EGP did not differ between the groups but correlated positively with BGU in the whole population, and the correlation was driven by the HR group. Skeletal muscle, BAT, VAT, abdominal and femoral SAT GU were lower in the HR group as compared to the LR group. Muscle GU correlated negatively with BGU in the HR group but not in the LR group.

Conclusion: Increased BGU, alterations in insulin action in the brain–liver axis and decreased whole-body insulin sensitivity occur early in pre-obese state.

European Journal of
Endocrinology
(2022) **187**, 917–928

Introduction

Obesity is one of the leading health challenges of the 21st century, resulting in myriad health problems (1). Insulin resistance is a key characteristic of type 2 diabetes (T2D), and alterations in insulin sensitivity may occur even decades before the clinical onset of T2D (2). Obesity is associated with multiorgan insulin resistance (3, 4), impaired suppression of endogenous glucose production

(EGP) (5) and adipose tissue lipolysis defined as elevated free fatty acid (FFA) levels (6).

We have previously shown that obese had in spite of their peripheral insulin resistance an increased brain glucose uptake (BGU) during hyperinsulinemic–euglycemic clamp (7), and this finding has been replicated in both humans and animals (8, 9). Large-scale cohort data confirmed that

lower peripheral insulin sensitivity is the best predictor of increased BGU during insulin stimulation, and T2D elevates BGU further (10). In line with that, Eriksson and colleagues demonstrated that BGU during insulin clamp was increased in patients with T2D, while the whole-body and peripheral tissue glucose uptake (GU) rates were reduced (11).

Most prior studies evaluating the impact of insulin resistance on BGU have studied middle-aged, obese (BMI > 30 kg/m²) or severely obese (BMI > 35 kg/m²) individuals, with or without T2D (7, 11, 12). These studies cannot reveal the causality of the increased BGU and insulin sensitivity. It is thus not known whether altered BGU is a consequence of obesity-related metabolic disturbances or whether it can actually represent a further aggravating factor behind these.

BGU correlates positively with EGP in obese but not in lean individuals (5) and also in subjects with a genetic variant associated with impaired intracellular insulin signaling (13), suggesting that in humans, the brain is involved in the control of EGP, but in obese subjects, the insulin action in the brain–liver axis is aberrant. It still remains unresolved whether this is an early characteristic of insulin resistance.

Recently, we have shown that parental overweight and T2D was associated with lower μ -opioid receptor (MOR) and endocannabinoid receptor 1 (CB1R) availability in the brain in overweight but otherwise healthy young males (14). Endogenous opioid system and CB1Rs are involved in the control of food intake and energy homeostasis (15, 16), and previous positron emission tomography (PET) studies have shown downregulation of MOR availability in morbidly obese subjects and normalization after weight loss following bariatric surgery (17). Also, the increased familial obesity risk was associated with increased BGU, while BMI had only a moderate association with BGU (14). However, the association of BGU and insulin sensitivity was not evaluated. The aim of this study is to assess with the same study population, by comparing groups with low vs high obesity risk (LR vs HR), whether alterations in BGU, insulin action in the brain–liver axis and whole-body insulin sensitivity occur already in pre-obese state with risk factors for obesity.

Subjects and Methods

Study subjects and study design

We determined the sample size by *a priori* power analysis based on earlier PET studies on obesity (18), suggesting that

a sample size of 16 +16 would be sufficient for establishing the predicted effects at $P < 0.05$ with actual power exceeding 0.95, assuming a regional effect size of $r=0.5$. We recruited 43 healthy young males with LR ($n=24$) or HR ($n=19$), as previously described (14). Inclusion criteria for the LR group were male sex, age 20–35 years, BMI 18.5–24.9 kg/m², free time physical activity 4 h or more per week and no maternal or paternal overweight or obesity or T2D. Inclusion criteria for the HR group were male sex, age 20–35 years, BMI 25–30 kg/m², free time physical activity less than 4 h per week and maternal or paternal overweight or obesity or T2D. Overweight, physical inactivity and parental obesity and T2D have been established as risk factors for obesity (19, 20, 21, 22, 23, 24). Exclusion criteria were any chronic disease or medication that would affect glucose metabolism or neurotransmission, history of eating disorder or psychiatric disease, use of nicotine products or abusive use of alcohol. Two LR subjects were excluded because they stopped corresponding. Thus, the study population consisted of 22 LR and 19 HR subjects. One LR subject's thigh, neck and brain PET scans were not completed according to his wish. Two LR subjects' brain and one LR subject's thigh scan were not completed because of scheduling problems.

All subjects underwent a screening consisting of physical examination, anthropometric measurements, fasting blood samples, a 75 g oral glucose tolerance test (OGTT), urine drug-screening test and an inquiry regarding medical history. Body fat mass percentage was measured with an air displacement plethysmograph (the Bod Pod system, software version 5.4.0, COSMED, Inc., Concord, CA, USA) after at least 4 h of fasting. Whole-body magnetic resonance imaging (MRI) and PET studies were performed at the Turku PET Centre (Turku, Finland). The study protocol was approved by the Ethics Committee of the Hospital District of Southwest Finland and conducted in according with the principles of the Declaration of Helsinki. All subjects gave written informed consent prior to inclusion. The study is a part of PROSPECT project registered at ClinicalTrials.gov (Neuromolecular Risk Factors for Obesity, PROSPECT, NCT03106688).

PET study protocols

We performed the PET studies after a 12-h overnight fast with the GE Discovery (Discovery 690 PET/CT, GE Healthcare) PET camera with [¹⁸F]fluoro-D-glucose ([¹⁸F]FDG). Tracer production has been previously described (25). Hyperinsulinemic–euglycemic clamp was applied as previously described (26, 27) in order to measure whole-

body insulin sensitivity (Supplementary Text 1). After reaching steady glycemia (80 ± 13 min from the start of the insulin infusion), 156 ± 10 MBq [^{18}F]FDG was injected intravenously and dynamic PET scanning was started with the clamp ongoing. Dynamic data of the thoracic region (0–40 min using 4×15 , 6×20 , 2×60 , 2×150 and 6×300 s frames), upper abdomen (40–55 min; 3×300 s) and thighs (55–70 min; 3×300 s) and static data of the neck (10 min; 1×600 s) and brain (10 min; 1×600 s) were collected. Arterialized venous blood samples at 4.5, 7.5, 10, 20 and 30 min from the [^{18}F]FDG injection and in the middle time points of the abdomen, thigh, neck and brain scans were taken to measure plasma activity.

Quantification of tissue glucose uptake

PET data were corrected for dead time, decay and measured photon attenuation before analysis. Input function was quantified by combining image-derived arterial activity data from the left ventricle (28, 29, 30, 31, 32, 33, 34) from 0 to 4.5 min to arterialized plasma sampling taken from 4.5 min to the end of the scan and analyzed with an automatic γ -counter (Wizard 1480 3", Wallac, Turku, Finland). Tissue activity was determined using Carimas Software (version 2.9, Turku PET Centre, downloadable at <https://turkupetcentre.fi/software/>) and freehand drawing regions of interest (ROI) or volume of interest (VOI) to both quadriceps femoris and hamstrings muscles, the right lobe of the liver, the supraclavicular brown adipose tissue (BAT) depots and several volumes of abdominal s.c. (SAT) and intraperitoneal visceral adipose tissue (VAT). To limit the effect of spillover due to partial volume effect and motion, several ROIs and VOIs in several slices of images were drawn, avoiding large vessels. For myocardium, a segmenting tool of Carimas Software was used to include the left ventricular wall and septum in the analysis. Computed tomography (CT) images were used as references for outlining the regions.

Dynamic tissue time–activity curves and input functions were used to determine the fractional uptake (K_i) of [^{18}F]FDG using the Patlak–Gjedde plot (35) or its approximation fractional uptake rate (FUR) (36). The Patlak–Gjedde plot was used in the analyses of myocardium, liver and femoral skeletal muscle. The mean K_i values were extracted from each tissue and used in the analysis. FUR was used in the analyses of VAT, SAT, BAT and brain. Tissue-specific GU ($\mu\text{mol/kg/min}$) was calculated by multiplying K_i or FUR by plasma glucose concentration during scanning and dividing by the tissue density and a lumped constant that accounts for the differences in

transport and phosphorylation rates between [^{18}F]FDG and glucose. A lumped constant value of 1.2 for skeletal muscle (37, 38), 1.0 for liver (39) and 1.14 for adipose tissue (40) was used. BGU was obtained using an automated processing tool Magia (41) (<https://github.com/tkkarjal/magia>), as recently described (14). Magia uses FreeSurfer (<http://surfer.nmr.mgh.harvard.edu/>) to define the ROIs.

Measurement of endogenous glucose production

EGP during the clamp was determined as previously described (42). Briefly, EGP was calculated by subtracting glucose infusion rate (GIR) from the rate of disappearance of glucose (R_d) during the clamp. Detailed description about the quantification of EGP is described in the Supplementary Text 1.

Measurement of tissue masses

The abdominal SAT and VAT masses were analyzed from MRI images using sliceOmatic® (Tomovision, Montreal, Quebec, Canada). The femoral SAT and skeletal muscle masses were analyzed from CT images. Detailed description about the tissue mass analyses is provided in the Supplementary Text 3.

Biochemical analysis

Detailed description about the methods of the biochemical analysis is presented in the Supplementary Text 2.

Statistical analysis

Data are presented as mean \pm S.D. (or median (interquartile range) for non-normally distributed variables). Between-group comparisons were performed with independent samples *t*-test or Wilcoxon rank-sum test as appropriate. Categorical variables were compared with the χ^2 test. Statistical analyses were performed with SPSS statistical software, version 27. A general linear model and SPM12 (<https://www.fil.ion.ucl.ac.uk/spm/software/spm12/>) software was used to mode associations between BGU and different predictor variables. The comparison between the groups was performed with a two-sample independent *t*-tests. The statistical threshold in statistical parametric mapping (SPM) analysis was set at a cluster level and corrected with false discovery rate (FDR) with $P < 0.05$. Age was included as a covariate in SPM analysis as age-related brain metabolic changes have been reported (43). Correlations with ROI-specific BGU values and clinical and

metabolic variables, BGU were adjusted for each subject to the average age in the whole sample, as previously described (44).

Results

Clinical and metabolic characteristics of the study subjects

The HR subjects had less favorable metabolic profile as compared to the LR subjects, comprising of higher weight, BMI, waist-to-hip ratio (WHR), total body fat mass and fat percentage and VAT and abdominal SAT masses. The HR group also had higher blood pressure, worse glycemic and lipid profile, higher values of liver enzymes, high-sensitivity C-reactive protein and glycoprotein acetyls (GlycA) than the LR group. There was a small difference in terms of age between the two study groups (Table 1).

Risk group differences in the whole-body insulin sensitivity

During the clamp, plasma glucose levels were steady at 5.3 mmol/L in both groups. The HR group had higher steady-state insulin levels and smaller suppression of FFA as compared to the LR group (Table 1 and Supplementary Fig. 1, see section on supplementary materials given at the end of this article), and these two measurements were reciprocally related ($r = -0.41$, $P = 0.009$).

Whole-body insulin sensitivity indexed by the M value and the whole-body Rd were significantly lower in the HR group than in the LR group. Insulin-suppressed EGP did not significantly differ between the groups (Table 1). In the whole dataset, M value and Rd correlated negatively with FFA levels during the clamp, and the correlation was driven by the HR group. Furthermore, M value correlated positively with Rd and negatively with EGP in both groups and in the whole dataset. M value correlated negatively with VAT and abdominal SAT masses (Fig. 2), while no association was found between EGP and adipose tissue masses.

The HR group was characterized by a multi-tissue insulin resistance, as demonstrated by lower rates of GU in skeletal muscle, liver, VAT, abdominal and femoral SAT and BAT (Fig. 1B). In line with this, the M value correlated positively with the GU rate in the skeletal muscle, BAT, VAT and femoral SAT, and the associations were driven by the HR group, but no association was found between the M value and liver or abdominal SAT GU (Fig. 3 and

Supplementary Table 2). Myocardial left ventricle GU rates were not different between groups (Fig. 1C) and correlated negatively with the M value (Fig. 3G and Supplementary Table 2).

When calculated the depot-specific GU, we found a lower rate of GU in the skeletal muscle in the HR group than in the LR group, but higher rates of GU in the VAT and abdominal SAT because of the fat mass expansion in the HR group. The depot-specific GU in the femoral SAT did not significantly differ between the groups, although the HR subjects had higher proportion of fat in the analyzed femoral section as compared to the LR group (Table 2).

Increased BGU in the high-risk group

At the voxel-by-voxel level, insulin-stimulated BGU was higher in the HR group as compared to the LR group (Fig. 4A), as reported previously (14). Cross-sectionally, the M value correlated negatively with BGU, but the correlation was driven by the HR group (Fig. 4B and Supplementary Table 2). Insulin-stimulated BGU correlated positively with insulin-suppressed EGP in the whole dataset (Fig. 4C), and the association was driven by the HR subjects (Supplementary Tables 2–3).

FFA levels during the clamp correlated positively with BGU in the ROI level in the whole dataset, and the association was driven by the HR group (Supplementary Table 3).

Insulin-stimulated BGU correlated positively with 2-h plasma glucose level in OGTT among all study subjects and negatively with Matsuda-ISI in the HR group but not in the LR group (Fig. 4D, E).

Inter-tissue associations between the insulin sensitivity and body composition

BGU in the HR group correlated negatively with skeletal muscle GU and showed a trend toward a negative correlation with BAT GU (Fig. 4F, G), whereas no correlation was found in the LR group. In both HR and LR groups, we did not find an association between BGU and liver, abdominal SAT, VAT, or femoral SAT GU rates, but we did find a positive association between BGU and myocardial left ventricle GU (Supplementary Table 1). In the whole dataset, BGU correlated positively with several measures of adiposity comprising VAT and abdominal SAT masses, which were mainly driven by the HR group (Supplementary Table 4).

WHR and total body fat percentage were positively associated with BGU at the ROI level in the HR group. In the LR group, there was a tendency of negative association

Table 1 Anthropometric and metabolic characteristics of the study subjects.

	Low risk (<i>n</i> = 22)		High risk (<i>n</i> = 19)		<i>P</i>
	Mean (s.d.)	Range	Mean (s.d.)	Range	
Age (years)	23 ± 3	20–30	27 ± 4	22–34	0.0005
Weight (kg)	70.3 ± 7.5	57.0–90.9	90.1 ± 9.3	69.4–109.8	<0.0001
BMI (kg/m ²)	21.9 ± 2.0	18.5–25.1	27.1 ± 1.9	24.8–31.1	<0.0001
WHR	0.9 ± 0.05	0.8–0.9	0.9 ± 0.05	0.8–1.0	0.002
Body fat mass (kg) ^a	11.7 ± 4.3	5.6–20.6	26.9 ± 9.1	11.4–40.7	<0.0001
Body fat mass (%) ^a	16.4 ± 5.5	7.7–27.9	29.1 ± 7.6	13.9–39.2	<0.0001
Fat-free mass (kg) ^a	59.2 ± 6.6	48.0–76.5	62.8 ± 5.7	51.0–73.3	0.07
Total abdominal VAT (kg)	1.4 ± 0.7	0.3–3.1	3.7 ± 1.2	1.5–5.8	<0.0001
Total abdominal SAT (kg)	2.7 ± 1.0	1.1–5.2	6.8 ± 2.4	2.9–10.4	<0.0001
Systolic blood pressure (mmHg)	123 ± 11	101–145	127 ± 11	117–157	0.001
Diastolic blood pressure (mmHg)	70 ± 10	51–90	74 ± 9	65–101	0.02
Fasting					
Plasma glucose (mmol/L)	4.9 ± 0.5	3.0–5.6	5.5 ± 0.4	4.8–6.3	<0.0001
Plasma insulin (pmol/L)	38.7 ± 21.0	13.9–91.3	61.8 ± 20.8	34.7–97.2	0.0006
Plasma FFA (mmol/L)	0.3 ± 0.1	0.1–0.5	0.3 ± 0.1	0.1–0.7	0.3
2-h OGTT					
Plasma glucose (mmol/L)	4.8 ± 1.0	2.6–6.3	5.9 ± 1.4	3.4–8.2	0.004
Plasma insulin (pmol/L)	160.7 ± 140.1	20.8–694.5	328.2 ± 236.5	34.7–909.8	0.01
Matsuda-ISI	11.0 ± 7.0	3.3–30.6	4.9 ± 2.4	2.1–10.3	0.0008
HbA _{1c} (mmol/mol)	29 ± 2	25–35	32 ± 3	27–38	0.004
HbA _{1c} (%)	4.8 ± 0.2	4.4–5.4	5.1 ± 0.3	4.6–5.6	0.007
Total cholesterol (mmol/L)	3.5 ± 0.8	1.8–5.8	4.4 ± 0.9	3.0–6.1	0.002
HDL cholesterol (mmol/L)	1.4 ± 0.3	0.9–1.9	1.3 ± 0.3	0.9–2.1	0.2
LDL cholesterol (mmol/L)	2.1 ± 0.8	0.4–3.7	2.9 ± 0.8	1.8–4.1	0.0009
Triglycerides (mmol/L)	0.7 ± 0.3	0.3–1.4	1.2 ± 0.6	0.3–2.9	0.004
ApoB (g/L)	0.6 ± 0.1	0.4–0.7	0.8 ± 0.2	0.6–1.3	<0.0001
ApoA1 (g/L)	1.3 ± 0.2	1.1–1.6	1.3 ± 0.1	1.1–1.6	0.8
ApoB/ApoA1	0.5 ± 0.1	0.3–0.7	0.6 ± 0.1	0.4–1.0	0.0001
ALT (U/L)	22 ± 8	14–43	32 ± 10	13–49	0.001
AFOS	70 ± 17	50–119	60 ± 19	35–100	0.08
GGT (U/L)	15 ± 5	8–27	33 ± 28	6–124	0.008
hs-CRP (mg/L)	0.5 ± 0.5	0.1–2.4	1.1 ± 1.1	0.1–4.6	0.01
GlycA (mmol/L)	0.7 ± 0.06	0.6–0.8	0.8 ± 0.06	0.7–0.9	<0.0001
Steady-state glucose (mmol/L)	5.3 ± 0.2	4.6–5.9	5.3 ± 0.3	4.8–5.6	0.5
Steady-state insulin (pmol/L)	510.5 ± 76.8	349.6–632.0	581.7 ± 94.9	476.4–801.5	0.01
M value (μmol/kg/min)	58.0 ± 14.7	30.2–86.1	38.7 ± 13.7	17.4–72.3	0.0001
M value (μmol/kg _{FFM} /min)	69.6 ± 17.3	35.2–102.3	53.0 ± 17.1	24.1–100.7	0.004
EGP (μmol/kg/min) ^b	–3.4 ± 6.7	–13.5 to 10.5	0.9 ± 6.0	–13.5 to 7.9	0.2
EGP (μmol/kg _{FFM} /min) ^b	–2.2 ± 8.9	–19.2 to 13.2	–0.6 ± 8.9	–16.1 to 11.7	0.6
Clamp FFA (mmol/L)	0.03 ± 0.01	0.01–0.1	0.05 ± 0.03	0.02–0.1	0.03

^aBody fat mass (kg and %) for high-risk subjects is calculated with *n* = 18, since one high-risk subject did not complete the body composition measurement.

^bEGP for low-risk subjects is calculated with *n* = 21, since one low-risk subject did not feel the need to urinate.

AFOS, alkaline phosphatase; ALT, alanine transaminase; ApoB, apolipoprotein B; ApoA1, apolipoprotein A1; BMI, body mass index; EGP, endogenous glucose production; FFA, free fatty acids; FFM, fat-free mass; GlycA, gGlycoprotein acetyls; GGT, gamma-glutamyltransferase; hs-CRP, high-sensitivity C-reactive protein; Matsuda-ISI, insulin sensitivity index by Matsuda; OGTT, oral glucose tolerance test; SAT, s.c. adipose tissue; VAT, visceral adipose tissue; WHR, waist-to-hip ratio.

between WHR and BGU and no association between total body fat percentage and BGU (Supplementary Table 4).

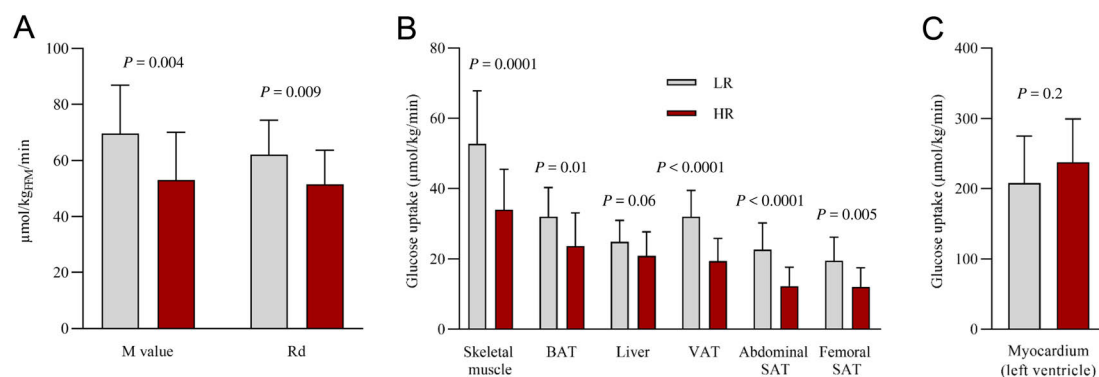
Inter-tissue associations between GU rates in brain and peripheral tissues are presented in Supplementary Table 1.

Furthermore, GU rates in skeletal muscle, BAT, and abdominal and femoral SAT, but not BGU, correlated negatively with apolipoprotein B (ApoB), apolipoprotein A1 (ApoA1) and ApoB/ApoA1 ratio, total and LDL

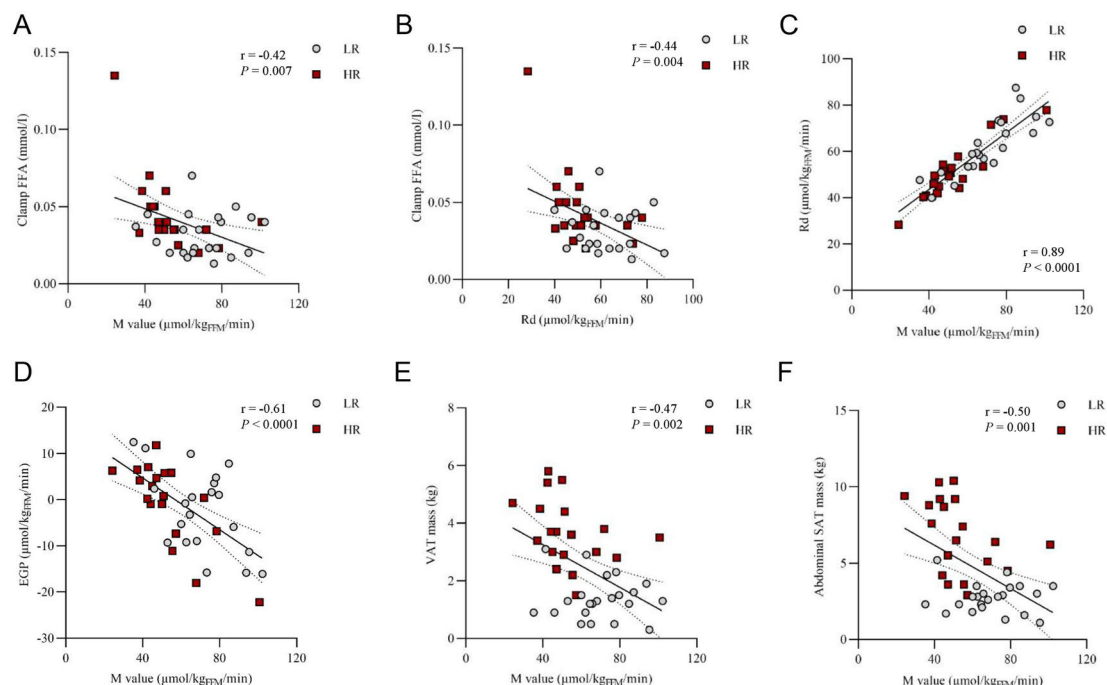
cholesterol, triglycerides and inflammatory marker GlycA (Supplementary Table 2).

Discussion

Our main finding based on the risk-group comparison was that both an increased BGU during hyperinsulinemic–

**Figure 1**

Whole-body and tissue-specific glucose uptake rates. (A) Whole-body insulin sensitivity indexed by the M value and whole-body glucose disposal rate (Rd) calculated with the fat-free mass in the low-risk (LR) and in the high-risk (HR) group. (B) Glucose uptake rates in skeletal muscle, brown adipose tissue (BAT), liver, visceral adipose tissue (VAT) and abdominal and femoral s.c. adipose tissue (SAT) and (C) myocardium (left ventricle) in the LR and in the HR group. Bar heights represent sample means. Vertical lines represent sample s.d. P values for comparison of LR vs HR group.

**Figure 2**

Association between the whole-body insulin sensitivity indexes and adipose tissue masses. (A) Association between the M value and free fatty acid (FFA) levels and (B) Rd and FFA levels during the hyperinsulinemic-euclycemic clamp, (C) M value and the rate of disappearance (Rd), (D) M value and endogenous glucose production (EGP), (E) M value and visceral adipose tissue (VAT) mass, and (F) M value and abdominal s.c. adipose tissue (SAT) mass.

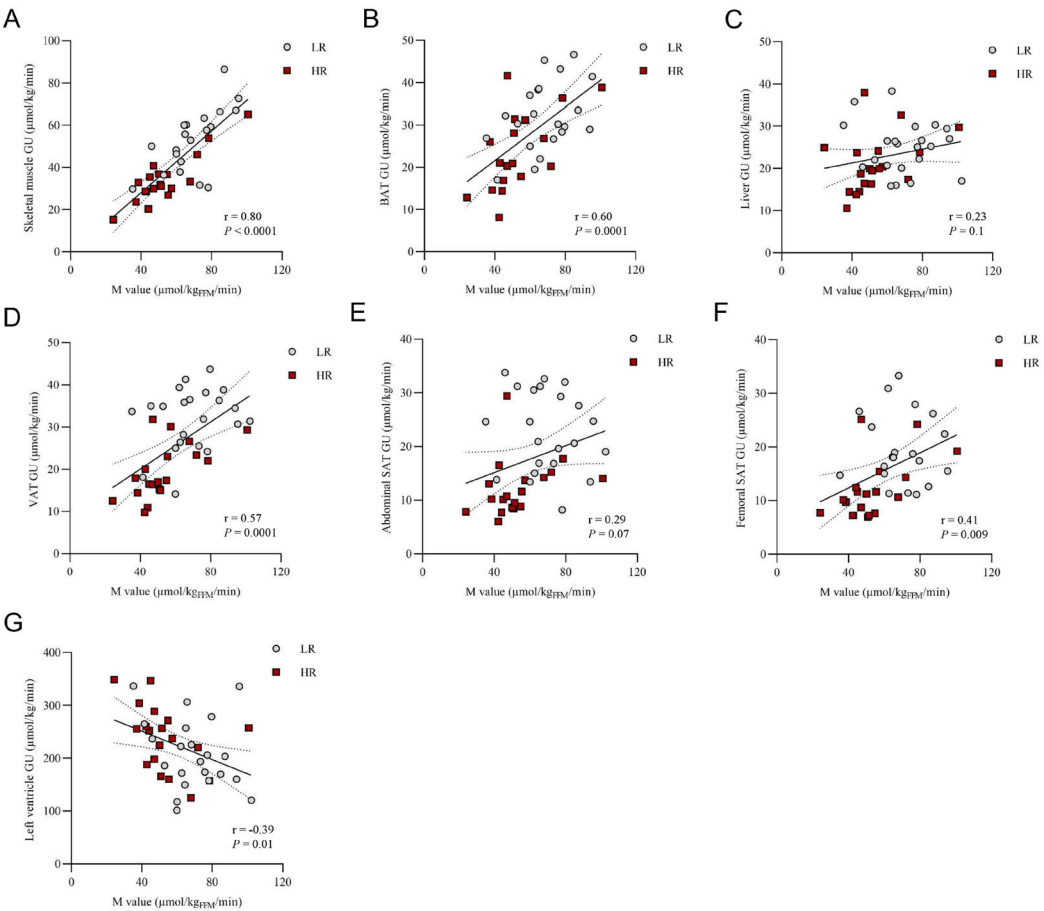
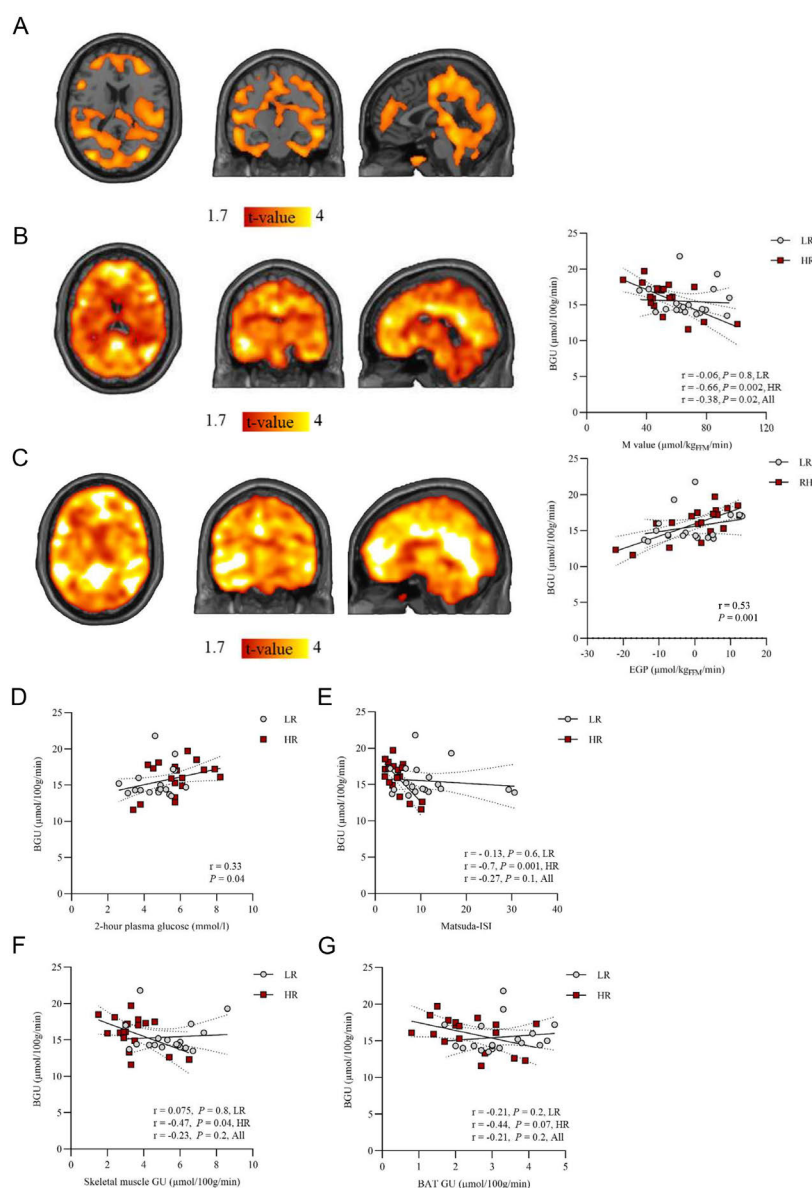


Figure 3 Association between the whole-body insulin sensitivity (M value) and the tissue-specific glucose uptake rates (GU) in (A) femoral skeletal muscle, (B) brown adipose tissue (BAT), (C) liver, (D) visceral adipose tissue (VAT), (E) abdominal s.c. adipose tissue (SAT), (F) femoral SAT and (G) myocardium left ventricle in the low-risk (LR) and in the high-risk (HR) group.

Table 2 Tissue masses and tissue depot-specific insulin-stimulated glucose uptake (GU) rates in the low-risk (LR) and in the high-risk (HR) group. Data presented as mean \pm s.d.

	Tissue mass (kg)		<i>P</i> *	Depot-specific GU (μ mol/min)		<i>P</i> **
	LR	HR		LR	HR	
Brain	1.7 \pm 0.2	1.7 \pm 0.1	0.5	258.1 \pm 46.2	270.2 \pm 43.2	0.4
Femoral skeletal muscle ^a	5.6 \pm 0.6	5.8 \pm 0.5	0.1	292.5 \pm 80.3	199.9 \pm 75.5	0.0007
VAT	1.4 \pm 0.7	3.7 \pm 1.2	<0.0001	42.1 \pm 18.4	68.8 \pm 27.0	0.0006
Abdominal SAT	2.7 \pm 1.0	6.8 \pm 2.4	<0.0001	52.2 \pm 23.3	79.7 \pm 34.8	0.02
Femoral SAT	2.1 \pm 0.7	2.8 \pm 0.8	0.01	40.0 \pm 19.2	31.7 \pm 14.6	0.1

^aCovering the 15 cm section of the mid-thigh in both groups
**P* value is for two-tailed independent samples *t*-test for tissue mass between the two groups.
***P* value is for two-tailed independent samples *t*-test for depot-specific GU between the two groups.
SAT, s.c. adipose tissue; VAT, visceral adipose tissue.

**Figure 4**

Brain glucose uptake (BGU) in the high-risk (HR) and the low-risk (LR) group. (A) A statistical parametric mapping (SPM) two-sample *t*-test between the HR and the LR group. Marked brain areas show regions with significantly higher insulin-stimulated BGU in the HR group as compared to the LR group. Higher T values denote larger differences between the groups. *P* values <0.05 at a cluster level and false discovery rate (FDR) corrected. (B) Brain clusters (as defined by FDR-corrected SPM one-sample *t*-test) for the association between BGU and M value and (C) BGU and EGP in the whole study group and the corresponding scatterplots. For the scatterplots, global region of interest (ROI) was extracted and used. (D) Association between the BGU and 2-h plasma glucose level in oral glucose tolerance test, (E) BGU and insulin sensitivity index by Matsuda (Matsuda-ISI), (F) BGU and skeletal muscle glucose uptake (GU) and (G) BGU and brown adipose tissue GU in the LR group and in the HR group.

euglycemic clamp and a defective insulin action in the brain–liver axis are early features of insulin resistance, being present already in healthy pre-obese subjects with increased adiposity, in early adulthood. These results accord with prior studies showing that during euglycemic hyperinsulinemia BGU is increased in conditions with systemic insulin resistance (8, 10, 11, 13). Even though the molecular mechanisms of this phenomenon are not known, our study demonstrates that relatively mild alterations in metabolic regulation are sufficient for this change to occur. Indeed, the inclusion criterion to the HR group was obesity risk in the early adulthood.

The HR group was characterized by impaired systemic insulin sensitivity. Compared with the LR group, they had reduced whole-body and tissue-specific GU rates and impaired suppression of adipose tissue lipolysis during the clamp. EGP, however, did not significantly differ between the groups. The HR subjects had worse metabolic profile based on general risk factors such as blood pressure, lipid values, OGTT, WHR and body adiposity, and coherently there were significant associations between these and the clamp-derived measurements (Supplementary Table 2). Considering this and the increased insulin-stimulated BGU found in the HR as compared to the LR group, our results are converging with the previous findings in obese subjects (7) and subjects with impaired glucose tolerance (8, 12).

There is long-standing debate regarding when and where insulin resistance starts, with some researchers proposing an important role of the brain in the regulation of energy balance and glucose homeostasis (45). Taking together both the enhanced BGU and the impaired insulin action in the brain–liver axis already in early adulthood, our data further contribute to the increasing understanding that brain metabolism is linked to impairments of whole-body homeostasis.

It is now well-established that accumulation of fat in the femoral SAT may play a protective metabolic role (46, 47), whereas expansion of fat mass in the abdominal SAT and VAT is associated with metabolic abnormalities such as insulin resistance, hyperglycemia, hypertension, and dyslipidemia (48). In a recent study, it was shown that subjects with strong insulin-induced suppression in hypothalamic blood flow (measured with functional MRI) had significantly less VAT, but there was no association between central insulin action and SAT (49); there was no distinction between abdominal and femoral SAT. Interestingly, in the present dataset, insulin-stimulated BGU correlated positively both with VAT and with abdominal SAT mass but not with femoral SAT mass. Further, we found that a significantly higher proportion of

whole-body glucose metabolism during hyperinsulinemia occurs in VAT ($P=0.0008$) and abdominal SAT ($P=0.02$) in the HR subjects as compared to the LR subjects. Despite the correlational nature of our data which cannot explain the basis of this differential pattern of association between BGU and fat masses in different fat depots, this could be attributed to the differences in endocrine function (e.g. adipokine secretion and FFA metabolism) and neural innervation between the various fat depots (50, 51, 52).

We have previously shown that in a group of morbidly obese individuals studied before and 6 months after bariatric surgery, a higher BGU at baseline predicted worse glycemic control at 2 and 3 years of follow-up (5). Also, in a similar group studied with a fatty acid PET tracer 14(R,S)-[^{18}F]fluoro-6-thia-heptadecanoic acid, enhanced brain fatty acid uptake at baseline predicted worse glycemic control following bariatric surgery (53). These findings would be essentially in line with the results of a previous intervention study (TULIP) where decreased cerebrocortical response to insulin in magnetoencephalography (defined by the authors as central insulin resistance) predicted a worse adhesion to the diet intervention and less weight loss (54). In this PROSPECT study design, we will further assess whether the BGU at baseline will predict weight and glycemic status at 5-year follow-up. This differs from the bariatric surgery setting, where significant weight loss occurs rapidly.

Strengths of the present study are the strict selection of the study participants after a thorough evaluation of their obesity risk factors, adiposity, and the application of PET, which not only represents the state-of-the art method for the assessment of glucose metabolic rates *in vivo* but also enables the contemporaneous assessment of EGP. Our study has certain limitations. First, we studied only males, and whether the results can be extrapolated to women is not known. In the previous large-scale study, BGU under insulin stimulation was not significantly affected by sex (10), and therefore it is possible that the effect we found could be similar with women. Subjects in the HR group were somewhat older than those in the LR group, and age represents an important determinant of BGU in both fasting and clamp conditions (55). To circumvent this problem, age was used as a covariate in the BGU analyses, and the results were unchanged. Unfortunately, one LR subject had BMI 25.1 kg/m² and one HR subject 24.8 kg/m² although otherwise fulfilling the group criteria. For the consistency of the statistics, we decided not to exclude them. EGP values in both study groups were mainly negative, indicating EGP suppression under insulin stimulation. A previous study showed a progressive decline

in insulin suppression of EGP with increasing VAT mass and hepatic lipid content (HLC) (56). We did not measure HLC in the this study; however, in a recent study, 95% percentile of HLC of lean non-Asian Indian participants was shown to be 1.85% (57), considerably lower than the previously determined upper limit of normal HLC 5.56% (58). Thus, it can be assumed that in the present study where the LR subjects are lean and the HR subjects are only overweight, not obese, it is likely that most of the subjects would have HLC under 1.85% and have effective suppression of EGP. Also, large variability and negative EGP values has been shown also in previous studies (59).

In conclusion, this risk-group comparison demonstrates that an increased BGU and a dysregulated insulin action in the brain–liver axis occur already in the pre-obese state in young healthy subjects, in the age range of early adulthood and with only mild extra adiposity. This cross-sectional study cannot resolve the causality of the effect, and longitudinal and intervention studies are needed to address this. The follow-up period may potentially show whether the enhanced BGU has an impact on metabolic deterioration with advancing age.

Supplementary materials

This is linked to the online version of the paper at <https://doi.org/10.1530/EJE-220509>.

Declaration of interest

The authors declare that there is no conflict of interest that could be perceived as prejudicing the impartiality of the research reported.

Funding

The study was supported by Center of Excellence funding (no. 307402) to PN, Academy of Finland grant nos 294897 and 332225 to LN, Jalmari and Rauha Ahokas Foundation, Turunmaa Duodecim Society, Turku University Hospital Foundation for Education and Research and The Diabetes Research Foundation to LP, Finnish Cultural Foundation (Southwest Finland Fund), Emil Aaltonen Foundation and Jenny and Antti Wihuri Foundation to TK, Finnish Cultural Foundation and Maud Kuistila Memorial Foundation to ER, and Sigrid Juselius Foundation.

Data availability

The data from this study are available from the corresponding author PN on reasonable request.

Author contribution statement

LP: first author, study design, study coordination, data acquisition, data modeling, statistical analysis, interpretation of the results, tables and figures and main writer of the manuscript. TK: study design, study coordination, data acquisition, data modeling, statistical analysis, interpretation of the results and writing of the manuscript. ER: brain PET data modeling,

statistical analysis, interpretation of the results, figures and writing of the manuscript. AL-R and PD: participation in the PET data analysis and writing of the manuscript. ToK and MB: brain PET data modeling. KK: study design, especially effects of exercise on metabolism. AKK: radiotracer production. KL and NH: measurement of the body fat percentage. TR: study design, expertise in metabolic risk factors and writing of the manuscript. LN: study design, study coordination, interpretation of the results, writing of the manuscript and supervision of the study. All authors approved the final version of the manuscript. PN: corresponding author, study design, study coordination, interpretation of the results, writing of the manuscript and supervision of the study. As a guarantor of the work has full access to all the data in the study and takes responsibility for the integrity of the data analysis.

Acknowledgements

The authors thank the volunteers who participated in this study and the staff of the Turku PET Centre for performing the PET imaging.

References

- 1 Nguyen DM & El-Serag HB. The epidemiology of obesity. *Gastroenterology Clinics of North America* 2010 **39** 1–7. (<https://doi.org/10.1016/j.gtc.2009.12.014>)
- 2 Martin BC, Warram JH, Krolewski AS, Bergman RN, Soeldner JS & Kahn CR. Role of glucose and insulin resistance in development of type 2 diabetes mellitus: results of a 25-year follow-up study. *Lancet* 1992 **340** 925–929. ([https://doi.org/10.1016/0140-6736\(92\)92814-v](https://doi.org/10.1016/0140-6736(92)92814-v))
- 3 Dadson P, Landini L, Helmiö M, Hannukainen JC, Immonen H, Honka MJ, Bucci M, Savisto N, Soinio M, Salminen P *et al.* Effect of bariatric surgery on adipose tissue glucose metabolism in different depots in patients with or without type 2 diabetes. *Diabetes Care* 2016 **39** 292–299. (<https://doi.org/10.2337/dc15-1447>)
- 4 Virtanen KA, Lönnroth P, Parkkola R, Peltoniemi P, Asola M, Viljanen T, Tolvanen T, Knuuti J, Rönnemaa T, Huupponen R *et al.* Glucose uptake and perfusion in subcutaneous and visceral adipose tissue during insulin stimulation in nonobese and obese humans. *Journal of Clinical Endocrinology and Metabolism* 2002 **87** 3902–3910. (<https://doi.org/10.1210/jcem.87.8.8761>)
- 5 Rebelos E, Immonen H, Bucci M, Hannukainen JC, Nummenmaa L, Honka MJ, Soinio M, Salminen P, Ferrannini E, Iozzo P *et al.* Brain glucose uptake is associated with endogenous glucose production in obese patients before and after bariatric surgery and predicts metabolic outcome at follow-up. *Diabetes, Obesity and Metabolism* 2019 **21** 218–226. (<https://doi.org/10.1111/dom.13501>)
- 6 Kovacs P & Stumvoll M. Fatty acids and insulin resistance in muscle and liver. *Best Practice and Research. Clinical Endocrinology and Metabolism* 2005 **19** 625–635. (<https://doi.org/10.1016/j.beem.2005.07.003>)
- 7 Tuulari JJ, Karlsson HK, Hirvonen J, Hannukainen JC, Bucci M, Helmiö M, Ovaska J, Soinio M, Salminen P, Savisto N *et al.* Weight loss after bariatric surgery reverses insulin-induced increases in brain glucose metabolism of the morbidly obese. *Diabetes* 2013 **62** 2747–2751. (<https://doi.org/10.2337/db12-1460>)
- 8 Boersma GJ, Johansson E, Pereira MJ, Heurling K, Skrtic S, Lau J, Katsogiannis P, Panagiotou G, Lubberink M, Kullberg J *et al.* Altered glucose uptake in muscle, visceral adipose tissue, and brain predict whole-body insulin resistance and may contribute to the development of Type 2 diabetes: a combined PET/MR study. *Hormone and Metabolic Research* 2018 **50** 627–639. (<https://doi.org/10.1055/a-0643-4739>)
- 9 Bahri S, Horowitz M & Malbert CH. Inward glucose transfer accounts for insulin-dependent increase in brain glucose metabolism associated with diet-induced obesity. *Obesity* 2018 **26** 1322–1331. (<https://doi.org/10.1002/oby.22243>)

- 10 Rebelos E, Buccì M, Karjalainen T, Oikonen V, Bertoldo A, Hannukainen JC, Virtanen KA, Latva-Rasku A, Hirvonen J, Heinonen I *et al.* Insulin resistance is associated With enhanced brain glucose uptake During euglycemic hyperinsulinemia: a large-scale PET cohort. *Diabetes Care* 2021 **44** 788–794. (<https://doi.org/10.2337/dc20-1549>)
- 11 Eriksson JW, Visvanathan R, Kullberg J, Strand R, Skrtic S, Ekström S, Lubberink M, Lundqvist MH, Katsogiannis P, Pereira MJ *et al.* Tissue-specific glucose partitioning and fat content in prediabetes and type 2 diabetes: whole-body PET/MRI during hyperinsulinemia. *European Journal of Endocrinology* 2021 **184** 879–889. (<https://doi.org/10.1530/EJE-20-1359>)
- 12 Hirvonen J, Virtanen KA, Nummenmaa L, Hannukainen JC, Honka MJ, Buccì M, Nesterov SV, Parkkola R, Rinne J, Iozzo P *et al.* Effects of insulin on brain glucose metabolism in impaired glucose tolerance. *Diabetes* 2011 **60** 443–447. (<https://doi.org/10.2337/db10-0940>)
- 13 Latva-Rasku A, Honka MJ, Stančáková A, Koistinen HA, Kuusisto J, Guan L, Manning AK, Stringham H, Gloyn AL, Lindgren CM *et al.* A partial loss-of-function variant in AKT2 is associated with reduced insulin-mediated glucose uptake in multiple insulin-sensitive tissues: a genotype-based callback positron emission tomography study. *Diabetes* 2018 **67** 334–342. (<https://doi.org/10.2337/db17-1142>)
- 14 Kantonen T, Pekkarinen L, Karjalainen T, Buccì M, Kalliokoski K, Haaparanta-Solin M, Aarnio R, Dickens AM, von Eyken A, Laitinen K *et al.* Obesity risk is associated with altered cerebral glucose metabolism and decreased μ -opioid and CB1 receptor availability. *International Journal of Obesity* 2022 **46** 400–407. (<https://doi.org/10.1038/s41366-021-00996-y>)
- 15 Gosnell BA & Levine AS. Reward systems and food intake: role of opioids. *International Journal of Obesity* 2009 **33**(Supplement 2) S54–S58. (<https://doi.org/10.1038/ijo.2009.73>)
- 16 Bermudez-Silva FJ, Cardinal P & Cota D. The role of the endocannabinoid system in the neuroendocrine regulation of energy balance. *Journal of Psychopharmacology* 2012 **26** 114–124. (<https://doi.org/10.1177/0269881111408458>)
- 17 Karlsson HK, Tuulari JJ, Tuominen L, Hirvonen J, Honka H, Parkkola R, Helin S, Salminen P, Nuutila P & Nummenmaa L. Weight loss after bariatric surgery normalizes brain opioid receptors in morbid obesity. *Molecular Psychiatry* 2016 **21** 1057–1062. (<https://doi.org/10.1038/mp.2015.153>)
- 18 Karlsson HK, Tuominen L, Tuulari JJ, Hirvonen J, Parkkola R, Helin S, Salminen P, Nuutila P & Nummenmaa L. Obesity is associated with decreased μ -opioid but unaltered dopamine D2 receptor availability in the brain. *Journal of Neuroscience* 2015 **35** 3959–3965. (<https://doi.org/10.1523/JNEUROSCI.4744-14.2015>)
- 19 Juonala M, Juhola J, Magnussen CG, Würtz P, Viikari JSA, Thomson R, Seppälä I, Hernesniemi J, Kähönen M, Lehtimäki T *et al.* Childhood environmental and genetic predictors of adulthood obesity: the cardiovascular risk in young Finns study. *Journal of Clinical Endocrinology and Metabolism* 2011 **96** E1542–E1549. (<https://doi.org/10.1210/jc.2011-1243>)
- 20 Juhola J, Magnussen CG, Viikari JSA, Kähönen M, Hutri-Kähönen N, Jula A, Lehtimäki T, Åkerblom HK, Pietikäinen M, Laitinen T *et al.* Tracking of serum lipid levels, blood pressure, and body mass index from childhood to adulthood: the cardiovascular Risk in Young Finns Study. *Journal of Pediatrics* 2011 **159** 584–590. (<https://doi.org/10.1016/j.jpeds.2011.03.021>)
- 21 Endalifer ML & Diress G. Epidemiology, predisposing factors, biomarkers, and prevention mechanism of obesity: a systematic review. *Journal of Obesity*. C Stocker, Ed. 2020 **2020** 6134362. (<https://doi.org/10.1155/2020/6134362>)
- 22 Mattsson N, Rönnemaa T, Juonala M, Viikari JSA & Raitakari OT. Childhood predictors of the metabolic syndrome in adulthood. The cardiovascular Risk in Young Finns Study. *Annals of Medicine* 2008 **40** 542–552. (<https://doi.org/10.1080/07853890802307709>)
- 23 Cederberg H, Stančáková A, Kuusisto J, Laakso M & Smith U. Family history of type 2 diabetes increases the risk of both obesity and its complications: is type 2 diabetes a disease of inappropriate lipid storage? *Journal of Internal Medicine* 2015 **277** 540–551. (<https://doi.org/10.1111/ijom.12289>)
- 24 Anjana RM, Lakshminarayanan S, Deepa M, Farooq S, Pradeepa R & Mohan V. Parental history of type 2 diabetes mellitus, metabolic syndrome, and cardiometabolic risk factors in Asian Indian adolescents. *Metabolism: Clinical and Experimental* 2009 **58** 344–350. (<https://doi.org/10.1016/j.metabol.2008.10.006>)
- 25 Hamacher K, Coenen HH & Stöcklin G. Efficient stereospecific synthesis of no-carrier-added 2-[18F]-fluoro-2-deoxy-D-glucose using aminopolyether supported nucleophilic substitution. *Journal of Nuclear Medicine* 1986 **27** 235–238.
- 26 DeFronzo RA, Tobin JD & Andres R. Glucose clamp technique: a method for quantifying insulin secretion and resistance. *American Journal of Physiology* 1979 **237** E214–E223. (<https://doi.org/10.1152/ajpendo.1979.237.3.E214>)
- 27 Nuutila P, Koivisto VA, Knuuti J, Ruotsalainen U, Teräs M, Haaparanta M, Bergman J, Solin O, Voipio-Pulkki LM & Wegelius U. Glucose-free fatty acid operates in human heart and skeletal muscle in vivo. *Journal of Clinical Investigation* 1992 **89** 1767–1774. (<https://doi.org/10.1172/JCI115780>)
- 28 Henze E, Huang SC, Ratib O, Hoffman E, Phelps ME & Schelbert HR. Measurements of regional tissue and blood-pool radiotracer concentrations from serial tomographic images of the heart. *Journal of Nuclear Medicine* 1983 **24** 987–996.
- 29 Weinberg IN, Huang SC, Hoffman EJ, Araujo L, Nienaber C, Grover-McKay M, Dahlbom M & Schelbert H. Validation of PET-acquired input functions for cardiac studies. *Journal of Nuclear Medicine* 1988 **29** 241–247.
- 30 Gambhir SS, Schwaiger M, Huang SC, Krivokapich J, Schelbert HR, Nienaber CA & Phelps ME. Simple noninvasive quantification method for measuring myocardial glucose utilization in humans employing positron emission tomography and fluorine-18 deoxyglucose. *Journal of Nuclear Medicine* 1989 **30** 359–366.
- 31 Ohtake T, Kosaka N, Watanabe T, Yokoyama I, Moritan T, Masuo M, Iizuka M, Kozeni K, Momose T & Oku S. Noninvasive method to obtain input function for measuring tissue glucose utilization of thoracic and abdominal organs. *Journal of Nuclear Medicine* 1991 **32** 1432–1438.
- 32 van der Weerd AP, Klein LJ, Boellaard R, Visser CA, Visser FC & Lammertsma AA. Image-derived input functions for determination of MRGlu in cardiac (18)F-FDG PET scans. *Journal of Nuclear Medicine* 2001 **42** 1622–1629.
- 33 de Geus-Oei LF, Visser EP, Krabbe PFM, van Hoorn BA, Koenders EB, Willemsen AT, Pruim J, Corstens FHM & Oyen WJG. Comparison of image-derived and arterial input functions for estimating the rate of glucose metabolism in therapy-monitoring 18F-FDG PET studies. *Journal of Nuclear Medicine* 2006 **47** 945–949.
- 34 Horsager J, Munk OL & Sørensen M. Metabolic liver function measured in vivo by dynamic (18)F-FDG PET/CT without arterial blood sampling. *EJNMMI Research* 2015 **5** 32. (<https://doi.org/10.1186/s13550-015-0110-6>)
- 35 Patlak CS & Blasberg RG. Graphical evaluation of blood-to-brain transfer constants from multiple-time uptake data. Generalizations. *Journal of Cerebral Blood Flow and Metabolism* 1985 **5** 584–590. (<https://doi.org/10.1038/jcbfm.1985.87>)
- 36 Ishizu K, Nishizawa S, Yonekura Y, Sadato N, Magata Y, Tamaki N, Tsuchida T, Okazawa H, Miyatake S & Ishikawa M. Effects of hyperglycemia on FDG uptake in human brain and glioma. *Journal of Nuclear Medicine* 1994 **35** 1104–1109.
- 37 Peltoniemi P, Lönnroth P, Laine H, Oikonen V, Tolvanen T, Grönroos T, Strindberg L, Knuuti J & Nuutila P. Lumped constant for [(18)F]fluorodeoxyglucose in skeletal muscles of obese and nonobese humans. *American Journal of Physiology. Endocrinology and Metabolism* 2000 **279** E1122–E1130. (<https://doi.org/10.1152/ajpendo.2000.279.5.E1122>)

- 38 Kelley DE, Williams KV, Price JC & Goodpaster B. Determination of the lumped constant for [18F] fluorodeoxyglucose in human skeletal muscle. *Journal of Nuclear Medicine* 1999 **40** 1798–1804.
- 39 Iozzo P, Jarvisalo MJ, Kiss J, Borra R, Naum GA, Viljanen A, Viljanen T, Gastaldelli A, Buzzigoli E, Guiducci L *et al.* Quantification of liver glucose metabolism by positron emission tomography: validation study in pigs. *Gastroenterology* 2007 **132** 531–542. (<https://doi.org/10.1053/j.gastro.2006.12.040>)
- 40 Virtanen KA, Peltoniemi P, Marjamäki P, Asola M, Strindberg L, Parkkola R, Huupponen R, Knuuti J, Lönnroth P & Nuutila P. Human adipose tissue glucose uptake determined using [(18)F]-fluoro-deoxy-glucose ([18F]FDG) and PET in combination with microdialysis. *Diabetologia* 2001 **44** 2171–2179. (<https://doi.org/10.1007/s001250100026>)
- 41 Karjalainen T, Tuisku J, Santavirta S, Kantonen T, Bucci M, Tuominen L, Hirvonen J, Hietala J, Rinne JO & Nummenmaa L. Magia: robust automated image processing and kinetic modeling toolbox for PET neuroinformatics [Internet]. *Frontiers in Neuroinformatics* 2020 **14** 3. (<https://doi.org/10.3389/fninf.2020.00003>)
- 42 Iozzo P, Gastaldelli A, Jarvisalo MJ, Kiss J, Borra R, Buzzigoli E, Viljanen A, Naum G, Viljanen T, Oikonen V *et al.* 18F-FDG assessment of glucose disposal and production rates during fasting and insulin stimulation: a validation study. *Journal of Nuclear Medicine* 2006 **47** 1016–1022.
- 43 Loessner A, Alavi A, Lewandrowski KU, Mozley D, Souder E & Gur RE. Regional cerebral function determined by FDG-PET in healthy volunteers: normal patterns and changes with age. *Journal of Nuclear Medicine* 1995 **36** 1141–1149.
- 44 Hirvonen J, Goodwin RS, Li CT, Terry GE, Zoghbi SS, Morse C, Pike VW, Volkow ND, Huestis MA & Innis RB. Reversible and regionally selective downregulation of brain cannabinoid CB1 receptors in chronic daily cannabis smokers. *Molecular Psychiatry* 2012 **17** 642–649. (<https://doi.org/10.1038/mp.2011.82>)
- 45 Pagotto U. Where does insulin resistance start? The brain. *Diabetes Care* 2009 **32**(Supplement 2) S174–S177. (<https://doi.org/10.2337/dc09-S305>)
- 46 Goss AM & Gower BA. Insulin sensitivity is associated with thigh adipose tissue distribution in healthy postmenopausal women. *Metabolism: Clinical and Experimental* 2012 **61** 1817–1823. (<https://doi.org/10.1016/j.metabol.2012.05.016>)
- 47 Goodpaster BH, Krishnaswami S, Harris TB, Katsiaras A, Kritchevsky SB, Simonsick EM, Nevitt M, Holvoet P & Newman AB. Obesity, regional body fat distribution, and the metabolic syndrome in older men and women. *Archives of Internal Medicine* 2005 **165** 777–783. (<https://doi.org/10.1001/archinte.165.7.777>)
- 48 Després JP & Lemieux I. Abdominal obesity and metabolic syndrome. *Nature* 2006 **444** 881–887. (<https://doi.org/10.1038/nature05488>)
- 49 Kullmann S, Valenta V, Wagner R, Tschritter O, Machann J, Häring HU, Preissl H, Fritsche A & Heni M. Brain insulin sensitivity is linked to adiposity and body fat distribution. *Nature Communications* 2020 **11** 1841. (<https://doi.org/10.1038/s41467-020-15686-y>)
- 50 Boivin A, Brochu G, Marceau S, Marceau P, Hould FS & Tchernof A. Regional differences in adipose tissue metabolism in obese men. *Metabolism: Clinical and Experimental* 2007 **56** 533–540. (<https://doi.org/10.1016/j.metabol.2006.11.015>)
- 51 Fontana L, Eagon JC, Trujillo ME, Scherer PE & Klein S. Visceral fat adipokine secretion is associated with systemic inflammation in obese humans. *Diabetes* 2007 **56** 1010–1013. (<https://doi.org/10.2337/db06-1656>)
- 52 Jensen MD. Role of body fat distribution and the metabolic complications of obesity. *Journal of Clinical Endocrinology and Metabolism* 2008 **93**(Supplement 1) S57–S63. (<https://doi.org/10.1210/jc.2008-1585>)
- 53 Rebelos E, Hirvonen J, Bucci M, Pekkarinen L, Nyman M, Hannukainen JC, Iozzo P, Salminen P, Nummenmaa L, Ferrannini E *et al.* Brain free fatty acid uptake is elevated in morbid obesity, and is irreversible 6 months after bariatric surgery: a positron emission tomography study. *Diabetes, Obesity and Metabolism* 2020 **22** 1074–1082. (<https://doi.org/10.1111/dom.13996>)
- 54 Tschritter O, Preissl H, Hennige AM, Sartorius T, Stingl KT, Heni M, Ketterer C, Stefan N, Machann J, Schleicher E *et al.* High cerebral insulin sensitivity is associated with loss of body fat during lifestyle intervention. *Diabetologia* 2012 **55** 175–182. (<https://doi.org/10.1007/s00125-011-2309-z>)
- 55 Rebelos E, Rinne JO, Nuutila P & Ekblad LL. Brain glucose metabolism in health, obesity, and cognitive decline—does insulin have anything to do with it? A narrative review. *Journal of Clinical Medicine* 2021 **10**. (<https://doi.org/10.3390/jcm10071532>)
- 56 Gastaldelli A, Cusi K, Pettiti M, Hardies J, Miyazaki Y, Berria R, Buzzigoli E, Sironi AM, Cersosimo E, Ferrannini E *et al.* Relationship between hepatic/visceral fat and hepatic insulin resistance in nondiabetic and type 2 diabetic subjects. *Gastroenterology* 2007 **133** 496–506. (<https://doi.org/10.1053/j.gastro.2007.04.068>)
- 57 Petersen KF, Dufour S, Li F, Rothman DL & Shulman GI. Ethnic and sex differences in hepatic lipid content and related cardiometabolic parameters in lean individuals. *JCI Insight* 2022 **7**. (<https://doi.org/10.1172/jci.insight.157906>)
- 58 Szczepaniak LS, Nurenberg P, Leonard D, Browning JD, Reingold JS, Grundy S, Hobbs HH & Dobbins RL. Magnetic resonance spectroscopy to measure hepatic triglyceride content: prevalence of hepatic steatosis in the general population. *American Journal of Physiology. Endocrinology and Metabolism* 2005 **288** E462–E468. (<https://doi.org/10.1152/ajpendo.00064.2004>)
- 59 Natali A, Toschi E, Camastra S, Gastaldelli A, Groop L & Ferrannini E. Determinants of postabsorptive endogenous glucose output in non-diabetic subjects. European Group for the study of insulin Resistance (EGIR). *Diabetologia* 2000 **43** 1266–1272. (<https://doi.org/10.1007/s001250051522>)

Received 8 June 2022

Revised version received 9 October 2022

Accepted 26 October 2022

**Pekkarinen, L., Kantonen, T., Oikonen, V., Haaparanta-Solin, M.,
Aarnio, R., Dickens, A. M., von Eyken, A., Latva-Rasku, A., Dadson, P.,
Kirjavainen, A. K., Rajander, J., Kalliokoski, K., Rönnemaa, T.,
Nummenmaa, L., & Nuutila, P. (2023)
Lower abdominal adipose tissue cannabinoid type 1 receptor
availability in young men with overweight.
Obesity**

ORIGINAL ARTICLE

Obesity Biology and Integrated Physiology



Lower abdominal adipose tissue cannabinoid type 1 receptor availability in young men with overweight

Laura Pekkarinen^{1,2} | Tatu Kantonen^{1,3} | Vesa Oikonen¹ |
 Merja Haaparanta-Solin^{1,4} | Richard Aarnio¹ | Alex M. Dickens^{5,6} |
 Annie von Eyken^{5,6} | Aino Latva-Rasku¹ | Prince Dadson¹ |
 Anna K. Kirjavainen¹ | Johan Rajander⁷ | Kari Kalliokoski¹ |
 Tapani Rönnemaa^{2,8} | Lauri Nummenmaa^{1,9} | Pirjo Nuutila^{1,2}

¹Turku PET Centre, University of Turku, Turku, Finland

²Department of Endocrinology, Turku University Hospital, Turku, Finland

³Clinical Neurosciences, Turku University Hospital, Turku, Finland

⁴MediCity Research Laboratory, University of Turku, Turku, Finland

⁵Turku Bioscience Centre, University of Turku, Turku, Finland

⁶Åbo Akademi University, Turku, Finland

⁷Turku PET Centre, Åbo Akademi University, Turku, Finland

⁸Department of Medicine, University of Turku, Turku, Finland

⁹Department of Psychology, University of Turku, Turku, Finland

Correspondence

Pirjo Nuutila, Turku PET Centre, University of Turku, and Department of Endocrinology, Turku University Hospital, Turku, Finland.
 Email: pirjo.nuutila@utu.fi

Funding information

Academy of Finland, Grant/Award Numbers: 294897, 307402, 332225; Diabetestutkimussäätiö; Emil Aaltosen Säätiö; Jenny ja Antti Wihurin Rahasto; Orionin Tutkimussäätiö; Turun Yliopistollisen Keskussairaalan Koulutus- ja Tutkimussäätiö; Varsinais-Suomen Rahasto

Abstract

Objective: Cannabinoid type 1 receptors (CB1R) modulate feeding behavior and energy homeostasis, and the CB1R tone is dysregulated in obesity. This study aimed to investigate CB1R availability in peripheral tissue and brain in young men with overweight versus lean men.

Methods: Healthy males with high (HR, $n = 16$) or low (LR, $n = 20$) obesity risk were studied with fluoride 18-labeled FMPEP- d_2 positron emission tomography to quantify CB1R availability in abdominal adipose tissue, brown adipose tissue, muscle, and brain. Obesity risk was assessed by BMI, physical exercise habits, and familial obesity risk, including parental overweight, obesity, and type 2 diabetes. To assess insulin sensitivity, fluoro- $[^{18}\text{F}]$ -deoxy-2-D-glucose positron emission tomography during hyperinsulinemic-euglycemic clamp was performed. Serum endocannabinoids were analyzed.

Results: CB1R availability in abdominal adipose tissue was lower in the HR than in the LR group, whereas no difference was found in other tissues. CB1R availability of abdominal adipose tissue and brain correlated positively with insulin sensitivity and negatively with unfavorable lipid profile, BMI, body adiposity, and inflammatory markers. Serum arachidonoyl glycerol concentration was associated with lower CB1R availability of the whole brain, unfavorable lipid profile, and higher serum inflammatory markers.

Conclusions: The results suggest endocannabinoid dysregulation already in the pre-obesity state.

INTRODUCTION

The number of people with obesity is increasing worldwide [1]. Obesity is a complex disease characterized by excess adipose tissue accumulation increasing the risk for other diseases and metabolic abnormalities [2]. Because of the significant burden to individuals and community due to obesity, effective tools for preventing and treating obesity are needed.

The endocannabinoid system (ECS) plays a central role in regulating food intake, energy homeostasis, and lipid metabolism at both the central and peripheral level [3, 4]. ECS consists of two G protein-coupled receptors: cannabinoid type 1 and type 2 (CB1R and CB2R, respectively) receptors, their ligands endocannabinoids, and the ligand-metabolizing enzymes [4]. CB1Rs, which are essential in energy homeostasis, are widely expressed in the central nervous system, notably in brain regions controlling energy balance and feeding behavior such as the hypothalamus, corticolimbic circuits, ventral tegmental area, and brain stem [5, 6]. Peripherally, CB1Rs are expressed in tissues controlling energy homeostasis, including gastrointestinal tract, adipose tissue, liver, skeletal muscle, and endocrine pancreas.

Endocannabinoids, of which the most studied are anandamide (AEA) and 2-arachidonoylglycerol (2-AG), act as ligands to CB1Rs, which exert a cascade promoting energy preservation leading to increased food intake, adipose tissue accumulation, increased levels of proinflammatory markers, decreased energy expenditure and thermogenesis, insulin resistance, and weight gain [3–7]. Endocannabinoids are synthesized and released locally on demand under tight regulation by neurons [3, 4]. During a prolonged metabolic dysregulation, however, the ECS tone can become upregulated; CB1R upregulation and increased levels of endocannabinoids in brain, peripheral tissue, and circulation have been found in animals and humans with obesity [7, 8].

Antagonism of CB1Rs contributes to reductions of food intake, body weight, adiposity, insulin resistance, and plasma triglycerides and an increase in the high-density lipoprotein (HDL)/low-density lipoprotein (LDL) cholesterol ratio [4, 7, 8]. After withdrawal of the first CB1R inverse agonist rimonabant (SR141716) from clinical use because of its neuropsychiatric side effects, therapeutic strategies targeting the peripheral ECS have been investigated. In murine models, peripherally restricted CB1R antagonists or inverse agonists and allosteric inhibitors of CB1Rs, compounds decreasing endocannabinoid synthesis or increasing endocannabinoid degradation, have been shown to have beneficial effects by reducing food intake, weight, hyperleptinemia, insulin resistance, and dyslipidemia without central side effects [6, 9].

Recently, we found no significant difference in CB1R availability in brain of healthy lean males versus males with overweight studied using positron emission tomography (PET) imaging and CB1R inverse agonist radioligand fluoride 18-labeled FMPEP- d_2 ([3R,5R]-5-[3-methoxy-phenyl]-3-[[R]-1-phenyl-ethylamino]-1-[4-trifluoro-methyl-phenyl]-pyrrolidin-2-one). However, BMI and parental history of overweight, obesity, and type 2 diabetes (T2D) had a negative association with CB1R availability [10]. Here, we investigated CB1R availability in peripheral tissues and in the whole brain in the same sample with [18 F]FMPEP- d_2 PET imaging [11] and compared the tissue CB1R availability with insulin sensitivity, body adiposity, and related cardiometabolic risk factors and circulating endocannabinoid levels. We found

Study Importance

What is already known?

- Cannabinoid type 1 receptors (CB1Rs) participate in the control of energy balance and lipid and glucose metabolism at the central and peripheral level, and obesity is associated with dysregulation of the endocannabinoid system.
- CB1R availability can be studied *in vivo* using positron emission tomography (PET) imaging and CB1R inverse agonist radioligand [18 F]FMPEP- d_2 .

What does this study add?

- We found lower abdominal adipose tissue CB1R availability in young men with overweight, as compared with lean men, and an association between lower CB1R availability and decreased insulin sensitivity, unfavorable lipid profile, and higher body adiposity and inflammatory markers.
- Whole-brain CB1R availability did not differ between the groups, but lower cerebral CB1R availability was associated with decreased whole-body insulin sensitivity and higher body adiposity.

How might these results change the direction of research or the focus of clinical practice?

- The study findings provide further knowledge about the endocannabinoid system dysregulation that may take place already in the preobesity state and encourage further effort for investigating CB1Rs as a target to treat obesity and metabolic disorders.

that obesity risk was associated with lowered CB1R availability in abdominal adipose tissue, which, in turn, was associated with decreased insulin sensitivity, unfavorable lipid profile, and higher weight, BMI, body adiposity, and inflammatory markers.

METHODS

Study participants

We studied 21 healthy young male participants with low (LR) and 16 with high (HR) obesity risk. A detailed description of the recruitment, inclusion, and exclusion criteria and a screening visit has been previously published [10]. Briefly, inclusion criteria for the LR group were male sex, age 20 to 35 years, BMI of 18.5 to 24.9 kg/m², leisure time physical activity ≥ 4 hours per week, and no parental overweight, obesity, or T2D. Inclusion criteria for the HR group were male sex, age 20 to 35 years, BMI of 25 to 30, leisure time physical activity < 4 hours per week, and parental overweight, obesity, or T2D. Overweight,

physical inactivity, and parental obesity and T2D have been established as risk factors for future obesity [12–17]. One HR participant's [^{18}F]FMPEP- d_2 uptake in brown adipose tissue (BAT) was not possible to analyze reliably because of marked spillover from adjacent structures.

The sample size was determined by a priori power analysis based on earlier PET studies on obesity [18] suggesting that a sample size of $16 + 16$ would be sufficient for power of 0.95 at $p < 0.05$, assuming effect size (r) = 0.5. Each participant provided written informed consent. The study protocol was approved by the Ethics Committee of the Hospital District of Southwest Finland and conducted in accordance with the principles of the Declaration of Helsinki. The study is a part of the PROSPECT project registered at ClinicalTrials.gov (Neuromolecular Risk Factors for Obesity, PROSPECT, NCT03106688).

Study design

CB1R availability was measured with dynamic PET/computed tomography (CT) using the CB1R inverse agonist radioligand [^{18}F]FMPEP- d_2 . Tissue glucose uptake (GU) rates were determined with fluoro- ^{18}F -deoxy-2-D-glucose (FDG) PET/CT during a hyperinsulinemic-euglycemic clamp. Whole-body insulin sensitivity (M value) and endogenous glucose production (EGP) were calculated. Magnetic resonance imaging (MRI) was conducted to assess abdominal subcutaneous (SAT) and visceral (VAT) adipose tissue masses. PET/CT and MRI studies were performed at room temperature on separate days at the Turku PET Centre, Finland. Body fat mass percentage was measured with an air displacement plethysmograph (the Bod Pod system, software version 5.4.0, COSMED, Inc.) after at least 4 hours of fasting. Serum endocannabinoid levels and metabolic biomarkers were quantified.

Radiochemistry

The radioligand [^{18}F]FMPEP- d_2 was synthesized according to the standard operating procedure of the Turku PET Centre as previously described [10, 19]. FDG was produced using the FASTlab synthesis platform (GE Healthcare) according to the modified method of Hamacher et al. [20] and Lemaire et al. [21].

[^{18}F]FMPEP- d_2 PET/CT scanning protocol

[^{18}F]FMPEP- d_2 PET images were acquired with PET/CT (GE Discovery VCT PET/CT, GE Healthcare) after a 6- to 12-hour fast. The study protocol has been described in detail in our previous report [10]. In brief, two catheters were inserted in veins of opposite forearms, one for blood sampling and one for [^{18}F]FMPEP- d_2 injection. Blood samples were collected to measure hematocrit and serum endocannabinoid concentrations before the scan. A heating pillow was used on the arm to obtain arterialized blood samples. Then 147 to 215 MBq of [^{18}F]FMPEP- d_2 was injected intravenously, and dynamic scans of the brain (60 minutes), neck (12 minutes), and

abdomen (9 minutes) and a late scan of the brain were conducted. CT scans of each region were performed for photon attenuation and anatomical reference. Arterialized venous blood samples were drawn on the opposite arm from the injection site to measure plasma radioactivity and [^{18}F]FMPEP- d_2 radio-metabolites. Radioactivity was measured with an automatic gamma counter (Wizard 1480 3", Wallac).

[^{18}F]FMPEP- d_2 PET/CT image analysis

CB1R availability of tissues was quantified from [^{18}F]FMPEP- d_2 PET/CT images by determining fractional uptake rate (FUR) and volume distribution (V_T) of the radioligand as previously described [11]. Carimas Software (version 2.9, Turku PET Centre, <https://turkupetcentre.fi/software/>) was used for image analysis of SAT, intraperitoneal white adipose tissue (IWAT) and retroperitoneal white adipose tissue (RWAT), BAT, and muscle. Regions of interest (ROI) were manually drawn on the fused PET/CT images to several volumes of abdominal SAT, IWAT, and RWAT. BAT ROIs were drawn bilaterally in supraclavicular adipose tissue depots. For ROIs of adipose tissue, only voxels of Hounsfield units (HU) within the range of -50 to -250 HU were included [22]. Muscle ROIs were drawn bilaterally in the deltoid muscle. To limit the effect of spillover due to partial volume effect and motion, several ROIs in several slices of images for each tissue were drawn avoiding large vessels. Radio-metabolite corrected plasma input for image analysis was determined by correcting the acquired plasma time-activity curve (TAC) with the parent tracer fraction measured using thin layer chromatography and digital autoradiography as previously described [6].

FUR of the [^{18}F]FMPEP- d_2 in each peripheral tissue was calculated by dividing the tissue radioactivity concentration at time X by the Area Under the Curve $_{0-X}$ of the radio-metabolite corrected plasma TAC. V_T of each peripheral tissue was calculated by dividing the radioactivity concentration in tissue by radio-metabolite corrected plasma TAC, whereas the tissue scans were performed as late scans. V_T of the [^{18}F]FMPEP- d_2 in the whole brain was determined by applying the reversible one-tissue compartmental model using the radio-metabolite corrected plasma TAC as model input as presented earlier [10, 11, 23]. Mean V_T of brain was computed as the average of all white and gray matter voxels within the Montreal Neurological Institute (MNI) space template.

FDG PET/CT scanning protocol and image analysis

The FDG PET/CT scanning protocol has been detailed in our previous report [10]. Studies were done after a 12-hour overnight fast with the GE Discovery (Discovery 690 PET/CT, GE Healthcare) PET camera. Hyperinsulinemic-euglycemic clamp was applied as previously described [24] in order to measure whole-body insulin sensitivity. A detailed description of the FDG PET/CT scanning protocol, hyperinsulinemic-euglycemic clamp execution, PET/CT image analysis, determination of plasma input, quantification of tissue-specific GU rates, and measurement of EGP is available in the online Supporting Information.

TABLE 1 Characteristics of the study participants in the LR and HR groups

	LR (n = 21)	HR (n = 16)	p value
Age (y)	23 ± 3	28 ± 4	0.0008
Weight (kg)	70.6 ± 7.6	92.1 ± 7.9	<0.0001
BMI (kg/m ²)	22.1 ± 2.0	27.3 ± 1.9	<0.0001
Body fat mass (kg)	11.9 ± 4.3	28.4 ± 8.9	<0.0001
Body fat mass (%)	16.7 ± 5.4	30.0 ± 7.9	<0.0001
Fat-free mass (kg)	59.2 ± 6.8	63.8 ± 5.3	0.03
Abdominal SAT mass (kg)	2.8 ± 1.0	7.2 ± 2.4	<0.0001
VAT mass (kg)	1.4 ± 0.8	3.8 ± 1.2	<0.0001
Systolic blood pressure (mm Hg)	124 ± 12	135 ± 12	0.008
Diastolic blood pressure (mm Hg)	76 ± 10	82 ± 9	0.08
<i>Fasting</i>			
Plasma glucose (mmol/L)	4.9 ± 0.5	5.5 ± 0.4	0.0004
Plasma insulin (pmol/L)	38.7 ± 21.2	63.9 ± 22.3	0.001
Serum FFA (mmol/L)	0.30 ± 0.11	0.32 ± 0.14	0.8
<i>2-Hour OGTT</i>			
Plasma glucose (mmol/L)	4.7 ± 1.0	6.0 ± 1.4	0.002
Plasma insulin (pmol/L)	163.7 ± 144.5	360.9 ± 244.3	0.004
HbA _{1c} (mmol/mol)	29 ± 2	32 ± 3	0.0008
HbA _{1c} (%)	4.8 ± 0.2	5.1 ± 0.3	0.001
hs-CRP (mg/L)	0.4 ± 0.3	1.2 ± 1.1	0.001
M value (μmol/kg/min)	57.0 ± 14.2	36.5 ± 12.0	<0.0001
M value (μmol/kg _{FFM} /min)	68.8 ± 17.3	50.4 ± 13.7	0.001
Rd (μmol/kg/min)	50.7 ± 10.6	35.7 ± 10.0	0.0001
Rd (μmol/kg _{FFM} /min)	61.1 ± 11.6	50.8 ± 11.0	0.01
EGP (μmol/kg/min) ^a	−3.3 ± 6.8	0.6 ± 4.7	0.06
EGP (μmol/kg _{FFM} /min) ^a	−2.0 ± 9.1	1.4 ± 7.2	0.2
Clamp serum FFA (mmol/L)	0.03 ± 0.01	0.05 ± 0.03	0.6
<i>Glucose uptake (μmol/100 g/min)</i>			
Abdominal SAT	2.2 ± 0.8	1.2 ± 0.6	0.0001
VAT	3.2 ± 0.7	1.9 ± 0.6	<0.0001
BAT ^b	3.1 ± 0.8	2.3 ± 0.9	0.005
Muscle ^c	5.1 ± 1.3	3.3 ± 0.9	<0.0001
Femoral SAT ^c	1.9 ± 0.7	1.2 ± 0.6	0.001
Liver	2.5 ± 0.6	2.1 ± 0.7	0.09

Note: Data presented as mean ± SD.

Abbreviations: BAT, brown adipose tissue; EGP, endogenous glucose production; FFA, free fatty acids; FFM, fat-free mass; HbA_{1c}, glycated hemoglobin; HR, high risk; hs-CRP, high-sensitivity C-reactive protein; LR, low risk; M value, whole-body insulin sensitivity; OGTT, oral glucose tolerance test; Rd, rate of disappearance of glucose; SAT, subcutaneous adipose tissue; VAT, visceral adipose tissue.

^aMean and SD for the LR (n = 20) and HR (n = 16) participants who gave a urine sample.

^bMean and SD for the LR (n = 20) and HR (n = 16) participants who completed the FDG scan successfully.

^cMean and SD for the LR (n = 19) and HR (n = 16) participants who completed the FDG scan successfully.

Biochemical analysis

A detailed description of the methods of the biochemical analysis of plasma glucose and insulin and serum free fatty acids (FFA) and high-sensitivity C-reactive protein is provided in the online Supporting Information. Metabolic biomarkers were quantified from serum

from 19 LR and 16 HR subjects at fasting using high-throughput proton nuclear magnetic resonance (NMR) [25] metabolomics (Nightingale Health Oy, Helsinki, Finland). Eight different serum endocannabinoids and related structures were measured: arachidonic acid, AEA, 1- and 2-arachidonoyl glycerol (AG 1 + 2), α-linolenic acid (α-LEA), γ-linolenic acid (γ-LEA), docosatetraenoyl ethanolamide

TABLE 2 Serum metabolic biomarkers in the LR and HR groups

	LR (n = 19)	HR (n = 16)	p value
<i>Cholesterol (mmol/L)</i>			
Total cholesterol	3.6 ± 0.4	4.5 ± 0.9	0.0008
Remnant cholesterol	1.0 ± 0.2	1.4 ± 0.4	0.001
VLDL cholesterol	0.4 ± 0.1	0.6 ± 0.2	0.0009
LDL cholesterol	1.3 ± 0.2	1.9 ± 0.5	<0.0001
HDL cholesterol	1.3 ± 0.2	1.2 ± 0.2	0.1
Total esterified cholesterol	2.6 ± 0.3	3.3 ± 0.6	0.0002
<i>Glycerides and phospholipids (mmol/L)</i>			
Total triglycerides	0.8 ± 0.2	1.3 ± 0.7	0.005
VLDL triglycerides	0.5 ± 0.2	1.0 ± 0.6	0.005
LDL triglycerides	0.09 ± 0.01	0.1 ± 0.03	0.001
HDL triglycerides	0.07 ± 0.02	0.09 ± 0.03	0.06
Phosphoglycerides	2.0 ± 0.2	2.2 ± 0.4	0.03
Ratio of triglycerides to phosphoglycerides	0.4 ± 0.1	0.6 ± 0.2	0.005
Total cholines	2.3 ± 0.2	2.5 ± 0.4	0.03
Phosphatidylcholines	1.9 ± 0.2	2.1 ± 0.4	0.03
Sphingomyelins	0.4 ± 0.04	0.4 ± 0.05	0.002
<i>Apolipoproteins (g/L)</i>			
ApoB	0.6 ± 0.1	0.8 ± 0.2	0.0002
ApoA1	1.3 ± 0.2	1.3 ± 0.1	0.7
ApoB/ApoA1	0.5 ± 0.1	0.6 ± 0.2	0.0003
<i>Fatty acids (mmol/L)</i>			
Total fatty acids	9.4 ± 1.0	11.6 ± 2.7	0.003
Omega-3 fatty acids	0.4 ± 0.1	0.5 ± 0.2	0.1
Omega-6 fatty acids	4.0 ± 0.3	4.5 ± 0.6	0.004
PUFA	4.4 ± 0.4	5.0 ± 0.8	0.006
MUFA	2.2 ± 0.3	3.0 ± 0.9	0.002
Saturated fatty acids	2.8 ± 0.4	3.7 ± 1.1	0.004
Linoleic acid	3.5 ± 0.3	4.0 ± 0.6	0.003
Docosahexaenoic acid	0.2 ± 0.1	0.3 ± 0.05	0.3
<i>Fatty acids (% of total fatty acids)</i>			
Omega-3 fatty acids	4.4 ± 1.4	4.2 ± 0.8	0.7
Omega-6 fatty acids	42.3 ± 1.7	39.3 ± 3.7	0.004
PUFA	46.7 ± 2.2	43.6 ± 3.4	0.003
MUFA	23.4 ± 2.0	25.2 ± 1.8	0.01
Saturated fatty acids	29.9 ± 1.5	31.3 ± 2.3	0.04
Linoleic acid	37.5 ± 1.8	35.3 ± 3.5	0.03
Docosahexaenoic acid	2.5 ± 0.6	2.2 ± 0.3	0.1
<i>Ketone bodies (mmol/L)</i>			
3-Hydroxybutyrate	0.05 ± 0.05	0.04 ± 0.03	0.2
Acetate	0.07 ± 0.03	0.05 ± 0.02	0.02
Acetoacetate	0.05 ± 0.03	0.04 ± 0.02	0.2
Acetone	0.02 ± 0.01	0.02 ± 0.01	0.1
<i>Glycolysis related metabolites (mmol/L)</i>			
Glucose	4.9 ± 0.1	5.4 ± 0.4	<0.0001
Lactate	1.8 ± 0.3	2.1 ± 0.4	0.02

(Continues)

TABLE 2 (Continued)

	LR (n = 19)	HR (n = 16)	p value
Pyruvate	0.1 ± 0.02	0.08 ± 0.03	0.05
Citrate	0.1 ± 0.01	0.06 ± 0.01	0.5
<i>Amino acids (mmol/L)</i>			
Alanine	0.3 ± 0.1	0.3 ± 0.1	0.1
Glutamine	0.8 ± 0.1	0.8 ± 0.1	0.5
Glycine	0.3 ± 0.1	0.2 ± 0.03	0.2
Histidine	0.1 ± 0.01	0.08 ± 0.01	0.5
<i>Branched-chain amino acids</i>			
Isoleucine	0.1 ± 0.02	0.1 ± 0.01	0.5
Leucine	0.1 ± 0.02	0.1 ± 0.01	0.07
Valine	0.2 ± 0.04	0.3 ± 0.03	0.4
<i>Aromatic amino acids</i>			
Phenylalanine	0.06 ± 0.01	0.06 ± 0.01	0.2
Tyrosine	0.06 ± 0.01	0.07 ± 0.01	0.4
<i>Fluid balance</i>			
Creatinine (μmol/L)	76.8 ± 10.1	82.9 ± 10.5	0.09
Albumin (g/L)	41.5 ± 2.4	41.9 ± 2.3	0.7
<i>Inflammation (mmol/L)</i>			
GlycA	0.7 ± 0.1	0.8 ± 0.1	<0.0001

Note: Data presented as mean ± SD. Serum samples of 35 participants (19 LR and 16 HR participants) were analyzed. Abbreviations: ApoA1, apolipoprotein A1; ApoB, apolipoprotein B; GlycA, glycoprotein acetyls; HDL, high-density lipoprotein; HR, high risk; LDL, low-density lipoprotein; LR, low risk; MUFA, monounsaturated fatty acids; PUFA, polyunsaturated fatty acids; VLDL, very low-density lipoprotein.

(DEA), *N*-arachidonoyl-L-serine, and oleyl ethanolamide. Because of rapid isomerization of 1-AG and 2-AG at room temperature, a total concentration of AG (1 + 2) was reported. Fasting-state blood samples collected during the [¹⁸F]FMPEP-*d*₂ study day were used and analyzed as previously described [10, 26].

Measurement of tissue masses

The abdominal SAT and VAT masses were analyzed from MRI images using sliceOmatic (Tomovision). A detailed description of the tissue mass analyses is provided in the online Supporting Information.

Statistical methods

Data are presented as mean ± SD. Between-group comparisons were performed with independent samples *t* test or Wilcoxon rank sum test as appropriate. Categorical variables were compared with χ^2 test. Statistical analyses were performed with SPSS Statistics software, version 28.0 (IBM Corp.). Associations between study variables were tested using Pearson or Spearman correlation tests. *P* values < 0.05 were considered statistically significant.

RESULTS

Participant characteristics

The HR participants had higher weight, BMI, total body fat mass, and abdominal SAT and VAT masses than the LR participants. The HR group also had worse glycemic profiles and lower insulin-stimulated tissue-specific GU rates and *M* values compared with the LR group, indicating lower insulin sensitivity; however, insulin-suppressed EGP did not differ between the groups. High-sensitivity C-reactive protein level was higher in the HR than in the LR group. The HR participants were older than the LR group (Table 1). Serum metabolite levels were higher in the HR group for total, remnant, very low-density lipoprotein (VLDL), and LDL cholesterol, triglycerides, apolipoprotein B (ApoB), ApoB/ApoA1 ratio, and fatty acids than in the LR group. Also, glycoprotein acetyls (GlycA), a biomarker of systemic inflammation, was higher in the HR than in the LR group (Table 2).

Lower CB1R availability in abdominal adipose tissue in the HR than in the LR group

The HR group exhibited lower *FUR* and *V_T* of the [¹⁸F]FMPEP-*d*₂ in abdominal SAT, IWAT, and RWAT, indicating lower CB1R availability as compared with the LR group. The muscle *FUR* and *V_T* were numerically

lower in the HR than in the LR group but this did not reach statistical significance. No difference was found in CB1R availability of BAT and the whole brain between the groups (Figure 1). As the V_T and FUR of [^{18}F]FMPEP- d_2 are both assumed to represent CB1R availability in tissue, the V_T and FUR values in each tissue correlated positively with each other ($r = 0.80$, $p < 0.0001$ for abdominal SAT; $r = 0.72$, $p < 0.0001$ for IWAT; $r = 0.78$, $p < 0.0001$ for RWAT; $r = 0.87$, $p < 0.0001$ for BAT; $r = 0.58$, $p = 0.0002$ for muscle). Intertissue associations of CB1R availability are presented in Supporting Information Table S1.

Association between CB1R availability and insulin sensitivity

When comparing the tissue CB1R availability with tissue-specific GU rates, we found a positive association between the two in abdominal adipose tissue (Table 3 and Figure 2A–C). CB1R availability of IWAT and RWAT correlated positively also with BAT, skeletal muscle, and femoral SAT GU, and CB1R availability of SAT with femoral SAT GU. CB1R availability of BAT correlated positively only with VAT GU.

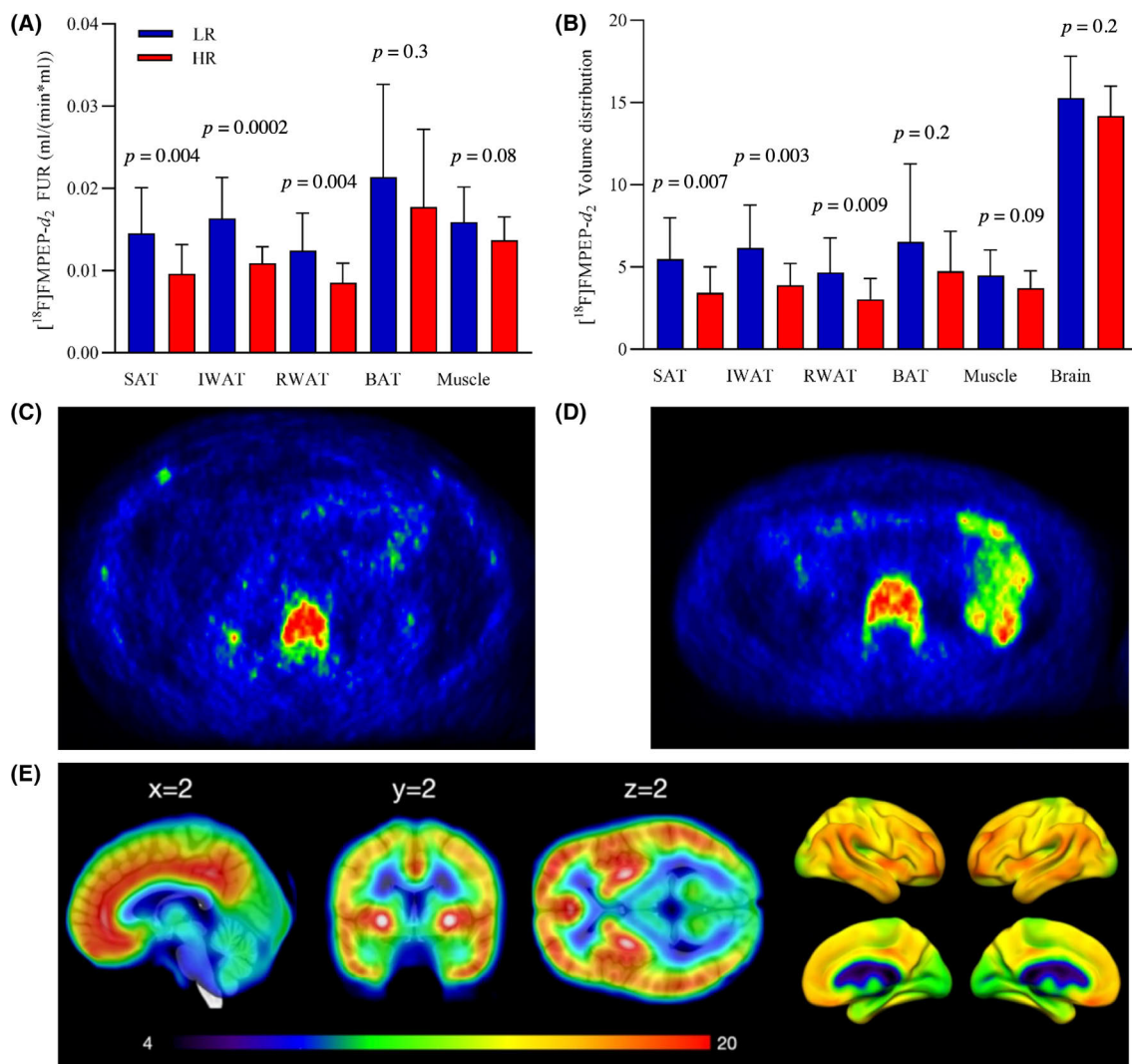


FIGURE 1 Lower CB1R availability in abdominal SAT, IWAT, and RWAT in the HR as compared with the LR group. (A) FUR of [^{18}F]FMPEP- d_2 in abdominal SAT, IWAT, RWAT, BAT, and muscle in the LR and HR groups. (B) [^{18}F]FMPEP- d_2 volume distribution (V_T) of SAT, IWAT, RWAT, BAT, muscle, and the whole brain in the LR and HR groups. PET abdomen images depicting FUR of [^{18}F]FMPEP- d_2 of (C) one HR and (D) one LR participant. (E) Mean V_T for the [^{18}F]FMPEP- d_2 scans. BAT, brown adipose tissue; FUR, fractional uptake rate; HR, high risk; IWAT, intraperitoneal white adipose tissue; LR, low risk; RWAT, retroperitoneal white adipose tissue; SAT, subcutaneous adipose tissue

CB1R availability of muscle and the whole brain correlated positively only with BAT GU (Table 3).

Considering whole-body insulin sensitivity, we found a positive correlation between CB1R availability of RWAT and M value and the rate of disappearance of glucose (Rd), and CB1R availability of IWAT and Rd. CB1R availability of the whole brain correlated positively with M value and negatively with insulin-suppressed EGP adjusted with fat-free mass (EGP_{FFM}; Table 3 and Supporting Information Figure S1). CB1R availability of abdominal adipose tissue depots correlated negatively with serum insulin-suppressed FFA level (Table 3).

Association between CB1R availability and body composition

CB1R availability of abdominal adipose tissue depots correlated negatively with weight, BMI, total body fat, and abdominal SAT and VAT masses. CB1R availability of muscle correlated negatively with weight, BMI, VAT mass, and FFM. CB1R availability of the whole brain correlated negatively with weight, BMI, total body fat mass, and VAT mass. CB1R availability of BAT did not correlate with any of these measures (Table 3).

TABLE 3 Associations between [¹⁸F]FMPEP-*d*₂ FUR values of abdominal SAT, IWAT, RWAT, BAT, and muscle and V_T of the whole brain and anthropometric and metabolic characteristics and insulin-stimulated tissue-specific glucose uptake rates

	[¹⁸ F]FMPEP- <i>d</i> ₂ FUR (mL/[min × mL])					V _T Brain
	SAT	IWAT	RWAT	BAT	Muscle	
Age (y)	−0.31	−0.42**	−0.42**	−0.16	−0.33*	−0.24
Weight (kg)	−0.49**	−0.59***	0.57***	−0.25	−0.40*	−0.39*
BMI (kg/m ²)	−0.49**	−0.57***	−0.59***	−0.29	−0.40*	−0.44**
Body fat mass (kg)	−0.56***	−0.63***	−0.65***	−0.13	−0.31	−0.36*
Body fat mass (%)	−0.53***	−0.63***	−0.68***	−0.07	−0.25	−0.36*
Fat-free mass (kg)	−0.15	−0.16	−0.09	−0.32	−0.35*	−0.08
Abdominal SAT mass (kg)	−0.55***	−0.60***	−0.59***	−0.09	−0.29	−0.28
VAT mass (kg)	−0.50**	−0.66***	−0.60***	−0.10	−0.33*	−0.37*
Systolic blood pressure (mm Hg)	−0.19	−0.34*	−0.35*	0.11	−0.10	−0.50**
Diastolic blood pressure (mm Hg)	−0.07	−0.23	−0.22	0.15	−0.17	−0.42**
HbA _{1c} (mmol/mol)	−0.23	−0.37*	−0.20	−0.004	0.09	−0.10
hs-CRP (mg/L)	−0.32	−0.31	−0.26	−0.07	−0.17	−0.28
Fasting serum FFA (mmol/L)	0.078	−0.04	−0.10	0.14	−0.02	−0.25
Clamp serum FFA (mmol/L)	−0.39*	−0.39*	−0.38*	−0.007	−0.13	−0.31
M value (μmol/kg/min)	0.28	−0.27	0.39*	0.17	0.19	0.38*
M value (μmol/kg _{FFM} /min)	0.16	0.14	0.24	0.17	0.16	0.35*
Rd (μmol/kg/min)	0.26	0.36*	0.42*	0.14	0.20	0.23
Rd (μmol/kg _{FFM} /min)	0.15	0.20	0.28	0.14	0.18	0.24
EGP (μmol/kg/min) ^a	−0.05	0.08	0.02	0.10	0.06	−0.33
EGP (μmol/kg _{FFM} /min) ^a	−0.12	−0.01	−0.08	0.08	0.05	−0.43*
<i>Glucose uptake (μmol/100 g/min)</i>						
Abdominal SAT	0.56***	0.64***	0.60***	0.31	0.24	0.30
VAT	0.57***	0.67***	0.62***	0.37*	0.32	0.32
BAT ^b	0.33	0.43*	0.50**	0.03	0.34*	0.34*
Muscle ^c	0.25	0.34*	0.41*	0.18	0.21	0.20
Femoral SAT ^c	0.41*	0.45**	0.51**	0.03	0.11	0.34
Liver	0.15	−0.002	0.02	0.09	−0.02	−0.23

Note: Data are Pearson *r* values. Significant associations are indicated by bold font.

Abbreviations: BAT, brown adipose tissue; EGP, endogenous glucose production; FFA, free fatty acids; FFM, fat-free mass; FUR, fractional uptake rate; HbA_{1c}, glycated hemoglobin; HR, high risk; hs-CRP, high-sensitivity C-reactive protein; IWAT, intraperitoneal white adipose tissue; LR, low risk; M value, whole-body insulin sensitivity; Rd, rate of disappearance of glucose; RWAT, retroperitoneal white adipose tissue; SAT, subcutaneous adipose tissue; VAT, visceral adipose tissue; V_T, volume distribution.

^aAssociations with the LR (*n* = 20) and HR (*n* = 16) participants who gave a urine sample.

^bAssociations with the LR (*n* = 20) and HR (*n* = 16) participants who completed the FDG scan successfully.

^cAssociations with the LR (*n* = 19) and HR (*n* = 16) participants who completed the FDG scan successfully.

**p* < 0.05.

***p* < 0.01.

****p* < 0.001.

*****p* < 0.0001.

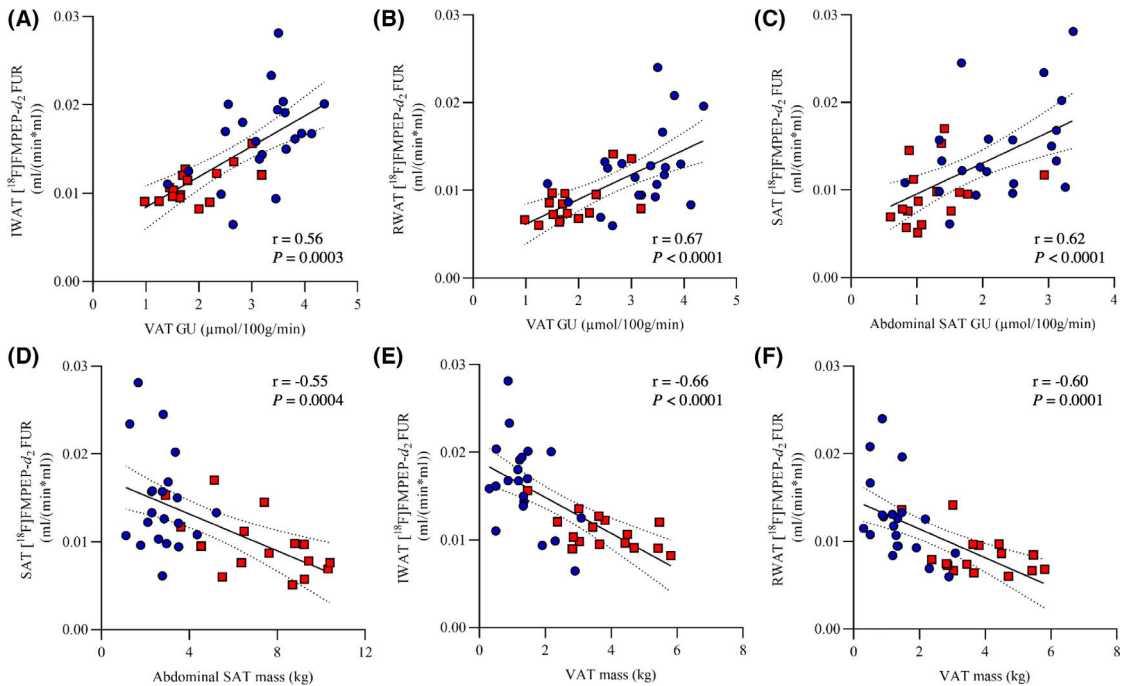


FIGURE 2 Associations between abdominal adipose tissue CB1R availability and tissue GU rates and tissue masses. Pearson correlation between $[^{18}\text{F}]\text{FMPEP-d}_2$ FUR values of (A) abdominal SAT and SAT GU, (B) intraperitoneal WAT and VAT GU, (C) retroperitoneal WAT and VAT GU, (D) abdominal SAT and abdominal SAT mass, (E) intraperitoneal WAT and VAT mass, and (F) retroperitoneal WAT and VAT mass in the LR (blue circle) and HR (red square) groups. FUR, fractional uptake rate; GU, glucose uptake; HR, high risk; IWAT, intraperitoneal white adipose tissue; LR, low risk; RWAT, retroperitoneal white adipose tissue; SAT, subcutaneous adipose tissue; VAT, visceral adipose tissue

Association between CB1R availability and serum metabolomics

Lower CB1R availability in abdominal adipose tissue, muscle, and the whole brain was associated with unfavorable lipid profile (Figure 3). CB1R availability of abdominal adipose tissue depots and the whole brain correlated negatively with total, non-HDL, remnant, VLDL, and LDL cholesterol, triglycerides, free cholesterol, ratio of triglycerides to phosphoglycerides, ApoB, and ApoB/ApoA1 ratio. CB1R availability of IWAT, RWAT, and brain also correlated negatively with fatty acids, including omega-6 fatty acids and linoleic acid. CB1R availability of abdominal SAT correlated positively with HDL cholesterol. CB1R availability of muscle correlated negatively with total, non-HDL, remnant, VLDL, and LDL cholesterol, ApoB, ApoB/ApoA1 ratio, and fatty acids. CB1R availability of abdominal adipose tissue depots and brain correlated negatively with GlycA. CB1R availability of BAT did not correlate with serum metabolomics.

Association between CB1R availability and serum endocannabinoid levels

Serum endocannabinoid levels did not differ between the groups as reported previously [10] (Supporting Information Table S3). CB1R availability in the whole brain correlated negatively with AG (1 + 2), whereas no significant association was found between the peripheral tissue CB1R availability and serum endocannabinoid levels (Table 4).

Associations between serum endocannabinoid levels and insulin sensitivity, body composition, and serum metabolomics

Serum arachidonic acid and AEA levels correlated negatively with M value_{FFM}, and AEA level also correlated negatively with M value, Rd, and Rd_{FFM}. Serum AG (1 + 2) and docosatetraenoyl ethanolamide

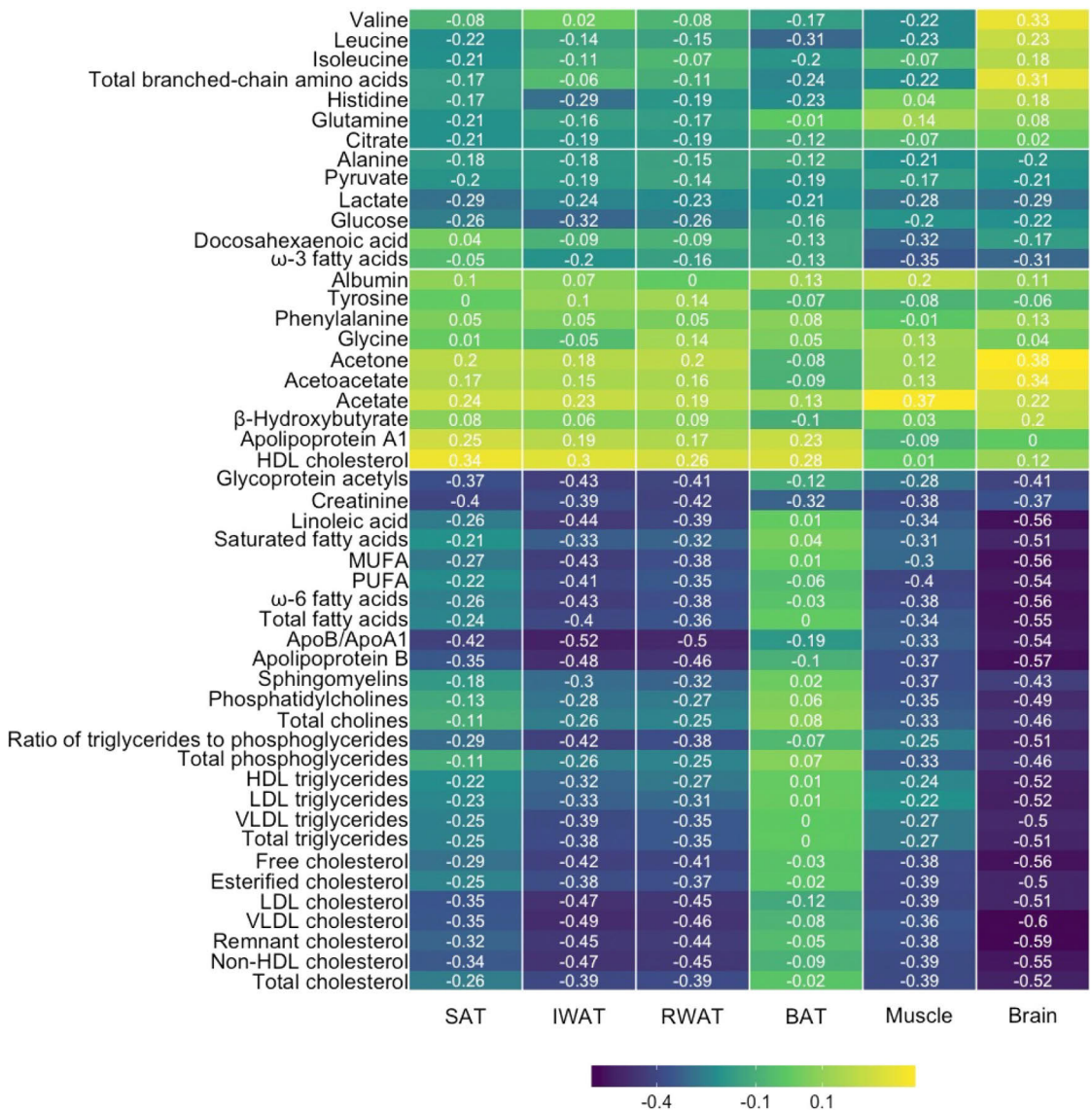


FIGURE 3 Correlation heat map between CB1R availability of abdominal SAT, IWAT, RWAT, BAT, muscle, and the whole brain with serum metabolomics across the whole study sample size. BAT, brown adipose tissue; IWAT, interperitoneal white adipose tissue; RWAT, retroperitoneal white adipose tissue; SAT, subcutaneous adipose tissue

levels correlated positively with EGP and EGP_{FFM}. No significant association was found between serum endocannabinoids and insulin-suppressed FFA levels. Regarding serum endocannabinoid levels and tissue-specific GU rates, γ-LEA was the only endocannabinoid to exhibit a significant correlation; serum γ-LEA correlated positively with abdominal SAT GU (Table 4).

Serum AG (1 + 2) level correlated positively with BMI. No association was found between serum endocannabinoid levels and weight or fat masses (Table 4).

Serum AG (1 + 2) level was associated with higher lipid levels including total, non-HDL, remnant, VLDL, and LDL cholesterol, as well as triglycerides, ApoB, ApoB/ApoA1 ratio, and fatty acids. AG (1 + 2) correlated positively also with GlycA. γ-LEA had a positive association with HDL cholesterol and ApoA1 (Figure 4).

Omega-6 polyunsaturated fatty acid linoleic acid correlated positively with abdominal SAT ($r = 0.40$, $p = 0.004$), VAT ($r = 0.60$, $p = 0.0001$), and total body fat ($r = 0.53$, $p = 0.001$) masses, weight ($r = 0.57$, $p = 0.0003$), and BMI ($r = 0.53$, $p = 0.001$). Omega-3 fatty

TABLE 4 Associations between circulating endocannabinoid concentrations and selected variables of body composition, insulin sensitivity, [18 F]FMPEP- d_2 FUR values of abdominal SAT, IWAT, and RWAT, BAT, and muscle, and [18 F]FMPEP- d_2 V_T of the whole brain

	AA	AEA	AG (1 + 2)	α -LEA	γ -LEA	DEA	NALS	OEA
Weight (kg)	0.04	0.23	0.26	0.16	0.14	0.09	-0.09	-0.06
BMI (kg/m ²)	0.16	0.22	0.36*	0.07	0.03	0.10	-0.08	-0.09
Body fat mass (kg)	0.06	0.24	0.23	0.02	-0.01	0.23	-0.08	0.02
Abdominal SAT mass (kg)	0.05	0.21	0.16	0.02	-0.04	0.24	-0.14	0.04
VAT mass (kg)	0.13	0.26	0.26	-0.02	-0.05	0.24	-0.06	0.09
M value (μ mol/kg/min)	-0.31	-0.43**	-0.24	-0.16	-0.13	-0.33	-0.14	-0.26
M value (μ mol/kg _{FFM} /min)	-0.34*	-0.44**	-0.23	-0.22	-0.20	-0.29	-0.18	-0.29
Rd (μ mol/kg/min)	-0.25	-0.37*	-0.12	-0.02	-0.03	-0.22	-0.10	-0.19
Rd (μ mol/kg _{FFM} /min)	-0.24	-0.43**	-0.03	-0.11	-0.12	-0.19	-0.06	-0.19
EGP (μ mol/kg/min) ^a	0.28	0.24	0.40*	0.29	0.25	0.35*	0.29	0.26
EGP (μ mol/kg _{FFM} /min) ^a	0.33	0.28	0.39*	0.22	0.22	0.41*	0.30	0.30
Clamp serum FFA (mmol/L)	0.03	0.02	0.02	-0.20	-0.15	0.04	-0.18	-0.10
<i>Glucose uptake (μmol/100 g/min)</i>								
Abdominal SAT	0.04	-0.10	-0.01	0.29	0.37*	-0.17	0.28	0.10
VAT	0.02	-0.12	-0.08	0.23	0.28	-0.26	0.14	-0.04
BAT ^b	-0.14	-0.33	0.10	0.08	0.08	-0.31	-0.03	-0.10
Muscle ^c	-0.19	-0.24	-0.06	-0.03	-0.01	-0.17	0.07	0.03
Femoral SAT ^c	0.00	0.01	-0.05	0.26	0.30	-0.05	0.22	0.22
Liver	0.23	0.01	0.23	-0.25	-0.13	-0.05	0.11	0.03
<i>[18F]FMPEP-d_2 FUR (mL/[min \times mL])</i>								
SAT	0.24	-0.11	-0.15	0.25	0.32	-0.19	0.23	0.16
IWAT	0.19	-0.12	-0.22	0.26	0.22	-0.21	0.18	0.12
RWAT	0.19	-0.19	-0.20	0.25	0.25	-0.20	0.22	0.14
BAT ^d	-0.004	-0.07	-0.02	0.08	0.15	-0.06	-0.10	0.07
Muscle	-0.01	-0.26	-0.29	0.03	0.03	-0.11	0.09	-0.05
[18 F]FMPEP- d_2 V_T of the whole brain	-0.28	-0.20	-0.34*	0.03	-0.05	-0.03	-0.11	-0.03

Note: Data are Pearson r values. Significant associations are indicated by bold font.

Abbreviations: AA, arachidonic acid; AEA, anandamide; AG (1 + 2), arachidonoyl glycerol (1 + 2); α -LEA, α -linolenic acid; BAT, brown adipose tissue; DEA, docosatetraenoyl ethanolamide; EGP, endogenous glucose production; FFA, free fatty acids; FFM, fat-free mass; FUR, fractional uptake rate; IWAT, intraperitoneal white adipose tissue; γ -LEA, γ -linolenic acid; M value, whole-body insulin sensitivity; NALS, N-arachidonoyl-L-serine; OEA, oleyl ethanolamide; Rd, rate of disappearance of glucose; RWAT, retroperitoneal white adipose tissue; SAT, subcutaneous adipose tissue; VAT, visceral adipose tissue; V_T , volume distribution.

^aAssociations with the LR ($n = 20$) and HR ($n = 16$) participants who gave a urine sample.

^bAssociations with the LR ($n = 20$) and HR ($n = 16$) participants who completed the FDG scan successfully.

^cAssociations with the LR ($n = 19$) and HR ($n = 16$) participants who completed the FDG scan successfully.

^dAssociations with the LR ($n = 20$) and HR ($n = 16$) participants whose [18 F]FMPEP- d_2 image analysis was able to be conducted.

* $p < 0.05$.

** $p < 0.01$.

acids in turn correlated positively with AG (1 + 2; Figure 4) and negatively with CB1R availability of muscle (Figure 3).

DISCUSSION

Our main finding was that CB1R availability of abdominal adipose tissue was lower in young healthy patients with overweight and risk for obesity in comparison with lean patients. This suggests an impairment of peripheral ECS related to increased risk for developing obesity. Lower CB1R availability in abdominal adipose tissue was associated with

decreased adipose tissue and whole-body insulin sensitivity, unfavorable lipid profile, and higher body adiposity and inflammatory markers. Whole-brain CB1R availability did not differ between the groups, but lower cerebral CB1R availability was associated with decreased whole-body insulin sensitivity and higher body adiposity. Higher serum endocannabinoid levels were associated with decreased whole-body insulin sensitivity, unfavorable lipid profile, and higher serum inflammatory markers.

Only a few studies have quantified peripheral tissue CB1R availability in humans using [18 F]FMPEP- d_2 PET. A 2018 study [11] showed lower [18 F]FMPEP- d_2 binding in abdominal SAT, WAT, and brain in

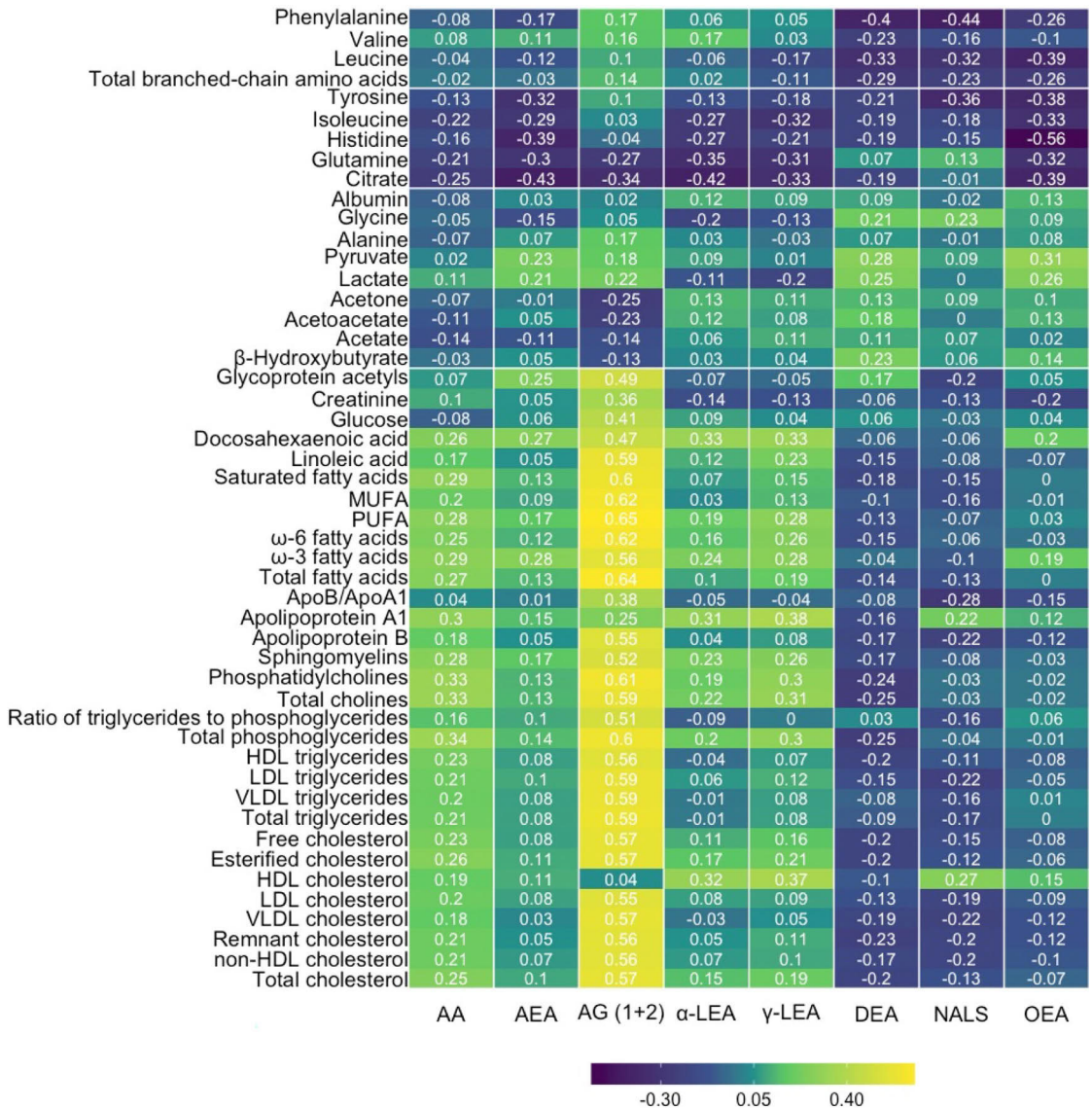


FIGURE 4 Correlation heat map between serum endocannabinoid levels and serum metabolomics across the whole study sample size. AA, arachidonic acid; AEA, anandamide; AG (1 + 2), arachidonoyl glycerol (1 + 2); α-LEA, α-linolenic acid; γ-LEA, γ-linolenic acid; DEA, docosatetraenoyl ethanolamide; NALS, N-arachidonoyl-L-serine; OEA, oleyl ethanolamide

healthy males with obesity (BMI: 32.9 ± 4.6) as compared with lean (BMI: 24.9 ± 1.7) males. Our study yielded converging results: lower CB1R availability in abdominal adipose tissue depots in the HR group than in the LR group. Compared with the previous report [11], the participants in the current study had overweight not obesity. This could contribute to the finding that CB1R availability of the whole brain did not differ between the groups, although lower CB1R availability was associated with decreased whole-body insulin sensitivity and

unfavorable body composition and serum metabolomics. Cerebral ECS regulates food intake and energy balance by interacting with reward pathways and orexigenic and anorexigenic hormones. It seems that, during a sustained positive energy balance, the cerebral ECS may become dysregulated, accompanied by defective leptin and insulin signaling, resulting in peripheral WAT accumulation and increased EGP [4], whereas pharmacologic or genetic inhibition of CB1Rs results in reduced food intake and it has antiobesity effects [4, 5, 9].

In white adipocytes, CB1R activation has several effects promoting the development of obesity and insulin resistance. CB1R activation increases adipocyte differentiation and adipogenesis, enhances fatty acid synthesis and triglyceride accumulation, reduces lipolysis, and decreases mitochondrial biogenesis favoring white and inhibiting the brown and beige phenotype, thus participating in the regulation of thermogenesis and energy expenditure. CB1R inhibition has reverse actions [4, 7, 9]. So far, the role of adipose tissue ECS in human obesity has been investigated mainly by measuring circulating and tissue endocannabinoid levels and by studying the gene expression of CB1Rs and endocannabinoid degrading enzymes [27–31]. Higher levels of circulating endocannabinoids have been observed in patients with obesity as compared with lean patients and they have been shown to decrease after weight loss [27, 28, 32, 33]. Circulating 2-AG levels were found to correlate positively with fasting insulin and triglycerides and negatively with HDL cholesterol levels [29]. Higher 2-AG levels have also been measured in VAT [33, 34], but they have been shown to be reduced in abdominal SAT [31, 35] in obesity; thus it has been proposed that alterations in endocannabinoid levels might occur in a WAT-depot-specific manner [4]. Discrepancy exists concerning CB1R expression in obesity. In high-fat fed [36] and obese Zucker rats [37], adipocyte hypertrophy has been shown to associate with increased CB1R expression in adipose tissue, whereas in humans with obesity, increased endocannabinoid levels in VAT were observed simultaneously with a trend toward a decrease of CB1R levels in VAT [34]. Also, lower CB1R gene expression has been found in abdominal SAT and VAT in patients with obesity compared with lean patients [27, 28, 31], and weight loss was followed by an increase of CB1R gene expression in abdominal SAT [31]. The expression of endocannabinoid degrading enzymes has been found to be differently affected by obesity, adipose tissue depot, and weight loss [27, 28, 30, 31, 38].

Unlike studying gene expression rate from tissue biopsies, [^{18}F]FMPEP- d_2 PET does not reveal the total CB1R density in the tissue. Instead, [^{18}F]FMPEP- d_2 binds to CB1Rs that are not occupied with their ligands endocannabinoids. Therefore, the reduced binding of [^{18}F]FMPEP- d_2 in tissues or reduced CB1R availability in tissues of the HR participants we found can either reflect increased endocannabinoid levels and their binding to CB1Rs, decreased CB1R expression in the tissue, or reduced CB1R affinity. Tissue endocannabinoid levels were not assessed in our study. Circulating endocannabinoid levels did not differ between the study groups, although we observed correlations between endocannabinoid levels and BMI, insulin sensitivity, and serum lipid and GlycA levels consistent with previous findings [27, 29]. It is acknowledged that a positive energy balance results in ECS dysregulation and an increase in the peripheral endocannabinoid tone [4, 8, 34], but the mechanisms of action of the ECS are still not fully understood. The regulation of CB1R expression seems to be complex.

Insulin has a central role in endocannabinoid metabolism in WAT [34]. In cultured adipocytes, insulin reduces intracellular endocannabinoid levels, but it does not affect the expression of CB1Rs. In insulin-resistant adipocytes, the insulin action on the endocannabinoid tone is absent or reversed. Similar observations were made with insulin-

resistant obese mice [33]. It is thus possible that the negative correlations between endocannabinoid levels and whole-body insulin sensitivity and the positive correlations between WAT CB1R availability and GU rates we found would represent the relationship between insulin action, or insulin resistance, and ECS dysregulation in WAT. In addition to insulin, the endocannabinoid tone in WAT is under control of central leptin signaling [39]. As obesity is characterized by leptin resistance, a study with obese mice showed that a peripherally restricted CB1R inverse agonist reduced food intake, body weight, and adiposity by suppressing the secretion and increasing the clearance of leptin [40].


In skeletal muscle, CB1Rs are thought to participate in the glucose homeostasis by decreasing GU after CB1R activation. There are differing results whether the ECS tone in muscle becomes dysregulated under conditions of obesity [4, 8, 9]. In the present study, CB1R availability of skeletal muscle did not differ between the groups, nor did it correlate with insulin sensitivity, possibly because of the young and healthy state of the participants. Our study did not show differences in CB1R availability of BAT. In a previous study [11], the difference was observed under cold exposure: the increase in CB1R availability of BAT in cold was blunted in participants with obesity as compared with lean participants.

Interestingly, linoleic acid, a precursor for endocannabinoids, correlated positively with AG (1 + 2) level and negatively with CB1R availability of IWAT. Excessive intake of linoleic acid has been implicated in the development of obesity, in which one possible pathway is the formation of endocannabinoids [41]. In mice, a diet enriched with linoleic acid increased liver endocannabinoid and plasma leptin levels, food intake, body weight, and adiposity, whereas adding dietary omega-3 fatty acids along with linoleic acid reversed the actions [42]. Accordingly, we observed positive correlations with linoleic acid and body adiposity, weight, and BMI. However, also ω -3 fatty acid level correlated positively with AG (1 + 2) and negatively with CB1R availability of muscle, and we do not have a suggested explanation for this. To control the overactive ECS, promising results have been found in studies with diets enriched in omega-3 fatty acids: reduced peripheral endocannabinoid levels, reduced waist to hip and visceral fat/skeletal muscle mass ratios, and improved lipid profile in participants with obesity [43].

This study had some limitations. We found lower [^{18}F]FMPEP- d_2 binding in abdominal adipose tissue in HR as compared with LR participants. However, the PET measurement is not able to distinguish a change in total CB1R density or affinity or whether CB1R availability is a consequence of a change in tissue or circulating endocannabinoid levels. We only studied males. The ECS interacts with gonadal hormones; central endocannabinoid signaling primarily reduces the release of gonadal hormones, whereas gonadal hormones cause changes in protein expression in ECS [44]. Estrogen negatively modulates ECS-induced changes in appetite, body temperature, and hypothalamic proopiomelanocortin (POMC) neurons [45]. It is thus not certain whether our result can be generalized to females. Because endocannabinoids are produced and released on demand, it is not possible to distinguish the source of the measured compounds. However, the similar associations with previously published studies with

circulating endocannabinoids and different variables we found encourage us to believe that the measured endocannabinoids do represent a metabolic situation of the body. Finally, the cross-sectional nature of the study precludes causal inference regarding the observed associations.

CONCLUSION

Here we have demonstrated lower CB1R availability of abdominal adipose tissue in young healthy patients with overweight and risk for obesity as compared with lean patients with no obesity risk and associations between CB1R availability of abdominal adipose tissue and the whole brain and insulin sensitivity and serum metabolomics. Our results suggest altered endocannabinoid tone in abdominal adipose tissue of participants with overweight, possibly reflecting a broader dysregulation of ECS with energy imbalance. 

AUTHOR CONTRIBUTIONS

Laura Pekkarinen: study design, coordination, data acquisition, modeling, statistical analysis, interpretation of results, tables and figures, main writer of the manuscript. Tatu Kantonen: study design, coordination, data acquisition, modeling, statistical analysis, interpretation of results. Vesa Oikonen: [^{18}F]FMPEP- d_2 data modeling. Merja Haaparanta-Solin, Richard Aarnio: analysis of [^{18}F]FMPEP- d_2 metabolites. Alex M. Dickens, Annie von Eyken: endocannabinoid measurements. Aino Latva-Rasku: participation in FDG PET data analysis. Prince Dadson: analysis of tissue masses. Anna K. Kirjavainen, Johan Rajander: radiotracer production. Kari Kalliokoski, Tapani Rönnemaa: study design. Lauri Nummenmaa: study design, coordination, statistical analysis, interpretation of results, figures, manuscript editing, study supervision. Pirjo Nuutila: study design, coordination, interpretation of results, study supervision. All authors were involved in writing the paper and had final approval of the submitted and published versions.

ACKNOWLEDGMENTS

The authors thank the volunteers who participated in this study and the staff of the Turku PET Centre.

FUNDING INFORMATION

The study was supported by Center of Excellence funding #307402 to Pirjo Nuutila, Academy of Finland grants #294897 and #332225 to Lauri Nummenmaa, Turku University Hospital Foundation for Education and Research, The Diabetes Research Foundation and Orion Research Foundation to Laura Pekkarinen, Finnish Cultural Foundation (Southwest Finland Fund), Emil Aaltonen Foundation, and Jenny and Antti Wihuri Foundation to Tatu Kantonen.

CONFLICT OF INTEREST STATEMENT

The authors declared no conflict of interest.

ORCID

Laura Pekkarinen  <https://orcid.org/0000-0002-5596-0485>

Pirjo Nuutila  <https://orcid.org/0000-0001-9597-338X>

REFERENCES

- World Health Organization. World Obesity Day 2022 – Accelerating action to stop obesity. Published March 4, 2022. <https://www.who.int/news/item/04-03-2022-world-obesity-day-2022-accelerating-action-to-stop-obesity>
- Pi-Sunyer FX. The obesity epidemic: pathophysiology and consequences of obesity. *Obes Res.* 2002;10(suppl 2):97S-104S. doi:10.1038/oby.2002.202
- Bermudez-Silva FJ, Viveros MP, McPartland JM, Rodriguez de Fonseca F. The endocannabinoid system, eating behavior and energy homeostasis: the end or a new beginning? *Pharmacol Biochem Behav.* 2010;95(4):375-382.
- Silvestri C, Di Marzo V. The endocannabinoid system in energy homeostasis and the etiopathology of metabolic disorders. *Cell Metab.* 2013;17(4):475-490.
- Di Marzo V, Matias I. Endocannabinoid control of food intake and energy balance. *Nat Neurosci.* 2005;8(5):585-589.
- Gatta-Cherifi B, Cota D. New insights on the role of the endocannabinoid system in the regulation of energy balance. *Int J Obes.* 2016;40(2):210-219. doi:10.1038/ijo.2015.179
- Quarta C, Mazza R, Obici S, Pasquali R, Pagotto U. Energy balance regulation by endocannabinoids at central and peripheral levels. *Trends Mol Med.* 2011;17(9):518-526.
- Di Marzo V. The endocannabinoid system in obesity and type 2 diabetes. *Diabetologia.* 2008;51(8):1356-1367.
- Simon V, Cota D. Mechanisms in endocrinology: endocannabinoids and metabolism: past, present and future. *Eur J Endocrinol.* 2017;176(6):R309-R324.
- Kantonen T, Pekkarinen L, Karjalainen T, et al. Obesity risk is associated with altered cerebral glucose metabolism and decreased μ -opioid and CB1 receptor availability. *Int J Obes.* 2022;46(2):400-407.
- Lahesmaa M, Eriksson O, Gnad T, et al. Cannabinoid type 1 receptors are upregulated during acute activation of brown adipose tissue. *Diabetes.* 2018;67(7):1226-1236.
- Juonala M, Juhola J, Magnussen CG, et al. Childhood environmental and genetic predictors of adulthood obesity: the cardiovascular risk in young Finns study. *J Clin Endocrinol Metab.* 2011;96(9):E1542-E1549.
- Juhola J, Magnussen CG, Viikari JSA, et al. Tracking of serum lipid levels, blood pressure, and body mass index from childhood to adulthood: the cardiovascular risk in young Finns study. *J Pediatr.* 2011;159(4):584-590.
- Endalifer ML, Diress G. Epidemiology, predisposing factors, biomarkers, and prevention mechanism of obesity: a systematic review. *J Obes.* 2020;2020:6134362. doi:10.1155/2020/6134362
- Mattsson N, Rönnemaa T, Juonala M, Viikari JSA, Raitakari OT. Childhood predictors of the metabolic syndrome in adulthood. The cardiovascular risk in young Finns study. *Ann Med.* 2008;40(7):542-552.
- Cederberg H, Stančáková A, Kuusisto J, Laakso M, Smith U. Family history of type 2 diabetes increases the risk of both obesity and its complications: is type 2 diabetes a disease of inappropriate lipid storage? *J Intern Med.* 2015;277(5):540-551. doi:10.1111/joim.12289
- Anjana RM, Lakshminarayanan S, Deepa M, Farooq S, Pradeepa R, Mohan V. Parental history of type 2 diabetes mellitus, metabolic syndrome, and cardiometabolic risk factors in Asian Indian adolescents. *Metabolism.* 2009;58(3):344-350.

18. Karlsson HK, Tuominen L, Tuulari JJ, et al. Obesity is associated with decreased μ -opioid but unaltered dopamine D2 receptor availability in the brain. *J Neurosci*. 2015;35(9):3959-3965.
19. Lahdenpohja S, Keller T, Forsback S, et al. Automated GMP production and long-term experience in radiosynthesis of CB(1) tracer [(18) F]FMPEP-d(2). *J Labelled Comp Radiopharm*. 2020;63(9):408-418.
20. Hamacher K, Coenen HH, Stöcklin G. Efficient stereospecific synthesis of no-carrier-added 2-[18F]-fluoro-2-deoxy-D-glucose using aminopolyether supported nucleophilic substitution. *J Nucl Med*. 1986; 27(2):235-238.
21. Lemaire C, Damhaut P, Lauricella B, et al. Fast F-18 FDG synthesis by alkaline hydrolysis on a low polarity solid phase supports. *Labelled Comp Radiopharm*. 2002;45(5):435-447.
22. Din M U, Raiko J, Saari T, et al. Human brown fat radiodensity indicates underlying tissue composition and systemic metabolic health. *J Clin Endocrinol Metab*. 2017;102(7):2258-2267.
23. Eriksson O, Mikkola K, Espes D, et al. The cannabinoid receptor-1 is an imaging biomarker of brown adipose tissue. *J Nucl Med*. 2015; 56(12):1937-1941.
24. DeFronzo RA, Tobin JD, Andres R. Glucose clamp technique: a method for quantifying insulin secretion and resistance. *Am J Physiol*. 1979;237(3):E214-E223.
25. Soininen P, Kangas AJ, Würtz P, Suna T, Ala-Korpela M. Quantitative serum nuclear magnetic resonance metabolomics in cardiovascular epidemiology and genetics. *Circ Cardiovasc Genet*. 2015;8(1): 192-206.
26. Dickens AM, Borgan F, Laurikainen H, et al. Links between central CB1-receptor availability and peripheral endocannabinoids in patients with first episode psychosis. *NPJ Schizophr*. 2020;6(1):21. doi:10.1038/s41537-020-00110-7
27. Blüher M, Engeli S, Klötting N, et al. Dysregulation of the peripheral and adipose tissue endocannabinoid system in human abdominal obesity. *Diabetes*. 2006;55(11):3053-3060.
28. Engeli S, Böhne J, Feldpausch M, et al. Activation of the peripheral endocannabinoid system in human obesity. *Diabetes*. 2005;54(10): 2838-2843.
29. Côté M, Matias I, Lemieux I, Petrosino S, et al. Circulating endocannabinoid levels, abdominal adiposity and related cardiometabolic risk factors in obese men. *Int J Obes*. 2007;31(4):692-699.
30. Sarzani R, Bordinchia M, Marcucci P, et al. Altered pattern of cannabinoid type 1 receptor expression in adipose tissue of dysmetabolic and overweight patients. *Metabolism*. 2009;58(3):361-367.
31. Bennetzen MF, Wellner N, Ahmed SS, et al. Investigations of the human endocannabinoid system in two subcutaneous adipose tissue depots in lean subjects and in obese subjects before and after weight loss. *Int J Obes*. 2011;35(11):1377-1384.
32. Di Marzo V, Côté M, Matias I, et al. Changes in plasma endocannabinoid levels in visceraally obese men following a 1 year lifestyle modification programme and waist circumference reduction: associations with changes in metabolic risk factors. *Diabetologia*. 2009;52(2): 213-217.
33. D'Eon TM, Pierce KA, Roix JJ, Tyler A, Chen H, Teixeira SR. The role of adipocyte insulin resistance in the pathogenesis of obesity-related elevations in endocannabinoids. *Diabetes*. 2008;57(5):1262-1268.
34. Matias I, Gonthier MP, Orlando P, et al. Regulation, function, and dysregulation of endocannabinoids in models of adipose and beta-pancreatic cells and in obesity and hyperglycemia. *J Clin Endocrinol Metab*. 2006;91(8):3171-3180.
35. Izzo AA, Piscitelli F, Capasso R, et al. Peripheral endocannabinoid dysregulation in obesity: relation to intestinal motility and energy processing induced by food deprivation and re-feeding. *Br J Pharmacol*. 2009;158(2):451-461.
36. Yan ZC, Liu DY, Zhang LL, et al. Exercise reduces adipose tissue via cannabinoid receptor type 1 which is regulated by peroxisome proliferator-activated receptor-delta. *Biochem Biophys Res Commun*. 2007;354(2):427-433.
37. Bensaid M, Gary-Bobo M, Esclangon A, et al. The cannabinoid CB1 receptor antagonist SR141716 increases Acrp30 mRNA expression in adipose tissue of obese fa/fa rats and in cultured adipocyte cells. *Mol Pharmacol*. 2003;63(4):908-914.
38. Bordinchia M, Battistoni I, Mancinelli L, et al. Cannabinoid CB1 receptor expression in relation to visceral adipose depots, endocannabinoid levels, microvascular damage, and the presence of the Cnr1 A3813G variant in humans. *Metabolism*. 2010;59(5):734-741.
39. Buettner C, Muse ED, Cheng A, et al. Leptin controls adipose tissue lipogenesis via central, STAT3-independent mechanisms. *Nat Med*. 2008;14(6):667-675.
40. Tam J, Cinar R, Liu J, et al. Peripheral cannabinoid-1 receptor inverse agonism reduces obesity by reversing leptin resistance. *Cell Metab*. 2012;16(2):167-179.
41. Naughton SS, Mathai ML, Hryciw DH, McAinch AJ. Linoleic acid and the pathogenesis of obesity. *Prostaglandins Other Lipid Mediat*. 2016; 125:90-99.
42. Alveheim AR, Malde MK, Osei-Hyiaman D, et al. Dietary linoleic acid elevates endogenous 2-AG and anandamide and induces obesity. *Obesity*. 2012;20(10):1984-1994.
43. Berge K, Piscitelli F, Hoem N, et al. Chronic treatment with krill powder reduces plasma triglyceride and anandamide levels in mildly obese men. *Lipids Health Dis*. 2013;12:78. doi:10.1186/1476-511X-12-78
44. Gorzalka BB, Dang SS. Minireview: endocannabinoids and gonadal hormones: bidirectional interactions in physiology and behavior. *Endocrinology*. 2012;153(3):1016-1024.
45. Kellert BA, Nguyen MC, Nguyen C, Nguyen QH, Wagner EJ. Estrogen rapidly attenuates cannabinoid-induced changes in energy homeostasis. *Eur J Pharmacol*. 2009;622(1-3):15-24.

SUPPORTING INFORMATION

Additional supporting information can be found online in the Supporting Information section at the end of this article.

How to cite this article: Pekkarinen L, Kantonen T, Oikonen V, et al. Lower abdominal adipose tissue cannabinoid type 1 receptor availability in young men with overweight. *Obesity (Silver Spring)*. 2023;31(7):1844-1858. doi:10.1002/oby.23770



**TURUN
YLIOPISTO**
UNIVERSITY
OF TURKU

ISBN 978-951-29-9574-5 (PRINT)
ISBN 978-951-29-9575-2 (PDF)
ISSN 0355-9483 (Print)
ISSN 2343-3213 (Online)